

MOTOR BUS TRANSFER SYSTEM MODELING with PSCAD/EMTDC

A Thesis

Presented in Partial Fulfillment of the Requirements for the

Degree of Master in Science

with a

Major in Electrical Engineering

in the

College of Graduate Studies

University of Idaho

by

Arturo Barradas Munoz

Major Professor: Brian K. Johnson, Ph.D.

Committee Members: Herbert L. Hess, Ph.D.; Joseph Law, Ph.D.

Department Administrator: Mohsen Guizani, Ph.D.

May 2018

**AUTHORIZATION TO SUBMIT THESIS**

This thesis of Arturo Barradas Munoz, submitted for the degree of Master of Science with a Major in Electrical Engineering and titled "MOTOR BUS TRANSFER SYSTEM MODELING WITH PSCAD/EMTDC," has been reviewed in final form. Permission, as indicated by the signatures and dates given below, is now granted to submit final copies to the College of Graduate Studies for approval.

Major Professor: \_\_\_\_\_ Date: \_\_\_\_\_

Brian K. Johnson, Ph.D.

Committee

Members: \_\_\_\_\_ Date: \_\_\_\_\_

Herbert L. Hess, Ph.D.

\_\_\_\_\_ Date: \_\_\_\_\_

Joseph Law, Ph.D.

Department

Administrator: \_\_\_\_\_ Date: \_\_\_\_\_

Mohsen Guizani, Ph.D.

**ABSTRACT**

When starting-up or shutting-down a power generator, there is a need to transfer the generator auxiliary load bus, known as the motor bus, from the start-up source to the generator or from the generator to the start-up source respectively. In the course of the transfer process, the auxiliary induction and synchronous motors are exposed to electromechanical and electromagnetic forces that could damage them if an improper transfer is performed. There is also a need to avoid paralleling sources that could increase the short circuit levels during faults causing auxiliary equipment damage. Similar but not less important, is the coasting down duration of the motor bus voltage under the open circuit conditions, which is a complex process owing to the fast voltage, frequency, and phase angle variations at the motor bus.

During the past twenty years, digital power system simulators have seen very significant technological advances on their numerical algorithms. This has allowed them not only to have more exact and sophisticated power system models, but also to include tools to simulate complex protective relays and control system interactions with the power system simulation. Until a few years ago, such cases were not only difficult to simulate but also time consuming to carry out.

The main purpose of this thesis is the modeling of a motor bus transfer case using three methods: fast transfer, in-phase, and residual voltage. Modeling the motor bus transfer using any of these three methods previously mentioned, may allow the power plant or industrial protection and control engineers to study and analyze the induction motor transient behavior during a motor bus transfer in order to implement or upgrade their current motor bus transfer schemes and strategies.

Another purpose of this thesis was to analyze the electromagnetic transient behavior of the induction motor during the motor load transfer process. To test and analyze the performance of the motor bus transfer model, several motor transfer simulations, under normal and emergency conditions, were developed and validated. The simulation results are analyzed and discussed. Although the examples presented in the simulations in this research refer to motor buses generating power plants, the concepts and the analysis of the motors' behavior as well as of the transfer system implemented in PSCAD/EMTDC are of a general application, and may be easily applied to industrial systems.

**ACKNOWLEDGMENTS**

I would like to thank my main advisor, Dr. Brian Johnson, for his guidance and support throughout my master's degree studies and research to complete this project.

Also, I extend my gratitude to Dr. Herbert Hess and Dr. Joseph Law for their valuable time and dedication to review and evaluate this thesis.

Finally, Mr. Alberto Gutierrez is gratefully thanked for his support and guidance to accomplish this work, and specially for his mentoring during my professional career.



## TABLE OF CONTENTS

Authorization to Submit Thesis.....	ii
Abstract.....	iii
Acknowledgments.....	iv
List of Figures .....	x
List of Tables .....	xxv
CHAPTER 1 - INTRODUCTION.....	1
1.1 Thesis Overview.....	1
1.2 Literature Review.....	2
1.3 Outline of Thesis .....	8
1.4 Research Purpose .....	9
CHAPTER 2 - Motor Bus Transfer Systems.....	10
2.1 Introduction.....	10
2.2 Motor Bus Transfer Classification (IEEE) .....	10
2.2.1 Open Transition Transfer – Methods and Modes.....	10
2.2.1.1 Methods.....	11
2.2.1.1.1 Fast Transfer.....	11
2.2.1.1.2 In-Phase.....	11
2.2.1.1.3 Residual Voltage .....	11
2.2.1.1.4 Slow Time Transfer .....	11
2.2.1.2 Modes.....	12
2.2.1.2.1 Sequential .....	12
2.2.1.2.2 Simultaneous.....	12
2.2.2 Bus Transfer Initiation .....	12

2.2.2.1 Manual Transfer .....	12
2.2.2.2 Automatic Transfer.....	13
2.2.2.3 Protective Transfer.....	13
2.3 Common Bus Transfer Topologies.....	13
2.3.1 Type I Bus Configuration Used in Thermal Power Plants.....	14
2.3.2 Type II Bus Configuration Used in Industrial Plants.....	15
2.3.3 Type III Bus Configuration Used in Nuclear Power Plants.....	16
CHAPTER 3 - Transient Analysis of Induction Motors.....	17
3.1 Introduction.....	17
3.2 Induction Motor Equations .....	18
3.2.1 Induction Motor Equations in Machine Variables .....	18
3.2.2 Induction Motor Equations in Arbitrary Reference-Frame Variables.....	26
3.2.3 Single Induction Motor on Loss of Power Supply .....	29
3.3 Analysis of Induction Motors Behavior on Motor Bus Transfer .....	32
3.3.1 Analysis of a Single Induction Motor During Loss of Power Supply.....	32
3.3.2 Analysis of a Group of Induction Motors on Loss of Power Supply.....	38
3.3.3 Analysis of a Group of Induction Motors During Reconnection on Maximum Voltage Phasor Difference.....	43
3.3.4 Analysis of a Group of Induction Motors During Reconnection on Large Frequency Difference .....	53
3.3.5 Analysis of a Motor Bus on Different Closing Times.....	56
CHAPTER 4 - Power Station System Model For Simulation of a Motor Bus Transfer System .....	68
4.1 Introduction.....	68
4.2 PSCAD/EMTDC.....	68
4.2.1 Introduction.....	68

4.3 Power System Model .....	69
4.3.1 One-Line Diagram .....	69
4.3.2 Western Equivalent System.....	70
4.3.3 Eastern Equivalent System .....	71
4.3.4 Start-up Transformer .....	72
4.3.5 Auxiliary Transformer.....	72
4.3.6 Power Station Generator Equivalent .....	73
4.3.7 Power Station Main Transformer .....	74
4.3.8 Induction Motors .....	74
CHAPTER 5 - Motor Bus Transfer System Model .....	83
5.1 Control Panel for the Motor Bus Transfer Simulation Modes.....	84
5.2 Relay Trip and Manual Command.....	85
5.3 Auxiliary Controls.....	86
5.4 Motor Bus Transfer System Process Unit.....	86
5.4.1 Motor Bus Transfer System Undervoltage Unit.....	90
5.4.2 Motor Bus Transfer System Fast Transfer Module .....	91
5.4.2.1 Voltage Phase Angle Difference .....	95
5.4.2.2 New Source Upper and Lower Voltage Supervision.....	95
5.4.2.3 Frequency Difference .....	95
5.4.2.4 Voltage Phasor Difference .....	96
5.4.3 Motor Bus Transfer System In-Phase Transfer Module .....	97
5.4.3.1 Frequency Difference .....	101
5.4.3.2 New Source Upper and Lower Voltage Supervision.....	101
5.4.3.3 Motor Bus Transfer System Circuit Breaker Close Angle.....	101
5.4.4 Motor Bus Transfer System Residual Voltage Transfer Module.....	103

5.4.4.1 Lower Residual Voltage Limit.....	106
5.4.4.2 Volts/Hertz.....	106
5.5 Circuit Breaker Control Block.....	107
CHAPTER 6 - Simulations and Results.....	110
6.1 Introduction.....	110
6.2 Testing Mode.....	110
6.2.1 Fast Transfer Algorithm Component Response.....	110
6.2.2 In-Phase Transfer Algorithm Component Response.....	129
6.2.3 Residual Voltage Algorithm Component Response .....	147
6.3 Manual Transfer.....	190
6.3.1 Transfer from Start-up System to Auxiliary System.....	190
6.3.2 Manual Transfer from Auxiliary System to Start-up System .....	195
6.4 Automatic Transfer .....	200
6.4.1 Automatic Transfer Initiated by the Auxiliary Transformer Differential Protective Relay .	200
6.4.2 Automatic Transfer Initiated by a Transmission Line Impedance Protective Relay.....	205
6.4.3 Automatic Transfer Initiated by Motor Bus Undervoltage Conditions .....	210
6.5 Motor Bus Transfer System Model Performance Summary .....	215
CHAPTER 7 - Conclusions and Future Work.....	216
CHAPTER 8 - Bibliography .....	219
Appendix A.....	223
A.1 Western System PSCAD/EMTDC Input Parameters.....	223
A.2 Auxiliary Transformer PSCAD/EMTDC Input Parameters .....	234
A.3 Eastern System PSCAD/EMTDC Input Parameters .....	236
A.4 Main Generator PSCAD/EMTDC Input Parameters.....	242
A.5 Main Station Transformer PSCAD/EMTDC Input Parameters.....	243

A.6 9000 HP Induction Motor PSCAD/EMTDC Input Parameters.....	244
A.7 6000 HP Induction Motor PSCAD/EMTDC Input Parameters.....	245
A.8 3200 HP Induction Motor PSCAD/EMTDC Input Parameters.....	246
A.9 1400 HP Induction Motor PSCAD/EMTDC Input Parameters.....	247
A.10 1000 HP Induction Motor PSCAD/EMTDC Input Parameters.....	248
A.11 470 HP Induction Motor PSCAD/EMTDC Input Parameters.....	249
A.12 9000 HP Induction Motor PSCAD/EMTDC Input Parameters.....	250
A.13 6000 HP Induction Motor PSCAD/EMTDC Input Parameters.....	251
A.14 4000 HP Induction Motor PSCAD/EMTDC Input Parameters.....	252
A.15 3500 HP Induction Motor PSCAD/EMTDC Input Parameters.....	253
A.16 2500 HP Induction Motor PSCAD/EMTDC Input Parameters.....	254
A.17 2000 HP Induction Motor PSCAD/EMTDC Input Parameters.....	255

## LIST OF FIGURES

Figure 2-1 Type I bus configuration.....	14
Figure 2-2 Type II bus configuration.....	15
Figure 2-3 Type III bus configuration used in nuclear power plants .....	16
Figure 3-1 Two-pole, 3-phase, symmetrical induction machine.....	18
Figure 3-2 Per-phase equivalent circuit of the induction motor with the mechanical load represented .....	19
Figure 3-3 Per-phase Steinmetz equivalent circuit for an induction motor with rotor parameters referred to the stator side. ....	29
Figure 3-4 System to analyze and compare the behavior of a medium and a high inertia induction motors on loss of power supply simulation.....	33
Figure 3-5 Motor terminal voltage magnitude change during a coast down simulation of a medium inertia 6000 HP induction motor pump and a high inertia 3200 induction motor fan. ....	35
Figure 3-6 Frequency of motor terminal voltage change during a coast down simulation of a medium inertia 6000 HP induction motor pump and a high inertia 3200 induction motor fan. ....	36
Figure 3-7 Motor terminal voltage phase angle change during a coast down simulation of a medium inertia 6000 HP induction motor pump and a high inertia 3200 induction motor fan. ....	37
Figure 3-8 Motor torques during a coast down simulation of a medium inertia 6000 HP induction motor pump and a high inertia 3200 induction motor fan. ....	38
Figure 3-9 Motor bus voltage magnitude during a motor bus coast down simulation.....	39
Figure 3-10 Motor bus voltage frequency during a motor bus coast down simulation.....	40
Figure 3-11 Motor bus voltage phase angle during a motor bus coast down simulation. ....	40
Figure 3-12 Motor torques during a motor bus coast down simulation. ....	41
Figure 3-13 Motor currents during a motor bus coast down simulation, a) instantaneous current in kA, b) current magnitude in per unit.....	42

Figure 3-14 Voltage phasor difference between the new source voltage and motor residual voltage during a motor bus coast down simulation. ....	44
Figure 3-15 New source and motor residual voltage difference in time domain during a motor bus coast down simulation, a) Voltage magnitudes in per unit, b) Voltage phase angle in degrees. ....	45
Figure 3-16 New incoming power supply voltage and motor bus voltage behavior during a simulation of induction motor starting, loss of power supply, and reconnection for maximum motor bus-new source voltage difference, a) instantaneous voltage in kV, b) voltage magnitude in per unit, c) zoom in time of the instantaneous voltage in kV and d) zoom in time of the voltage magnitude in per unit. ...	47
Figure 3-17 High and medium inertia motor currents behavior during a simulation of induction motor starting, loss of power supply, and reconnection for maximum motor bus-new source voltage difference, a) instantaneous current in kA, b) current magnitude in per unit, c) zoom in time of the instantaneous current in kA and d) zoom in time of the current magnitude in per unit. ....	48
Figure 3-18 Motor bus frequency and phase angle behavior during a simulation of induction motor starting, loss of power supply, and reconnection for maximum motor bus-new source voltage difference, a) Frequency in Hertz, b) Voltage phase angle in degrees, c) Zoom in time of the frequency in Hertz and d) Zoom in time of the voltage phase angle in degrees. ....	49
Figure 3-19 High and medium inertia motor load and electromagnetic torque behavior during a simulation of induction motor starting, loss of power supply, and reconnection for maximum motor bus-new source voltage difference, a) Mechanical torque in per unit, b) Electromagnetic torque in per unit, c) Zoom in time of the mechanical torque in per unit, d) Zoom in time of the electromagnetic torque in per unit. ....	51
Figure 3-20 High and medium inertia motor currents behavior during a simulation of induction motor starting, loss of power supply, and reconnection for a high motor bus-new source voltage frequency difference, a) Instantaneous current in kA, b) Current magnitude in per unit, c) Zoom in time of the instantaneous current in kA, d) Zoom in time of the current magnitude in per unit. ....	54
Figure 3-21 High and medium inertia motor electromagnetic torques behavior during a simulation of induction motor starting, loss of power supply, and reconnection for a high motor bus-new source voltage frequency difference, a) Instantaneous electromagnetic torque in per unit, b) Zoom in time of the electromagnetic torque in per unit. ....	55

Figure 3-22 System 01 to analyze the induction motor currents and electromagnetic torques behavior during different reclosing times of the new source's breaker.....	57
Figure 3-23 System 01 induction motor current behavior during different closing times of the new source's breaker.....	58
Figure 3-24 System 01 induction motor electromagnetic torques behavior during different closing times of the new source's breaker.....	60
Figure 3-25 System 02 to analyze the induction motor currents and electromagnetic torques behavior during different closing times of the new source's breaker.....	62
Figure 3-26 System 02 induction motor currents behavior during different closing times of the new source's breaker.....	63
Figure 3-27 System 02 induction motor electromagnetic torques behavior during different closing times of the new source's breaker.....	65
Figure 4-1 Power system model one-line diagram .....	70
Figure 4-2 Western equivalent system.....	71
Figure 4-3 Eastern equivalent system .....	71
Figure 4-4 Start-up transformer circuit .....	72
Figure 4-5 Auxiliary transformer circuit.....	73
Figure 4-6 Power station generator equivalent.....	73
Figure 4-7 Main Station Transformer Model in PSCAD/EMTDC .....	74
Figure 4-8 9000 HP motor starting performance simulation with PSCAD/EMTDC.....	77
Figure 4-9 6000 HP motor starting performance simulation with PSCAD/EMTDC.....	78
Figure 4-10 3200 HP motor starting performance simulation with PSCAD/EMTDC.....	79
Figure 4-11 1400 HP motor starting performance simulation with PSCAD/EMTDC.....	80
Figure 4-12 1000 HP motor starting performance simulation with PSCAD/EMTDC.....	81
Figure 4-13 470 HP motor starting performance simulation with PSCAD/EMTDC.....	82
Figure 5-1 Motor bus transfer system model implemented in PSCAD/EMTDC.....	83



Figure 5-2 Control panel to control the motor bus transfer simulation modes .....	84
Figure 5-3 Relay trip and manual command.....	85
Figure 5-4 Auxiliary controls section .....	86
Figure 5-5 Motor bus transfer process unit.....	86
Figure 5-6 Voltage phasors calculation using standard PSCAD/EMTDC build-in modules.....	88
Figure 5-7 Motor bus transfer system process unit internal components.....	89
Figure 5-8 Motor bus transfer system under-voltage unit .....	90
Figure 5-9 Motor bus transfer system under voltage unit details .....	91
Figure 5-10 Motor bus transfer system fast transfer modules.....	92
Figure 5-11 Fast transfer concept .....	93
Figure 5-12 MBTS fast transfer module details.....	94
Figure 5-13 Motor bus transfer system in-phase module.....	98
Figure 5-14 In-Phase transfer concept .....	99
Figure 5-15 MBTS in-phase module details .....	100
Figure 5-16 Motor bus transfer system residual voltage module.....	103
Figure 5-17 Residual voltage transfer concept .....	104
Figure 5-18 MBTS residual voltage module components.....	105
Figure 5-19 Circuit breaker control block .....	107
Figure 5-20 Circuit breaker controls block in details.....	108
Figure 6-1 Motor bus transfer system controls for a fast transfer test, initiated at t=14 sec. ....	111
Figure 6-2 Phase A instantaneous voltage in kV during a fast transfer test, initiated at t=14 sec. ....	112
Figure 6-3 Phase A RMS voltage in per unit during a fast transfer test, initiated at t=14 sec. ....	113
Figure 6-4 Voltage frequency in Hertz during a fast transfer test, initiated at t=14 sec. ....	113
Figure 6-5 Phase A voltage phase angle in degrees during a fast transfer test, initiated at t=14 sec.	114

Figure 6-6 Motor bus transfer system element and circuit breaker contact operations during a fast transfer test, initiated at t=14 sec.....	115
Figure 6-7 9000 HP Motor phase A instantaneous and RMS current, and torque transient response during a fast transfer test, initiated at t=14 sec.....	117
Figure 6-8 6000 HP Motor phase A instantaneous and RMS current, and torque transient response during a fast transfer test, initiated at t=14 sec.....	118
Figure 6-9 3200 HP Motor phase A instantaneous and RMS current, and torque transient response during a fast transfer test, initiated at t=14 sec.....	120
Figure 6-10 1400 HP Motor phase A instantaneous and RMS current, and torque transient response during a fast transfer test, initiated at t=14 sec.....	121
Figure 6-11 1000 HP Motor phase A instantaneous and RMS current, and torque transient response during a fast transfer test, initiated at t=14 sec.....	122
Figure 6-12 470 HP Motor phase A instantaneous and RMS current, and torque transient response during a fast transfer test, initiated at t=14 sec.....	124
Figure 6-13 Phase A instantaneous voltage in kV, phase A RMS voltage in p.u., voltage frequency in Hz and phase A voltage phase angle during a fast transfer test, initiated at t=14.004167 sec.....	125
Figure 6-14 Phase A instantaneous voltage in kV, phase A RMS voltage in p.u., voltage frequency in Hz and phase A voltage phase angle during a fast transfer test, initiated at t=14.00833 sec.....	126
Figure 6-15 Phase A instantaneous voltage in kV, phase A RMS voltage in p.u., voltage frequency in Hz and phase A voltage phase angle during a fast transfer test, initiated at t=14.0125 sec. ....	127
Figure 6-16 Motor bus transfer system controls for an in-phase test, initiated at t=14 sec.....	129
Figure 6-17 Phase A Instantaneous Voltage in kV during an in-phase transfer test, initiated at t=14 sec. ....	130
Figure 6-18 Phase A RMS voltage in per unit during an in-phase transfer test, initiated at t=14 sec.	131
Figure 6-19 Voltage frequency in Hertz during an in-phase transfer test, initiated at t=14 sec.....	131
Figure 6-20 Phase A Voltage phase angle in degrees during an in-phase transfer test, initiated at t=14 sec.....	132

Figure 6-21 Motor bus transfer system element and circuit breaker contact operations during an in-phase transfer test, initiated at t=14 sec.....	133
Figure 6-22 9000 HP Motor phase A instantaneous and RMS current and torque transient response during an in-phase transfer test, initiated at t=14 sec. ....	135
Figure 6-23 6000 HP Motor phase A instantaneous and RMS current and torque transient response during an in-phase transfer test, initiated at t=14 sec. ....	136
Figure 6-24 3200 HP Motor phase A instantaneous and RMS current and torque transient response during an in-phase transfer test, initiated at t=14 sec. ....	138
Figure 6-25 1400 HP Motor phase A instantaneous and RMS current and torque transient response during an in-phase transfer test, initiated at t=14 sec. ....	139
Figure 6-26 1000 HP Motor phase A instantaneous and RMS current and torque transient response during an in-phase transfer test, initiated at t=14 sec. ....	141
Figure 6-27 470 HP Motor phase A instantaneous and RMS current and torque transient response during an in-phase transfer test, initiated at t=14 sec. ....	142
Figure 6-28 Phase A instantaneous voltage in kV, phase A RMS voltage in p.u., voltage frequency in Hz and phase A voltage phase angle during an in-phase transfer test, initiated at t=14.004167 sec. ....	143
Figure 6-29 Phase A instantaneous voltage in kV, phase A RMS voltage in p.u., voltage frequency in Hz and phase A voltage phase angle during an in-phase transfer test, initiated at t=14.00833 sec. ....	144
Figure 6-30 Phase A instantaneous voltage in kV, phase A RMS voltage in p.u., voltage frequency in Hz and phase A voltage phase angle during an in-phase transfer test, initiated at t=14.0125 sec. ....	145
Figure 6-31 Motor bus transfer system controls for the residual voltage transfer test, initiated at t=14 sec.....	147
Figure 6-32 Phase A Instantaneous voltage in kV during a residual voltage transfer test, initiated at t=14 sec.....	148
Figure 6-33 Phase A RMS voltage in per unit during a residual voltage transfer test, initiated at t=14 sec.....	149
Figure 6-34 Voltage frequency in Hertz during a residual voltage transfer test, initiated at t=14 sec. ....	150

Figure 6-35 Phase A Voltage phase angle in degrees during a residual voltage transfer test, initiated at t=14 sec.....	150
Figure 6-36 Motor bus transfer system element and circuit breaker contact operations during a residual voltage transfer test, initiated at t=14 sec.....	152
Figure 6-37 9000 HP Motor phase A instantaneous current and electromagnetic torque transient response comparison between the motor starting process and the reconnection after a residual voltage transfer test, initiated at t=14 sec.....	153
Figure 6-38 9000 HP Motor phase A instantaneous current and electromagnetic torque transient response at the moment of reconnection to the start-up system during a residual voltage transfer test, initiated at t=14 sec.....	153
Figure 6-39 9000 HP Motor phase A current versus speed in per unit transient response comparison between the motor starting process and the reconnection after a residual voltage transfer test, initiated at t=14 sec.....	154
Figure 6-40 9000 HP Motor electromagnetic torque versus speed transient response comparison during starting process and at the reconnection after a residual voltage transfer test, initiated at t=14 sec.....	155
Figure 6-41 6000 HP Motor phase A instantaneous current and electromagnetic torque transient response comparison between the motor starting process and the reconnection after a residual voltage transfer test, initiated at t=14 sec.....	156
Figure 6-42 6000 HP Motor phase A instantaneous current and electromagnetic torque transient response at the moment of reconnection to the start-up system during a residual voltage transfer test, initiated at t=14 sec.....	157
Figure 6-43 6000 HP Motor phase A current versus speed in per unit transient response comparison between the motor starting process and the reconnection after a residual voltage transfer test, initiated at t=14 sec.....	158
Figure 6-44 6000 HP Motor electromagnetic torque versus speed transient response comparison during starting process and at the reconnection after a residual voltage transfer test, initiated at t=14 sec.....	159

Figure 6-45 3200 HP Motor phase A instantaneous current and electromagnetic torque transient response during a residual voltage transfer test, initiated at t=14 sec.....	160
Figure 6-46 3200 HP Motor phase A instantaneous current and electromagnetic torque transient response at the moment of reconnection to the start-up system during a residual voltage transfer test, initiated at t=14 sec.....	160
Figure 6-47 3200 HP Motor phase A current versus speed in per unit transient response comparison between the motor starting process and the reconnection after a residual voltage transfer test, initiated at t=14 sec.....	161
Figure 6-48 3200 HP Motor electromagnetic torque versus speed transient response comparison during starting process and at the reconnection after a residual voltage transfer test, initiated at t=14 sec.....	162
Figure 6-49 1400 HP Motor phase A instantaneous current and electromagnetic torque transient response during a residual voltage transfer test, initiated at t=14 sec.....	163
Figure 6-50 1400 HP Motor phase A instantaneous current and electromagnetic torque transient response at the moment of reconnection to the start-up system during a residual voltage transfer test, initiated at t=14 sec.....	163
Figure 6-51 1400 HP Motor phase A current versus speed in per unit transient response comparison between the motor starting process and the reconnection after a residual voltage transfer test, initiated at t=14 sec.....	164
Figure 6-52 1400 HP Motor electromagnetic torque versus speed transient response comparison during starting process and at the reconnection after a residual voltage transfer test, initiated at t=14 sec.....	165
Figure 6-53 1000 HP Motor phase A instantaneous current and electromagnetic torque transient response during a residual voltage transfer test, initiated at t=14 sec.....	166
Figure 6-54 1000 HP Motor phase A instantaneous current and electromagnetic torque transient response at the moment of reconnection to the start-up system during a residual voltage transfer test, initiated at t=14 sec.....	166

Figure 6-55 1000 HP Motor phase A current versus speed in per unit transient response comparison between the motor starting process and the reconnection after a residual voltage transfer test, initiated at t=14 sec.....	167
Figure 6-56 1000 HP Motor electromagnetic torque versus speed transient response comparison during starting process and at the reconnection after a residual voltage transfer test, initiated at t=14 sec.....	168
Figure 6-57 470 HP Motor phase A instantaneous current and electromagnetic torque transient response during a residual voltage transfer test, initiated at t=14 sec.....	169
Figure 6-58 470 HP Motor phase A instantaneous current and electromagnetic torque transient response at the moment of reconnection to the start-up system during a residual voltage transfer test, initiated at t=14 sec.....	169
Figure 6-59 470 HP Motor phase A current versus speed in per unit transient response comparison between the motor starting process and the reconnection after a residual voltage transfer test, initiated at t=14 sec.....	170
Figure 6-60 470 HP Motor electromagnetic torque versus speed transient response comparison during starting process and at the reconnection after a residual voltage transfer test, initiated at t=14 sec.....	171
Figure 6-61 Phase A instantaneous voltage in kV, during a residual voltage transfer test, initiated at t=14.004167 sec.....	172
Figure 6-62 9000 HP motor phase A current and electromagnetic torque versus speed in per unit transient response comparison during starting process and at the reconnection after a residual voltage transfer test, initiated at t=14.004167 sec.....	172
Figure 6-63 6000 HP motor phase A current and electromagnetic torque versus speed in per unit transient response comparison during starting process and at the reconnection after a residual voltage transfer test, initiated at t=14.004167 sec.....	173
Figure 6-64 3200 HP motor phase A current and electromagnetic torque versus speed in per unit transient response comparison during starting process and at the reconnection after a residual voltage transfer test, initiated at t=14.004167 sec.....	173

Figure 6-65 1400 HP motor phase A current and electromagnetic torque versus speed in per unit transient response comparison during starting process and at the reconnection after a residual voltage transfer test, initiated at t=14.004167 sec. ....	174
Figure 6-66 1000 HP motor phase A current and electromagnetic torque versus speed in per unit transient response comparison during starting process and at the reconnection after a residual voltage transfer test, initiated at t=14.004167 sec. ....	174
Figure 6-67 470 HP motor phase A current and electromagnetic torque versus speed in per unit transient response comparison during starting process and at the reconnection after a residual voltage transfer test, initiated at t=14.004167 sec. ....	175
Figure 6-68 Phase A instantaneous voltage in kV, during a residual voltage transfer test, initiated at t=14.00833 sec. ....	176
Figure 6-69 9000 HP motor phase A current and electromagnetic torque versus speed in per unit transient response comparison during starting process and at the reconnection after a residual voltage transfer test, initiated at t=14.00833 sec. ....	176
Figure 6-70 6000 HP motor phase A current and electromagnetic torque versus speed in per unit transient response comparison during starting process and at the reconnection after a residual voltage transfer test, initiated at t=14.00833 sec. ....	177
Figure 6-71 3200 HP motor phase A current and electromagnetic torque versus speed in per unit transient response comparison during starting process and at the reconnection after a residual voltage transfer test, initiated at t=14.00833 sec. ....	177
Figure 6-72 1400 HP motor phase A current and electromagnetic torque versus speed in per unit transient response comparison during starting process and at the reconnection after a residual voltage transfer test, initiated at t=14.00833 sec. ....	178
Figure 6-73 1000 HP motor phase A current and electromagnetic torque versus speed in per unit transient response comparison during starting process and at the reconnection after a residual voltage transfer test, initiated at t=14.00833 sec. ....	178
Figure 6-74 470 HP motor phase A current and electromagnetic torque versus speed in per unit transient response comparison during starting process and at the reconnection after a residual voltage transfer test, initiated at t=14.004167 sec. ....	179

Figure 6-75 Phase A instantaneous voltage in kV, during a residual voltage transfer test, initiated at t=14.0125 sec.....	180
Figure 6-76 9000 HP motor phase A current and electromagnetic torque versus speed in per unit transient response comparison during starting process and at the reconnection after a residual voltage transfer test, initiated at t=14.0125 sec. ....	180
Figure 6-77 6000 HP motor phase A current and electromagnetic torque versus speed in per unit transient response comparison during starting process and at the reconnection after a residual voltage transfer test, initiated at t=14.0125 sec. ....	181
Figure 6-78 3200 HP motor phase A current and electromagnetic torque versus speed in per unit transient response comparison during starting process and at the reconnection after a residual voltage transfer test, initiated at t=14.0125 sec. ....	181
Figure 6-79 1400 HP motor phase A current and electromagnetic torque versus speed in per unit transient response comparison during starting process and at the reconnection after a residual voltage transfer test, initiated at t=14.0125 sec. ....	182
Figure 6-80 1000 HP motor phase A current and electromagnetic torque versus speed in per unit transient response comparison during starting process and at the reconnection after a residual voltage transfer test, initiated at t=14.0125 sec. ....	182
Figure 6-81 470 HP motor phase A current and electromagnetic torque versus speed in per unit transient response comparison during starting process and at the reconnection after a residual voltage transfer test, initiated at t=14.0125 sec. ....	183
Figure 6-82 Phase A instantaneous voltage in kV, during a residual voltage transfer test, initiated at t=14.02 sec.....	183
Figure 6-83 9000 HP motor phase A current and electromagnetic torque versus speed in per unit transient response comparison during starting process and at the reconnection after a residual voltage transfer test, initiated at t=14.02 sec. ....	184
Figure 6-84 9000 HP motor phase A current and electromagnetic torque transient response at the reconnection after a residual voltage transfer test, initiated at t=14.02 sec. ....	184



Figure 6-85 6000 HP motor phase A current and electromagnetic torque versus speed in per unit transient response comparison during starting process and at the reconnection after a residual voltage transfer test, initiated at t=14.02 sec.....	185
Figure 6-86 3200 HP motor phase A current and electromagnetic torque versus speed in per unit transient response comparison during starting process and at the reconnection after a residual voltage transfer test, initiated at t=14.02 sec.....	185
Figure 6-87 1400 HP motor phase A current and electromagnetic torque versus speed in per unit transient response comparison during starting process and at the reconnection after a residual voltage transfer test, initiated at t=14.02 sec.....	186
Figure 6-88 1000 HP motor phase A current and electromagnetic torque versus speed in per unit transient response comparison during starting process and at the reconnection after a residual voltage transfer test, initiated at t=14.0125 sec.....	186
Figure 6-89 470 HP motor phase A current and electromagnetic torque versus speed in per unit transient response comparison during starting process and at the reconnection after a residual voltage transfer test, initiated at t=14.02 sec.....	187
Figure 6-90 Motor bus transfer system controls for a manual transfer test, initiated at t=14.1312 sec.....	190
Figure 6-91 Phase A Instantaneous voltage in kV during a manual transfer test, initiated at t=14.1312 sec.....	191
Figure 6-92 Phase A RMS voltage in per unit during a manual transfer test, initiated at t=14.1312 sec.....	192
Figure 6-93 Voltage frequency in Hertz during a manual transfer test, initiated at t=14.1312 sec....	192
Figure 6-94 Phase A voltage phase angle in degrees during a manual transfer test, initiated at t=14.1312 sec.....	193
Figure 6-95 Motor bus transfer system element and circuit breaker contact operations during a manual transfer test, initiated at t=14.1312 sec.....	194
Figure 6-96 Motor bus transfer system controls for a manual transfer test, initiated at t=14.1042 sec.....	195

Figure 6-97 Phase A Instantaneous voltage in kV during a manual transfer test, initiated at t=14.1042 sec.....	196
Figure 6-98 Phase A RMS voltage in per unit during a manual transfer test, initiated at t=14.1042 sec. ....	196
Figure 6-99 Voltage frequency in Hertz during a manual transfer test, initiated at t=14.1042 sec....	197
Figure 6-100 Phase A voltage phase angle in degrees during a manual transfer test, initiated at t=14.1042 sec.....	197
Figure 6-101 Motor bus transfer system element and circuit breaker contact operations during a manual transfer test, initiated at t=14.1042 sec.....	199
Figure 6-102 Motor bus transfer system controls for the automatic transfer .....	200
Figure 6-103 Phase A Instantaneous voltage in kV during an automatic transfer initiated by the auxiliary transformer differential protective relay operation under a phase-to-ground C-G fault initiated at t=14.000 seconds .....	201
Figure 6-104 Phase A RMS voltage in per unit during an automatic transfer initiated by the auxiliary transformer differential protective relay operation under a phase-to-ground C-G fault initiated at t=14.000 seconds .....	202
Figure 6-105 Frequency in Hertz during an automatic transfer initiated by the auxiliary transformer differential protective relay operation under a phase-to-ground C-G fault initiated at t=14.000 seconds .....	202
Figure 6-106 Phase A Voltage phase angle in degrees during an automatic transfer initiated by the auxiliary transformer differential protective relay operation under a phase-to-ground C-G fault initiated at t=14.000 seconds.....	203
Figure 6-107 Motor bus transfer system element and circuit breaker contact operations during an automatic transfer initiated by the auxiliary transformer differential protective relay operation under a phase-to-ground C-G fault initiated at t=14.000 seconds.....	204
Figure 6-108 Motor bus transfer system controls for the automatic transfer .....	205

Figure 6-109 Phase A instantaneous voltage in kV during an automatic transfer initiated by the Eastern transmission line impedance protective relay operation under a phase-to-phase BC fault initiated at t=14.000 seconds .....	206
Figure 6-110 Phase A RMS voltage in per unit during an automatic transfer initiated by the Eastern transmission line impedance protective relay operation under a phase-to-phase BC fault initiated at t=14.000 seconds .....	207
Figure 6-111 Voltage frequency in Hertz during an automatic transfer initiated by the Eastern transmission line impedance protective relay operation under a phase-to-phase BC fault initiated at t=14.000 seconds .....	207
Figure 6-112 Phase A Voltage phase angle in degrees during an automatic transfer initiated by the Eastern transmission line impedance protective relay operation under a phase-to-phase BC fault initiated at t=14.000 seconds.....	208
Figure 6-113 Motor bus transfer system element and circuit breaker contact operations during an automatic transfer initiated by the Eastern transmission line impedance protective relay operation under a phase-to-phase BC fault initiated at t=14.000 seconds.....	209
Figure 6-114 Motor bus transfer system controls for the automatic transfer .....	210
Figure 6-115 Phase A instantaneous voltage in kV during an automatic transfer initiated by the Eastern transmission line impedance protective relay operation under a phase-to-phase BC fault initiated at t=14.000 seconds .....	211
Figure 6-116 Phase A RMS voltage in per unit during an automatic transfer initiated by the Eastern transmission line impedance protective relay operation under a phase-to-phase BC fault initiated at t=14.000 seconds .....	212
Figure 6-117 Voltage frequency in Hertz during an automatic transfer initiated by the Eastern transmission line impedance protective relay operation under a phase-to-phase BC fault initiated at t=14.000 seconds .....	212
Figure 6-118 Phase A Voltage phase angle in degrees during an automatic transfer initiated by the Eastern transmission line impedance protective relay operation under a phase-to-phase BC fault initiated at t=14.000 seconds.....	213

Figure 6-119 Motor bus transfer system element and circuit breaker contact operations during an automatic transfer initiated by the motor bus under voltage relay operation under low voltage conditions initiated at t=14.000 seconds..... 214

## LIST OF TABLES

Table 3-1 Induction motor parameters to compare the behavior of a medium and a high inertia induction motors on loss of power supply simulation. ....	34
Table 3-2 Summary of simulation results of induction motor current and torque when reconnecting to a new source under maximum voltage difference.....	52
Table 3-3 Summary of simulation results of induction motor current and torque when reconnecting to a new source under large frequency difference. ....	56
Table 4-1 Induction Motor Parameters.....	75
Table 4-2 PSCAD/EMTDC induction motor model validation comparing simulation results with given values.....	76
Table 6-1 Summary of the fast transfer component response.....	128
Table 6-2 Summary of the in-phase transfer component response .....	146
Table 6-3 Summary of maximum current and electromagnetic torque of the 6000 HP motor during several motor bus transfer conditions .....	188
Table 6-4 Summary of maximum current and electromagnetic torque of the 3200 HP motor during several motor bus transfer conditions .....	189
Table 6-5 Summary of response of the motor bus transfer system .....	215
Table A-1 PSCAD/EMTDC input parameters of the Western system equivalent source 1.....	223
Table A-2 PSCAD/EMTDC input parameters of the Western system equivalent source 2.....	224
Table A-3 PSCAD/EMTDC input parameters of the Western system transmission line from bus BusA to bus BusB – Part 1.....	225
Table A-4 PSCAD/EMTDC input parameters of the Western system transmission line from bus BusA to bus BusB – Part 2.....	226
Table A-5 PSCAD/EMTDC input parameters of the Western system transmission line from bus BusB to bus BusFlt_1 – Part 1.....	227
Table A-6 PSCAD/EMTDC input parameters of the Western system transmission line from bus BusB to bus BusFlt_1 – Part 2 .....	228

Table A-7 PSCAD/EMTDC input parameters of the Western system transmission line from bus BusFlt_1 to bus BusC – Part 1.....	229
Table A-8 PSCAD/EMTDC input parameters of the Western system transmission line from bus BusFlt_1 to bus BusC – Part 2.....	230
Table A-9 PSCAD/EMTDC input parameters of the Western system transmission line from bus BusBF to bus BusC – Part 1.....	231
Table A-10 PSCAD/EMTDC input parameters of the Western system transmission line from bus BusBF to bus BusC – Part 2.....	232
Table A-11 PSCAD/EMTDC input parameters of the Western system three phase fault control.....	233
Table A-12 PSCAD/EMTDC input parameters of the auxiliary transformer.....	234
Table A-13 PSCAD/EMTDC input parameters of the auxiliary transformer three phase fault control.....	235
Table A-14 PSCAD/EMTDC input parameters of the Eastern system equivalent source .....	236
Table A-15 PSCAD/EMTDC input parameters of the Eastern system transmission line from bus BusB to bus BusFlt_1 – Part 1 .....	237
Table A-16 PSCAD/EMTDC input parameters of the Eastern system transmission line from bus BusB to bus BusFlt_1 – Part 2 .....	238
Table A-17 PSCAD/EMTDC input parameters of the Eastern system transmission line from bus BusFlt_1 to bus BusC – Part 1.....	239
Table A-18 PSCAD/EMTDC input parameters of the Eastern system transmission line from bus BusFlt_1 to bus BusC – Part 2.....	240
Table A-19 PSCAD/EMTDC input parameters of the Eastern system three phase fault control .....	241
Table A-20 PSCAD/EMTDC input parameters of the main generator modeled by an equivalent source .....	242
Table A-21 PSCAD/EMTDC input parameters of the main station transformer .....	243
Table A-22 PSCAD/EMTDC input parameters of the 9000 HP induction motor .....	244
Table A-23 PSCAD/EMTDC input parameters of the 6000 HP induction motor .....	245
Table A-24 PSCAD/EMTDC input parameters of the 3200 HP induction motor .....	246

Table A-25 PSCAD/EMTDC input parameters of the 1400 HP induction motor .....	247
Table A-26 PSCAD/EMTDC input parameters of the 1000 HP induction motor .....	248
Table A-27 PSCAD/EMTDC input parameters of the 470 HP induction motor .....	249
Table A-28 PSCAD/EMTDC input parameters of the 9000 HP induction motor .....	250
Table A-29 PSCAD/EMTDC input parameters of the 6000 HP induction motor .....	251
Table A-30 PSCAD/EMTDC input parameters of the 4000 HP induction motor .....	252
Table A-31 PSCAD/EMTDC input parameters of the 3500 HP induction motor .....	253
Table A-32 PSCAD/EMTDC input parameters of the 2500 HP induction motor .....	254
Table A-33 PSCAD/EMTDC input parameters of the 2000 HP induction motor .....	255

## CHAPTER 1 - INTRODUCTION

### 1.1 Thesis Overview

In the course of a power generator start-up process, the power plant's auxiliary loads, many of which are induction motor or synchronous motors, are powered by what is called a start-up source. When the power generator has reached its rated or desired operating conditions, the auxiliary loads are transferred from the start-up source to the generator. When the generator needs to be shut down under normal or critical conditions, the auxiliary motor loads are transferred back to the start-up source. This process of transferring the auxiliary motor loads is known as motor bus transfer [1]. Without compromising the auxiliary motor loads or the integrity of other power system equipment such as the motor bus or auxiliary and/or start-up transformers, some requirements should be fulfilled to ensure perform of a successful and safe motor load transfer.

In most of cases, bus transfer systems' control settings are implemented based on field measurements and field testing only. Due to their inherent complexity, software simulations are not typically performed [1]. However, at present there are some electromagnetic transient programs with enough modeling capabilities to simulate the motor bus transfer processes including the electromagnetic and mechanical transients caused on motor loads to analytically support the transfer scheme control settings to be implemented in the field.

This thesis proposes and analyzes a motor bus transfer model using the electromagnetic transients program PSCAD/EMTDC [2], [3]. The motor bus transfer system model includes the following standard transfer methods: a) fast transfer, b) in-phase and c) residual voltage. The model also includes a circuit breaker control block to perform a manual motor bus transfer requested by the user, motor bus transfer initiated by time, and automatic transfer initiated directly by the operation of protective relays when the system is under emergency conditions. The simulation results include a number of plots describing the motor bus transfer system and the induction motors electromagnetic performances.

The implementation of the motor bus transfer system in PSCAD/EMTDC and the analysis of the induction motors are not only applicable to motor buses of generating power plants but also to industrial systems.



## 1.2 Literature Review

Following is a review on motor bus transfer literature. The review focuses on definitions, practices and considerations, algorithms used in implementing motor bus transfer schemes as well as the transient behavior of induction motors under motor bus transfer process. Brief comments and a summary of the most relevant papers are given in this section to provide a basic understanding about why motor bus transfer schemes have been implemented in the power industry as well as their advantages and disadvantages

Reference [4], *Simulation of Symmetrical Induction Machinery*, **P. C. Krause, C. H. Thomas**, IEEE Transactions on Power Apparatus and Systems, Vol. PAS-84, No. 11, pages 1038-1053, January 31<sup>st</sup>, 1965.

This is an excellent paper which describes the set of equations for symmetrical induction machines transformed to an arbitrary reference frame. The authors consider the equation development of 2-phase and 3-phase machines individually as well as the following modes of operation a) balanced conditions, b) unbalanced stator voltages, c) unequal rotor resistor, d) a combination of unbalanced stator voltages and unequal rotor resistor, and e) opening and closing of stator phases. Results of several simulations are presented and discussed.

Reference [5], *Universal Machine Modeling for the Representation of Rotating Electric Machinery in an Electromagnetic Transients Program*, **W. Scott Meyer, Hian K. Lauw**, Vol. PAS-101, No. 6, pages 1324-1351, July 26, 1981.

As a response to the increased interest to include several major types of rotating electrical machines in general transient simulation programs for digital computers, to allow the study of transients involving the interaction of electric machines with an electric power grid, as well as complex networks of mechanical components the authors present the implementation of the Universal Machine in the Electromagnetic Transients Program (EMTP).

The module can model: a) synchronous machines, b) induction machines, and c) direct-current machines. The general interface allows representation of the interaction of: a) mechanical system, b) universal machine, c) electrical power network, and d) control system. This model is implemented in the Alternative Transients Programs (ATP). The model is also implemented in the EMTDC according to [3].

Reference [6], *Analysis of Transient Electrical Torques and Shaft Torques in Induction Motors as a Result of Power Supply Disturbances*, **R. H. Daugherty**, IEEE Transactions on Power Apparatus and Systems, Vol. PAS-101, No. 8, pages 2826-2836, January 31<sup>st</sup>, 1982.

R. H. Daugherty presents an in-depth analysis of transient electrical torques and shaft torques in induction motors due to power supply disturbances. The author describes the set of differential equations that represent the induction motor and its mechanical load, which is solved at every time step.

The author talks in detail about the fundamentals of the electrical analysis of motor bus transfer during open circuit and re-connection from an alternate source considering the deceleration of the motor and the load rotating masses. The author also provides an example on how to compute: a) the motor residual voltage during the time the motor is disconnected from the power system and b) the phase angle between the motor residual voltage and the new power supply voltage.

The author discusses the results of a dynamic study performed simulating a 250 HP induction motor as well. The author shows the electrical and shaft torques, but no plots of motor stator currents, voltage, frequency decay and phase angle changes are presented.

Reference [7], *A Modern Automatic Bus Transfer Scheme*. **Tarlochan S. Sidhu, Vinayagam Balamourougan, Manish Thakur, and Bogdan Kasztenny**. International Journal of Control, Automation, and Systems. Vol. 3. No. 2, pages 376-385, June 2005.

Reference [8], *Robust Technique for fast and Safe Transfer of Power Plant Auxiliaries*. **Vinayagam Balamourougan, Tarlochan. S. Sidhu, Bogdam Kasztenny, and Manish. M. Thakur**. IEEE Transactions of Energy Conversion. Vol. 21. No. 2, pages 541-551, June 2006

In both papers the authors propose a high-speed bus transfer scheme using intelligent electronic devices, intra substation communication and two algorithms: a) one to estimate the residual voltage decay time constant, and b) and another with a recursive discrete Fourier transform based filter algorithm to estimate the voltage magnitude and frequency of the motor bus. The outputs of the two algorithms are used to automatically determine the type of suitable bus transfer method under emergency conditions. The proposed scheme is tested using the electromagnetic transients program PSCAD/EMTDC and Matlab. Four cases are described proving their methodology works as they expected, but there are no comments or plots regarding torques and currents.

It also mentions the settings for the fast, in-phase and residual voltage methods and some advantages and disadvantages of the residual voltage and in-phase methods. The authors point out that the simultaneous transfer is not possible when the main source is lost due to a short circuit or other abnormal conditions.

Reference [9], *Motor Bus Transfer: Considerations and Methods*. **Thomas R. Beckwith and Wayne G. Hartmann**. IEEE Transactions on Industry Applications. Vol. 42, No. 2, pp. 602-611, March 2006.

The authors discuss the classic motor bus transfer methods and the advanced in-phase transfer method and argue that the in-phase method, together with the fast transfer method offer an opportunity to synchronize a motor bus on the first available slip cycle when the residual voltage in the motors is still above 0.25 p.u.

The authors also argue about the effects that inertia, motor load size and the mix of synchronous and induction motors have on the coast down period and resultant voltage and frequency decay. The authors present a transfer sequence analysis and among other important considerations conclude that: a) the residual and long-time transfers may interrupt the plant process and b) the automatic synchronizing relays may lack the ability to account for the rapid deceleration of the motor bus.

Reference [10], *Design of a High-Speed Motor Bus Transfer System*. **Dr. Murty V. V. S. Yalla**: IEEE, 2009.

The author presents a detailed digital signal processing algorithm for the in-phase transfer method. While measuring the auxiliary source voltage magnitude and phase angle at rated frequency, it measures the magnitude and the phase angle of the decaying bus voltage and estimates the delta frequency change and the zero-phase prediction coincidence. Considering a second order differential equation used in the present research work, the zero-phase coincidence prediction uses the estimated delta frequency, the rate of change of delta frequency and the breaker closing time.

All related equations for each variable are provided. The complete system also includes fast and residual voltage methods, manual hot parallel transfer, sequential and simultaneous fast transfer methods among other key features.

Reference [11] , *Motor Bus Transfer, A Report Prepared by the Motor Bus Transfer Working Group of the Power System Relaying Committee*. **R. D. Pettigre, P. Powell**. IEEE Transactions on Power Delivery. Vol. 8, No. 4, pp. 1747-1758, October 1993.

This reference reports a survey performed on 89 received responses from several company types, regarding the present practices in the application of fast, parallel, residual voltage, slow and in-phase transfer schemes. The information presented includes: practices, design criteria, in-service experience and, advantages and disadvantages of every method.

Most of the parallel transfers are performed with sync-check close auto trip relays, and nearly 40% of the users select minimizing parallel time as a design criterion for their parallel transfer scheme.

The fast transfer is found to be the most popular method. Less than half of the fast transfer applications use a synch-check relay to supervise the transfer. Among the main reasons for selecting this method are: a) the speed of transfer minimized the interruption of power source to the motor bus, b) the method provides the minimum level of motor stress of all methods available and, c) simplest scheme to implement.

Reference [12], *Considerations and Methods for an Effective fast Bus Transfer System*. **Girish Hunswadkar, N.R. Viju**. Power System Protection and Automation, 2010.

The authors argue about the characteristics of the motor and the resultant voltage frequency ratio (Volts per Hertz) as the most important considerations for motor bus transfer. These methods and motor bus transfer are also described in detail. They provide useful comments about advantages and disadvantages of the hot parallel transfer, stressing that a fast motor bus transfer system must ensure the source parallel condition is temporal. The fast, in-phase, residual voltage, and fixed-time of the open transition transfer type are also covered in detail, including their advantages and disadvantages.

Reference [13], *Bus Transfer Systems: Requirements, Implementation, and Experiences*. **Amit Raje, Anil Raje, Jack McCall, and Arvind Chaudhary**. IEEE Transactions on Industry Applications. Vol. 30. No. 1, pages 34-44, January 2003.

This paper describes real-world bus transfer requirements such as: a) process requirements, which require that the bus transfer does not disturb the mechanical process, b) electrical requirements for avoiding excessive transient torques, high sustained transient currents and adverse effects and the protection system, and c) system requirements, which include the bus transfer system detection of

any breaker operation failure and functions which operate automatically on emergency conditions. In addition, the system should be simple to increase reliability.

This paper also shows the considerations and methods to effectively carry out a successful bus transfer, whether it is planned or is on emergency. According to the authors, the main three considerations are: a) the coasting down duration of a bus voltage on the open circuit conditions, b) the electrical and mechanical stress exerted on the motors and the connected loads during the source transfer, and c) the inclusion of high-speed motor bus transfer blocking during a short circuit conditions at the motor bus.

The authors consider that the worst condition to perform a transfer is under the first phase opposition between the new source and the decaying motor bus voltage. The authors also mention the advantages and disadvantages of each open transition motor bus transfer method.

Reference [14], In Phase Motor Bus Transfer. **Normann Fischer**. A Dissertation Presented in Partial Fulfillment of the Requirements for the Degree of Doctorate of Philosophy. College of Graduate Studies, University of Idaho, September 2014.

The author proposes a new in-phase transfer method in which it is not necessary advanced studies or field testing to set the transfer system. The author first analyzes the three-phase induction motor behavior. Next, the author presents the requirements of the motor bus transfer and explains the concepts for the new in-phase method. The author shows in detail the results of the induction motor behavior under several power system operating conditions modeled with the real time digital simulator RTDS.

The author mentions that “The IEEE C50.41 standard [15] state that if the p.u. volts per hertz ratio is less than 1.33 p.u. then the maximum transient torque developed by the motor would be less than 1.77 p.u.”, and he also shows that the volts per hertz p.u. on all simulation test runs performed are

less than 1.33 p.u. but the transient torques are considerably larger than 1.77 p.u. even in cases under perfect synchronism conditions.

### 1.3 Outline of Thesis

The thesis has two principal parts: background information about definitions and theory on motor bus transfer systems currently applied in the industry and the model implemented in PSCAD/EMTDC with the test results of its behavior during simulations.

First, the concepts and definitions provided by the IEEE including the common transfer topologies used in the industry are presented in Chapter 2. The set of equations that describe the induction motors and their behavior on loss of power supply and reconnection to a new source are analyzed and studied in Chapter 3. In that chapter, it is also explained that the oscillatory damped nature of the electromagnetic torques of induction motors during the reconnection is due to the interaction of the residual frequency in the rotor and the frequency of the new incoming power supply to which the bus is reconnected. It should be mentioned that in the literature reviewed there is no technical justification for this behavior.

Chapter 4, describes the power generation station system modeled in this research and its detailed implementation in the electromagnetic transient program PSCAD/EMTDC.

The motor bus transfer system model, including the standard motor bus transfer algorithms as well as the circuit breaker controls for manual and automatic motor bus transfer simulations, are described in detail in Chapter 5. The motor bus transfer system model and the circuit breaker control block are not in the PSCAD / EMTDC standard libraries or in other libraries of transient simulation programs such as the Alternative Transients Program ATP or the Electromagnetic Transients Program EMTP-RV. The implementation of these models has been described in detail in this chapter to be open source to users of any transient program.

The simulations and results of the performance of the motor bus transfer model are presented together with a discussion of the transient behavior of the induction motors during the simulations in Chapter 6.

Finally, the conclusion of the thesis is included in Chapter 7 together with future work that can be conducted regarding motor bus transfer modeling and simulation.

#### 1.4 Research Purpose

The purpose of this research was to model a motor bus transfer using three methods: Fast Transfer, In-Phase and Residual Voltage. Using any of these methods, power plant protection and control engineers may use the models used in this research to: a) study the performance of a motor bus transfer scheme, b) analyze the induction motor transient behavior during motor bus transfer processes, c) to suggest appropriate motor bus transfer system settings or d) improve their schemes. With respect to a particular power plant system, depending on the actual power plant characteristics and requirements, the motor bus transfer system model and controls were developed in such a way as to allow them to be easily varied.



## CHAPTER 2 - MOTOR BUS TRANSFER SYSTEMS

### 2.1 Introduction

This chapter focuses on the motor bus transfer terms, definitions, and fundamental theory. The report on motor bus transfer applications issues and considerations [1] defines terms used for motor bus transfer systems and applications and it also describes the most common motor bus transfer topologies, classification methods, and modes to perform manual or automatic transfers. It covers in detail the dynamic conditions during bus transfer as well. The terms for motor bus transfer defined by the IEEE are included here for reference.

### 2.2 Motor Bus Transfer Classification (IEEE)

The motor bus transfers may be classified as closed or open transition. In the closed transition also called hot parallel transfer, the new source breaker is closed before tripping the old source breaker. As it has been well documented in [1], [7], [9], and [10], during the closed transition there could occur some fault or emergency conditions that could result in direct equipment damage or unsuccessful proper power plant shutdown, causing major damage to the power plant equipment. Because of these reasons, the closed transition is rarely used.

An open transition transfer is designed to trip the old source breaker before closing the new source breaker. This condition forces the two source breakers to be open at the same time during the transfer time. Under such a condition, there is no opportunity to have both sources connected in parallel. For safety reasons the open transition is the most widely recommended one.

#### 2.2.1 Open Transition Transfer – Methods and Modes

There are three standard methods to supervise and open transition transfer namely: fast transfer, in-phase, and residual voltage. Some other references [7], [11], [12] consider a fourth method, the slow transfer in which the transfer is designed to wait for a determined fixed time, greater than 20 cycles, without any voltage relay supervising the transfer. The slow transfer is defined by the IEEE reference

[1], but it is not included in the Open Transition Transfer – Methods and Modes sections of the IEEE document.

#### *2.2.1.1 Methods*

##### 2.2.1.1.1 Fast Transfer

The fast transfer method is designed to trip the old source breaker before closing the new source breaker, whereby the closing is supervised to ensure that the voltage phase angle difference between the motor bus voltage and the new source voltage is within a predetermined acceptable limit. The method utilizes a high-speed sync-check relay that is accurate and fast enough to detect the change in relative phase angle between the disconnected motor bus and the new source [1].

##### 2.2.1.1.2 In-Phase

The in-phase method is designed to trip the old source breaker before closing the new source breaker, whereby the close command to the new breaker occurs at a phase angle in advance of phase coincidence between the motor bus and the new source, so that the new breaker closed just exactly when the voltages are in phase.

##### 2.2.1.1.3 Residual Voltage

The residual voltage method is designed to trip the old source breaker before closing the new source breaker, whereby the motor bus voltage magnitude must fall below a predetermined level before the close command is issued to the new breaker. According to reference [1] there is no supervision of conditions for synchronization between the motor bus and the new source.

##### 2.2.1.1.4 Slow Time Transfer

The slow time transfer method is designed to trip the old source breaker before closing the new source breaker, whereby a time interval, usually more than 20 cycles, occurs before the load is powered from another source. There is no supervision of the conditions for synchronization between the motor bus and the new source or of the voltage magnitude of the motor bus basically because the motor bus can

be considered as a dead bus. This method is outside of the scope of this work and no further comments are addressed.

#### *2.2.1.2 Modes*

##### *2.2.1.2.1 Sequential*

In the sequential mode, the old source breaker is tripped immediately, but closure of the new source breaker shall be attempted only upon confirmation by the breaker status contact that the old source breaker has opened. Upon receipt of this confirmation, the fast, in-phase or residual voltage methods of transfer must be employed to supervise closure of the new source breaker [1].

##### *2.2.1.2.2 Simultaneous*

In the simultaneous mode, the fast, in-phase or residual voltage methods of transfer must be employed to supervise closure of the new source breaker without waiting for the breaker status contact confirmation that the old source breaker has opened. Thus, with the fast transfer method, the commands for the old source breaker and the new source breaker to trip and close could be sent simultaneously if and only if the phase angle between the motor bus and the new source is within the phase angle limit immediately upon transfer initiation. Otherwise, the old source breaker will still be tripped, but closure of the new source breaker must wait for permitted conditions by the fast, in-phase or residual voltage transfer criteria [1].

This type of transfer method is not recommended and should be avoided in all cases when the old source is lost due to a short circuit or abnormal voltage conditions.

#### *2.2.2 Bus Transfer Initiation*

##### *2.2.2.1 Manual Transfer*

Manual bus transfer systems are designed to allow the power plant users to initialize the motor bus transfer by a manual command sent by the operator. The manual transfer is normally used to allow the motor bus transfer operation in either direction from the start-up to the auxiliary source side when

the plant is in the start-up process or from the auxiliary source side to the start-up side when the plant is in a planned shutdown process [1], [12], [13], [15].

#### *2.2.2.2 Automatic Transfer*

#### *2.2.2.3 Protective Transfer*

The automatic motor bus transfer may be initiated by a protective relay if the power plant is operating under emergency conditions [1], [12], [13], [15]. Some modern microprocessor-based motor bus transfer systems have built-in voltage and frequency relays to initiate the automatic transfer under abnormal operating conditions [15].

### 2.3 Common Bus Transfer Topologies

The power plant auxiliary system configuration may vary depending on the power plant operation practices. The most widely used configurations used in thermal power plants, and industrial process plants are briefly described in the following sections.

2.3.1 Type I Bus Configuration Used in Thermal Power Plants

Figure 2-1 shows the Type I bus configuration topology commonly used in thermal power plants in which a two-breaker scheme is employed to service a single motor bus from two alternate sources. It may be observed that under normal operating conditions, the auxiliary loads are supplied directly from the auxiliary transformer. On start-up, the loads are first fed from the start-up source and subsequently the loads are then transferred to the auxiliary system. When the plant has a planned shutdown or is under emergency conditions, all loads are transferred from the auxiliary transformer to the start-up source. The loads may include boiler feed pumps, forced draft fans, and cooling water pumps [7].

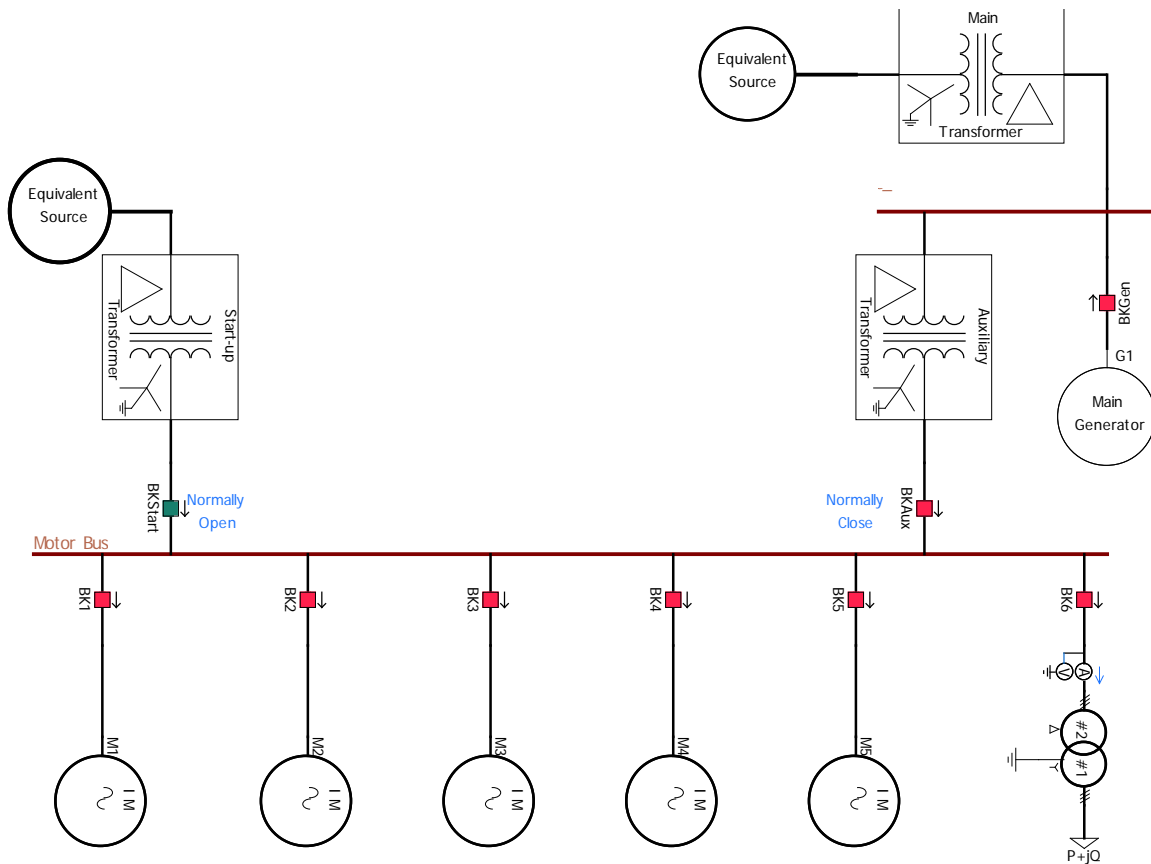


Figure 2-1 Type I bus configuration

### 2.3.2 Type II Bus Configuration Used in Industrial Plants

Figure 2-2 shows a typical bus configuration commonly used in process plants [7]. Each group of loads is fed from its normal power supply as shown and the tie breaker is normally operated in the open condition. Under emergency conditions of one source the tie breaker is used to transfer the loads from the compromised source bus to the other source bus and the breaker of the source under emergency conditions is opened.

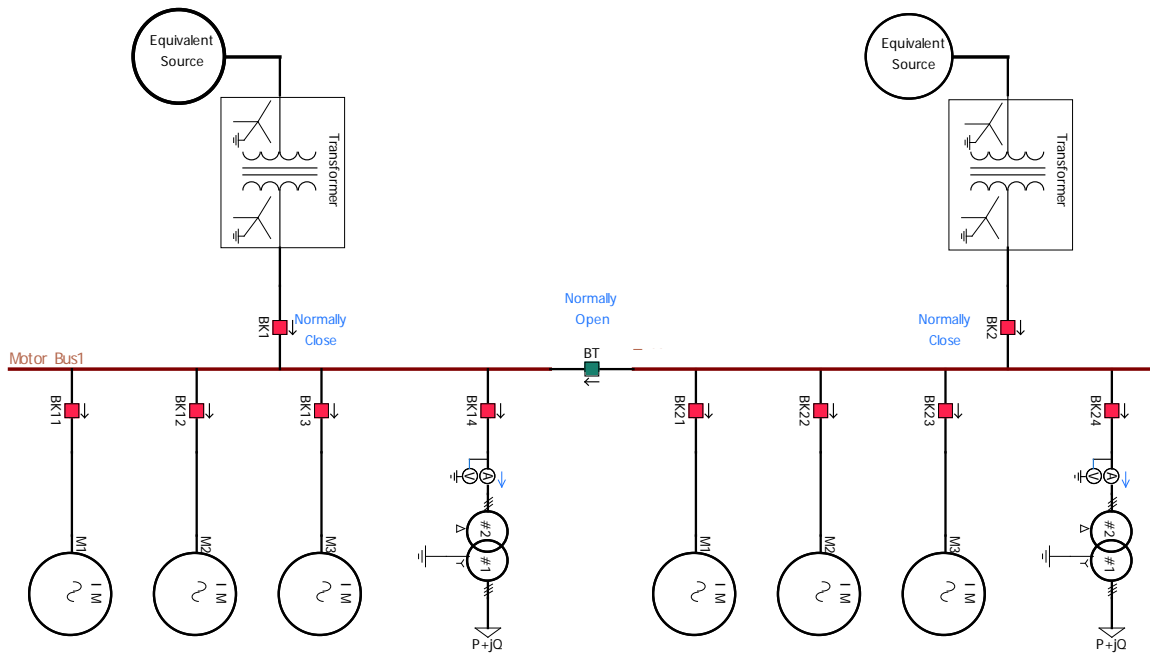


Figure 2-2 Type II bus configuration

### 2.3.3 Type III Bus Configuration Used in Nuclear Power Plants

Nuclear power plants use different topologies due to their safety related equipment requirements. Figure 2-3 shows a topology widely used in the United States and in the two nuclear power plants located in Mexico. In this topology, under normal operating conditions, the balance-of-plant loads and the class 1E (The IEEE Std. 308-2012 [16] defines class 1E as: “The safety classification of the electric equipment and systems that are essential to emergency reactor shutdown, containment isolation, reactor core cooling, and containment and reactor heat removal or that are otherwise essential in preventing significant release of radioactive material to the environment”) loads are fed from the main generator through the auxiliary transformer. During planned shutdown or under emergency conditions, both loads balance-of-plant and class 1E are transferred to the start-up source through the start-up transformer.

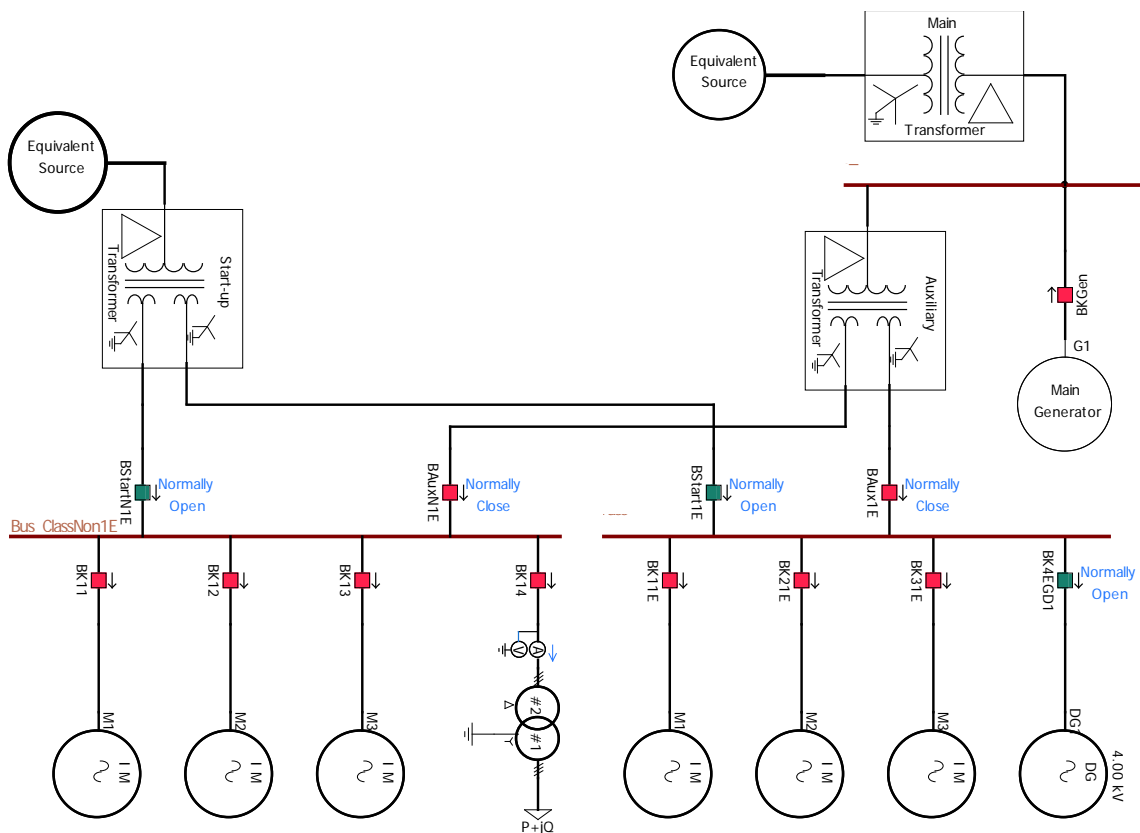


Figure 2-3 Type III bus configuration used in nuclear power plants

Some nuclear power plants use a bus configuration in which the class 1E loads are normally fed from a separate source [7].

## CHAPTER 3 - TRANSIENT ANALYSIS OF INDUCTION MOTORS

### 3.1 Introduction

During the motor bus transfer process, the motors are subjected to two transient states. The first state is the loss of the power supply when the old source breaker opens, and the second during reconnection when the new source breaker closes. To analyze the induction motors behavior in these two transient conditions, first in Section 3.23 it is presented the development of the set of equations of flux, voltage, current and electromagnetic torque in machines variables that describe the induction motors. The equations are also presented in the arbitrary reference frame using the Park's transformation. Finally, it is also shown the equations and mathematical analysis of the induction motor under open circuit conditions.

Section 3.3 presents four cases of simulations performed with PSCAD/EMTDC to analyze the transient behavior of various induction motors under different conditions. In the first case, the behavior of two individual motors is analyzed under loss of power supply conditions. In the second case, the behavior of a group of two motors is analyzed under loss of power supply conditions. In the third case, the transient response of a group of two induction motors is analyzed during the re-connection to the new power supply under conditions of maximum voltage difference between the voltage of the new power supply and the residual voltage of the motor bus. Then, in the fourth case, the re-connection of a group of motors is analyzed under conditions of a large frequency difference between the new source and the residual frequency of the motor bus. Finally, in cases five and six, two power generation station systems were modeled to analyze the transient response of the induction motors under different new source circuit breaker reclosing times.



## 3.2 Induction Motor Equations

### 3.2.1 Induction Motor Equations in Machine Variables

In this section it is presented the development of the set of equations of flux, voltage, current and electromagnetic torque in machines variables that describe the induction motors, which allow understanding the machine's functioning, so as to establish its analysis and transient behavior under different motor bus transfer conditions.

Figure 3-1 shows the schematic diagram of a two-pole, 3-phase, symmetrical induction machine taken from [17]. The stator windings are identical, displaced  $120^\circ$ . The rotor windings are also considered to be three identical windings, displaced  $120^\circ$ .

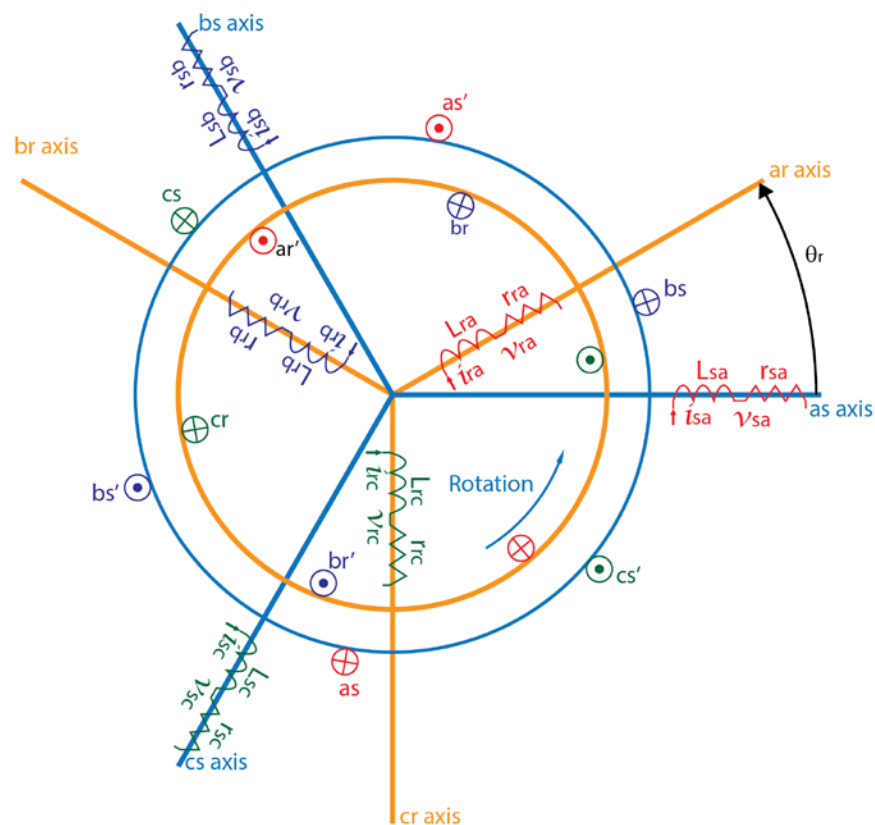


Figure 3-1 Two-pole, 3-phase, symmetrical induction machine

The stator windings are supplied by a three-phase system of balanced voltages with an angular frequency  $\omega_s$ . The response currents in the stator windings generate a rotating magnetic field of

constant magnitude in the air gap, which rotates at synchronous angular speed  $\omega_s$  (in the case where the stator has a number of  $P$  poles, the stator magnetic field is rotating at a synchronous speed  $\Omega_s = \omega_s/(P/2)$ ). This rotating field induces voltages in the rotor windings creating currents in the rotor windings, which in turn produce a second constant-amplitude magnetic field also rotating at a constant angular speed,  $\omega_r$ , lower than the synchronous angular speed. The interaction of these two magnetic fields creates a torque in the induction machine.

It should be noted that the magnetic field induced in the rotor rotates at the same angular velocity as the magnetic field of the stator. When operating as a motor, the rotor has a physical angular velocity slower than the stator magnetic field (and rotor magnetic field also). The interaction of these two magnetic fields does produce a torque, but this torque is the result of a phase angle difference between the two fields. When considered in the same reference frame, there is no difference in the angular velocity of those two fields in steady state operation. We can comment on the rotor frequency being somewhat smaller than the stator frequency and that is true, but the fields, when considered in the same reference frame, have the same frequency and differ by a phase angle that is related to torque produced.

Figure 3-2 shows the per-phase conventional equivalent circuit of the Steinmetz induction motor model with the mechanical load represented. The stator side, denoted by the  $s$  subscript, is shown on the left side, while the rotor side, denoted by the  $r$  subscript, is shown on the right. It is very important to observe that the stator current,  $I_s$ , has a synchronous frequency  $f_s$  whereas the rotor current has a frequency  $f_r$  which is related to the synchronous frequency by the slip  $s$ .

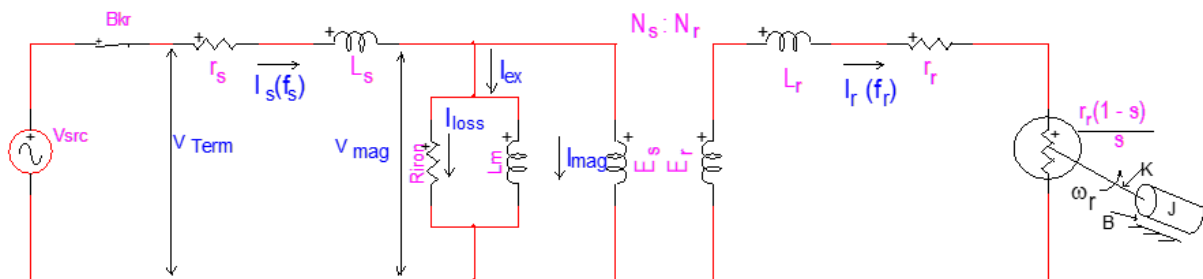


Figure 3-2 Per-phase equivalent circuit of the induction motor with the mechanical load represented

For the following mathematical analysis of the induction motor, it is supposed that: a) the air gap is uniform and the notching effects, generating space harmonics, are not included, b) the magnetic fields are not saturated, c) the skin effect is not considered, and d) the temperature in the motor is constant.

Per references [6], [18], and [19], the set of equations in machines variables describing a three-phase induction motor may be expressed as:

#### a) Flux equations

The self-phase inductances have two components, a leakage, and magnetizing inductances  $L_s = L_{ls} + L_{ms}$  for stator and  $L_r = L_{lr} + L_{mr}$  for rotor. For a magnetically linear system, the total flux linkage in each stator winding is given by the sum of its self-phase flux (linked by the inductance  $L_s$ ) with the other two stator-coupling fluxes (linked by mutual inductance  $M_s = L_{ms} \cos(\frac{2}{3}\pi) = -\frac{1}{2}L_{ms}$ ) and with three rotor-coupling fluxes ( $L_{sr}$  which is nonlinear function of rotor position  $\theta_r$  with respect to stator position).

$$\begin{bmatrix} \lambda_{as} \\ \lambda_{bs} \\ \lambda_{cs} \end{bmatrix} = \begin{bmatrix} L_{ls} + L_{ms} & -\frac{1}{2}L_{ms} & -\frac{1}{2}L_{ms} \\ -\frac{1}{2}L_{ms} & L_{ls} + L_{ms} & -\frac{1}{2}L_{ms} \\ -\frac{1}{2}L_{ms} & -\frac{1}{2}L_{ms} & L_{ls} + L_{ms} \end{bmatrix} \begin{bmatrix} i_{as} \\ i_{bs} \\ i_{cs} \end{bmatrix} + L_{sr} \begin{bmatrix} \cos(\theta_r) & \cos(\theta_r + \frac{2\pi}{3}) & \cos(\theta_r - \frac{2\pi}{3}) \\ \cos(\theta_r - \frac{2\pi}{3}) & \cos(\theta_r) & \cos(\theta_r + \frac{2\pi}{3}) \\ \cos(\theta_r + \frac{2\pi}{3}) & \cos(\theta_r - \frac{2\pi}{3}) & \cos(\theta_r) \end{bmatrix}^T \begin{bmatrix} i_{ar} \\ i_{br} \\ i_{cr} \end{bmatrix} \quad (3-1)$$

$$\begin{bmatrix} \lambda_{as} \\ \lambda_{bs} \\ \lambda_{cs} \end{bmatrix} = \begin{bmatrix} L_s & M_s & M_s \\ M_s & L_s & M_s \\ M_s & M_s & L_s \end{bmatrix} \begin{bmatrix} i_{as} \\ i_{bs} \\ i_{cs} \end{bmatrix} + L_{sr} \begin{bmatrix} \cos(\theta_r) & \cos(\theta_r + \frac{2\pi}{3}) & \cos(\theta_r - \frac{2\pi}{3}) \\ \cos(\theta_r - \frac{2\pi}{3}) & \cos(\theta_r) & \cos(\theta_r + \frac{2\pi}{3}) \\ \cos(\theta_r + \frac{2\pi}{3}) & \cos(\theta_r - \frac{2\pi}{3}) & \cos(\theta_r) \end{bmatrix} \begin{bmatrix} i_{ar} \\ i_{br} \\ i_{cr} \end{bmatrix} \quad (3-2)$$

The total flux linkage in each rotor winding is given by the sum of its self-phase flux (linked by the inductance  $L_r$ ) with the other two rotor coupling fluxes (linked by mutual inductance  $M_r = L_{mr} \cos(\frac{2}{3}\pi) = -\frac{1}{2}L_{mr}$ ) and with three stator-coupling fluxes ( $L_{sr}$ , which are a nonlinear function of rotor position  $\theta_r$  with respect to stator position).

$$\begin{bmatrix} \lambda_{ar} \\ \lambda_{br} \\ \lambda_{cr} \end{bmatrix} = \begin{bmatrix} L_{lr} + L_{mr} & -\frac{1}{2}L_{mr} & -\frac{1}{2}L_{mr} \\ -\frac{1}{2}L_{mr} & L_{lr} + L_{mr} & -\frac{1}{2}L_{mr} \\ -\frac{1}{2}L_{mr} & -\frac{1}{2}L_{mr} & L_{lr} + L_{mr} \end{bmatrix} \begin{bmatrix} i_{ar} \\ i_{br} \\ i_{cr} \end{bmatrix} + L_{sr} \begin{bmatrix} \cos(\theta_r) & \cos(\theta_r + \frac{2\pi}{3}) & \cos(\theta_r - \frac{2\pi}{3}) \\ \cos(\theta_r - \frac{2\pi}{3}) & \cos(\theta_r) & \cos(\theta_r + \frac{2\pi}{3}) \\ \cos(\theta_r + \frac{2\pi}{3}) & \cos(\theta_r - \frac{2\pi}{3}) & \cos(\theta_r) \end{bmatrix}^T \begin{bmatrix} i_{as} \\ i_{bs} \\ i_{cs} \end{bmatrix} \quad (3-3)$$

$$\begin{bmatrix} \lambda_{ar} \\ \lambda_{br} \\ \lambda_{cr} \end{bmatrix} = \begin{bmatrix} L_r & M_r & M_r \\ M_r & L_r & M_r \\ M_r & M_r & L_r \end{bmatrix} \begin{bmatrix} i_{ar} \\ i_{br} \\ i_{cr} \end{bmatrix} + L_{sr} \begin{bmatrix} \cos(\theta_r) & \cos(\theta_r + \frac{2\pi}{3}) & \cos(\theta_r - \frac{2\pi}{3}) \\ \cos(\theta_r - \frac{2\pi}{3}) & \cos(\theta_r) & \cos(\theta_r + \frac{2\pi}{3}) \\ \cos(\theta_r + \frac{2\pi}{3}) & \cos(\theta_r - \frac{2\pi}{3}) & \cos(\theta_r) \end{bmatrix}^T \begin{bmatrix} i_{as} \\ i_{bs} \\ i_{cs} \end{bmatrix} \quad (3-4)$$

For a 3-phase symmetrical machine with the stator and rotor connected as a three-wire system, the stator and rotor currents relationships may be written as:

$$i_{sa} + i_{sb} + i_{sc} = 0 \quad (3-5)$$

$$i_{ra} + i_{rb} + i_{rc} = 0 \quad (3-6)$$

By expressing the winding current  $i_c$  in terms of the other two winding currents, each phase flux is simplified as it is shown below:

$$\begin{aligned}
\begin{bmatrix} \lambda_{as} \\ \lambda_{bs} \\ \lambda_{cs} \end{bmatrix} &= \begin{bmatrix} L_s & M_s & M_s \\ M_s & L_s & M_s \\ M_s & M_s & L_s \end{bmatrix} \begin{bmatrix} i_{as} \\ i_{bs} \\ -i_{as} - i_{bs} \end{bmatrix} \\
&+ L_{sr} \begin{bmatrix} \cos(\theta_r) & \cos\left(\theta_r + \frac{2\pi}{3}\right) & \cos\left(\theta_r - \frac{2\pi}{3}\right) \\ \cos\left(\theta_r - \frac{2\pi}{3}\right) & \cos(\theta_r) & \cos\left(\theta_r + \frac{2\pi}{3}\right) \\ \cos\left(\theta_r + \frac{2\pi}{3}\right) & \cos\left(\theta_r - \frac{2\pi}{3}\right) & \cos(\theta_r) \end{bmatrix} \begin{bmatrix} i_{ar} \\ i_{br} \\ i_{cr} \end{bmatrix}
\end{aligned} \tag{3-7}$$

$$\begin{aligned}
\begin{bmatrix} \lambda_{as} \\ \lambda_{bs} \\ \lambda_{cs} \end{bmatrix} &= \begin{bmatrix} L_s i_{as} + M_s i_{bs} + M_s (-i_{as} - i_{bs}) \\ M_s i_{as} + L_s i_{bs} + M_s (-i_{as} - i_{bs}) \\ M_s i_{as} + M_s i_{bs} + L_s (-i_{as} - i_{bs}) \end{bmatrix} \\
&+ L_{sr} \begin{bmatrix} \cos(\theta_r) & \cos\left(\theta_r + \frac{2\pi}{3}\right) & \cos\left(\theta_r - \frac{2\pi}{3}\right) \\ \cos\left(\theta_r - \frac{2\pi}{3}\right) & \cos(\theta_r) & \cos\left(\theta_r + \frac{2\pi}{3}\right) \\ \cos\left(\theta_r + \frac{2\pi}{3}\right) & \cos\left(\theta_r - \frac{2\pi}{3}\right) & \cos(\theta_r) \end{bmatrix} \begin{bmatrix} i_{ar} \\ i_{br} \\ i_{cr} \end{bmatrix}
\end{aligned} \tag{3-8}$$

$$\begin{aligned}
\begin{bmatrix} \lambda_{as} \\ \lambda_{bs} \\ \lambda_{cs} \end{bmatrix} &= \begin{bmatrix} L_s - M_s & 0 & 0 \\ 0 & L_s - M_s & 0 \\ 0 & 0 & L_s - M_s \end{bmatrix} \begin{bmatrix} i_{as} \\ i_{bs} \\ i_{cs} \end{bmatrix} \\
&+ L_{sr} \begin{bmatrix} \cos(\theta_r) & \cos\left(\theta_r + \frac{2\pi}{3}\right) & \cos\left(\theta_r - \frac{2\pi}{3}\right) \\ \cos\left(\theta_r - \frac{2\pi}{3}\right) & \cos(\theta_r) & \cos\left(\theta_r + \frac{2\pi}{3}\right) \\ \cos\left(\theta_r + \frac{2\pi}{3}\right) & \cos\left(\theta_r - \frac{2\pi}{3}\right) & \cos(\theta_r) \end{bmatrix} \begin{bmatrix} i_{ar} \\ i_{br} \\ i_{cr} \end{bmatrix}
\end{aligned} \tag{3-9}$$

The rotor equations are obtained using a similar procedure:

$$\begin{aligned}
\begin{bmatrix} \lambda_{ar} \\ \lambda_{br} \\ \lambda_{cr} \end{bmatrix} &= \begin{bmatrix} L_r & M_r & M_r \\ M_r & L_r & M_r \\ M_r & M_r & L_r \end{bmatrix} \begin{bmatrix} i_{ar} \\ i_{br} \\ -i_{ar} - i_{br} \end{bmatrix} \\
&+ L_{sr} \begin{bmatrix} \cos(\theta_r) & \cos\left(\theta_r + \frac{2\pi}{3}\right) & \cos\left(\theta_r - \frac{2\pi}{3}\right) \\ \cos\left(\theta_r - \frac{2\pi}{3}\right) & \cos(\theta_r) & \cos\left(\theta_r + \frac{2\pi}{3}\right) \\ \cos\left(\theta_r + \frac{2\pi}{3}\right) & \cos\left(\theta_r - \frac{2\pi}{3}\right) & \cos(\theta_r) \end{bmatrix}^T \begin{bmatrix} i_{as} \\ i_{bs} \\ i_{cs} \end{bmatrix}
\end{aligned} \tag{3-10}$$

$$\begin{aligned}
\begin{bmatrix} \lambda_{ar} \\ \lambda_{br} \\ \lambda_{cr} \end{bmatrix} &= \begin{bmatrix} L_r i_{ar} + M_r i_{br} + M_r (-i_{ar} - i_{br}) \\ M_r i_{ar} + L_r i_{br} + M_r (-i_{ar} - i_{br}) \\ M_r i_{ar} + M_r i_{br} + L_r (-i_{ar} - i_{br}) \end{bmatrix} \\
&+ L_{sr} \begin{bmatrix} \cos(\theta_r) & \cos\left(\theta_r + \frac{2\pi}{3}\right) & \cos\left(\theta_r - \frac{2\pi}{3}\right) \\ \cos\left(\theta_r - \frac{2\pi}{3}\right) & \cos(\theta_r) & \cos\left(\theta_r + \frac{2\pi}{3}\right) \\ \cos\left(\theta_r + \frac{2\pi}{3}\right) & \cos\left(\theta_r - \frac{2\pi}{3}\right) & \cos(\theta_r) \end{bmatrix}^T \begin{bmatrix} i_{as} \\ i_{bs} \\ i_{cs} \end{bmatrix}
\end{aligned} \tag{3-11}$$

$$\begin{aligned}
\begin{bmatrix} \lambda_{ar} \\ \lambda_{br} \\ \lambda_{cr} \end{bmatrix} &= \begin{bmatrix} L_r - M_r & 0 & 0 \\ 0 & L_r - M_r & 0 \\ 0 & 0 & L_r - M_r \end{bmatrix} \begin{bmatrix} i_{ar} \\ i_{br} \\ i_{cr} \end{bmatrix} \\
&+ L_{sr} \begin{bmatrix} \cos(\theta_r) & \cos\left(\theta_r + \frac{2\pi}{3}\right) & \cos\left(\theta_r - \frac{2\pi}{3}\right) \\ \cos\left(\theta_r - \frac{2\pi}{3}\right) & \cos(\theta_r) & \cos\left(\theta_r + \frac{2\pi}{3}\right) \\ \cos\left(\theta_r + \frac{2\pi}{3}\right) & \cos\left(\theta_r - \frac{2\pi}{3}\right) & \cos(\theta_r) \end{bmatrix}^T \begin{bmatrix} i_{as} \\ i_{bs} \\ i_{cs} \end{bmatrix}
\end{aligned} \tag{3-12}$$

Defining:

$$\mathbf{L}_s = \begin{bmatrix} L_s - M_s & 0 & 0 \\ 0 & L_s - M_s & 0 \\ 0 & 0 & L_s - M_s \end{bmatrix} = \begin{bmatrix} L_{ls} + \frac{3}{2}L_{ms} & 0 & 0 \\ 0 & L_{ls} + \frac{3}{2}L_{ms} & 0 \\ 0 & 0 & L_{ls} + \frac{3}{2}L_{ms} \end{bmatrix} \tag{3-13}$$

$$\mathbf{L}_r = \begin{bmatrix} L_r - M_r & 0 & 0 \\ 0 & L_r - M_r & 0 \\ 0 & 0 & L_r - M_r \end{bmatrix} = \begin{bmatrix} L_{lr} + \frac{3}{2}L_{mr} & 0 & 0 \\ 0 & L_{lr} + \frac{3}{2}L_{mr} & 0 \\ 0 & 0 & L_{lr} + \frac{3}{2}L_{mr} \end{bmatrix} \tag{3-14}$$

$$\mathbf{L}_{sr} = L_{sr} \begin{bmatrix} \cos(\theta_r) & \cos\left(\theta_r + \frac{2\pi}{3}\right) & \cos\left(\theta_r - \frac{2\pi}{3}\right) \\ \cos\left(\theta_r - \frac{2\pi}{3}\right) & \cos(\theta_r) & \cos\left(\theta_r + \frac{2\pi}{3}\right) \\ \cos\left(\theta_r + \frac{2\pi}{3}\right) & \cos\left(\theta_r - \frac{2\pi}{3}\right) & \cos(\theta_r) \end{bmatrix} \quad (3-15)$$

The flux equation can be written as:

$$[\lambda_{abcs}] = [\mathbf{L}_s][i_{abcs}] + [\mathbf{L}_{sr}][i_{abcr}] \quad (3-16)$$

$$[\lambda_{abcr}] = [\mathbf{L}_r][i_{abcr}] + [\mathbf{L}_{sr}]^T[i_{abcs}] \quad (3-17)$$

$$\begin{bmatrix} \lambda_{abcs} \\ \lambda_{abcr} \end{bmatrix} = \begin{bmatrix} \mathbf{L}_s & \mathbf{L}_{sr} \\ \mathbf{L}_{sr}^T & \mathbf{L}_r \end{bmatrix} \begin{bmatrix} i_{abcs} \\ i_{abcr} \end{bmatrix} \quad (3-18)$$

Rotor variables can now be referred to the stator windings by appropriate turns ratios:  $i'_{abcr} = \left(\frac{N_r}{N_s}\right) i_{abcr}$ ,  $\lambda'_{abcr} = \left(\frac{N_s}{N_r}\right) \lambda_{abcr}$ ,  $L'_{ms} = \left(\frac{N_s}{N_r}\right) L_{sr}$ ,  $L'_{mr} = \left(\frac{N_r}{N_s}\right)^2 L_{ms}$ ,  $L'_r = \left(\frac{N_s}{N_r}\right)^2 L_r$ , and  $L'_{lr} = \left(\frac{N_s}{N_r}\right)^2 L_{lr}$ .

Equation (3-18) may now be expressed as:

$$\begin{bmatrix} \lambda_{abcs} \\ \lambda'_{abcr} \end{bmatrix} = \begin{bmatrix} \mathbf{L}_s & \mathbf{L}'_{sr} \\ \mathbf{L}'_{sr}^T & \mathbf{L}'_r \end{bmatrix} \begin{bmatrix} i_{abcs} \\ i'_{abcr} \end{bmatrix} \quad (3-19)$$

b) Voltage equations. The stator and rotor voltage equation may be written in matrix form as:

$$\begin{bmatrix} v_{as} \\ v_{bs} \\ v_{cs} \end{bmatrix} = \begin{bmatrix} r_s & 0 & 0 \\ 0 & r_s & 0 \\ 0 & 0 & r_s \end{bmatrix} \begin{bmatrix} i_{as} \\ i_{bs} \\ i_{cs} \end{bmatrix} + \frac{d}{dt} \begin{bmatrix} \lambda_{as} \\ \lambda_{bs} \\ \lambda_{cs} \end{bmatrix} \quad (3-20)$$

$$\begin{bmatrix} v_{ar} \\ v_{br} \\ v_{cr} \end{bmatrix} = \begin{bmatrix} r_r & 0 & 0 \\ 0 & r_r & 0 \\ 0 & 0 & r_r \end{bmatrix} \begin{bmatrix} i_{ar} \\ i_{br} \\ i_{cr} \end{bmatrix} + \frac{d}{dt} \begin{bmatrix} \lambda_{ar} \\ \lambda_{br} \\ \lambda_{cr} \end{bmatrix} \quad (3-21)$$

Or in a combined matrix form

$$\begin{bmatrix} v_{abcs} \\ v_{abcr} \end{bmatrix} = \begin{bmatrix} r_{abcs} & \mathbf{0}_{3 \times 3} \\ \mathbf{0}_{3 \times 3} & r_{abcr} \end{bmatrix} \begin{bmatrix} i_{abcs} \\ i_{abcr} \end{bmatrix} + \frac{d}{dt} \left( \begin{bmatrix} \mathbf{L}_s & \mathbf{L}_{sr} \\ (\mathbf{L}_{sr})^T & \mathbf{L}_r \end{bmatrix} \begin{bmatrix} i_{abcs} \\ i_{abcr} \end{bmatrix} \right) \quad (3-22)$$

The voltage equation in (3-22) may be expressed referred to the stator windings by appropriate turns

ratio  $v'_{abcr} = \left(\frac{N_s}{N_r}\right) v_{abcr}$  as:

$$\begin{bmatrix} v_{abcs} \\ v'_{abcr} \end{bmatrix} = \begin{bmatrix} r_{abcs} & \mathbf{0}_{3 \times 3} \\ \mathbf{0}_{3 \times 3} & r'_{abcr} \end{bmatrix} \begin{bmatrix} i_{abcs} \\ i'_{abcr} \end{bmatrix} + \frac{d}{dt} \left( \begin{bmatrix} \mathbf{L}_s & \mathbf{L}'_{sr} \\ (\mathbf{L}'_{sr})^T & \mathbf{L}'_r \end{bmatrix} \begin{bmatrix} i_{abcs} \\ i'_{abcr} \end{bmatrix} \right) \quad (3-23)$$

Rewriting the above equation:

$$\begin{aligned} \begin{bmatrix} v_{abcs} \\ v'_{abcr} \end{bmatrix} &= \begin{bmatrix} r_{abcs} & \mathbf{0}_{3 \times 3} \\ \mathbf{0}_{3 \times 3} & r'_{abcr} \end{bmatrix} \begin{bmatrix} i_{abcs} \\ i'_{abcr} \end{bmatrix} + \begin{bmatrix} \mathbf{L}_s & \mathbf{L}'_{sr} \\ (\mathbf{L}'_{sr})^T & \mathbf{L}'_r \end{bmatrix} \frac{\partial}{\partial t} \left( \begin{bmatrix} i_{abcs} \\ i'_{abcr} \end{bmatrix} \right) \\ &+ \frac{\partial}{\partial \theta_r} \left( \begin{bmatrix} \mathbf{L}_s & \mathbf{L}'_{sr} \\ (\mathbf{L}'_{sr})^T & \mathbf{L}'_r \end{bmatrix} \right) \begin{bmatrix} i_{abcs} \\ i'_{abcr} \end{bmatrix} \end{aligned} \quad (3-24)$$

c) Electromagnetic torque equation:

According to [19], the motor electromagnetic torque is given by:



$$\begin{aligned}
T_e &= \left(\frac{P}{2}\right) (i_{abc})^T \frac{\partial [L'_{sr}]}{\partial \theta_r} i'_{abcr} \\
&= -\left(\frac{P}{2}\right) L_{ms} \left\{ \left[ i_{as} \left( i'_{ar} - \frac{1}{2} i'_{br} - \frac{1}{2} i'_{cr} \right) + i_{bs} \left( i'_{br} - \frac{1}{2} i'_{ar} - \frac{1}{2} i'_{cr} \right) \right. \right. \\
&\quad \left. \left. + i_{cs} \left( i'_{cr} - \frac{1}{2} i'_{br} - \frac{1}{2} i'_{ar} \right) \right] \sin(\theta_r) \right. \\
&\quad \left. + \frac{\sqrt{3}}{2} [i_{as}(i'_{br} - i'_{cr}) + i_{bs}(i'_{cr} - i'_{ar}) + i_{cs}(i'_{ar} - i'_{br})] \cos(\theta_r) \right\}
\end{aligned} \tag{3-25}$$

Where P is the number of poles in the machine.

d) Mechanical load equation in terms of the motor electromagnetic torque:

The electromagnetic torque as a function of rotor position may be expressed as:

$$T_e = J \left(\frac{2}{P}\right) \frac{d^2}{dt^2} \theta_r(t) + \left(\frac{2}{P}\right) B_L \frac{d}{dt} \theta_r(t) + \left(\frac{2}{P}\right) K_L \theta_r(t) + T_L \tag{3-26}$$

Where J is the moment of inertia of the rotor and connected load, B is the coefficient of friction, K is the stiffness of the shaft, and the  $T_L$  is positive for a loading torque on the shaft of the induction motor.

### 3.2.2 Induction Motor Equations in Arbitrary Reference-Frame Variables

The voltage and electromagnetic torque equations (3-24) and (3-25) respectively described in Section 3.2.1 have time-dependent stator-rotor mutual inductances which make the analysis very complex. To solve this problem, the time-dependent mutual inductances can be removed by transforming the variables with respect to an arbitrary rotating reference frame called “qd0” using the Park’s transformation. This change of variables consists in referencing the three phase system variables, either rotor and start, to one coordinates system composed of two axes in quadrature and another axis, known as the zero-sequence axis. The variables of the new system are distinguished by the indices d, q and 0 representing the direct, quadrature axes and zero-sequence respectively.

The relationship between the variables of both coordinate systems is given by reference [19] as follows:

$$\mathbf{f}'_{qd0r} = \mathbf{K}_r \mathbf{f}'_{abcr} \quad (3-27)$$

Where:

$$(\mathbf{f}'_{qd0r})^T = [f'_{qr} \quad f'_{dr} \quad f'_{or}] \quad (3-28)$$

$$(\mathbf{f}'_{abcr})^T = [f'_{ar} \quad f'_{br} \quad f'_{cr}] \quad (3-29)$$

$$\mathbf{K}_r = \frac{2}{3} \begin{bmatrix} \cos \beta & \cos\left(\beta - \frac{2\pi}{3}\right) & \cos\left(\beta + \frac{2\pi}{3}\right) \\ \sin \beta & \sin\left(\beta - \frac{2\pi}{3}\right) & \sin\left(\beta + \frac{2\pi}{3}\right) \\ \frac{1}{2} & \frac{1}{2} & \frac{1}{2} \end{bmatrix} \quad (3-30)$$

$$\beta = \theta - \theta_r \quad (3-31)$$

The inverse transform is given by:

$$\mathbf{f}'_{qd0r} = \mathbf{K}_r^{-1} \mathbf{f}'_{abcr} \quad (3-32)$$

$$\mathbf{K}_r^{-1} = \frac{2}{3} \begin{bmatrix} \cos \beta & \sin \beta & 1 \\ \cos\left(\beta - \frac{2\pi}{3}\right) & \sin\left(\beta - \frac{2\pi}{3}\right) & 1 \\ \cos\left(\beta + \frac{2\pi}{3}\right) & \sin\left(\beta + \frac{2\pi}{3}\right) & 1 \end{bmatrix} \quad (3-33)$$

According to reference [4], the set of equations in the “qd0” reference frame that describe the induction motor is:

a) Flux equations:

$$\begin{bmatrix} \lambda_{qs} \\ \lambda_{ds} \\ \lambda_{os} \\ \lambda'_{qr} \\ \lambda'_{dr} \\ \lambda'_{or} \end{bmatrix} = \begin{bmatrix} L_{ls} + L_M & 0 & 0 & L_M & 0 & 0 \\ 0 & L_{ls} + L_M & 0 & 0 & L_M & 0 \\ 0 & 0 & L_{ls} & 0 & 0 & 0 \\ L_M & 0 & 0 & L'_{lr} + L_M & 0 & 0 \\ 0 & L_M & 0 & 0 & L'_{lr} + L_M & 0 \\ 0 & 0 & 0 & 0 & 0 & L'_{lr} \end{bmatrix} \begin{bmatrix} i_{qs} \\ i_{ds} \\ i_{os} \\ i'_{qr} \\ i'_{dr} \\ i'_{or} \end{bmatrix} \quad (3-34)$$

where

$$L_M = \frac{3}{2} L_{ms} \quad (3-35)$$

b) Voltage equations:

$$\begin{bmatrix} v_{qs} \\ v_{ds} \\ v_{os} \\ v'_{qr} \\ v'_{dr} \\ v'_{or} \end{bmatrix} = \begin{bmatrix} R_s & 0 & 0 & 0 & 0 & 0 \\ 0 & R_s & 0 & 0 & 0 & 0 \\ 0 & 0 & R_s & 0 & 0 & 0 \\ 0 & 0 & 0 & R'_r & 0 & 0 \\ 0 & 0 & 0 & 0 & R'_r & 0 \\ 0 & 0 & 0 & 0 & 0 & R'_r \end{bmatrix} \begin{bmatrix} i_{qs} \\ i_{ds} \\ i_{os} \\ i'_{qr} \\ i'_{dr} \\ i'_{or} \end{bmatrix} + \begin{bmatrix} \frac{d}{dt} & \omega & 0 & 0 & 0 & 0 \\ -\omega & \frac{d}{dt} & 0 & 0 & 0 & 0 \\ 0 & 0 & 0 & 0 & 0 & 0 \\ 0 & 0 & 0 & \frac{d}{dt} & (\omega - \omega_r) & 0 \\ 0 & 0 & 0 & -(\omega - \omega_r) & \frac{d}{dt} & 0 \\ 0 & 0 & 0 & 0 & 0 & \frac{d}{dt} \end{bmatrix} \begin{bmatrix} \lambda_{qs} \\ \lambda_{ds} \\ \lambda_{os} \\ \lambda'_{qr} \\ \lambda'_{dr} \\ \lambda'_{or} \end{bmatrix} \quad (3-36)$$

c) Electromagnetic torque equation:

$$T_e = \left(\frac{3}{2}\right) \left(\frac{P}{2}\right) (L_M) (i_{qs} i'_{dr} - i_{ds} i'_{qr}) \quad (3-37)$$

For the most common way that the problem is posed, an iterative method is indeed the solution method of choice. Depending on what variables are considered given and what variables are to be

solved for, solution methods vary. In some problem formulations, a closed form solution is possible. This formulation is not among such cases.

In 1981, Hian K. Lauw and W. Scott Meyer published a paper describing the theory and development of a new universal machine module for the BPA Electromagnetic Transients Program (EMTP) [5]. This model was later implemented in the PSCAD/EMTDC simulator, which will be used in this research.

### 3.2.3 Single Induction Motor on Loss of Power Supply

When a single motor is disconnected from its power supply source, the motor stator current  $I_s$  goes to zero. As the flux in the machine cannot change suddenly, the change in the stator currents must be accompanied by a change in the rotor currents to maintain constant flux linkages [20]. This flux will decay due to the combination of loss of power supply, energy dissipated in the rotor resistance, friction, and energy delivered to the load, and will induce a decaying voltage in the rotor windings that will produce currents in the rotor.

However, in an auxiliary motor bus isolated by breaker action there are multiple motors that interact. The larger inertia machines in general act as induction generator supplying current to the smaller inertia machines.

Figure 3-3 shows the per-phase Steinmetz equivalent circuit of an induction motor with the rotor parameters referred to the stator side.

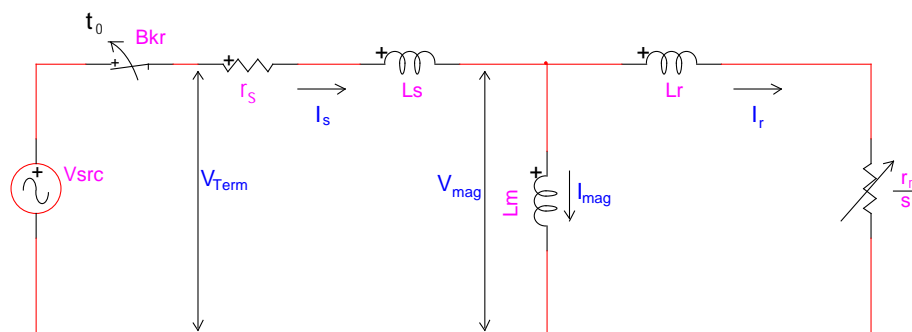


Figure 3-3 Per-phase Steinmetz equivalent circuit for an induction motor with rotor parameters referred to the stator side.

The differential equation of the circuit shown in Figure 3-3 that describes the behavior of an induction motor during open circuit conditions ( $I_s = 0$ ) is only determined by the rotor circuit and the magnetizing branch and could be written as follows:

$$\frac{r_r}{s} i_{\text{mag}} + (L_m + L_r) \frac{di_{\text{mag}}}{dt} = 0 \quad (3-38)$$

The solution for this differential equation is:

$$i_{\text{mag}}(t) = I_{\text{mag}_0} e^{-\left(\frac{r_r}{L_m + L_r} t\right)} = I_{\text{mag}_0} e^{-\left(\frac{t}{\frac{L_m + L_r}{r_r}}\right)} \quad (3-39)$$

Where  $I_{\text{mag}_0}$  is the magnetizing current of the motor at the moment of disconnection.

The induction motor time constant for open circuit conditions is defined as:

$$\tau_0 = \frac{L_m + L_r}{\frac{r_r}{s}} \quad (3-40)$$

The  $I_{\text{mag}_0}$  magnitude can be determined from the induction motor steady state operating point just before the open circuit conditions using the following steps.

a) Compute the equivalent impedance of the rotor circuit and the magnetization branch:

$$Z_{\text{mr}} = \frac{\left(\frac{r_r}{s} + j\omega L_r\right) j\omega L_m}{\left(\frac{r_r}{s} + j\omega(L_r + L_m)\right)} \quad (3-41)$$

b) Compute the total motor impedance seen from its terminal, adding the stator impedance to the equivalent impedance computed in step a):

$$Z_{eqtotal} = r_s + j\omega L_s + Z_{mr} \quad (3-42)$$

c) Compute the induction motor steady state current drawn from the power source using the source voltage and the equivalent motor impedance computed in step b):

$$I_{s\_ss} = \frac{V_{src}}{Z_{eqtotal}} \quad (3-43)$$

d) Subtract the voltage drop of the stator impedance from the power supply voltage and calculate the magnetizing current:

$$I_{mag\_ss} = I_{mag_0} = \frac{V_{src} - I_{s\_ss}(r_s + j\omega L_s)}{j\omega L_m} \quad (3-44)$$

As it has been previously mentioned, the magnetizing current after disconnection is a decaying current with DC offset which is flowing in the rotor windings. The motor rotor and its connected load are still rotating after the power supply disconnection due to the inertia. However, the motor rotor angular speed starts decaying due to the friction and the lack of supporting electromagnetic torque from the power supply. Therefore, this magnetizing decaying current with DC offset flowing in the rotor windings induces a voltage in the induction motor magnetizing branch with a frequency related to the decaying angular speed of the rotor and its load. The load mechanical angular speed and deceleration can be computed using equation (3-26) described in Section 3.2.

The equation for the residual induced voltage may be written as follows:

$$v_m = (j\omega L_m * I_{mag_0}) e^{-\left(\frac{t}{\frac{L_m + L_r}{R_r}}\right)} \{sin(\omega_r t)\} = E_{mag_0} e^{-\left(\frac{t}{\tau_0}\right)} \{sin(\omega_r t)\} \quad (3-45)$$

### 3.3 Analysis of Induction Motors Behavior on Motor Bus Transfer

As mentioned in the introduction to this chapter, during the motor bus transfer process, the motors are exposed to two transient states. The disconnection from the power supply and the connection to the new power supply. To analyze the behavior of the induction motors during various motor bus transfer conditions, six cases were prepared in PSCAD/EMTDC and multiple simulations were carried out.

The first case presents the analysis of individual induction motors before the loss of the power supply. The second case analyzes the behavior of a group of two motors during the loss of power supply. In the third case, the behavior of a group of induction motors is analyzed when the motors are reconnected to the new power supply under conditions of maximum voltage difference. The fourth case presents the behavior of the induction motors when the motors are reconnected to the new power supply under conditions of a large frequency difference. The fifth and sixth cases present the modeling of two power generation station systems and both systems are analyzed under different new source breaker closing times.

#### 3.3.1 Analysis of a Single Induction Motor During Loss of Power Supply

When a single motor is disconnected from its power supply source, the decaying flux in the machine will induce a decaying voltage in the rotor windings with a frequency related to the decaying angular speed of the rotor and its load. The residual voltage and frequency of the high inertia motors will decay more slowly than those with medium or low inertia [1].

The system shown in Figure 3-4 was modeled in PSCAD/EMTDC to analyze and compare the behavior of medium and a high inertia induction motors on loss of power supply through simulation. The motors were fed at their rated voltage of 4.0 kV by the power supply on the left connected to the motor bus through breaker BWStart. Breaker BWAux remained opened during the simulation. Both motor breakers BKM1\_W and BKM2\_W were then opened at  $t=12.00$  seconds. Therefore, the motors were not exchanging current between them during the coast down simulation.

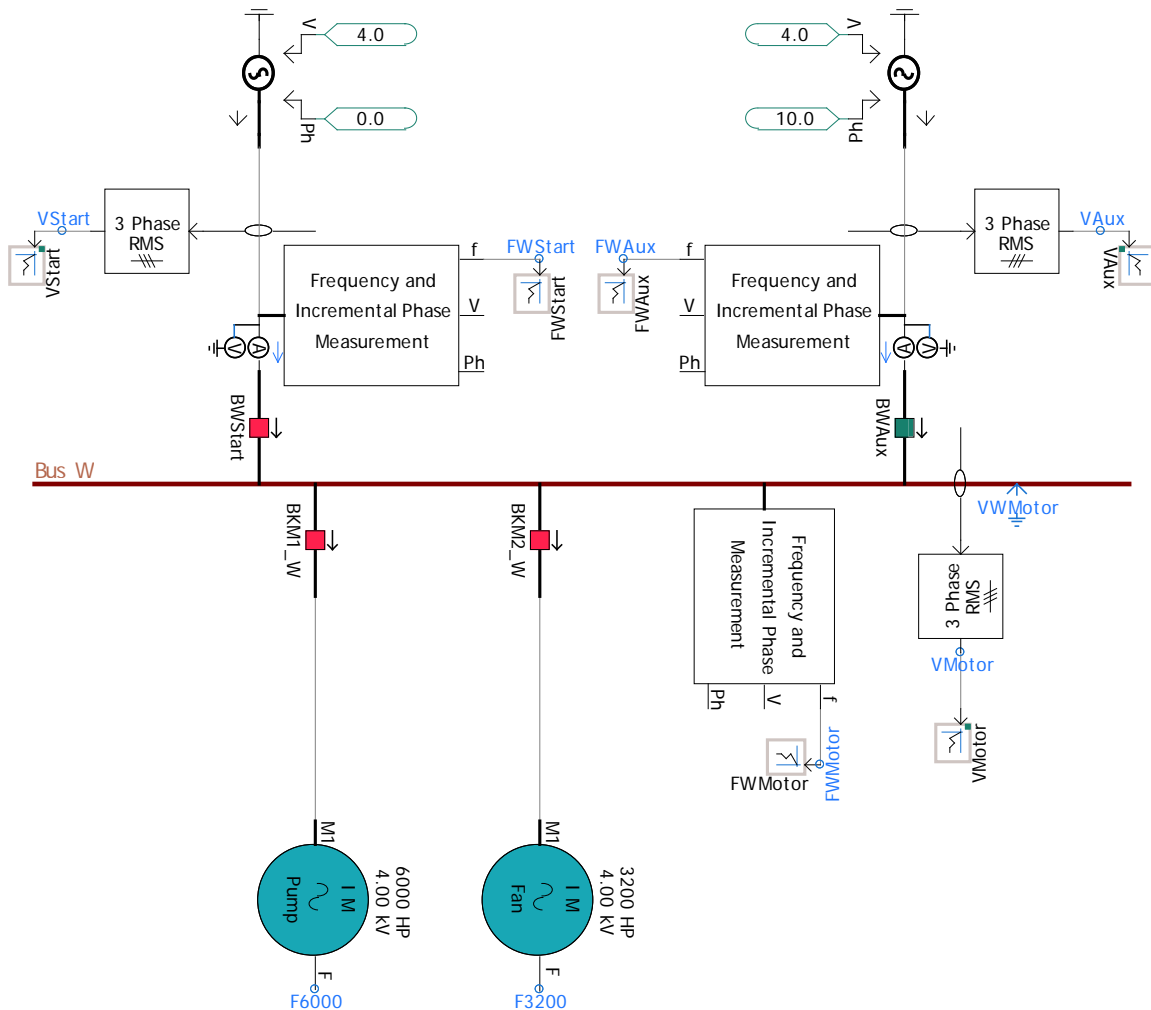


Figure 3-4 System to analyze and compare the behavior of a medium and a high inertia induction motors on loss of power supply simulation.

Signals VStart, Vaux, and VMotor are the RMS voltages measured at the start, auxiliary and motor buses respectively. These measurements are performed using the 3-Phase RMS PSCAD/EMTDC standard component. According to [3] if these meters are set to digital RMS measurements, then the meters take samples based on the specified frequency to compute the RMS value. In this case, if the fundamental frequency shifts, then it could introduce errors. These errors could be minimized by using a larger number of samples per cycle. If the meter is set to analog metering options, then it is frequency independent. For a single-phase system instantaneous signal is squared and integrated with a real pole ( $G/(1+sT)$ ) with the specified time constant to compute the RMS value. Three phase analog metering is carried out by measuring instantaneous peak to peak value of all the 3 phase quantities (i.e.  $\text{Maximum}(V_a, V_b, V_c) - \text{Minimum}(V_a, V_b, V_c)$ ). The average value of this is obtained with a smoothing filter. The average value is linearly proportional to the line-line RMS value in a balanced system. The



meters were set to digital RMS measurements with the number of samples per cycle set to 256 to reduce possible errors introduced by frequency shifts.

The current and voltage meters connected directly to the BWStart and BWAux breakers are used to measure the instantaneous three phase voltage and currents at the auxiliary and startup sides. The signal VWMotor is used to measure the instantaneous three phase voltage at the motor bus.

Signals FWStart, FWAux and FWMotor are the frequencies measured using the PSCAD/EMTDC “Frequency and Incremental Phase Measurements” standard component at the start, auxiliary and motor buses respectively. These signals together with the voltage measurements are used as inputs for the motor bus transfer system modeled in PSCAD/EMTDC.

The induction motor parameters are shown in Table 3-1. The table also shows the motor’s magnetizing branch voltages, rotor’s frequencies during their operating conditions prior to the loss of power supply and the magnetizing branch voltage and rotor frequency computed with PSCAD/EMTDC.

	6000 HP	3200 HP
	Pump	Fan
Rated Voltage kV L-L	4	4
Rated Power HP	6000	3200
Rated Current Amps	873.63	423.97
Efficiency	0.85	0.90
Power Factor	0.87	0.903
Synch Speed	1800	1200
Rated Speed	1785	1190
Rated Slip	0.0084	0.0084
Inertia of Motor (s)	0.554	0.41
Inertia of Load (s)	2.921	4.49
$E_{mag0}$ p.u. computed with PSCAD/EMTDC	0.875	0.901
$f_{rot0}$ Hz computed with PSCAD/EMTDC	58.78	58.98

*Table 3-1 Induction motor parameters to compare the behavior of a medium and a high inertia induction motors on loss of power supply simulation.*

Figure 3-5 to Figure 3-8 compare the behavior of the system shown in Figure 3-4 during a coast down simulation in PSCAD/EMTDC. The medium inertia induction motor pump results are plotted in blue and the high inertia induction motor fan results are plotted in red.

It can clearly be seen that the voltage magnitude, frequency, phase angle and the mechanical torque of the high inertia induction motor decay slower than the medium inertia motor.

Figure 3-5 shows the terminal voltage magnitude behavior for both motors. Before the loss of power supply, the terminal voltage magnitude was 1.0 p.u. and right after the loss of power supply, the high inertia motor terminal voltage changes its magnitude to  $E_{mag_0} = 0.901 \text{ p.u.}$  which was the magnetizing branch voltage before the motor disconnection. The medium inertia motor terminal voltage changes from 1.0 p.u. to  $E_{mag_0} = 0.875 \text{ p.u.}$ . From those values, both motor terminal voltages continued decaying at a rate of change dictated by the motor electrical parameters and the motor's connected load. The fundamental frequency RMS meter took approximately one cycle to track the sinusoidal voltage after the loss of power supply.

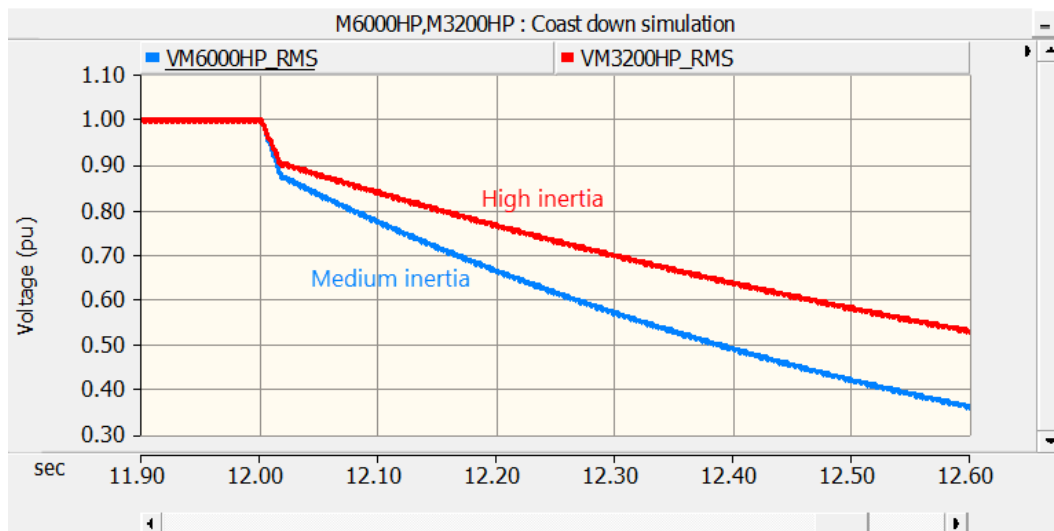


Figure 3-5 Motor terminal voltage magnitude change during a coast down simulation of a medium inertia 6000 HP induction motor pump and a high inertia 3200 HP induction motor fan.

Figure 3-6 below shows the frequency of motor terminal voltage behavior of both motors during the loss of power supply. The motors terminal voltage frequency before the loss of power supply was 60 Hz and just after the motor circuit breaker opening, both motors terminal frequency changed from 60 Hz

Hz to their respective rotor operating frequency prior to the motor circuit breaker operation. For the high inertia motor, the frequency changed from 60 Hz to 58.98 Hz whereas for the medium inertia motor, the frequency changed from 60 Hz to 58.78 Hz. It may be observed the transient response of the frequency meter after the loss of power supply. Reference [21] indicates that “In power system applications, discrete Fourier transform (DFT) is widely used, due to its simple structure and effective performance, to obtain the signal magnitudes and phase angles [5]. The standard DFT, however, fails to cope with frequency variations. If the DFT sampling rate is not synchronized with the system frequency, e.g., due to the frequency change during a bus transfer, the errors are produced in phasor measurements.”. The authors proposed a new implementation modifying the discrete Fourier Transform in order to avoid the errors presented by the DFT. The errors introduced by the standard meter of the PSCAD/EMTDC do not affect the performance of the transfer system implemented in the present research.

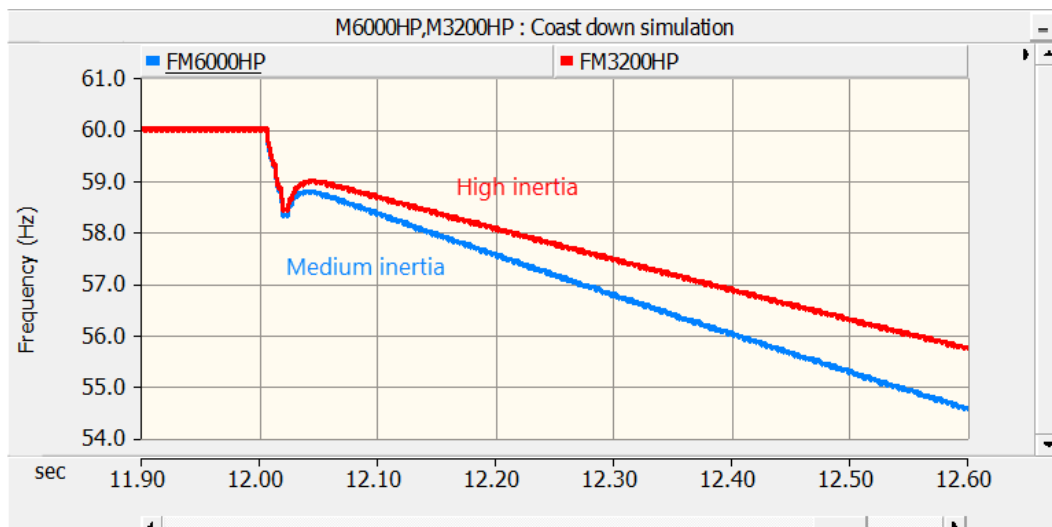


Figure 3-6 Frequency of motor terminal voltage change during a coast down simulation of a medium inertia 6000 HP induction motor pump and a high inertia 3200 induction motor fan.

Figure 3-7 shows phase angle of the motor terminal voltage behavior of both motors during the loss of power supply. As the motor terminal voltage frequency changes following the loss of power supply, the motor terminal voltage phasor changes its phase angle in relation to the reference voltage which has a fixed frequency of 60 Hz. Therefore, the motor terminal voltage phase angle starts to move apart from the reference at 60 Hz. Again, the motor terminal phase angle of the high inertia motor changes more slowly than the medium inertia motor.

The instant after opening the source breaker, the motor terminal voltage exhibits an essentially instantaneous phase angle shift that corresponds to phase angle of the magnetizing branch voltage that is governing during the open source condition. This effect is followed by impact of subsequent frequency decay on the angles which accelerates their rate of change.

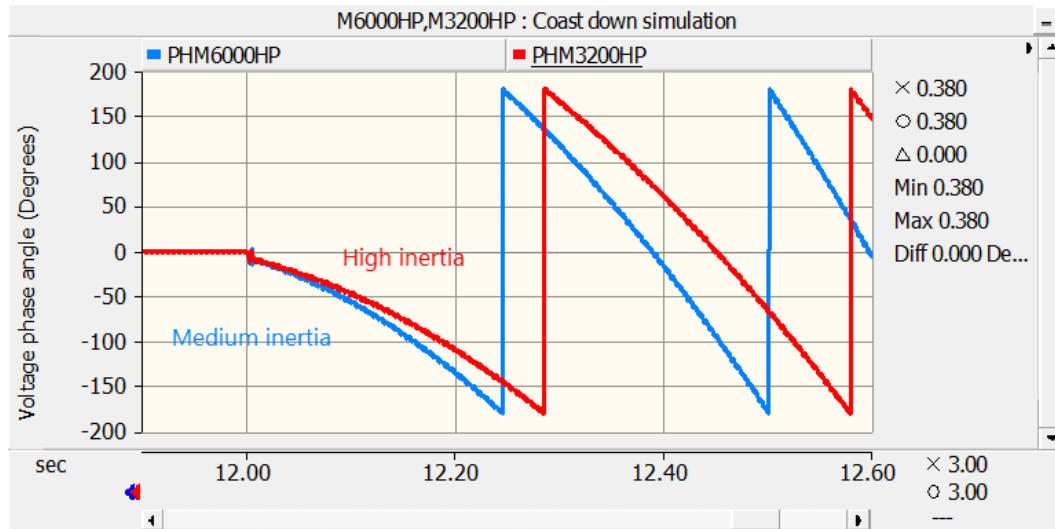


Figure 3-7 Motor terminal voltage phase angle change during a coast down simulation of a medium inertia 6000 HP induction motor pump and a high inertia 3200 induction motor fan.

Figure 3-8 shows the PSCAD/EMTDC computed electromagnetic and load torques for both motors during the coast down simulation. The electromagnetic torque of both motors goes to zero immediately when the power supply is lost due to the lack of power supply and hence the loss of stator current to sustain the electromagnetic field induced in the rotor. The mechanical load and the motor parameters govern the decaying behavior.

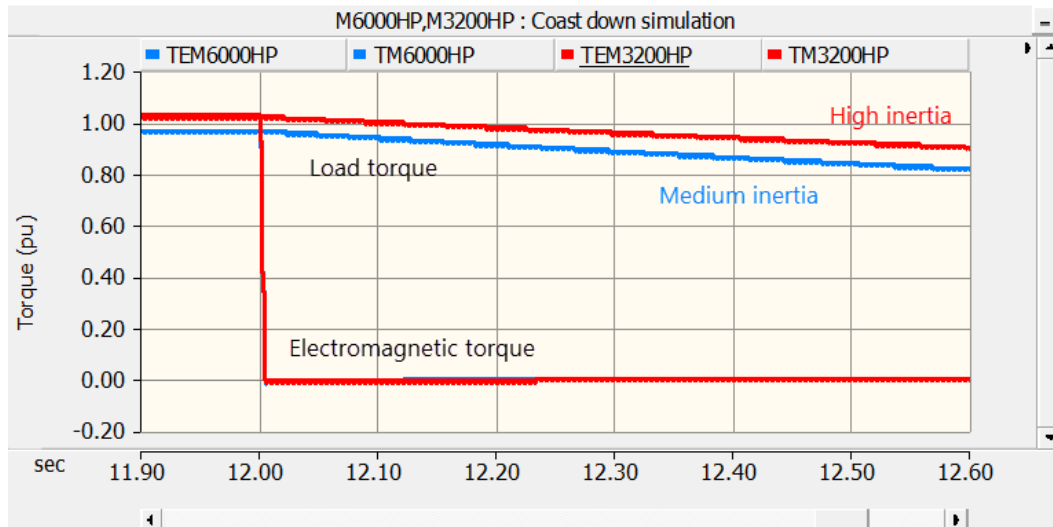


Figure 3-8 Motor torques during a coast down simulation of a medium inertia 6000 HP induction motor pump and a high inertia 3200 induction motor fan.

### 3.3.2 Analysis of a Group of Induction Motors on Loss of Power Supply

When an auxiliary motor bus is disconnected from the old source, the mix of motors develop a voltage on the motor bus depending on the loads inertia, motor types, motor sizes and the mix of motors [9]. The larger machines in general act as induction generators supplying current to the smaller machines [8].

The system described in Figure 3-4 was setup to observe the interactive behavior of the mix of motors upon loss of power supply by opening only the source breaker labeled BWStart and with the motor breakers labeled BKM1\_W and BKM2\_W remaining closed during the simulation. Breaker BWAux was kept open during the simulation. Figure 3-9 to Figure 3-13 show the behavior of bus voltage, frequency, phase angle, torque and current during this simulation.

Figure 3-9 shows the bus voltage behavior. Both motor terminal voltage magnitudes were the same because their breakers were not opened. Immediately after the loss of power supply (when the source breaker opened) the terminal voltage changed from 1 p.u. to 0.888 p.u., which was the average of the voltages of both motor's magnetizing branch voltages before the bus disconnection ( $E_{mag_0} = 0.901 \text{ p.u.}$  and  $E_{mag_0} = 0.875 \text{ p.u.}$ ). After that the voltage decayed according to the motor and load

inertias, motor electrical parameters, motor's feeder electrical parameters, load torque and load friction.

The right-side plot in Figure 3-9 shows the voltage phasor magnitude and angle behavior during the coast down simulation. The rotation speed and hence the phase angle depend on the frequency rate of change.

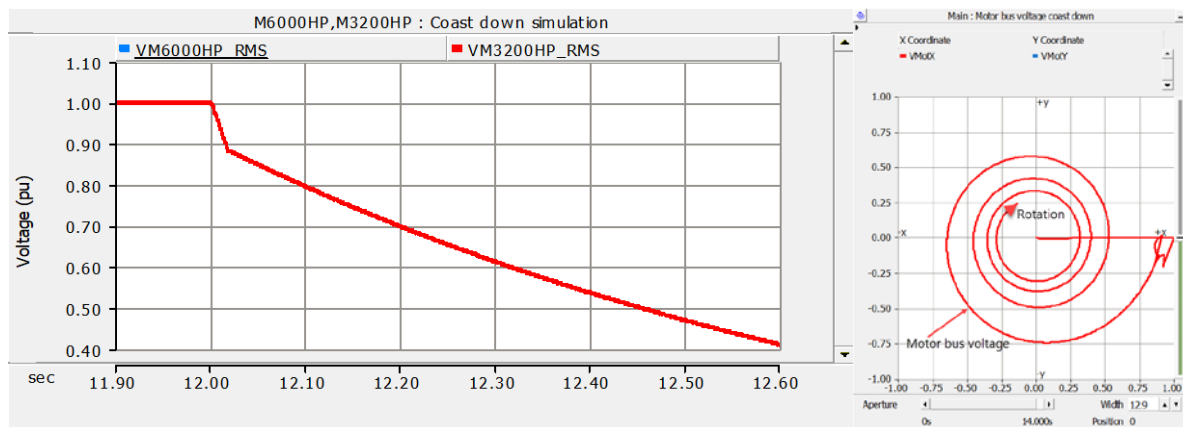


Figure 3-9 Motor bus voltage magnitude during a motor bus coast down simulation.

Figure 3-10 shows the bus frequency. The frequency of the terminal voltage of both motors was the same during the simulation because the motor breakers were not opened. Immediately after the loss of power supply (when the source breaker opened) the terminal voltage frequency changed from 60 Hz to 58.88 Hz, which is the average rotor frequency of the motors before the bus disconnection ( $F_{rot1} = 58.98 \text{ Hz}$  and  $F_{rot2} = 58.78 \text{ Hz}$ ). As was explained for the terminal voltage magnitude, the frequency decayed according to the motor and load parameters.

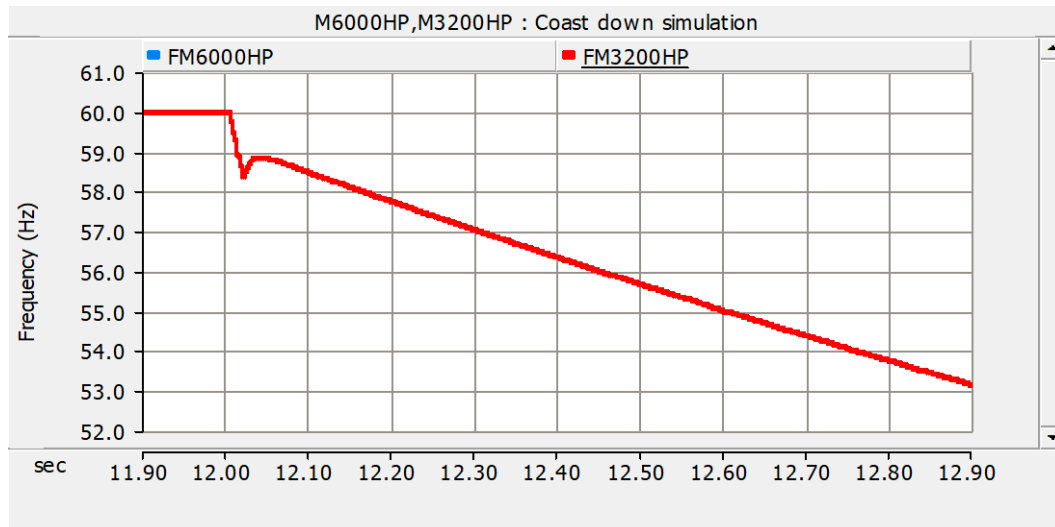


Figure 3-10 Motor bus voltage frequency during a motor bus coast down simulation.

Figure 3-11 shows the bus voltage phase angle. After the loss of power supply, the bus voltage phase angle changed from 0 to -9.5 degrees due to the slip frequency of the motor group's rotors.

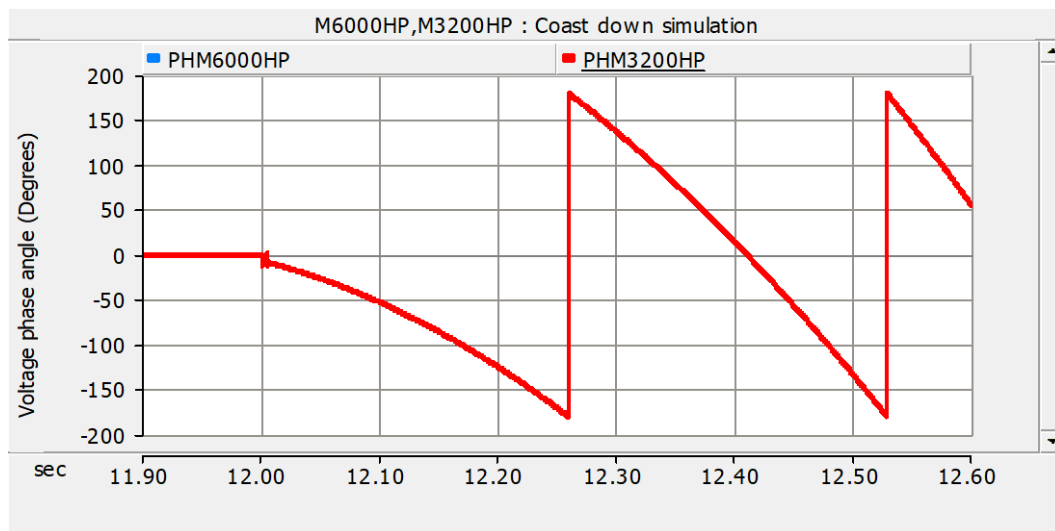


Figure 3-11 Motor bus voltage phase angle during a motor bus coast down simulation.

Figure 3-12 shows the motor electromagnetic torque and load torque behavior during the motor bus loss of supply. First, the high inertia load torque decayed more slowly than the medium inertia load, the red and blue plots in the figure's upper part. Second, the motor with high inertia after the power supply disconnection started behaving as an induction generator producing negative torque while the medium inertia motor produced positive torque. It is very important to point out that the mechanical

load of the motor behaving as induction generator is still producing positive torque with opposing rotating direction than its electromagnetic torque. Therefore, this way torsional stress is developed in the motor shaft.

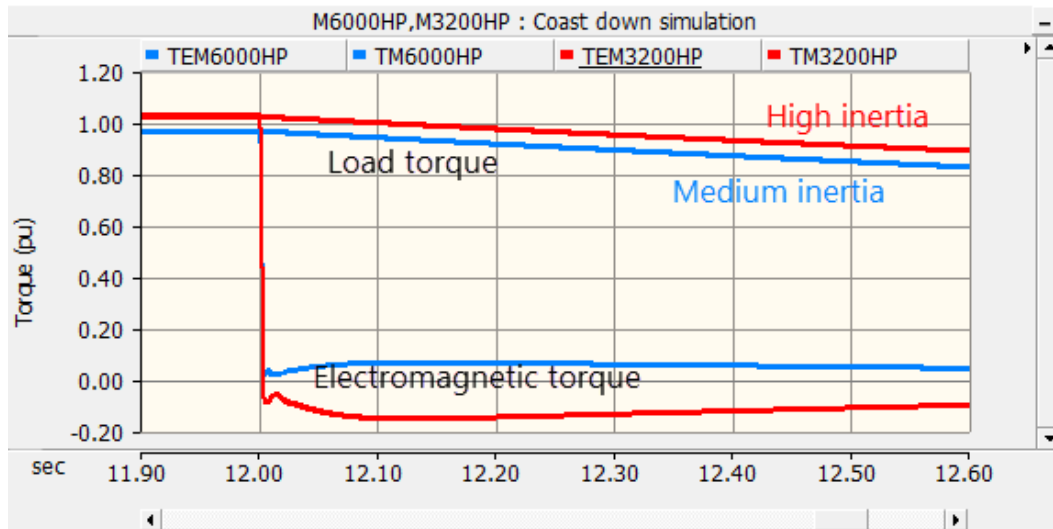


Figure 3-12 Motor torques during a motor bus coast down simulation.

Figure 3-13 shows the motor terminal currents behavior following the motor bus loss of power supply. First, the high inertia motor supplies current to the medium inertia load. It is clearly seen that there is a current phase angle opposition between both currents. Second, after a few cycles, both currents decayed to a minimum value and then the high inertia motor supplied current to the medium inertia motor. Third, comparing the instantaneous current and the RMS current the time response of the RMS meter at the beginning of the loss of power supply may be observed. The RMS meter took approximately one cycle to track the current change. After that period, it consistently followed the sinusoidal value.



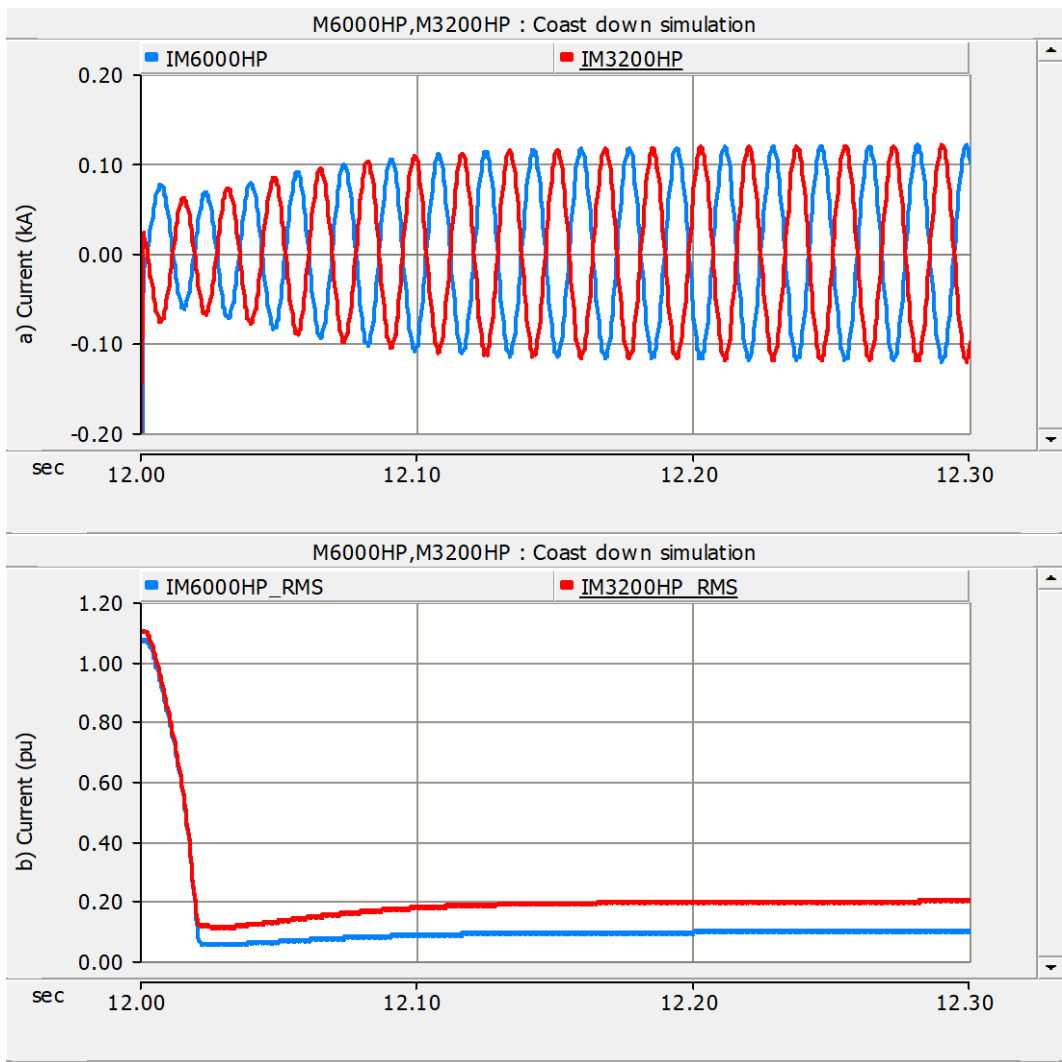


Figure 3-13 Motor currents during a motor bus coast down simulation, a) instantaneous current in kA, b) current magnitude in per unit.

### 3.3.3 Analysis of a Group of Induction Motors During Reconnection on Maximum Voltage Phasor Difference

The motor bus transient behavior during the reconnection to a new incoming source can be computed from equations (3-24) to (3-26) in Section 3.2 or their equivalents in the  $qd0$  domain provided in Section 3.2.2 knowing the stator and rotor currents and the residual motor bus voltage at the instant of switching [19] and [20].

The initial magnitude of the electromagnetic transient depends on the frequency difference and the magnitude of the voltage phasor difference between the new source and the decaying residual voltage of the magnetizing branch at the instant of closing the new source breaker.

According with references [22] and [20], if the voltage difference is maximum when reconnecting the motor bus to the new source, it may produce motor reconnecting currents higher than the motor starting currents and negative transient torques that may stress and even damage the motor shafts.

Figure 3-14 shows the voltage phasor plot of the new source voltage (blue phasor) and the motor bus residual voltage (red plot). The maximum voltage phasor difference between the motor bus residual voltage and the incoming power supply voltage during the loss of power supply may not occur in phase opposition [20]. For this example, the maximum difference occurred near phase opposition (black region).

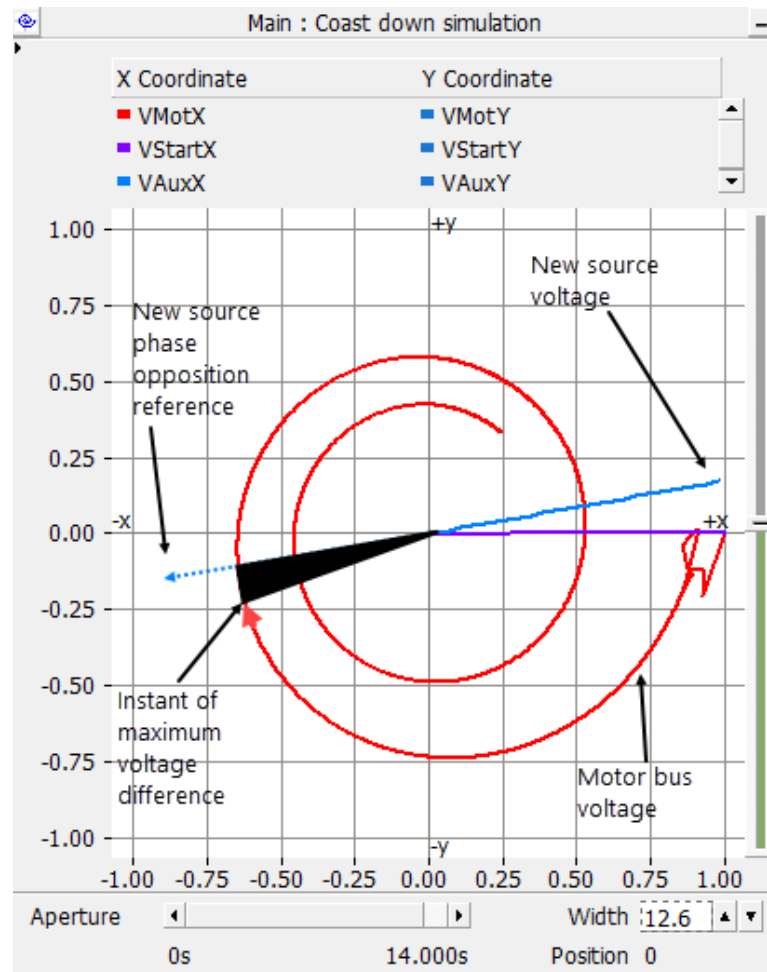


Figure 3-14 Voltage phasor difference between the new source voltage and motor residual voltage during a motor bus coast down simulation.

Figure 3-15 shows time domain magnitude and phase angle of the motor bus residual voltage (red plot), the new incoming power supply voltage (blue plot) and the magnitude of the voltage difference of the residual voltage and the incoming power supply (magenta plot). The magenta arrow shows the maximum magnitude of voltage difference for this example. “The maximum difference may not occur exactly at  $180^\circ$  phase opposition of the decaying motor voltage and the incoming power supply voltage” [20].

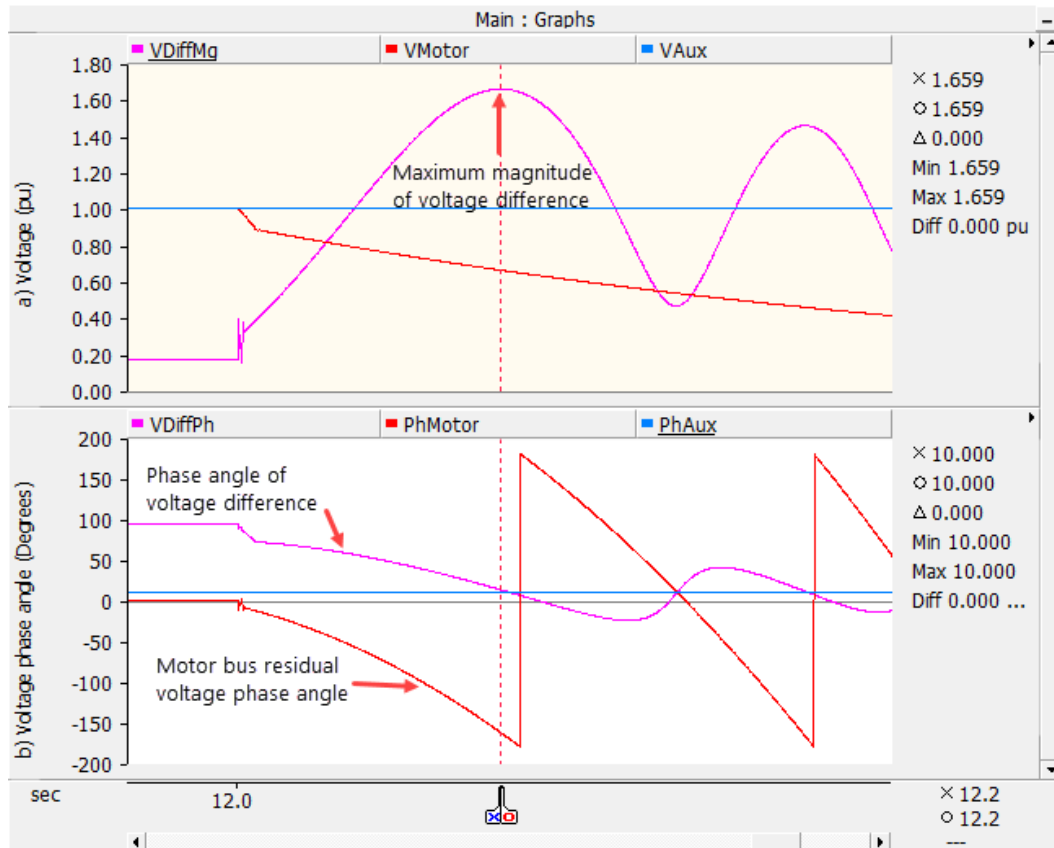


Figure 3-15 New source and motor residual voltage difference in time domain during a motor bus coast down simulation, a) Voltage magnitudes in per unit, b) Voltage phase angle in degrees.

The phasor voltage difference at the instant of switching may be computed using voltage phasor difference. Using trigonometric identities, the phasor voltage difference may be computed as:

$$E_{\text{diff}} = \sqrt{E_s^2 + E_m^2 - 2E_sE_m \cos \theta} \quad (3-46)$$

Where  $\theta$  is the angle between both voltage phasors,  $E_s$  is the new source voltage magnitude, and  $E_m$  is the residual motor bus voltage magnitude, at the instant of switching to the new source.

The system shown in Figure 3-4 was setup to simulate and compare the behavior of a medium and a high inertia induction motors when reconnecting after a loss of power supply simulation under maximum voltage difference between residual motor bus and new power supply voltage. The

maximum voltage difference occurs during the first cycle of the loss of power supply, and the decaying residual magnetizing voltage frequency is still close to the initial rotor slip frequency.

The startup breaker BWStart was opened at  $t=12.00$  seconds to simulate the loss of power supply and then, the breaker BWAux was closed at  $t=12.243$  seconds to simulate transients under maximum voltage difference between the motor bus residual voltage and the new incoming power supply. Both motor breakers BKM1\_W and BKM2\_W remained closed during the simulation. Therefore, both motors had the same terminal voltage during the time of the simulation.

Figure 3-16 shows the new incoming power supply and motor bus voltage behavior during a simulation that included the induction motor starting process, loss of power supply and finally the reconnection event under maximum phasor voltage difference between the new source and the motor bus. The first two graphs a) and b) at the top show the instantaneous voltage in kV and the voltage magnitude in p.u. during the simulation. The loss of power supply at  $t=12.00$  seconds with the reconnection at  $t=12.243$  seconds may be observed. The last two graphs c) and d) at the bottom show a zoom in time of the first two graphs. It may be observed that the motor bus voltage (red plot) is decaying before the reconnection and its phase angle is changing due to the frequency decay and is approaching the phase opposition with respect to the incoming source voltage phase (blue plot). The voltage difference between the residual motor bus voltage and the new incoming source voltage is maximum at the instant prior to reconnection.

At the instant of reconnection  $t=10.243$  seconds, the motor bus voltage phase angle changes abruptly to  $\theta=10$  degrees which is the phase angle of the new source voltage.

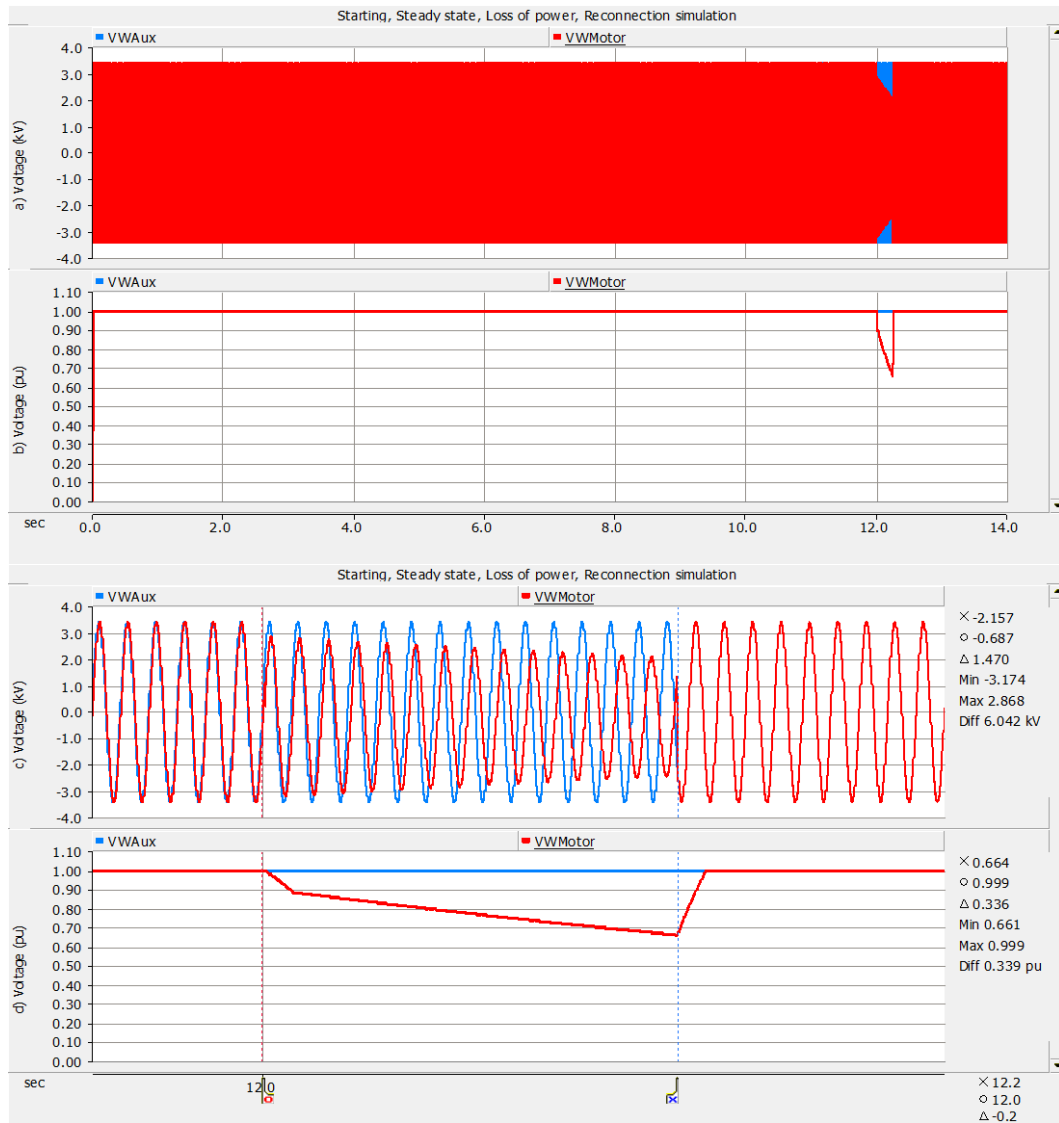


Figure 3-16 New incoming power supply voltage and motor bus voltage behavior during a simulation of induction motor starting, loss of power supply, and reconnection for maximum motor bus-new source voltage difference, a) instantaneous voltage in kV, b) voltage magnitude in per unit, c) zoom in time of the instantaneous voltage in kV and d) zoom in time of the voltage magnitude in per unit.

Figure 3-17 compares the high and medium inertia motor currents during a simulation of induction motor covering the startup process, loss of power supply and reconnection event under maximum phasor voltage difference between the new source and the motor bus. The first two graphs a) and b) on the top show the behavior during the simulation from startup of the motors to the reconnection to the new source and the two graphs c) and d) at the bottom show a zoom in time of the first two graphs to observe in detail the transient behavior during the reconnection to the new incoming source.

The induction motor startup shows that the high inertia motor starting current was near 6.8 p.u. whereas the medium inertia motor was 6 p.u. However, during the reconnection under maximum residual voltage-new incoming source voltage difference, the high inertia motor current increased to 11.2 p.u. while the medium inertia motor current increased to 9.53 p.u. The peak reconnecting current of the high inertia motor was 1.65 times its maximum starting current, while the peak reconnecting current of the medium inertia motor was 1.58 times its maximum starting current. The first four cycles after the reconnection show the impact of frequency difference between the new source and the residual voltage frequency on current and on the electromagnetic torque.

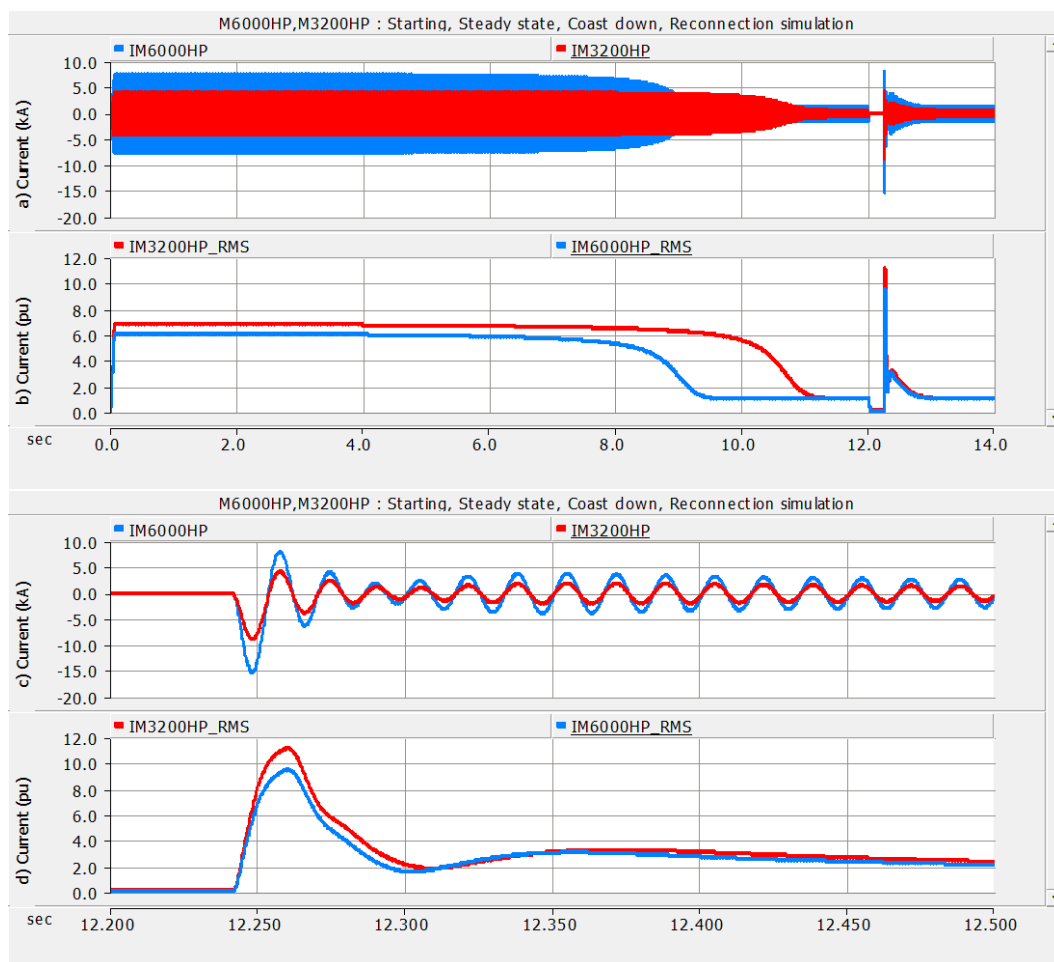


Figure 3-17 High and medium inertia motor currents behavior during a simulation of induction motor starting, loss of power supply, and reconnection for maximum motor bus-new source voltage difference, a) instantaneous current in kA, b) current magnitude in per unit, c) zoom in time of the instantaneous current in kA and d) zoom in time of the current magnitude in per unit.

Figure 3-18 shows the motor bus frequency and voltage phase angle behavior during a simulation that includes induction motor startup process, loss of power supply and reconnection event under maximum phasor voltage difference between the new source and the motor bus voltages. It may be observed that the motor bus frequency and voltage phase decayed during the loss of power supply. After reconnection, the new incoming power supply frequency dictates the motor bus frequency and the motor bus voltage phase angle.

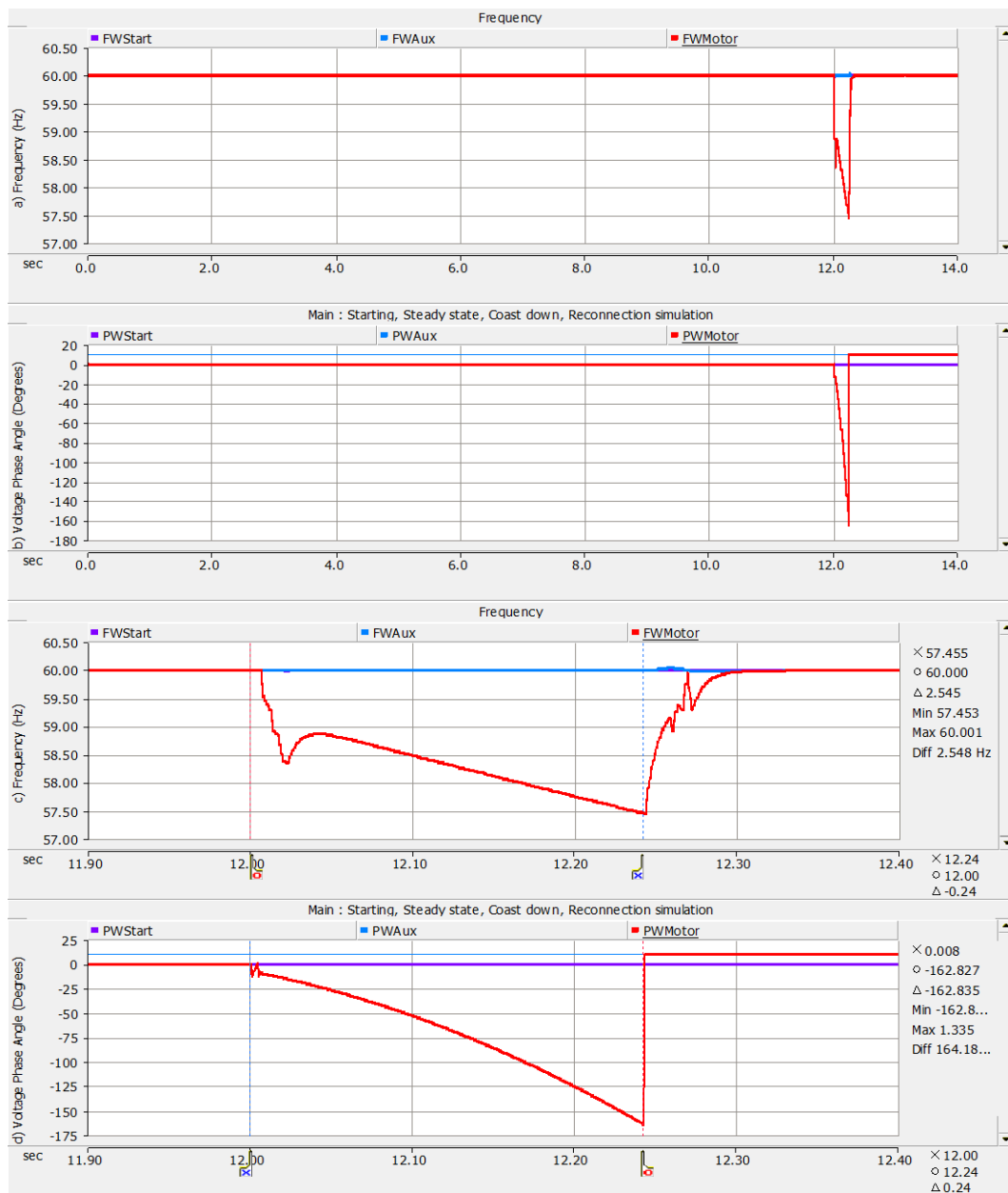


Figure 3-18 Motor bus frequency and phase angle behavior during a simulation of induction motor starting, loss of power supply, and reconnection for maximum motor bus-new source voltage difference, a) Frequency in Hertz, b) Voltage phase angle in degrees, c) Zoom in time of the frequency in Hertz and d) Zoom in time of the voltage phase angle in degrees.



Figure 3-19 compares the high and medium inertia motor load and electromagnetic torque behavior during a simulation including the process of induction motor starting, loss of power supply and reconnection of the motor bus for maximum motor – new source voltage difference. The first two graphs a) and b) at the top show the behavior during the whole simulation and the two graphs c) and d) at the bottom show a zoom in time of the first two graphs to observe in detail the transient behavior during the reconnection to the new incoming source.

The load torque for both motors decayed during the loss of power supply. The high inertia motor load torque decayed down to 0.934 p.u. and the medium inertia motor torque decayed down to 0.966 p.u. When the motor bus was reconnected both load torque recovered to their value before the loss of power without any further impact.

It may be seen in the two bottom plots that the maximum electromagnetic torque of both motors during the initial starting condition were nearly 2.4 p.u. During the reconnection under maximum voltage difference between the residual motor bus voltage and the new incoming source voltage, the high inertia motor electromagnetic torque was -7.45 p.u. (negative) and the maximum negative electromagnetic torque of the medium inertia motor was 6.4 p.u.

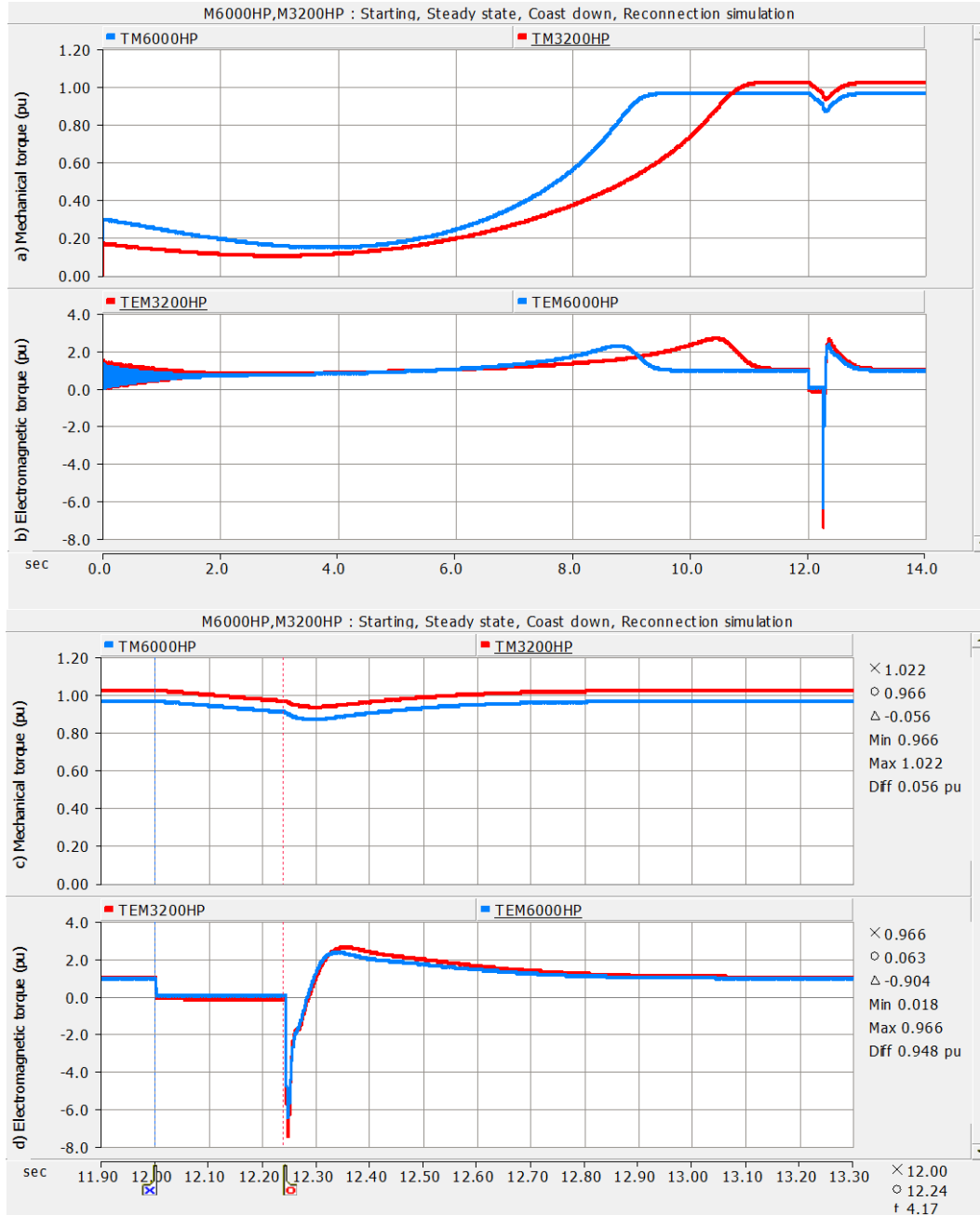


Figure 3-19 High and medium inertia motor load and electromagnetic torque behavior during a simulation of induction motor starting, loss of power supply, and reconnection for maximum motor bus-new source voltage difference, a) Mechanical torque in per unit, b) Electromagnetic torque in per unit, c) Zoom in time of the mechanical torque in per unit, d) Zoom in time of the electromagnetic torque in per unit.

Table 3-3 shows a summary of the simulation results, when reconnecting the motor bus under maximum motor bus – new source voltage difference. It may be observed the high magnitude of motor currents during reconnection, approximately twice the maximum starting current, when reconnecting under maximum motor bus – new source voltage difference. The electromagnetic torque of both motors is higher than negative 9.0 p.u.

Induction Motor	6000 HP	3200 HP
Reconnecting the motor bus under maximum motor bus – new source voltage difference		
Current		
a) Maximum starting current in p.u.	6.0	6.8
b) Maximum current during reconnection in p.u.	9.53	11.2
c) $I_{\text{reconnecting}} / I_{\text{starting}}$ in p.u.	1.59	1.65
Electromagnetic Torque		
a) Maximum starting torque in p.u.	2.3	2.6
b) Maximum torque during reconnection in p.u.	-6.39	-7.44
c) $T_{\text{reconnecting}} / T_{\text{starting}}$ in p.u.	2.78	2.86

*Table 3-2 Summary of simulation results of induction motor current and torque when reconnecting to a new source under maximum voltage difference.*

### 3.3.4 Analysis of a Group of Induction Motors During Reconnection on Large Frequency Difference

According with [20] and [6], if there is a significant frequency difference between the new source voltage frequency and the residual voltage frequency, when reconnecting the motor bus to the new source, the motor response produces damped oscillating currents and damped oscillating electromagnetic torques.

The motors system shown in Figure 3-4 was setup to show and compare the behavior of a medium and a high inertia induction motors when reconnecting after a loss of power supply simulation under a large voltage frequency difference between residual motor bus and new power supply voltage. The power system was on the same conditions as described before, and the loss of power lasted longer. The reconnection to the new incoming source was at  $t= 20.90$  seconds when the residual voltage was 0.22 per unit and the residual voltage frequency was 27.89 Hz.

Figure 3-20 above compares the high and medium inertia motor currents behavior during a simulation of induction motor covering the startup process, loss of power supply and reconnection event for a high motor – new source voltage frequency difference. The first two graphs a) and b) at the top show the behavior during the simulation from motor startup to motor bus reconnection and the two graphs c) and d) at the bottom show a zoom in time of the first two graphs to observe in detail the motor load current transient behavior during the reconnection to the new incoming source.

The high inertia motor maximum peak reconnection current was 8.7 p.u. in contrast the medium inertia motor maximum peak reconnecting current was 7.56 p.u. The first eleven cycles after the reconnection show the impact of frequency difference between the new source and the residual voltage frequency on current when comparing against the simulation results shown in Figure 3-17.

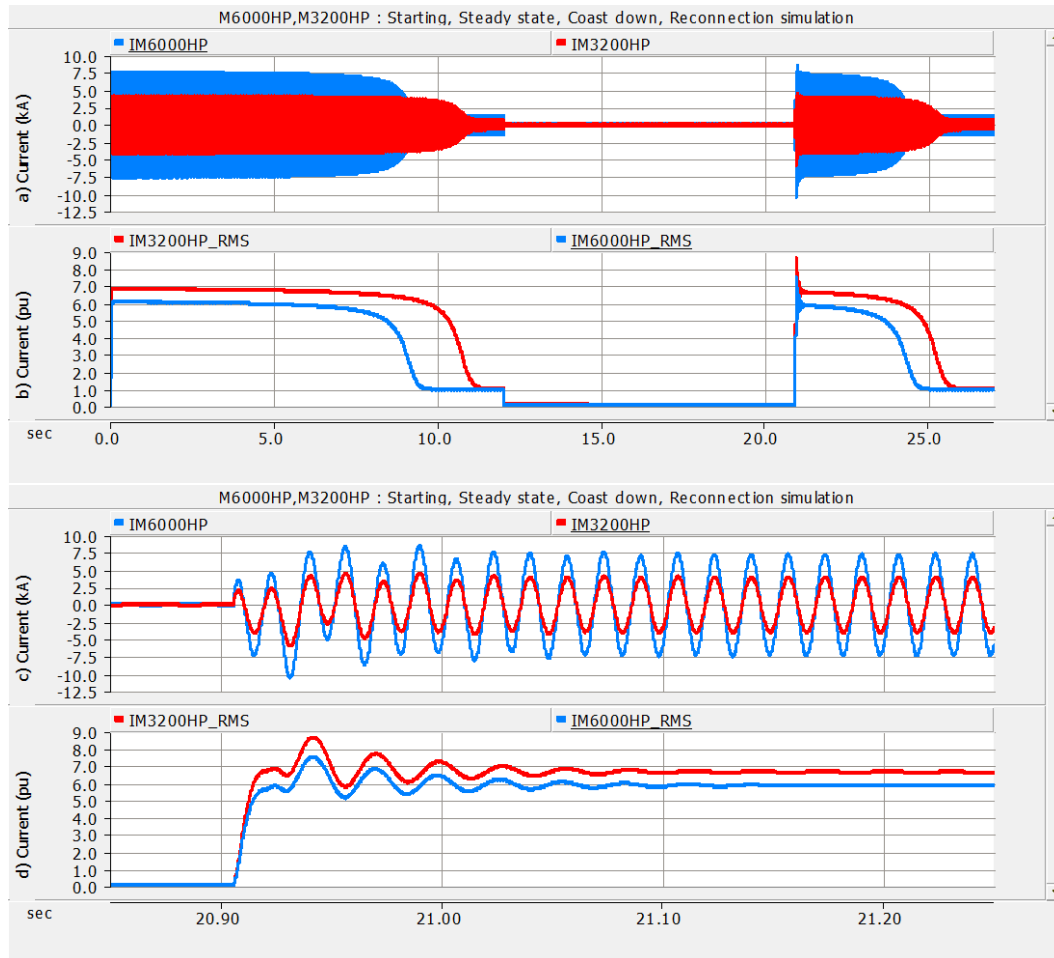


Figure 3-20 High and medium inertia motor currents behavior during a simulation of induction motor starting, loss of power supply, and reconnection for a high motor bus-new source voltage frequency difference, a) Instantaneous current in kA, b) Current magnitude in per unit, c) Zoom in time of the instantaneous current in kA, d) Zoom in time of the current magnitude in per unit.

Figure 3-21 compares the high and medium inertia motor electromagnetic torques behavior of induction motors during a simulation of induction motor covering the startup process, loss of power supply and reconnection event for a high motor – new source voltage frequency difference. The first graph a) at the top show the behavior during the simulation and the graph b) at the bottom show a zoom in time of the first graph to observe in detail the motor electromagnetic torque transient behavior during the reconnection to the new incoming source.

The high inertia motor maximum negative peak electromagnetic torque was 4.56 p.u. in contrast the medium inertia motor maximum peak electromagnetic torque was -3.62 p.u. There were 3 cycles with periods of negative torques, producing torsional stress to the motor's shaft. The first eleven cycles

after the reconnection show the oscillatory electromagnetic torques caused by the impact of frequency difference between the new source and the residual voltage frequency. These oscillatory electromagnetic torques can be compared against the simulation results shown in Figure 3-19 where there are negative torques but these are not oscillating.

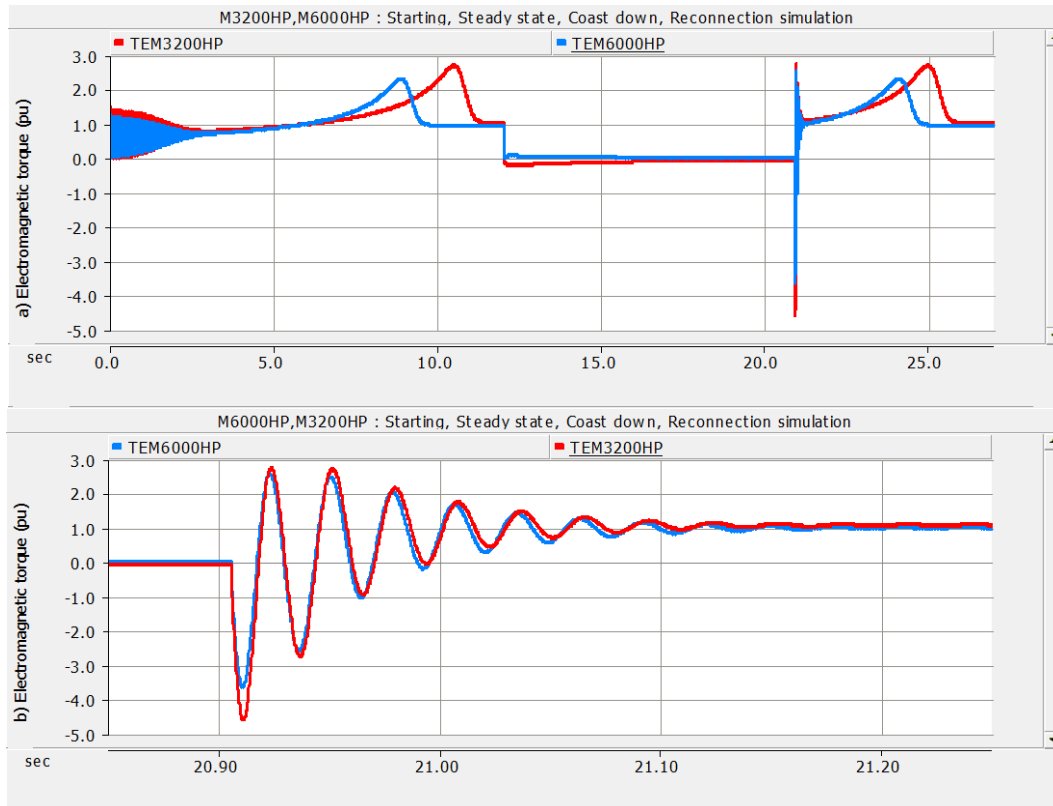


Figure 3-21 High and medium inertia motor electromagnetic torques behavior during a simulation of induction motor starting, loss of power supply, and reconnection for a high motor bus-new source voltage frequency difference, a) Instantaneous electromagnetic torque in per unit, b) Zoom in time of the electromagnetic torque in per unit.

The magnitude of such negative torques may cause damage to the motor's shaft and some related power plant equipment. The large negative torques and high currents during reconnection to the new incoming power supply can be avoided reconnecting the new incoming source under minimized voltage and frequency difference between the motor bus and the new incoming power supply. The large positive torques during the reconnection may be larger than those exerted during the startup process and could cause damage with time.

Table 3-3 shows a summary of the simulation results when reconnecting the motor bus under a high motor bus - new source voltage frequency difference. The maximum current of both motors when reconnecting under large motor bus - new source voltage frequency difference is approximately 30% larger than their respective starting current, and the torque is -6.8 p.u. for the high inertia motor and -5.3 for the medium inertia motor.

Induction Motor	6000 HP	3200 HP
Reconnecting the motor bus under a high motor bus - new source voltage frequency difference		
Current		
a) Maximum starting current in p.u.	6.0	6.8
b) Maximum current during reconnection in p.u.	7.55	8.71
c) $I_{\text{reconnecting}} / I_{\text{starting}}$ in p.u.	1.25	1.28
Electromagnetic Torque		
a) Maximum starting torque in p.u.	2.3	2.6
b) Maximum torque during reconnection in p.u.	-3.62	-4.56
c) $T_{\text{reconnecting}} / T_{\text{starting}}$ in p.u.	1.57	1.75

*Table 3-3 Summary of simulation results of induction motor current and torque when reconnecting to a new source under large frequency difference.*

### 3.3.5 Analysis of a Motor Bus on Different Closing Times

To analyze the impact of the reclosing time of the new source breaker in the magnitude of the induction motor current and electromagnetic torque, two power systems were prepared in PSCAD/EMTDC. Each system was set with six induction motors of different power and inertia, data of each motor are shown in Appendix A.

For system 01, shown in Figure 3-22, 2121 simulations were carried out in PSCAD/EMTDC increasing the reclosing time of the new source breaker in 0.5 milliseconds between each subsequent simulation. The closing of the new source breaker was  $t=12.0$  seconds for the first simulation and  $t=13.06$  seconds for the last simulation. Maximum current values and positive and negative maximum values of electromagnetic torque of each motor connected to the motor bus were recorded. The magnitude and the phase angle of residual voltage of the motor bus, and the volts/Hertz in p.u. of the voltage

difference between the voltage of the new source and the residual voltage of the motor bus were also computed.

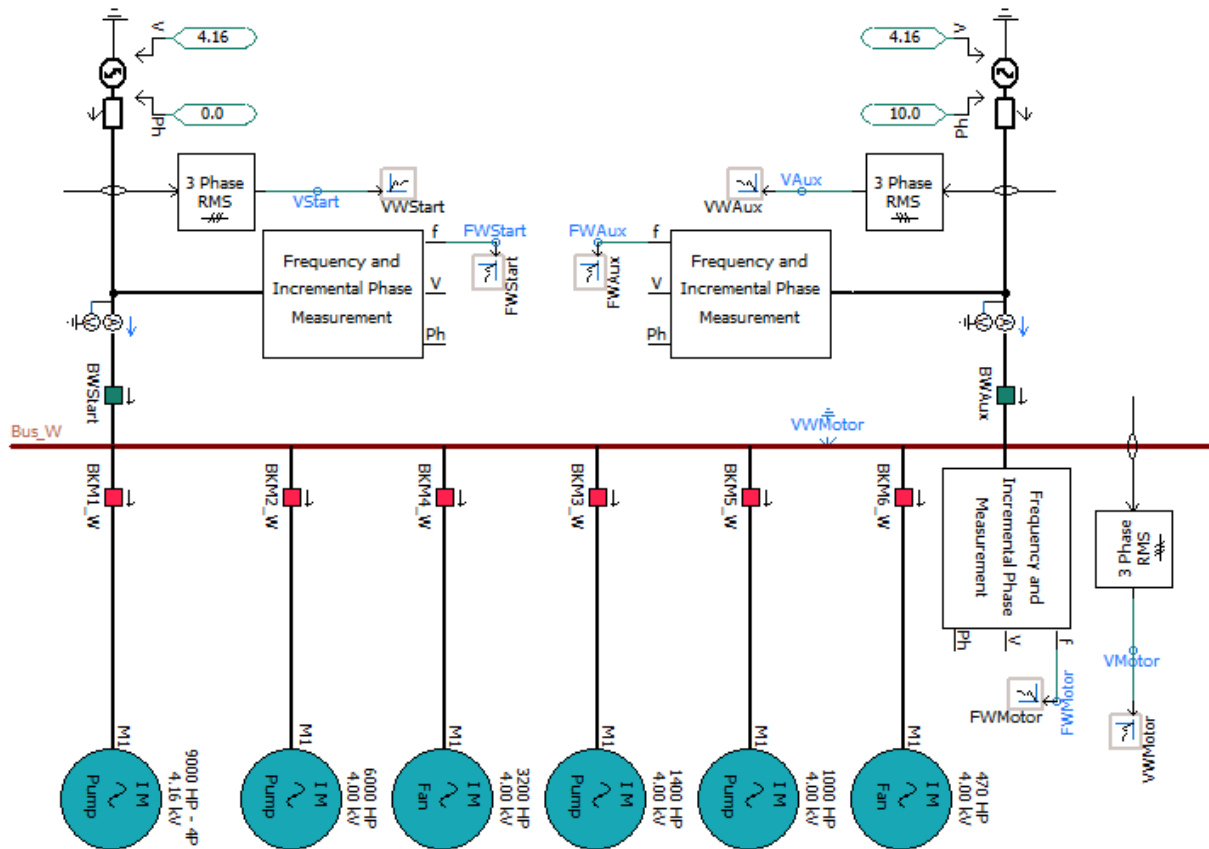


Figure 3-22 System 01 to analyze the induction motor currents and electromagnetic torques behavior during different reclosing times of the new source's breaker.

Figure 3-23 shows the results of maximum current of each induction motor for each simulation during the reconnection to the new source. It may be observed that all motors have the same behavior pattern. First, the current magnitude increases as the voltage phase angle of the motor bus moves forward from the voltage phase angle of the new power source. Second, the current magnitude decreases while the voltage phase angle of the motor bus approaches the voltage phase angle of the new source. Third, the current magnitude is maximum when the residual voltage phase angle is close to the phase opposition with respect to the phase angle of the new source. Fourth, the current magnitude is minimal in the phase coincidence between the voltage phase angle of residual voltage of the motor bus and the voltage phase angle of the new source. In the first phase coincidence, the induction motor current magnitudes are lower with respect to the subsequent phase coincidences.



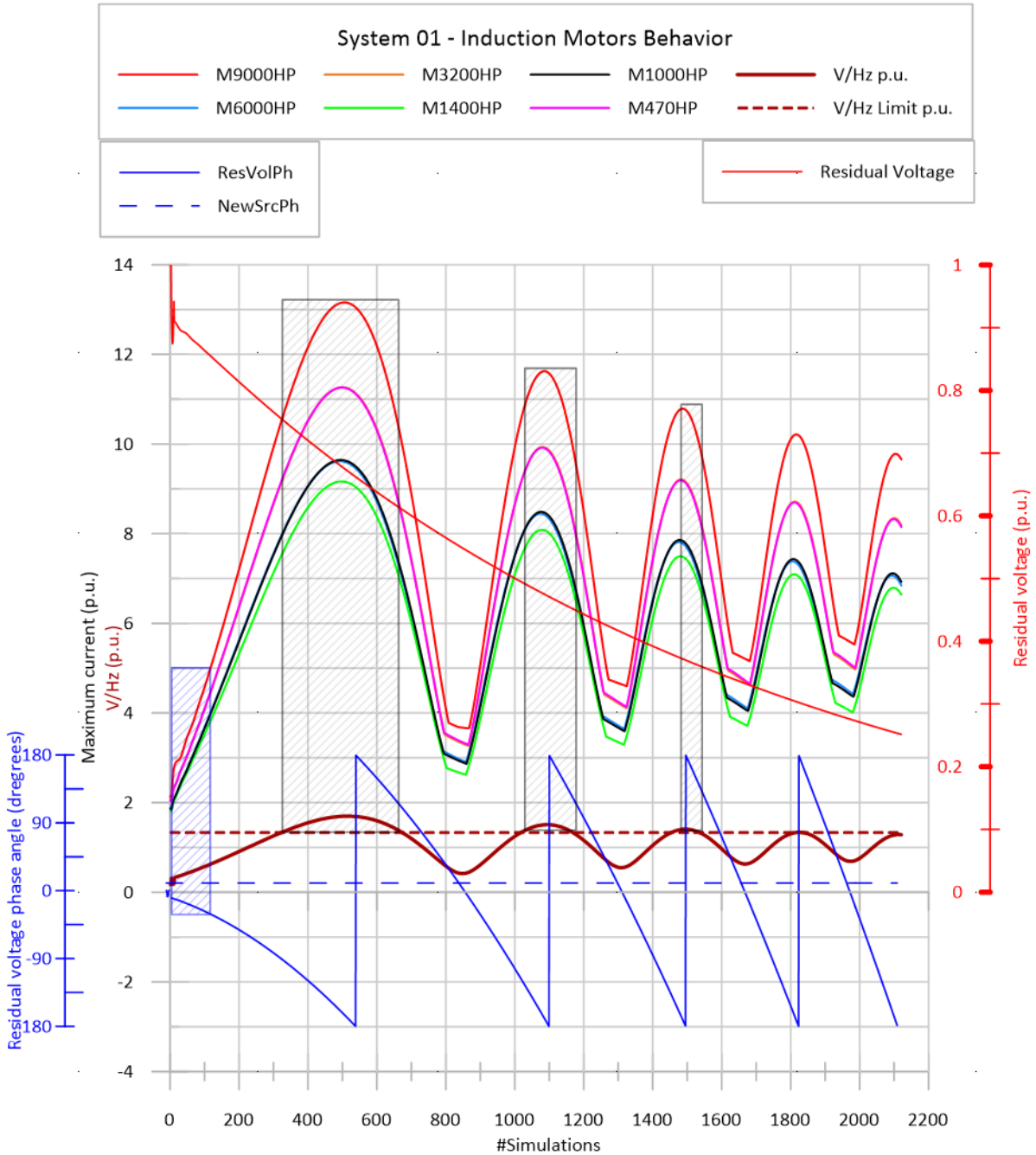


Figure 3-23 System 01 induction motor current behavior during different closing times of the new source's breaker.

The area in blue, corresponding to a difference of 30 degrees in the phase angle between residual voltage and that of the new source voltage, is the recommended region to perform the motor transfer using the fast-transfer method. It may be observed that in this region the volts/Hertz in p.u. are lower than the volts/Hertz limit of 1.33 p.u. and that the induction current magnitudes during the reconnection are lower than 5 p.u. for this system.

On the other hand, the areas in gray, are regions where the volts/Hertz in p.u. are greater than the limit of 1.33 p.u. In these regions, improper transfers may produce very high induction motor reconnection currents which may subsequently damage the induction motors. A proper volts/Hertz limit adjustment would avoid transfer of motors in these regions. The intermediate areas between the areas in gray, show volts/Hertz values lower than the limit 1.33 p.u. resulting in a volts/Hertz minimum value in the phase coincidence between the voltage of the motor bus and the voltage of the new source. However, while the reclosing time is approaching the areas in gray, the volts/Hertz in p.u. is increasing but its magnitude is still lower than the limit of 1.33 p.u. and transfers on those regions show high current magnitudes. In several simulations, the results have magnitudes higher than 10 p.u.

Finally, for this system and its set conditions, when the residual voltage is less than 0.35 p.u. the volts/Hertz magnitude is lower than the volts/Hertz limit of 1.33 p.u. Even under these conditions, some induction motors transfers result in high induction motor reconnection currents.

Figure 3-24 shows the results of maximum positive and negative electromagnetic torques of each induction motor for each simulation during reconnection to the new source. It can be observed that all motor electromagnetic torques follow the same behavior pattern. First, the magnitude of negative torques increases while the voltage phase angle of the motor bus moves forward from the voltage phase angle of the new source. Second, the negative torque magnitude decreases while the voltage phase angle of the motor bus approaches to the voltage phase angle of the new source. Third, the negative torque magnitude is maximum when the residual voltage phase angle is closer to the phase opposition with respect to the phase angle of the new source. Fourth, the negative torque magnitude is minimal in the phase coincidence between the residual voltage phase angle of the motor bus and the voltage phase angle of the new source.

Negative torques are minimum as from the first phase coincidence and during the following 90 degrees forward of the phase coincidence. In contrast, positive torques are more relevant in these zones. Reference [14] shows that higher torques may be developed when transferring using the in-phase method under fault conditions.

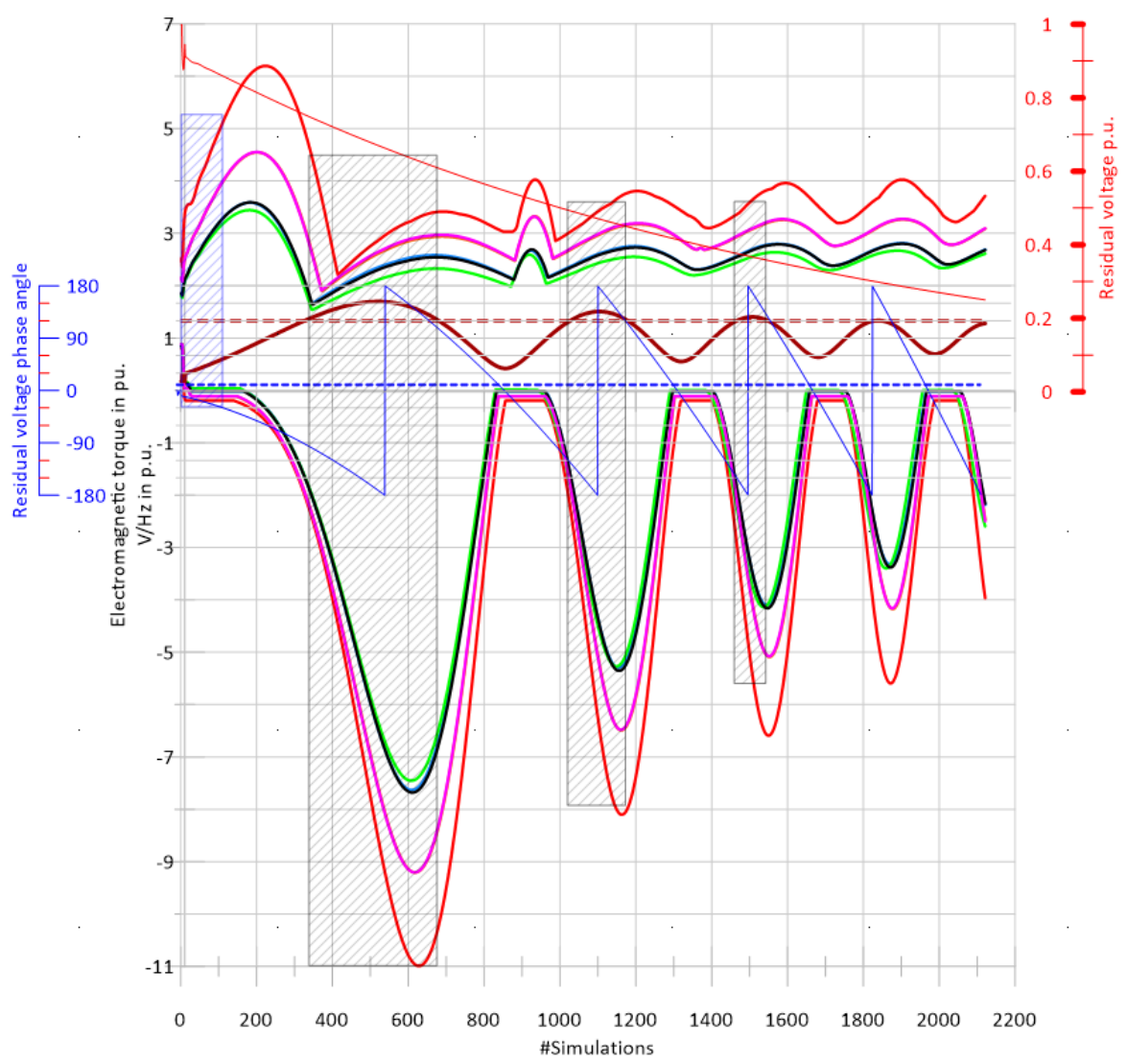
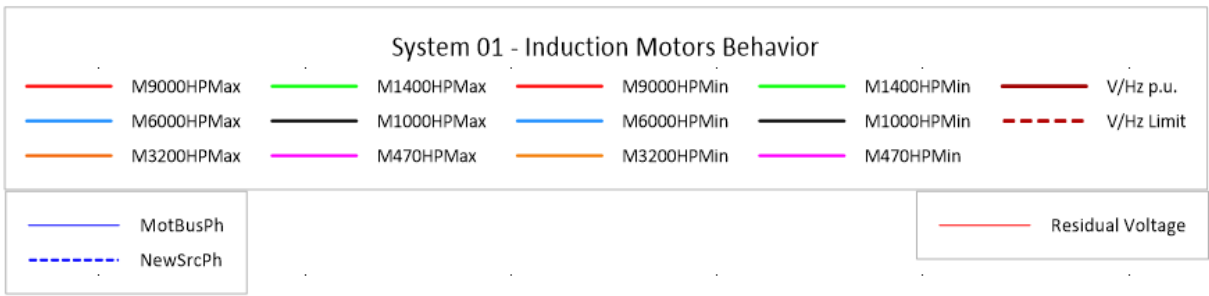


Figure 3-24 System 01 induction motor electromagnetic torques behavior during different closing times of the new source's breaker.

The area in blue corresponds to a phase angle difference of 30 degrees between residual voltage and that of the new source, it is the recommended region to perform motor transfer with the fast-transfer method. It can be observed that in this region the volts/Hertz in p.u. are lower than the 1.33 p.u.

volts/Hertz limit, and the induction motor negative torque magnitudes during the reconnection are lower than 0.5 p.u. while positive electromagnetic torques may reach up to 5 p.u. for this system.

On the other hand, the areas in gray are regions where the volts/Hertz magnitude in p.u. are above to the limit of 1.33 p.u. In these regions, improper transfers may produce very large positive and negative electromagnetic torques which may subsequently damage the induction motors. A proper adjustment of the volts/Hertz limit would avoid motor transfers in these regions. The intermediate areas between the regions in gray show volts/Hertz values lower than the limit 1.33 p.u. resulting in a minimum value of the volts/Hertz in the phase coincidence between the motor bus voltage and the voltage of the new source. However, while the reclosing time is approaching the areas in gray, the p.u. volts/Hertz value increases but is still lower than the limit of 1.33 p.u. and negative electromagnetic torques of high magnitude are developed. In several simulations, with reclosing times in these zones, negative electromagnetic torques of magnitudes above 7 p.u. for this system may be developed.

Finally, for this system and its set conditions, when a residual voltage is lower than 0.35 p.u. the volts/Hertz magnitude is lower than the volts/Hertz limit of 1.33 p.u. Under these transfer conditions, some motors show negative electromagnetic torques larger than 4 p.u.

In general, for transfers with reclosing times above the first 90 degrees of phase difference between the residual voltage of the motor bus and voltage of the new source, the motor positive electromagnetic torques of system 01 are kept lower than 4 p.u.

For the system 02, shown in Figure 3-25 , 2551 simulations in PSCAD/EMTDC were performed increasing the reclosing time of the new source breaker in 0.5 milliseconds between each subsequent simulation. The closing of the new source breaker was  $t=12.0$  seconds for the first simulation and  $t=13.275$  seconds for the last simulation. For each simulation, the maximum current values and maximum positive and negative values of electromagnetic torque were recorded of each motor connected to the motor bus. Also, the magnitude and residual voltage phase angle of the motor bus, and volts/Hertz in p.u. of the voltage difference between the new source voltage and the residual voltage of the motor bus were also calculated.

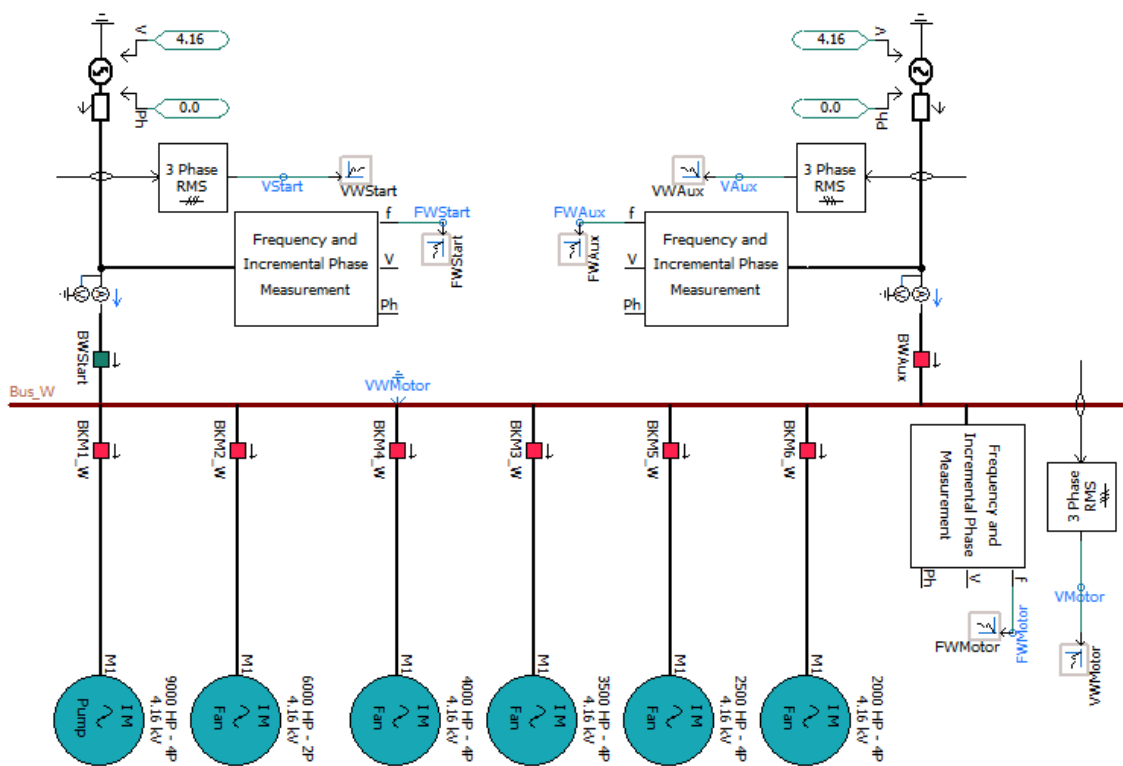


Figure 3-25 System 02 to analyze the induction motor currents and electromagnetic torques behavior during different closing times of the new source's breaker.

Figure 3-26 shows the results of the maximum current of each induction motor for each simulation during reconnection to the new source. As well as in system 01 all motors follow the same behavior pattern. First, the current magnitude increases as the voltage phase angle of the motor bus moves forward from the voltage phase angle of the new power source. Second, the current magnitude decreases while the voltage phase angle of the motor bus approaches the voltage phase angle of the new source. Third, the current magnitude is maximum when the residual voltage phase angle is close

to the phase opposition with respect to the phase angle of the new source. Fourth, the current magnitude is minimal in the phase coincidence between the voltage phase angle of residual voltage of the motor bus and the voltage phase angle of the new source. In the first phase coincidence, the induction motor current magnitudes are lower with respect to the subsequent phase coincidences.

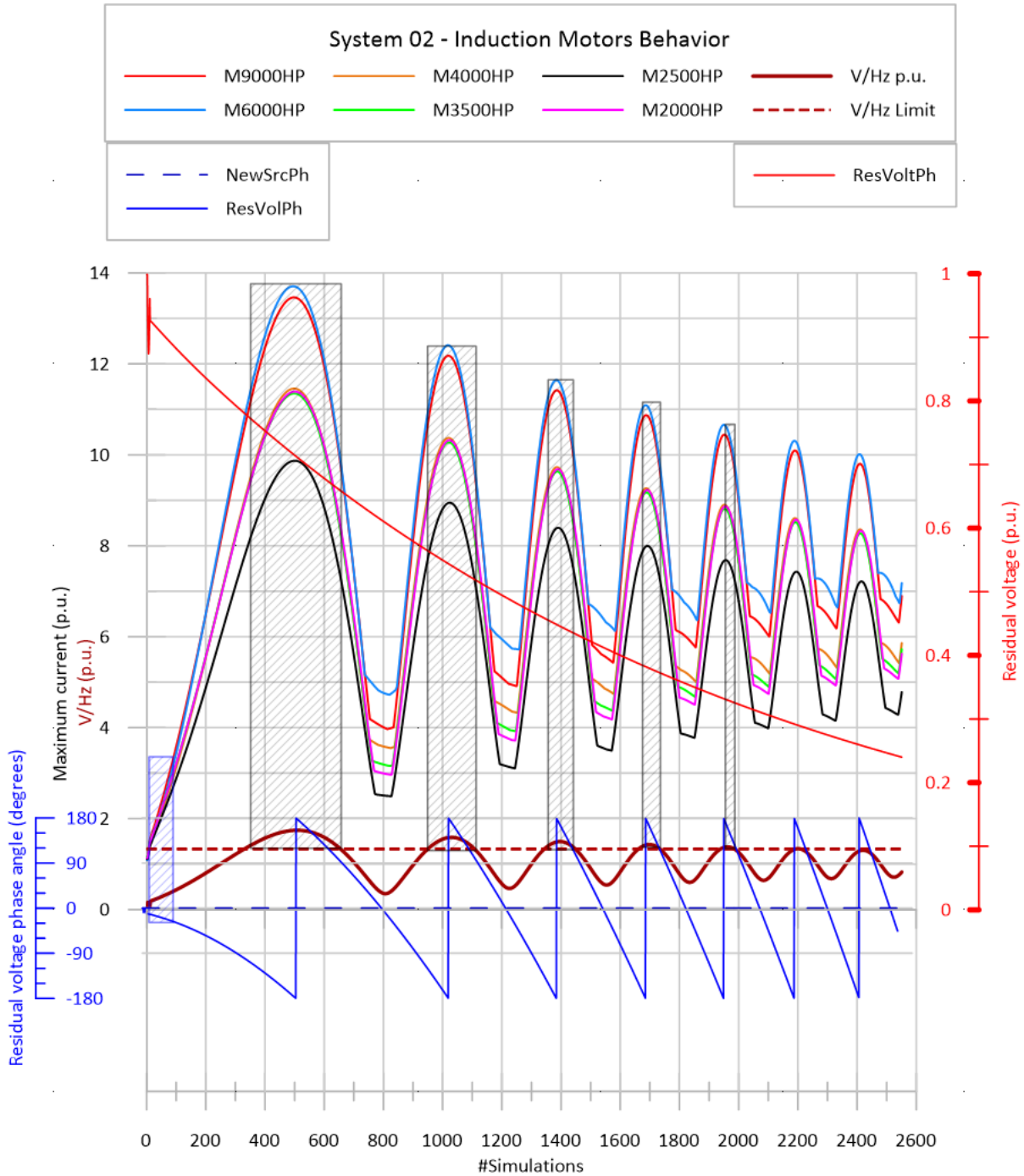


Figure 3-26 System 02 induction motor currents behavior during different closing times of the new source's breaker.

The area in blue corresponds to a phase angle difference of 30 degrees between residual voltage and the new source. This region is recommended for motor transfer using the fast It may be observed that in this region the volts/Hertz in p.u. are lower than the volts/Hertz limit of 1.33 p.u. and that the induction current magnitudes during the reconnection are lower than 4 p.u. for this system.

In contrast, the areas in gray, are regions where volts/Hertz magnitudes in p.u. are above the limit of 1.33 p.u. In these regions, improper transfers may produce very high reconnection currents that may subsequently damage the induction motors. For this system 02, currents close to 12 p.u. may be developed in the areas in gray. A proper adjustment of volts/Hertz would avoid motor transfers in these regions. Intermediate areas between the areas in gray, show volts/Hertz values lower than the limit 1.33 p.u. resulting in a volts/Hertz minimum value in the phase coincidence between the voltage of the motor bus and the voltage of the new source. However, while the reclosing time is approaching the areas in gray, the volts/Hertz in p.u. is increasing but its magnitude is still lower than the limit of 1.33 p.u. and transfers on those regions show high current magnitudes. In several simulations, the results have magnitudes higher than 10 p.u.

Finally, for this system and its set conditions, when the residual voltage is less than 0.35 p.u. the volts/Hertz magnitude is lower than the volts/Hertz limit of 1.33 p.u. Even under these conditions, some induction motors transfers result in reconnection currents higher than 8 p.u.

Figure 3-27 shows the results of maximum positive and negative electromagnetic torques of each induction motor for each simulation during reconnection to the new source. It can be observed that all motor electromagnetic torques follow the same behavior pattern similar to that shown in system 01. First, magnitude of negative torques increases while the voltage phase angle of the motor bus moves forward from the voltage phase angle of the new source. Second, the negative torque magnitude decreases while the voltage phase angle of the motor bus approaches to the voltage phase angle of the new source. Third, the negative torque magnitude is maximum when the residual voltage phase angle is closer to the phase opposition with respect to the phase angle of the new source. In some simulations, negative electromagnetic torques of all motors of this system are higher than 8 p.u. for the first region in gray.

Fourth, the negative torque magnitude is minimal in the phase coincidence between the residual voltage phase angle of the motor bus and the voltage phase angle of the new source. Negative torques are minimum as from the first phase coincidence and during the following 90 degrees forward of the phase coincidence. In contrast, positive torques are more relevant in these zones, and some cases reach positive torques of magnitudes greater than 4 p.u.

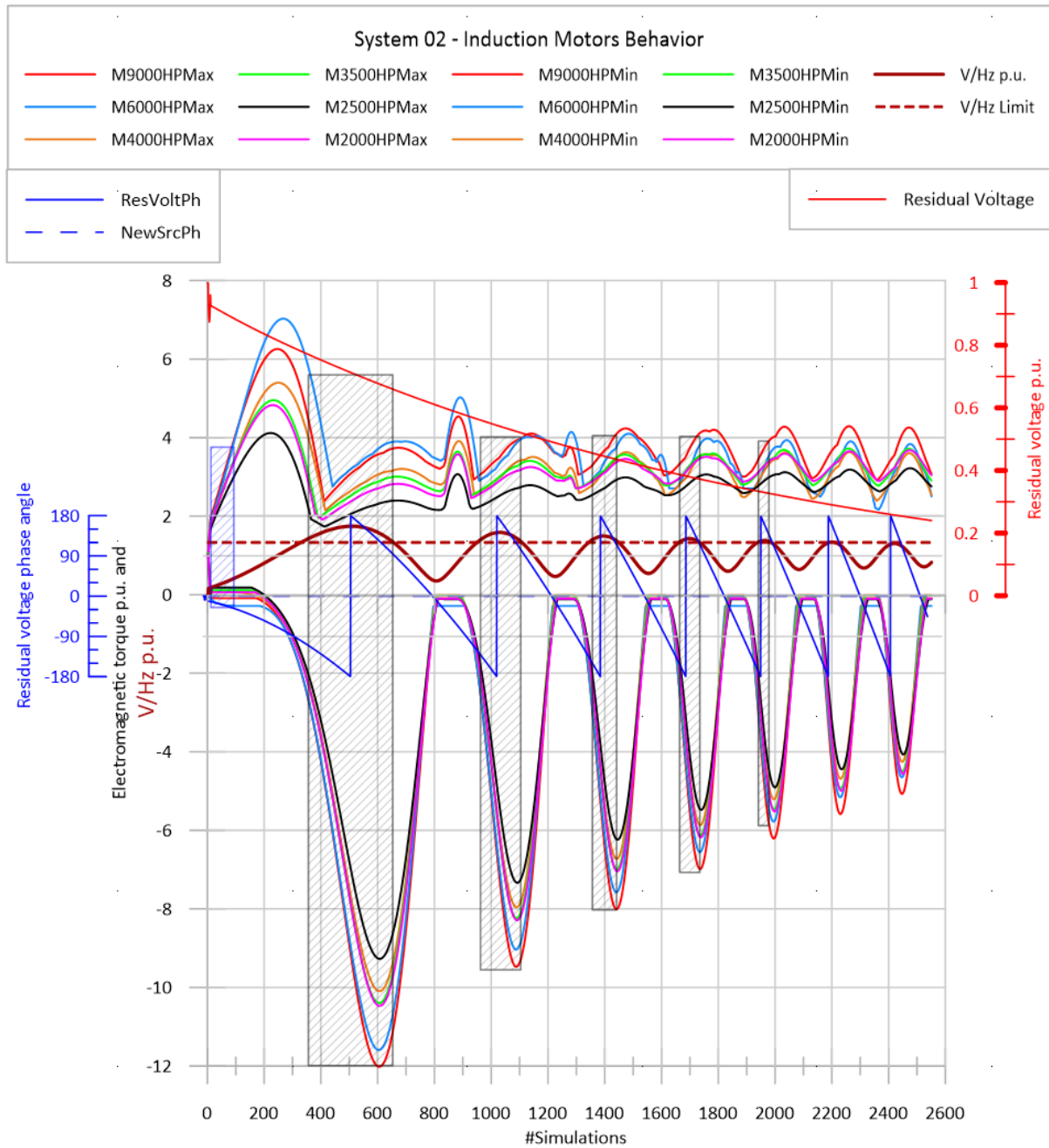


Figure 3-27 System 02 induction motor electromagnetic torques behavior during different closing times of the new source's breaker.



The area in blue corresponds to a phase angle difference of 30 degrees between residual voltage and the new source. It is the recommended region for motor transfer using the fast-transfer method. It may be observed that in this region the volts/Hertz in p.u. are lower than the volts/Hertz limit of 1.33 p.u., and the induction motor negative torque magnitudes during the reconnection are lower than 0.5 p.u. while positive electromagnetic torques may reach up to 3.5 p.u. for this system.

In contrast, the areas in gray are regions where the volts/Hertz magnitudes in p.u. are greater than the limit of 1.33 p.u. In these regions, improper transfers may produce very high positive and negative electromagnetic torques that may subsequently damage the induction motors. A proper adjustment of the volts/Hertz limit would avoid motor transfer in these regions. Intermediate areas between the regions in gray, show volts/Hertz values lower than the limit of 1.33 p.u. resulting in a minimum value of volts/Hertz in the phase coincidence between the motor bus voltage and the new source voltage. However, while the reclosing time is approaching the areas in gray, the p.u. volts/Hertz value increases but is still lower than the limit of 1.33 p.u. and negative electromagnetic torques of high magnitude are developed. In several simulations with reclosing times in these zones, negative electromagnetic torques of magnitudes above 9 p.u. for this system may be developed.

Finally, for this system and its set conditions, when a residual voltage is lower than 0.35 p.u. the volts/Hertz magnitude is lower than the volts/Hertz limit of 1.33 p.u. Under these transfer conditions, some motors show negative electromagnetic torques larger than 5 p.u.

In general, for transfers with reclosing times above the first 90 degrees of phase difference between the residual voltage of the motor bus and voltage of the new source, the motor positive electromagnetic torques of system 02 are kept lower than 4 p.u.

In summary, in the first case of simulation of power loss of individual motors, it may be observed that during the loss of power supply the motors with greater inertia show a slower residual voltage decay than the medium-and-low inertia motors. In the second case of simulations, it is analyzed and proved that, in general, larger machines act as induction generators by supplying current to smaller machines.

In the third case of simulations, it is analyzed and proved that if the voltage difference is maximum when the motor bus is reconnected to the new source, higher motor currents may be produced than the motor starting currents and negative electromagnetic torques may be developed that may stress and even damage the motor shaft.

In the fourth case of simulations, it is shown and analyzed that if there is a large frequency difference between the motor bus residual voltage and the new source voltage when reconnecting the motor bus to the new source, the motor response produces damped oscillating currents and damped oscillating electromagnetic torques. In some cases, the damped oscillating electromagnetic torques may have several cycles between positive and negative values.

In the fifth and sixth cases, it is shown in detail through more than 4600 simulations the effect in the current and in the electromagnetic torques as result of the new source breaker reclosing time. Although the volts /hertz criterion of 1.33 is suitable for some of the regions where the torques can be very large, in many of the simulations negative torques greater than 6 p.u. are developed in conditions of volts / hertz values lower than the limit of 1.33.

The next chapter describes the power system model for simulation of the motor bus transfer system and then Chapter 5 covers in detail the motor bus transfer model.

## **CHAPTER 4 - POWER STATION SYSTEM MODEL FOR SIMULATION OF A MOTOR BUS TRANSFER SYSTEM**

### 4.1 Introduction

The power system modeled in this work represents a typical power station consisting of: 1) an auxiliary motor bus with five induction motors, 2) an auxiliary transformer, 3) a start-up transformer, 4) an equivalent system connected to a high voltage transmission line that is connected to the start-up transformer, 5) an equivalent system connected to a high voltage transmission line that is connected to the station transformer, 6) the main station power transformer and 7) a power generator.

The complete system was modeled using the electromagnetic transients program PSCAD/EMTDC, which will be briefly described in the following section.

### 4.2 PSCAD/EMTDC

#### 4.2.1 Introduction

EMTDC stands for Electromagnetic Transients including DC, which represents and solves differential equations in the time domain and PSCAD stands for Power System Computer Aided Design which is a powerful and graphical user-friendly interface to the EMTDC. Two important strengths of PSCAD/EMTDC are its comprehensive library of components and its ability to allow the user to build complex electrical and control networks in a graphical environment. PSCAD/EMTDC is most suitable for simulating electromagnetic transients of electrical systems [3].

The main power system components included in PSCAD/EMTDC are:

- 1) Passive elements, R, L, and C lumped, distributed linear or non-linear.
- 2) Independent or controlled voltage sources and current sources.
- 3) Breakers controlled by time or by user developed modules.
- 4) Power transformers.
- 5) Induction motors, synchronous generators, and direct current machines.

- 6) Control systems such as governors, power system stabilizers, AC, DC and static exciters.
- 7) Transmission lines using Bergeron or frequency dependent phase domain and modal domain models.
- 8) Cables using Bergeron or frequency dependent phase domain and modal domain models.
- 9) Voltage, current, power, and frequency meters.
- 10) Protective relays schemes.
- 11) Continuous system model functions, digital and analog control blocks.

PSCAD/EMTDC has been widely used in power system planning, operation, design, commissioning, teaching, and research.

### 4.3 Power System Model

#### 4.3.1 One-Line Diagram

The one-line diagram of the power system used in this research is shown in Figure 4-1. It is a type I bus configuration with an auxiliary motor bus with 9000 HP, 6000 HP, 1400 HP and 1000 HP pumps and 3200 HP and 470 HP fans which will be described in detail in the following sections. The startup transformer is rated at 230 kV/4.36 kV, 28 MVA, Delta-Wye-grounded and the auxiliary transformer is rated at 20 kV/4.36 kV, 28 MVA, Delta-Wye-grounded.

The motor bus has a rated voltage of 4.16 kV. The western and eastern equivalent systems are both 230 kV systems. The main station generator is rated at 300 MVA, 20 kV and the main station transformer is rated 300MVA, delta-star grounded with a voltage transformation ratio of 20/230 kV.

The instantaneous current  $I_{WStart}$  and  $I_{WAux}$  and instantaneous voltages  $V_{WStart}$  and  $V_{WAux}$  are measured at the low voltage side of the startup and auxiliary buses respectively and together with the instantaneous voltage  $V_{WMotor}$  measured at the motor bus are inputs to the motor bus transfer module. Both frequencies  $F_{WStart}$  and  $F_{WAux}$  are measured at the low voltage side of the startup and auxiliary buses and are also inputs to the motor bus transfer module.

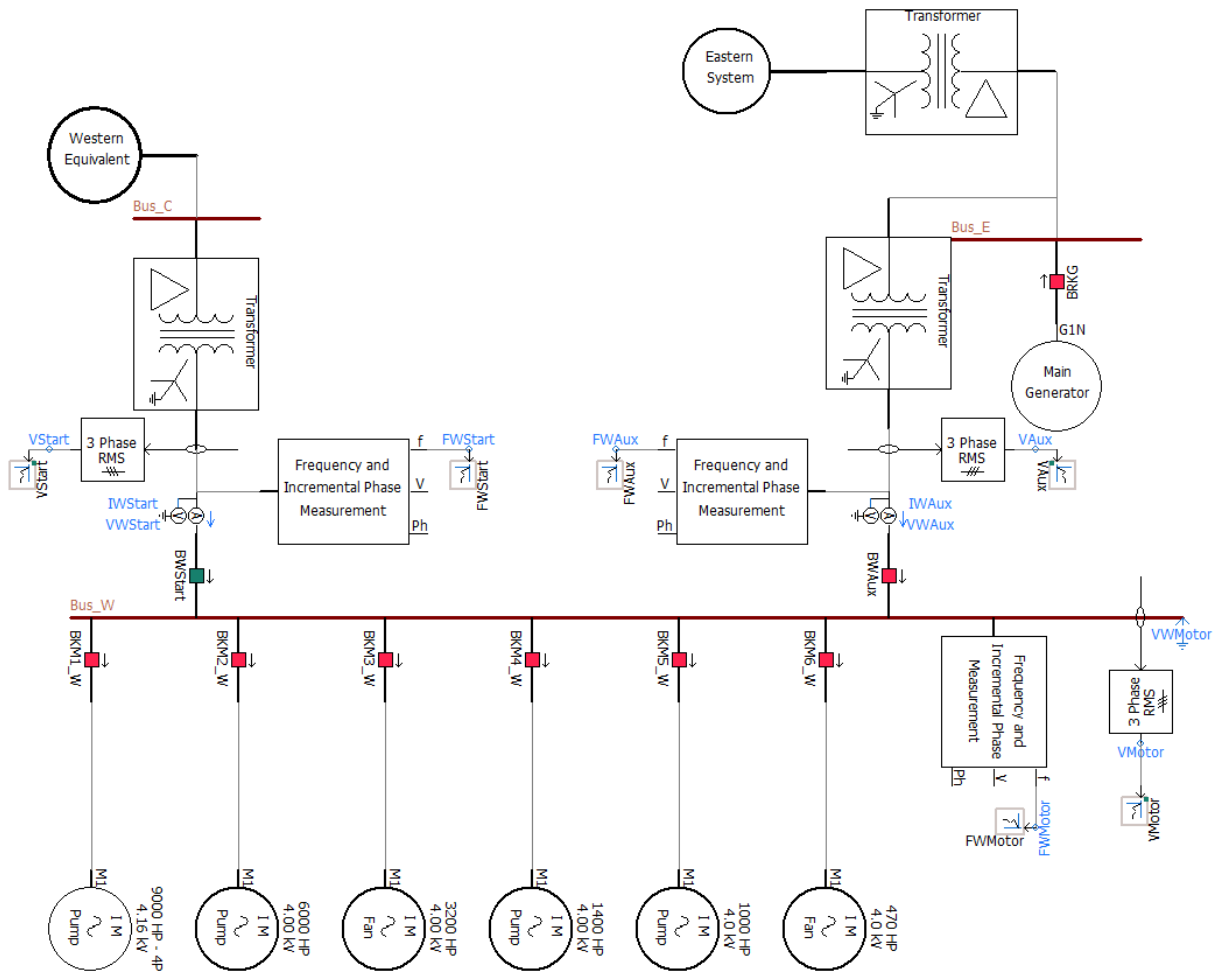


Figure 4-1 Power system model one-line diagram

### 4.3.2 Western Equivalent System

The detailed western equivalent system is shown in Figure 4-2. It consists of two 230 kV equivalent sources. Each one connected to the start-up high voltage transformer bus through a 230-kV transmission line.

The 230 kV transmission lines were modeled with the same conductors and tower configuration using the frequency dependent line model built-in in PSCAD/EMTDC and the data and configuration are shown in the Appendix A.

The equivalent system called EqSystem2 is sending active and reactive power to the system called EqSystem1. There is a transformer at bus C for the startup supply for the generator plant.

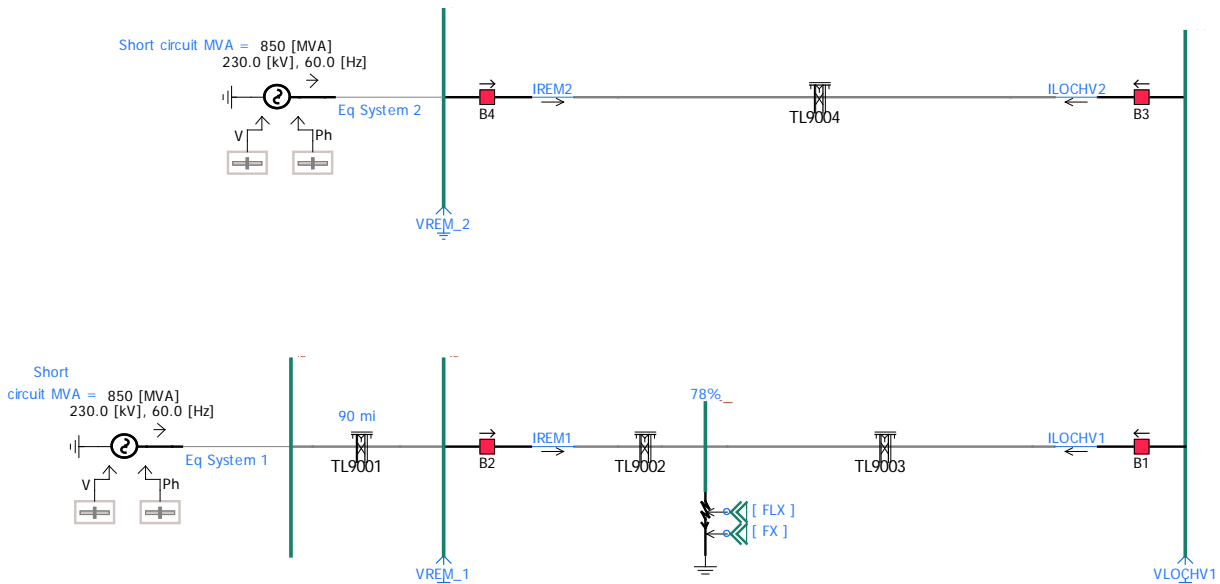


Figure 4-2 Western equivalent system

#### 4.3.3 Eastern Equivalent System

The Eastern equivalent system is shown in more detail in Figure 4-3. It consists of one 230 kV equivalent source connected to the power station high voltage transformer bus through a 230-kV transmission line. The transmission line has been modeled using the Frequency Dependent Model included in PSCAD/EMTDC and its data and geometrical configuration are shown in the Appendix A. The generator feeds the eastern system.

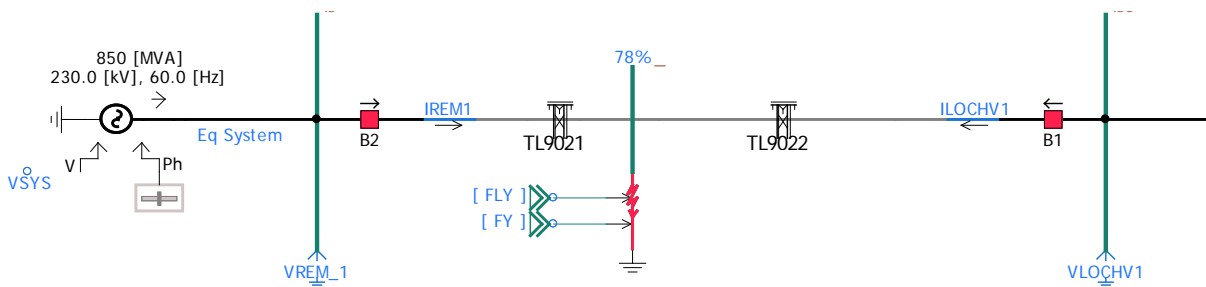


Figure 4-3 Eastern equivalent system

#### 4.3.4 Start-up Transformer

The start-up transformer circuit shown in Figure 4-4 is a three phase Delta-Wye-grounded connected, 230 kV / 4.36 kV, 28 MVA with a leakage reactance of 0.1 p.u. Capacitances and the magnetization branch have not been included in the model.

A PSCAD/EMTDC three phase fault component with signals named “FaultLoc” and “Fault” was added to the transformer module to simulate line-to-line as well as line-to-neutral faults.

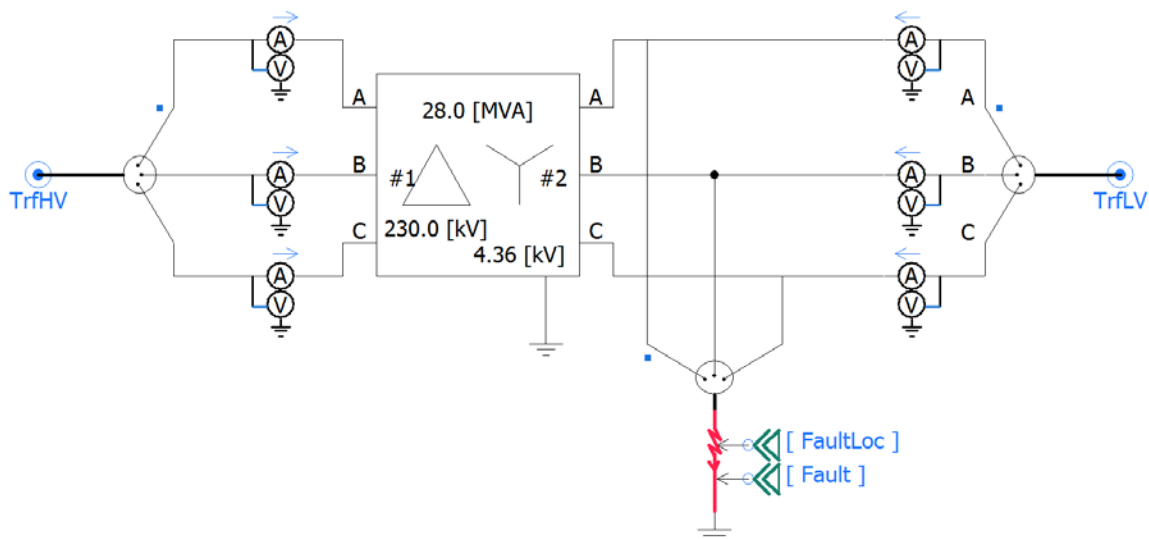


Figure 4-4 Start-up transformer circuit

#### 4.3.5 Auxiliary Transformer

The auxiliary transformer circuit shown in Figure 4-5 is a three phase Delta-Wye connected, 20 kV / 4.36 kV 28 MVA with a leakage reactance of 0.1 p.u. Capacitances and the magnetization branch have not been included in the model.

A PSCAD/EMTDC three phase fault component with signals named “FaultLoc” and “Fault” was added to the transformer module to simulate line-to-line as well as line-to-neutral faults.

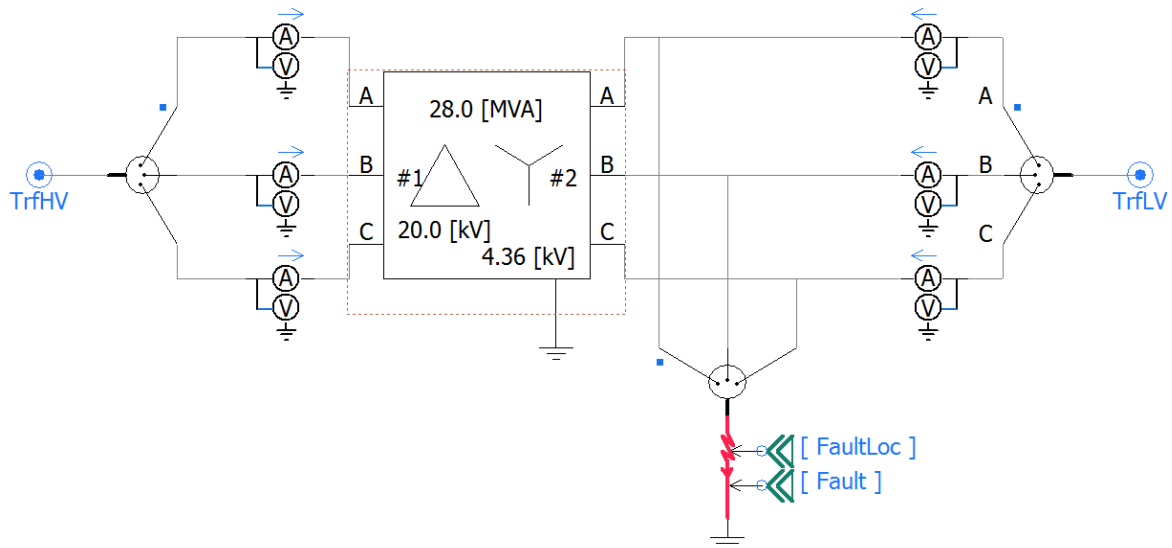


Figure 4-5 Auxiliary transformer circuit

#### 4.3.6 Power Station Generator Equivalent

Figure 4-6 shows the power station generator equivalent modeled using an equivalent source. The voltage magnitude of the simple equivalent voltage source has been configured to allow the source voltage to be reduced to 75% of the nominal operating voltage to initiate a motor bus transfer by the operation of an under-voltage relay.

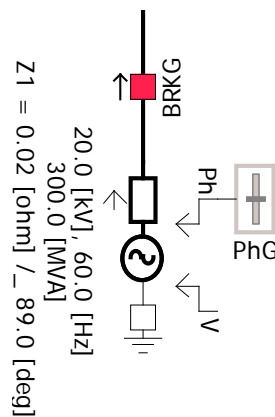


Figure 4-6 Power station generator equivalent



#### 4.3.7 Power Station Main Transformer

The power station main transformer is a 300MVA, Delta-Wye 230 kV / 20 kV with a leakage reactance of 0.7 p.u. The transformer circuit module used is shown in Figure 4-7.

A PSCAD/EMTDC three phase fault component with signals named "FaultLoc" and "Fault" was added to the transformer module to simulate line-to-line as well as line-to-neutral faults.

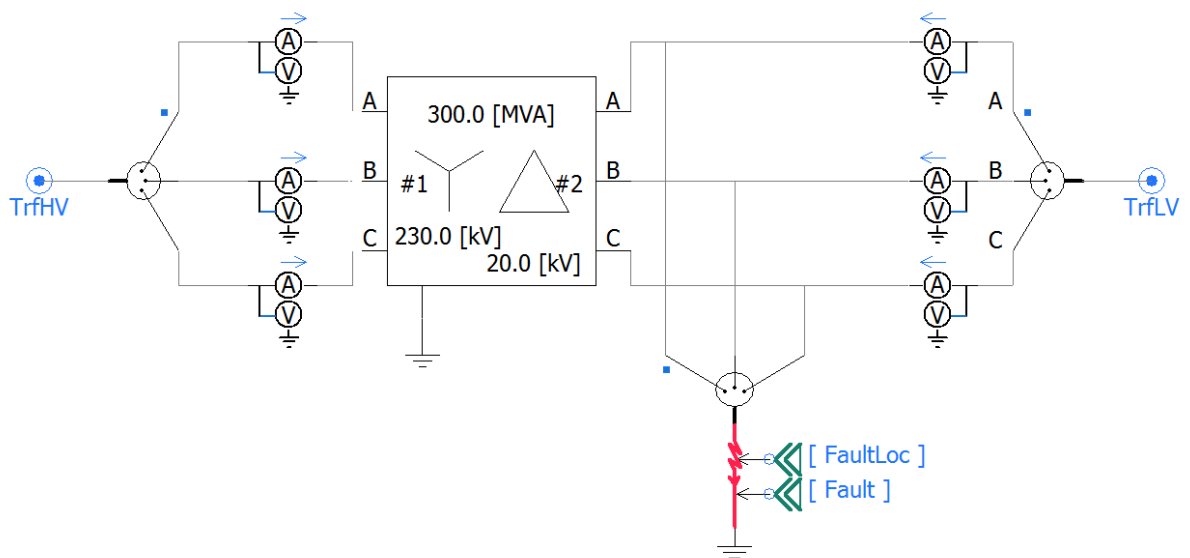


Figure 4-7 Main Station Transformer Model in PSCAD/EMTDC

#### 4.3.8 Induction Motors

The induction motors were represented using the built-in induction motor model of PSCAD. The load torque fitting factors were computed using the EDSA motor parameter estimation program [23]. The induction motor electrical parameters were computed directly by PSCAD/EMTDC using the EMTP type 40 model machine [2].

Table 4-1 shows the electrical and mechanical parameters of the five motors included in the power system modeled in the PSCAD/EMTDC.

	9000 HP	6000 HP	3200 HP	1400 HP	1000 HP	470 HP
	Pump	Pump	Fan	Pump	Pump	Fan
Rated Voltage kV L-L	4.16	4.0	4.0	4.0	4.0	4.0
Rated Voltage kV L-G	2.4017	2.3094	2.3094	2.3094	2.3094	2.3094
Rated Power HP	9000	6000	3200	1400	1000	470
Rated Phase Current	1075.46	873.63	423.97	203.84	145.606	62.27
Efficiency	0.973	0.85	0.90	0.87	0.87	0.90
Power Factor	0.89	0.87	0.903	0.85	0.85	0.903
Starting pf	0.2	0.2	0.2	0.2	0.25	0.25
Poles	4	4	6	4	4	6
Starting Tq (p.u.)	10	1.0	1.0	1.0	1.0	1.0
LRA/FLA (p.u.)	6.9	6.2	7.0	5.9	6.2	7.0
Motor Class	B	B	B	B	B	B
Synch Speed	1800	1800	1200	1800	1800	1200
Rated Speed	1787	1785	1190	1780	1780	1190
Slip	0.0072	0.0084	0.0084	0.01124	0.01124	0.0084
Inertia Motor (s)	0.5263	0.3606	0.3669	0.2061	0.1890	0.3501
Inertia Load (s)	4.0936	3.1143	4.5330	4.0138	3.6809	4.3248
Inertia (Motor and Load) (s)	4.62	3.475	4.9	4.229	3.87	4.678
Torque Fitting						
A0	0.3	0.3	0.17	0.3	0.3	0.17
A1	-1.171	-1.171	-0.696	-1.171	-1.171	-0.696
A2	2.413	2.413	1.948	2.413	2.413	1.948
A3	-0.543	-0.543	-0.371	-0.543	-0.543	-0.371

Table 4-1 Induction Motor Parameters

Table 4-2 compares the given rated parameters with their corresponding parameters computed with PSCAD/EMTDC. The simulation results from the induction motor modeled in PSCAD/EMTDC are consistent with the given parameters.

	9000 HP	6000 HP	3200 HP	1400 HP	1000 HP	470 HP
	Pump	Pump	Fan	Pump	Pump	Fan
Rated current (Given)	1 p.u.	1 p.u.	1 p.u.	1 p.u.	1 p.u.	1 p.u.
Rated current (Computed with PSCAD/EMTDC)	1.065	1.118 p.u.	1.147 p.u.	1.112 p.u.	1.126 p.u.	1.144 p.u.
Starting current (Given)	6.9 p.u.	6.2 p.u.	7.0 p.u.	5.9 p.u.	6.2 p.u.	7.0 p.u.
Starting current (Computed with PSCAD/EMTDC)	6.867 p.u.	5.92 p.u.	6.63 p.u.	5.643 p.u.	5.9 p.u.	6.63 p.u.
Slip p.u. (Given)	0.0072 p.u.	0.0084 p.u.	0.0084 p.u.	0.01124 p.u.	0.01124 p.u.	0.0084 p.u.
Slip (Computed with PSCAD/EMTDC)	0.011 p.u.	0.018 p.u.	0.015 p.u.	0.020 p.u.	0.018 p.u.	0.015 p.u.
Torque at nominal speed (Given)	1.0 p.u.	1.0 p.u.	1.0 p.u.	1.0 p.u.	1.0 p.u.	1.0 p.u.
Torque at nominal speed (Computed with PSCAD/EMTDC)	0.984 p.u.	0.964 p.u.	1.028 p.u.	0.967 p.u.	0.971 p.u.	1.028 p.u.
Starting torque (Given)	1.0 p.u.	1.0 p.u.	1.0 p.u.	1.0 p.u.	1.0 p.u.	1.0 p.u.
Starting torque (Computed with PSCAD/EMTDC)	1.0 p.u.	1.0 p.u.	1.0 p.u.	1.0 p.u.	1.0 p.u.	1.0 p.u.

*Table 4-2 PSCAD/EMTDC induction motor model validation comparing simulation results with given values*

Figure 4-9 shows the load torque, the electromagnetic torque and current versus speed plots of the 9000 HP induction motor modeled in this research plotted in PSCAD/EMTDC.

The 9000 HP computed motor maximum torque was 2.934 p.u. at a speed of 0.925 p.u. The steady state electromagnetic torque was 0.984 p.u. at a speed of 0.989 p.u. The computed starting current was 6.867 p.u. and the rated current was 1.065 p.u. at a speed of 0.989 p.u.

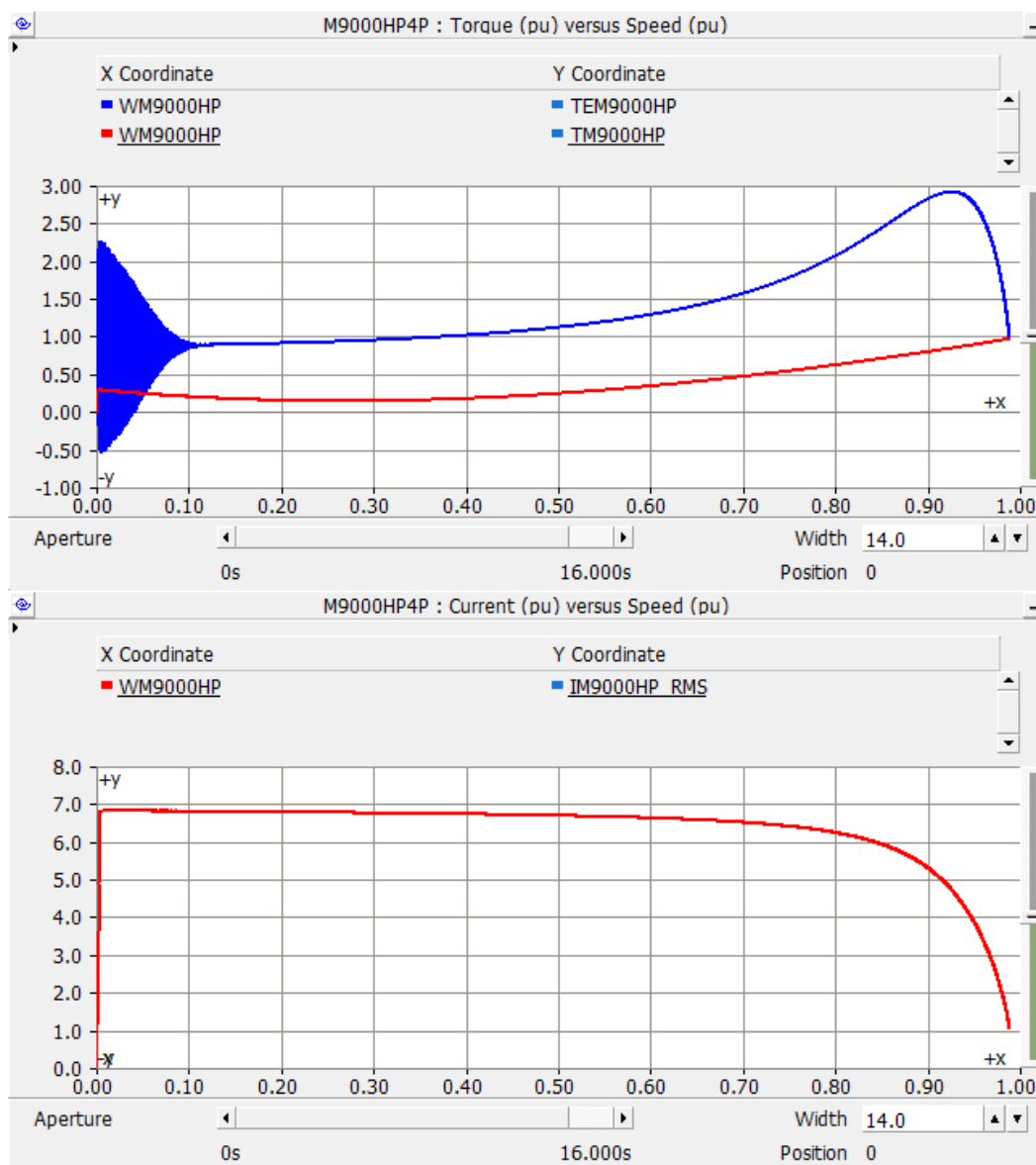


Figure 4-8 9000 HP motor starting performance simulation with PSCAD/EMTDC

Figure 4-9 shows the load torque, the electromagnetic torque and current versus speed plots of the 6000 HP induction motor modeled in this research plotted in PSCAD/EMTDC.

The 6000 HP computed motor maximum torque was 2.104 p.u. at a speed of 0.908 p.u. The steady state electromagnetic torque was 0.964 p.u. at a speed of 0.982 p.u. The computed starting current was 5.92 p.u. and the rated current was 1.118 p.u. at a speed of 0.982 p.u.

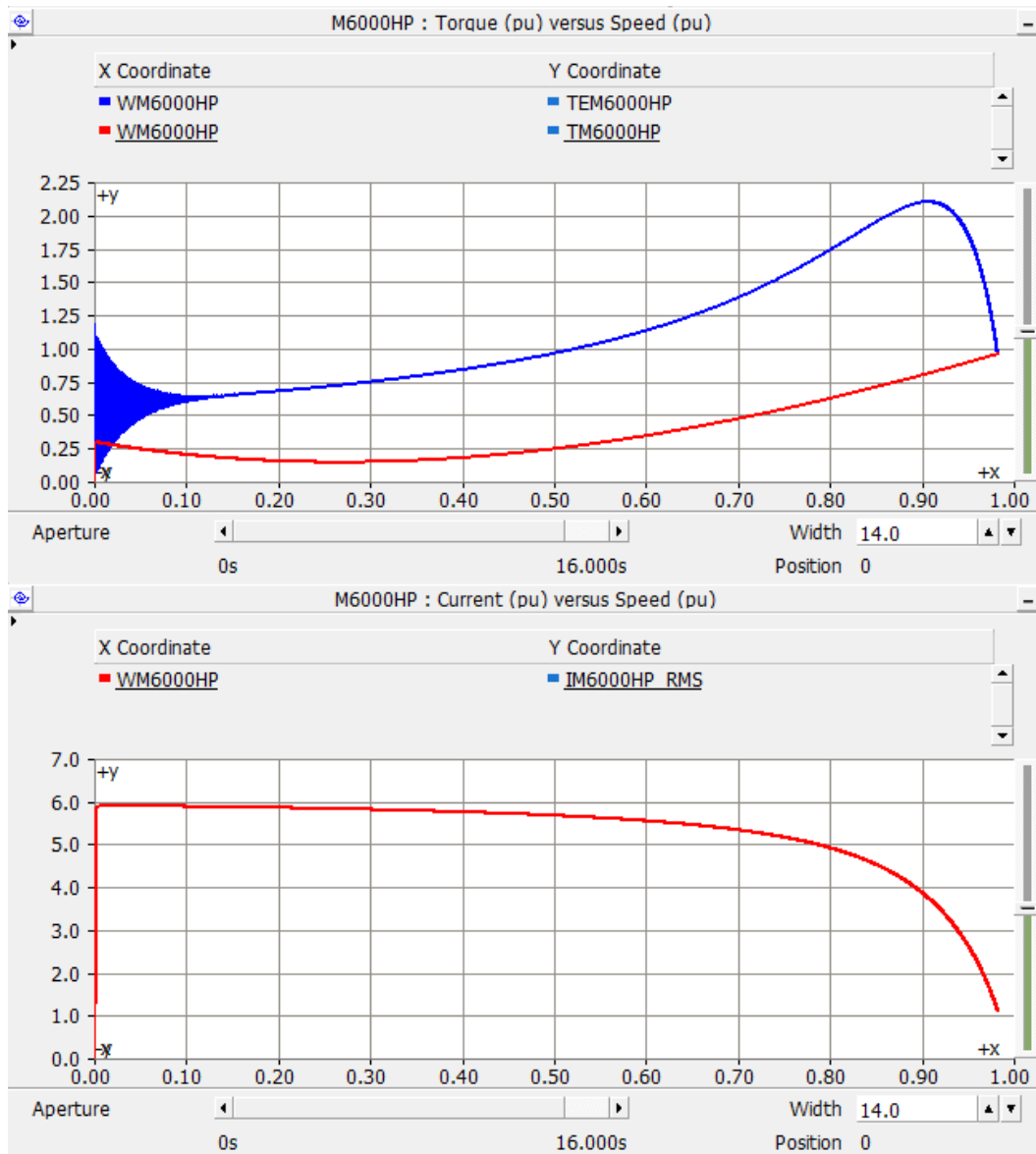


Figure 4-9 6000 HP motor starting performance simulation with PSCAD/EMTDC

Figure 4-10 shows the load torque, the electromagnetic torque and current versus speed plots of the 3200 HP induction motor modeled in this research.

The computed maximum torque was 2.463 p.u. at a speed of 0.916 p.u. The steady state electromagnetic torque was 1.028 p.u. at a speed of 0.985 p.u. The computed starting current was 6.63 p.u. and the rated current was 1.147 p.u. at a speed of 0.985 p.u.

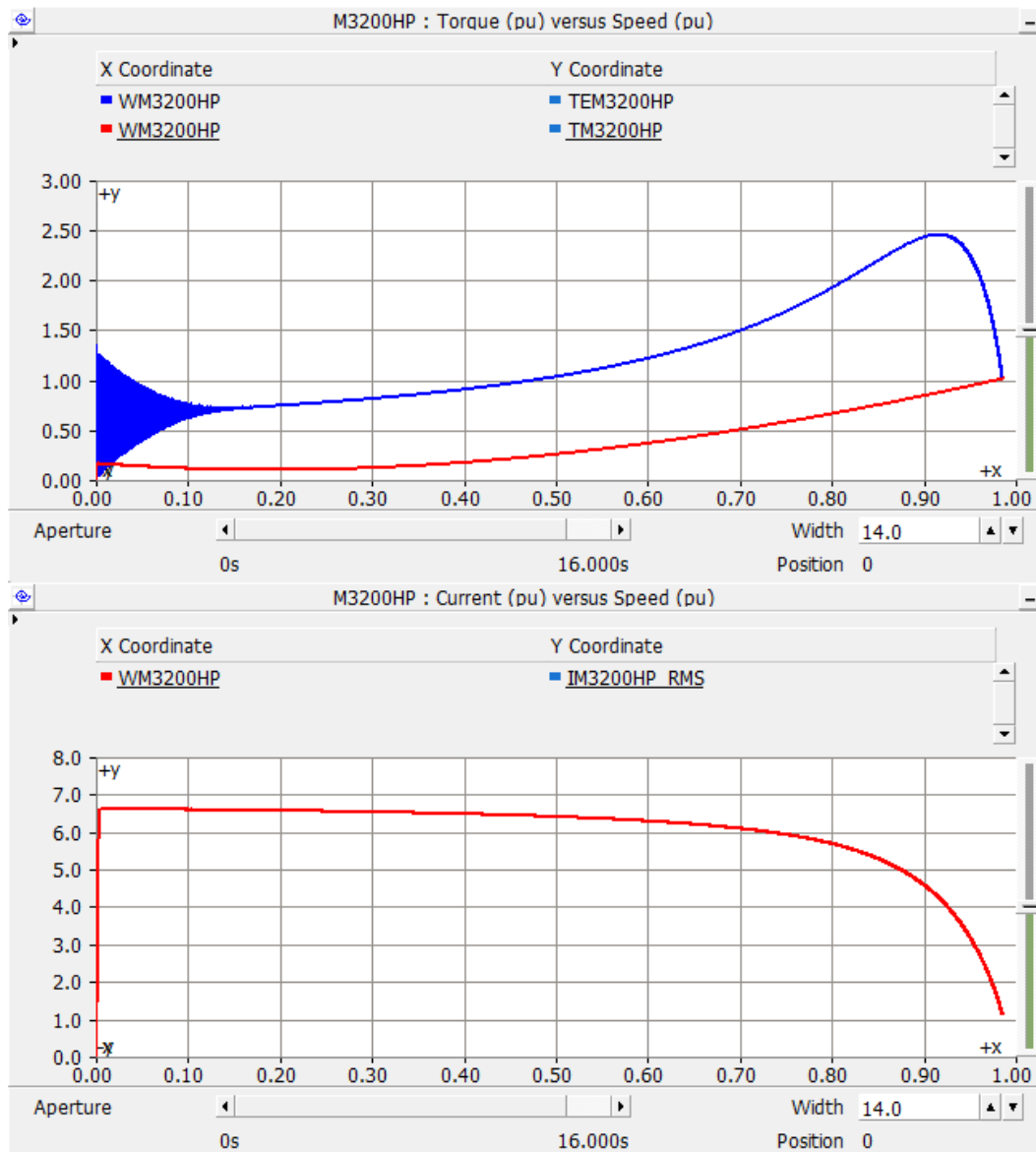


Figure 4-10 3200 HP motor starting performance simulation with PSCAD/EMTDC

Figure 4-11 shows the load torque, the electromagnetic torque and current versus speed plots of the 1400 HP induction motor modeled in this research.

The computed maximum torque was 2.047 p.u. at a speed of 0.902 p.u. The steady state electromagnetic torque was 0.967 p.u. at a speed of 0.98 p.u. The computed starting current was 5.643 p.u. and the rated current was 1.112 p.u. at a speed of 0.98 p.u.

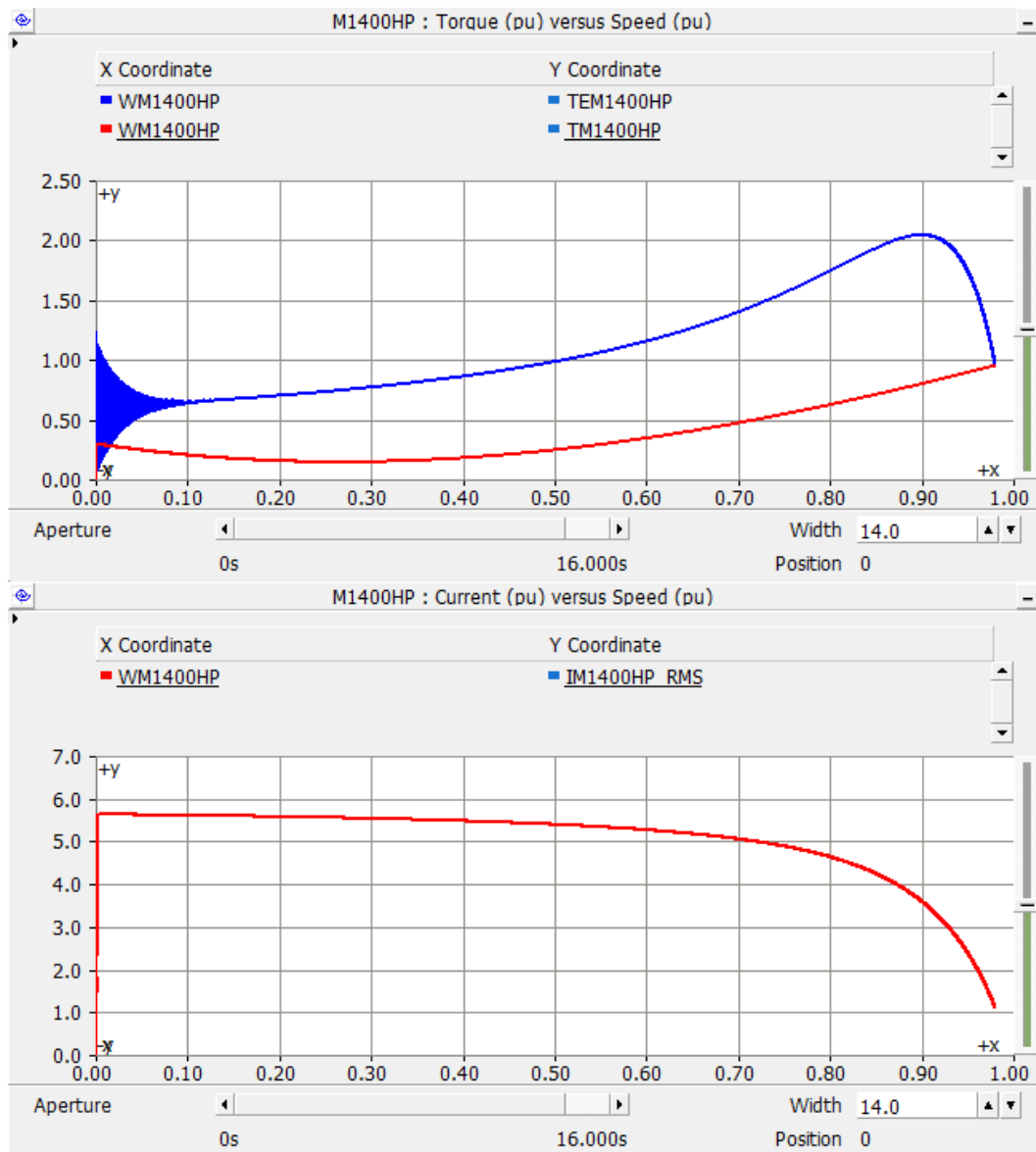


Figure 4-11 1400 HP motor starting performance simulation with PSCAD/EMTDC

Figure 4-12 shows the load torque, electromagnetic torque and current versus speed plots of the 1000 HP induction motor modeled in this research.

The computed maximum torque was 2.11 p.u. at a speed of 0.908 p.u. The steady state electromagnetic torque was 0.971 p.u. at a speed of 0.982 p.u. The computed starting current was 5.9 p.u. and the rated current was 1.126 p.u. at a speed of 0.982 p.u.

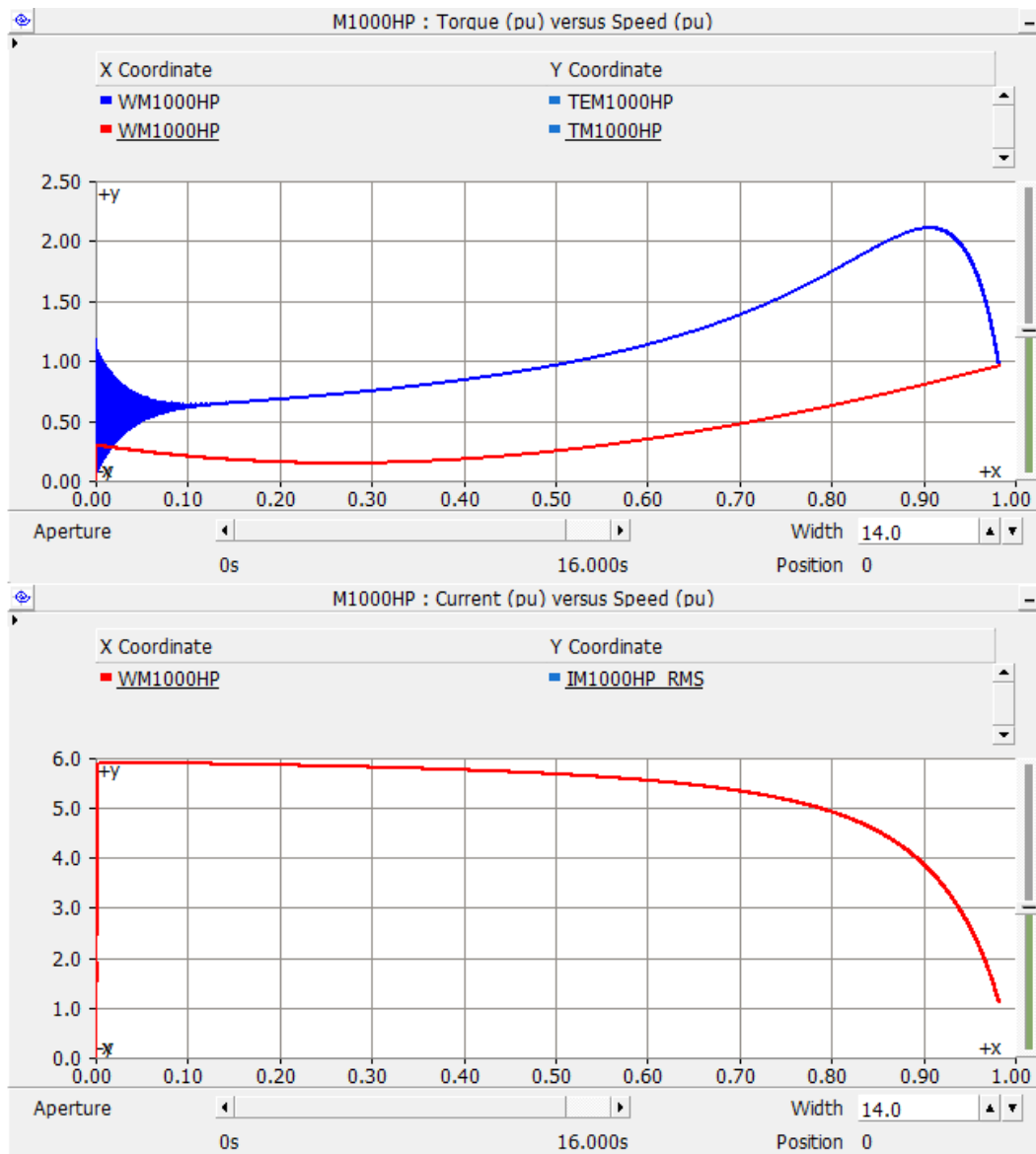


Figure 4-12 1000 HP motor starting performance simulation with PSCAD/EMTDC



Figure 4-13 shows the load torque, electromagnetic torque and current versus speed plots of the 470 HP induction motor modeled in this research.

The computed maximum torque was 2.462 p.u. at a speed of 0.923 p.u. The steady state electromagnetic torque was 1.028 p.u. at a speed of 0.985 p.u. The computed starting current was 6.63 p.u. and the rated current was 1.144 p.u. at a speed of 0.985 p.u.

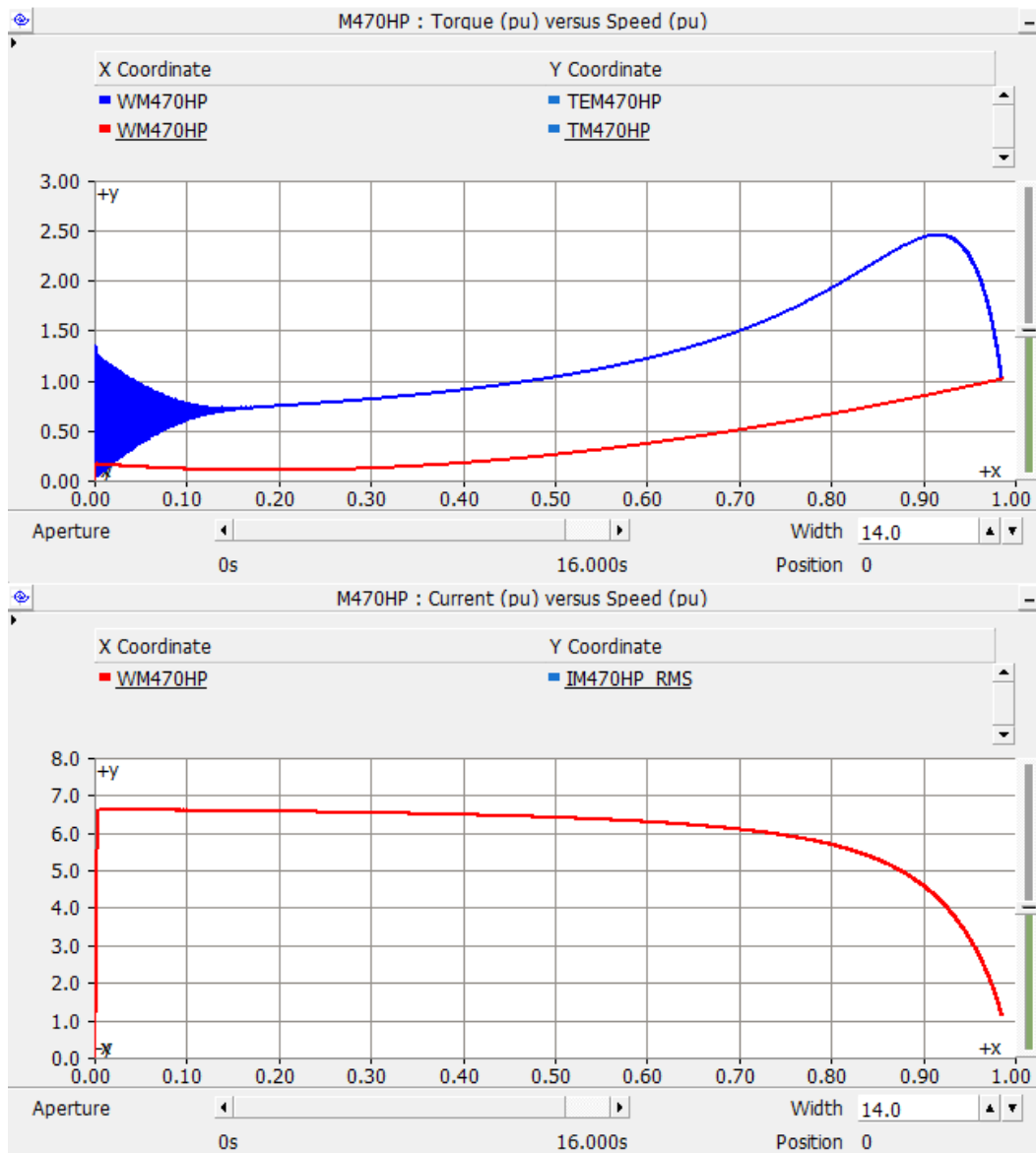


Figure 4-13 470 HP motor starting performance simulation with PSCAD/EMTDC

## CHAPTER 5 - MOTOR BUS TRANSFER SYSTEM MODEL

The motor bus transfer system (MBTS) modeled implemented in PSCAD/EMTDC in this research is shown in Figure 5-1 and it consists of five sections: a) the control panel to control the motor bus transfer simulation modes, b) the relay trip and manual command which initiates the motor bus transfer under fault conditions or manual transfer controlled by time, c) the auxiliary controls which take the signals from the motor bus transfer selector and the coast down simulation selector to control the auxiliary and start-up breakers, d) the motor bus transfer system process unit which takes the measurement inputs, performs the motor bus system algorithms, and outputs commands to control the auxiliary and start-up breakers, and e) the circuit breaker controls block which control the opening and closing of the auxiliary and start-up breakers.

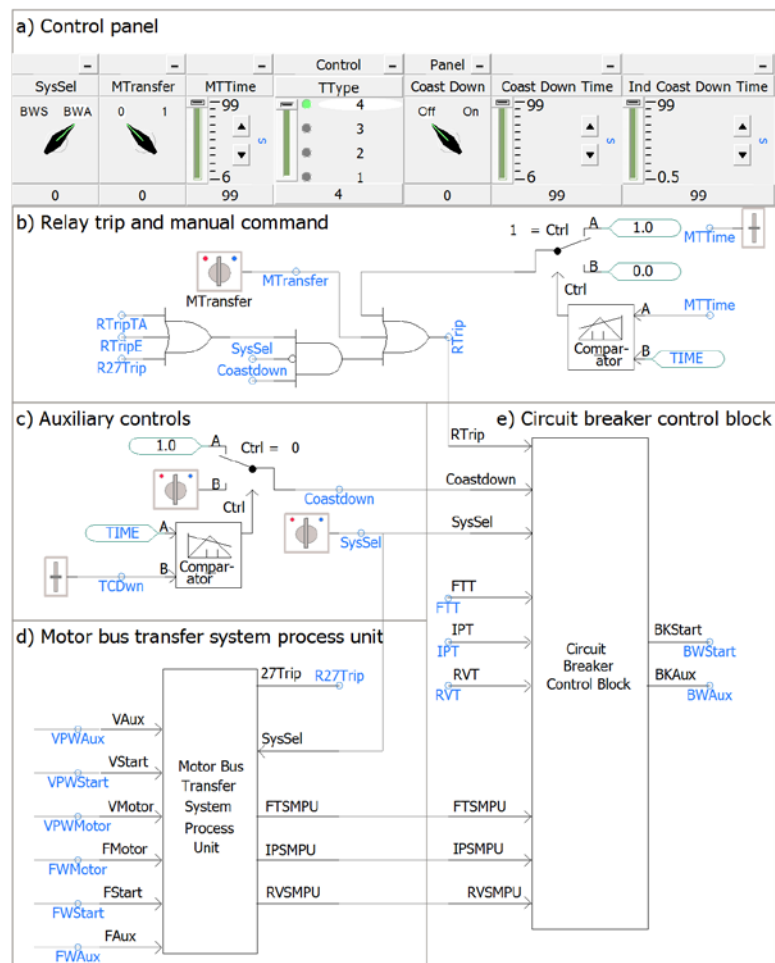


Figure 5-1 Motor bus transfer system model implemented in PSCAD/EMTDC

## 5.1 Control Panel for the Motor Bus Transfer Simulation Modes

Figure 5-2 shows the control panel for the motor bus transfer simulation modes. It uses built-in PSCAD sliders and switches. The control SysSel selects the power supply of the motor bus during the simulation. If the selector is on position BWS the motor bus will be fed from the start-up system whereas if the selector is on position BWA the auxiliary system will supply power to the motor bus.

The control MTransfer is set to activate the motor bus manual transfer simulations.

The control MTime sets the time to start testing the individual motor bus transfer algorithms. The default value has been set to 99 seconds.

The control TType is set to select the motor bus transfer method during the simulation. Position 1 selects the fast transfer method; position 2 selects the in-phase transfer method, position 3 selects the residual voltage transfer method and position 4 allows the simulation to automatically select the transfer mode based on the power system operating conditions.

The controls Coast Down and Coast Down Time set the model to run a coast down simulation blocking any motor bus transfer action. The Coast Down Time is used to set the time to start the coast down action. The controls Coast Down and Ind Coast Down Time set the model to run a coast down simulation opening the power supply breaker of each induction motor to observe each induction motor behavior during a coast down simulation without any current exchange between the motors. The Ind Coast Down Time control set the time to start the coast down action.

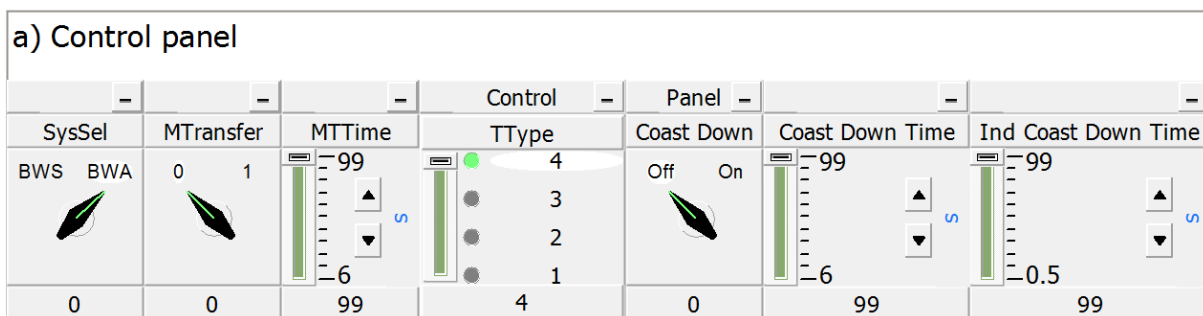


Figure 5-2 Control panel to control the motor bus transfer simulation modes

## 5.2 Relay Trip and Manual Command

The relay trip and manual command section shown in Figure 5-3 was implemented to allow the motor bus transfer system to initialize the transfer either by a relay tripping signal, a manual transfer signal or by a time-controlled test mode.

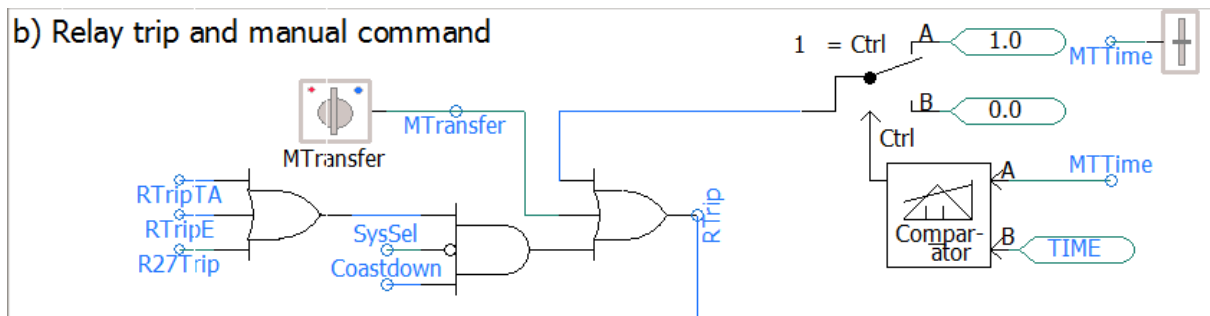


Figure 5-3 Relay trip and manual command

The signal MTransfer is activated when the user changes the status of the switch MTransfer located in the control panel.

The time-controlled signal MTime from Section 5.1 is compared against the running simulation time (TIME) and if it is lower or equal than the simulation running time the comparator output is 1 and the transfer is initiated.

The signal RTripA is received from an auxiliary transformer differential relay when the auxiliary transformer is under fault conditions. The signal RTripE is received from a distance relay when there is a fault in the Eastern transmission line system. The signal R27Trip is received from the motor bus transfer process unit when there is an under-voltage condition in the motor bus.

The signal Coastdown signal is received from the auxiliary controls section in Figure 5-2 to block the trip command if a coast down simulation has been selected in Figure 5-2.

The signal SysSel received from the auxiliary controls section in Figure 5-2 blocks the motor bus transfer if the motor bus is fed from the start-up system and there is a fault in the auxiliary side.

### 5.3 Auxiliary Controls

Figure 5-4 shows the Auxiliary controls section which allows the model to run a simulation of the induction motors either individually or as a group during a coast down test (from the auxiliary source to the start-up source or vice versa depending on signal SysSel). The motors coast down is initiated when the simulation running time reaches the threshold time TCDwn set in the “Coast Down Time Slider” shown in Figure 5-2.

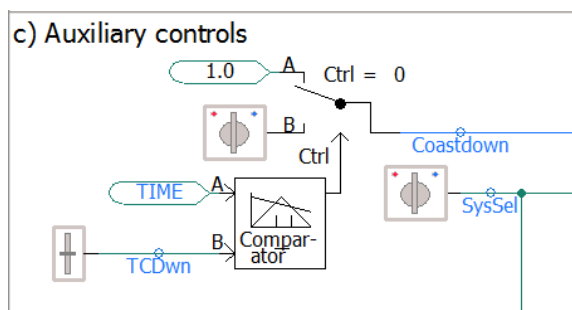


Figure 5-4 Auxiliary controls section

### 5.4 Motor Bus Transfer System Process Unit

The motor bus transfer system process unit is shown in Figure 5-5. The unit processes the inputs according to the standard fast, in-phase and residual voltage transfer algorithms and outputs transfer initiation signals to the circuit breaker control section.

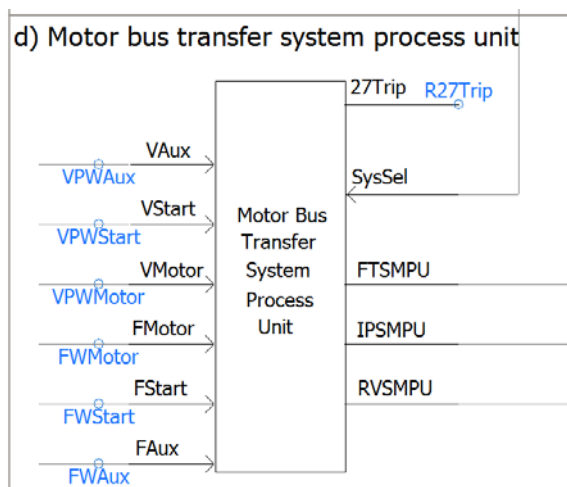


Figure 5-5 Motor bus transfer process unit

The unit has seven inputs: three 3-phase voltage signals identified as VPWMotor, VPWStart and VPWAux; three frequency signals identified as FWMotor, FWStart and FWAux; one signal SysSel that was described in Section 5.1. VPWMotor is the voltage phasor at the motor bus and FWMotor is instantaneous frequency reading from the meters at the motor bus. VPWStart is the voltage phasor at the connection between the start-up transformer low voltage side and the start-up breaker and the FWStart is the instantaneous frequency readings from the frequency meter. VPWAux is the voltage phasor at the connection between the auxiliary transformer low voltage side and the auxiliary breaker and the FWAux is the instantaneous frequency readings from the frequency meter located at the auxiliary low voltage side.

The unit also has four outputs: one from the internal under voltage relay (R27Trip), one from the fast transfer module (FTSMPU), one from the in-phase transfer module (IPSMPU) and, one from the residual voltage transfer module (RVSMPU). These outputs are passed to the circuit breaker control section.

Phasor signals VPWAux, VPWStart and VPWMotor are computed using standard build-in PSCAD/EMTDC components from the instantaneous readings of voltages as shown in Figure 5-6.

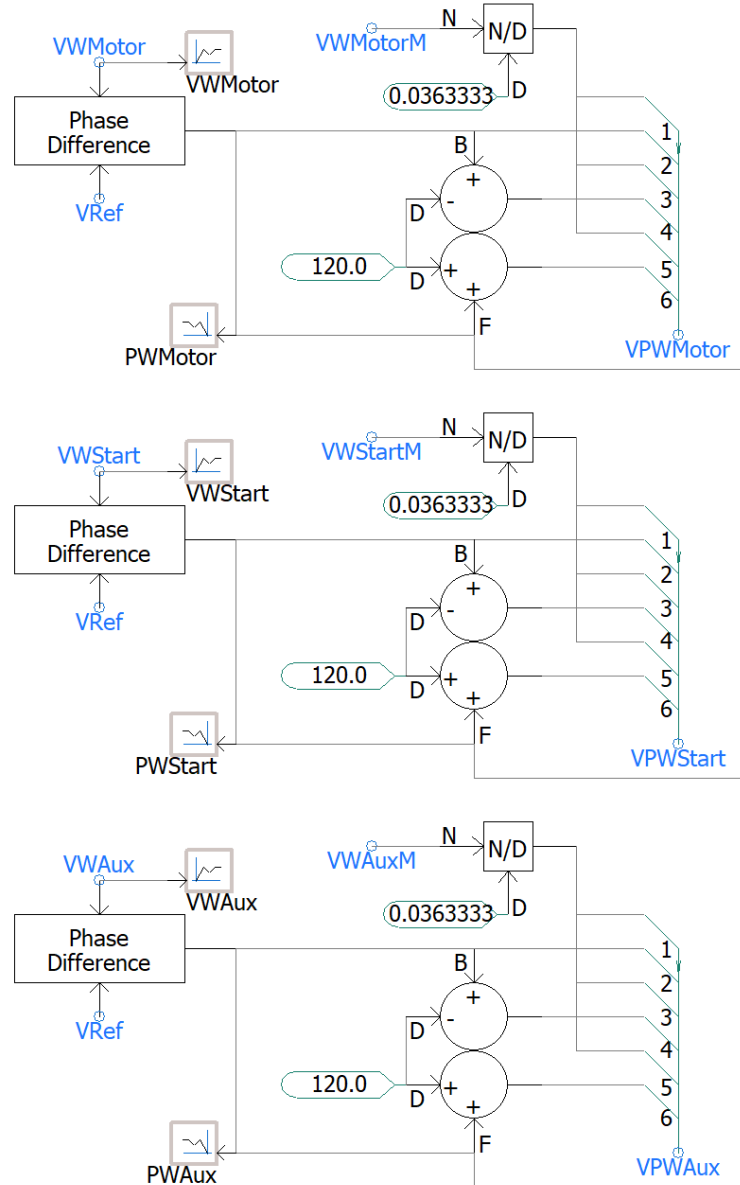


Figure 5-6 Voltage phasors calculation using standard PSCAD/EMTDC build-in modules

Figure 5-7 shows the motor bus transfer system process unit internal components. The 3-phase voltage phasors  $V_{Motor}$  at the motor bus are passed as inputs to the fast, in-phase and residual voltage transfer modules. The three 3-phase voltage phasors  $V_{Aux}$  at the auxiliary side or the 3-phase voltage phasors  $V_{Start}$  at the start-up side are passed to signal  $V_{NSrc}$  depending on the signal  $SysSel$ . If the motor transfer is from the start-up to auxiliary system, signal  $V_{Aux}$  is passed to  $V_{NSrc}$ , and if the motor transfer is from the auxiliary to start-up system, signal  $V_{Start}$  is passed to  $V_{NSrc}$ . The signal  $V_{NSrc}$  is then passed as input to the fast, in-phase and residual voltage modules.

The 3-phase motor bus voltage phasors are also passed to an under-voltage relay which initializes a motor bus transfer in case the motor bus has low voltage conditions.

The motor bus voltage frequency FMotor is passed as input to the three transfer modules. Depending on the signal SysSel value, the signal FStart (motor transfer from the auxiliary to the start-up side) or the signal FAux (motor transfer from the start-up to the auxiliary system) is passed to signal FNSrc. FNSrc is then passed to the transfer modules.

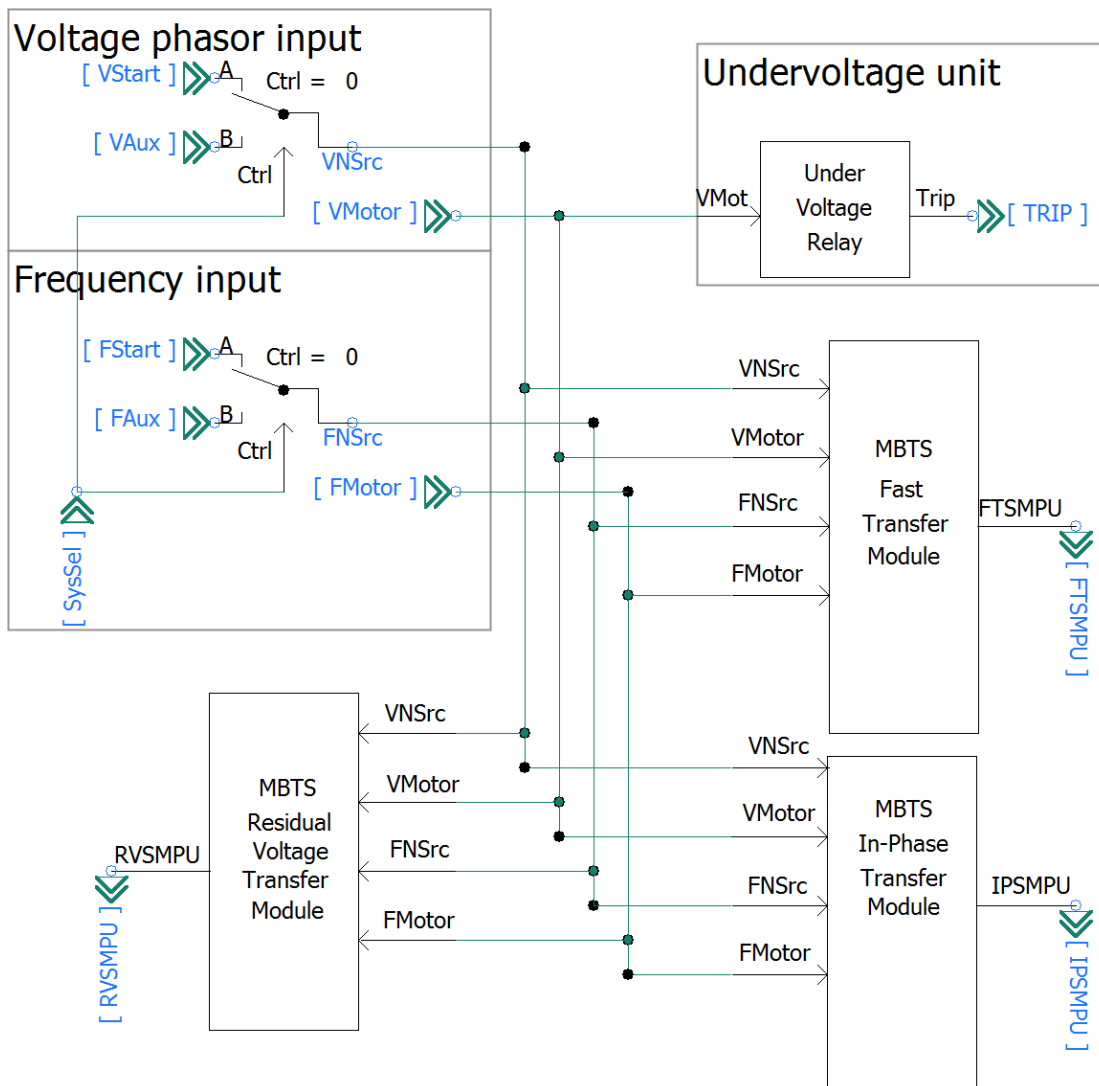


Figure 5-7 Motor bus transfer system process unit internal components



The outputs from the under-voltage relay (TRIP), fast transfer module (FTSMPU), in-phase transfer module (IPSMPU), and residual voltage transfer module (RVSMPU) are passed to the control breaker section.

The algorithms of each module are described in detail in the following subsections.

#### 5.4.1 Motor Bus Transfer System Undervoltage Unit

The motor bus transfer system under voltage unit is shown in Figure 5-8. This under-voltage relay supervises the low voltage condition at the motor bus, if there is a low voltage magnitude lower than the set point of 0.8 p.u. sends a trip output that initializes the motor bus transfer. The input for this under-voltage relay are the motor bus voltage magnitudes (phases a, b, and c), and the output is a trip signal TRIP.

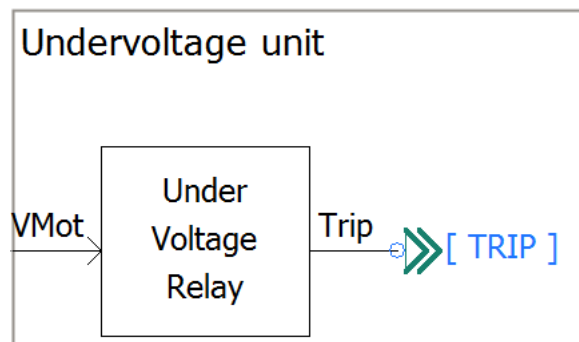


Figure 5-8 Motor bus transfer system under-voltage unit

Figure 5-9 shows the motor bus transfer system under voltage unit details. In the motor bus transfer system under voltage unit, the motor bus voltage magnitude of each phase is converted to per unit (p.u.) using the nominal voltage transformation secondary voltage level as the base voltage which is  $\frac{120Volts}{\sqrt{3}} = 69.2820 Volts$ . These per unit values are then compared to the set point, in this case is set to 0.8 p.u. and if any is lower than the set point a trip command (TRIP) is sent to the relay trip commands section and then to the circuit breaker control module to initiate the circuit breaker operations. When the PSCAD/EMTDC monostable module receives a positive edge, the output remains high for a set of time after being turned on and has been added to keep the trigger signal active.

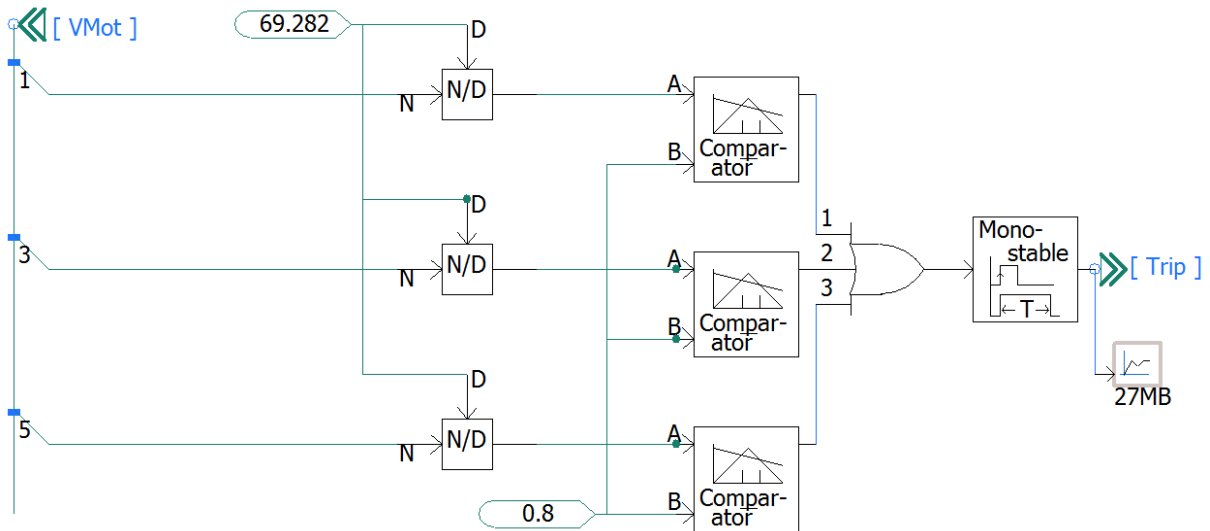


Figure 5-9 Motor bus transfer system under voltage unit details

#### 5.4.2 Motor Bus Transfer System Fast Transfer Module

The MBTS fast transfer module is shown in Figure 5-10. The module has four inputs and one output which are described as follows: a) VMotor that receives the motor bus voltage phasors, b) VNSrc that receives the new source voltage phasors (VAux if the transfer is from the start-up to the auxiliary system or VStart if the transfer is from the auxiliary to the start-up system), c) FMotor which receives the motor bus voltage frequency, and d) FNSrc that receives the new source voltage frequency (FAux if the transfer is from the start-up to the auxiliary system or FStart if the transfer is from the auxiliary to the start-up system)

The MBTS fast transfer module processes the inputs using the fast transfer algorithm and if the conditions are met then it outputs a command FTSMPI. This signal is then passed to the circuit breaker control block.

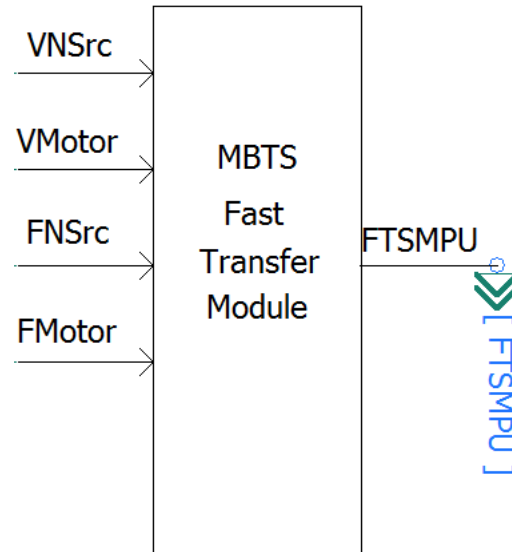


Figure 5-10 Motor bus transfer system fast transfer modules

The fast transfer module requires that the voltage phasor difference, the phase angle difference, and the frequency difference each meet their requirements to allow the motor bus transfer, otherwise the transfer is blocked. Reference [7] suggests a phase angle difference of 30 degrees and a lower limit of 0.90 p.u. and reference [8] suggest a phase angle difference of 20 degrees and a lower voltage limit of 0.85 p.u. These values change according to power plant requirements and operating conditions. In the present example, the phase angle difference was considered 20 degrees, the voltage upper limit was set to 1.15 p.u., and lower voltage limit was set to 0.85 p.u., and the voltage phasor difference magnitude was set to 20 volts.

The fast transfer concept and the phasor diagram representing the new source and the motor bus voltages is depicted in Figure 5-11. The lower and upper limits are shown with dotted lines and the voltage difference at instant time =  $t_x$  is shown with the green arrow.

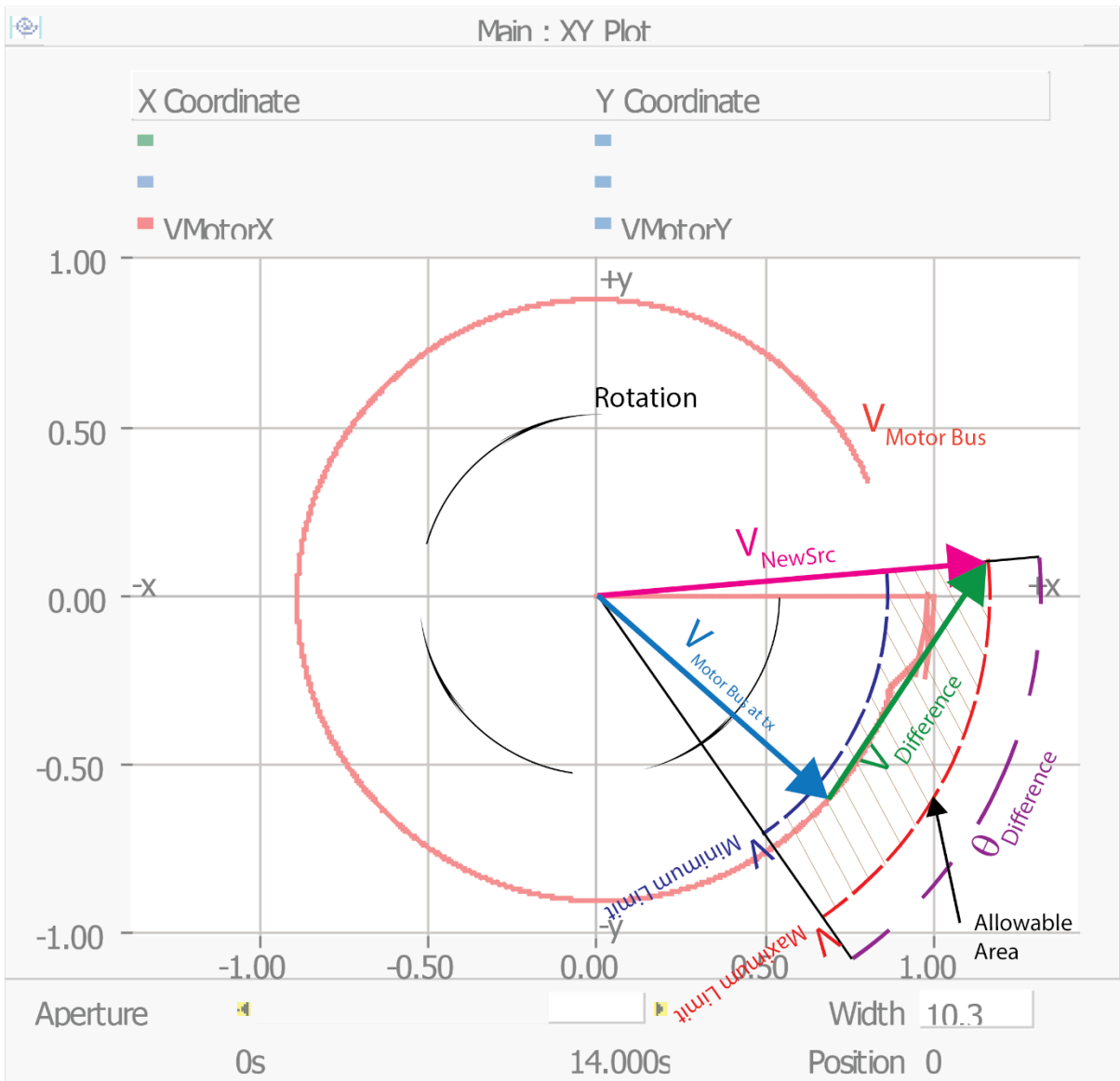


Figure 5-11 Fast transfer concept

The detailed MBTS fast transfer module is shown in Figure 5-12. The right upper part shows the voltage phase angle difference computation and the lower part performs the comparison against the upper and lower voltage limits. The part shown in the middle computes the voltage phasor difference whereas the part in the right middle performs the frequency difference comparison against the frequency slip limit.

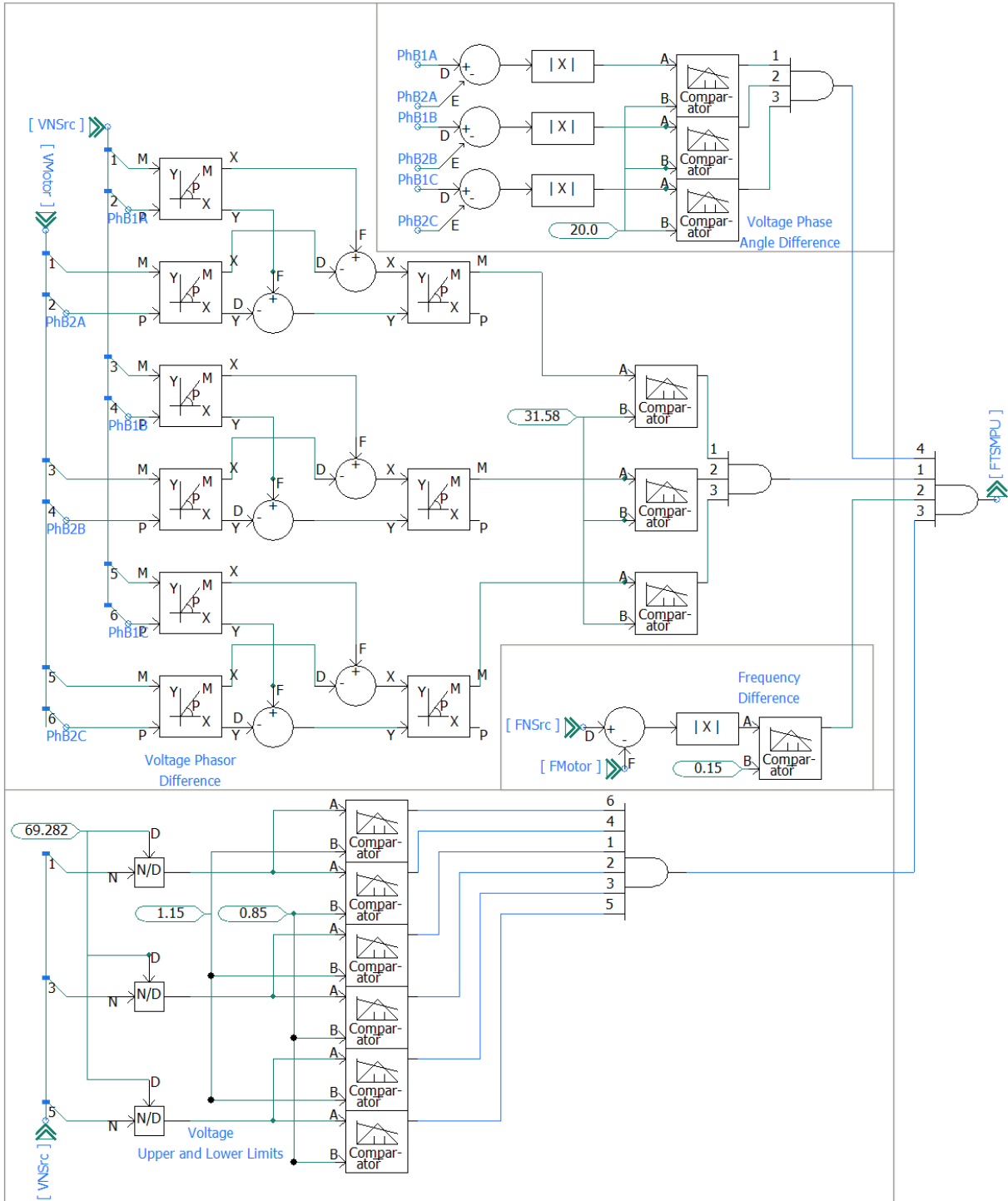


Figure 5-12 MBTS fast transfer module details

#### 5.4.2.1 Voltage Phase Angle Difference

The voltage phase angle difference check ensures that the new source and the motor bus voltage phase angle difference are under a limit avoiding motor bus transfers with high phase angle difference, reducing the risk of high transients when reconnecting to the new incoming source. The absolute voltage phase angle difference between the motor bus and the new source voltage is computed using PSCAD/EMTDC components. Basically, in phasor terms, it can be expressed as follows:

$$\Delta\theta = |\theta_{\text{NSrc}} - \theta_{\text{Motor}}| \quad (5-1)$$

Where the criterion for transfer is:

$$\Delta\theta \leq 20^\circ \quad (5-2)$$

The PSCAD/EMTDC controls for this section is shown in the right upper part of Figure 5-12, where the phase differences are computed from PhB1A, PhB2A, PhB1B, PhB2B, PhB1C, PhB2C for phases A, B and C respectively.

#### 5.4.2.2 New Source Upper and Lower Voltage Supervision

The voltage magnitude supervision section is shown in the lower part of Figure 5-12, and it verifies that the new source voltage magnitudes are between an upper and a lower limit. The 3-phase voltage magnitudes (input VNSrc) are converted to per unit on a 120 L-L volts' base reference (69.282 L-N volts) and then these per unit values are compared to the upper and lower limits. The limits were established as  $\pm 15\%$  of the rated voltage to coordinate such values with the motor bus under voltage unit.

#### 5.4.2.3 Frequency Difference

The absolute value of the difference between the new source and motor bus frequencies is also computed and the resultant absolute value is compared against a set value of 0.15Hz. Reference [15] recommends setting the frequency difference to 0.15Hz.

$$\Delta F = |F_{NSrc} - F_{Motor}| \quad (5-3)$$

Where the limit allowed for transfer is:

$$\Delta F \leq 0.15Hz \quad (5-4)$$

The controls for this section are shown in the right center part of Figure 5-12 where FNSrc and FMotor are the voltage frequency at the new source and at the motor bus respectively.

#### 5.4.2.4 Voltage Phasor Difference

The phasor diagram representing the new source and the motor bus voltage difference is shown in Figure 3-14. The magnitude of the voltage phasor difference may be computed using equation (3-46) or by computing the phasor difference as follows:

$$\begin{bmatrix} \Delta V_a \\ \Delta V_b \\ \Delta V_c \end{bmatrix} = \begin{bmatrix} V_{NSrc_a} \\ V_{NSrc_b} \\ V_{NSrc_c} \end{bmatrix} - \begin{bmatrix} V_{Motor_a} \\ V_{Motor_b} \\ V_{Motor_c} \end{bmatrix} \quad (5-5)$$

$$\begin{bmatrix} \Delta V_a \\ \Delta V_b \\ \Delta V_c \end{bmatrix} = \begin{bmatrix} V_{NSrc_{ax}} - V_{Motor_{ax}} \\ V_{NSrc_{bx}} - V_{Motor_{bx}} \\ V_{NSrc_{cx}} - V_{Motor_{cx}} \end{bmatrix} + j \begin{bmatrix} V_{NSrc_{ay}} - V_{Motor_{ay}} \\ V_{NSrc_{by}} - V_{Motor_{by}} \\ V_{NSrc_{cy}} - V_{Motor_{cy}} \end{bmatrix} \quad (5-6)$$

$$\begin{bmatrix} \Delta V_a \\ \Delta V_b \\ \Delta V_c \end{bmatrix} = \begin{bmatrix} \sqrt{(V_{NSrc_{ax}} - V_{Motor_{ax}})^2 + (V_{NSrc_{ay}} - V_{Motor_{ay}})^2} \\ \sqrt{(V_{NSrc_{bx}} - V_{Motor_{bx}})^2 + (V_{NSrc_{by}} - V_{Motor_{by}})^2} \\ \sqrt{(V_{NSrc_{cx}} - V_{Motor_{cx}})^2 + (V_{NSrc_{cy}} - V_{Motor_{cy}})^2} \end{bmatrix} \quad (5-7)$$

The threshold setting may be computed according to equation (3-46) which is repeated here for a prompt reference:

$$E_{\text{diff}} = \sqrt{E_s^2 + E_m^2 - 2E_sE_m \cos \theta} \quad (5-8)$$

Considering the maximum voltage of 1.15 p.u., a minimum allowable voltage of 0.85 p.u., and a maximum phase angle difference of 20 degrees, the maximum voltage difference is:

$$E_{\text{diff}} = \sqrt{(1.15)^2 + (0.85)^2 - 2(1.15)(0.85) \cos(20^\circ)} \quad (5-9)$$

$$E_{\text{diff}} = \sqrt{1.3225 + 0.7225 - 1.6930} = 0.4559\text{pu}$$

$$E_{\text{diff}} = 0.4559\text{pu} * \frac{120\text{V}}{\sqrt{3}} = 31.58 \text{ Volts}$$

Therefore, the setting threshold expressed in vector form is

$$\begin{bmatrix} \Delta V_a \\ \Delta V_b \\ \Delta V_c \end{bmatrix} \leq \begin{bmatrix} 31.58 \\ 31.58 \\ 31.58 \end{bmatrix} \text{ Volts} \quad (5-10)$$

Equations (5-7) and (5-10) were implemented in PSCAD/EMTDC as shown in the left middle part of Figure 5-12. If the magnitude of the phasor difference is less than 31.58 Volts, then a command signal is sent to allow the transfer to initialize.

#### 5.4.3 Motor Bus Transfer System In-Phase Transfer Module

The MBTS in-phase transfer module is shown in Figure 5-13. The in-phase transfer module has four inputs and one output which are described as follows: a) VMotor that receives the motor bus voltage phasor, b) VNSrc that receives the new source voltage phasor (VAux if the transfer is from the start-up to the auxiliary system or VStart if the transfer is from the auxiliary to the start-up system), c) FMotor which receives the motor bus voltage frequency, and d) FNSrc that receives the new source voltage frequency (FAux if the transfer is from the start-up to the auxiliary system or FStart if the transfer is from the auxiliary to the start-up system). The MBTS in-phase transfer module processes the inputs



using the standard in-phase algorithm and if the conditions are met then it outputs a command IPSMPU which is then passed to the circuit breaker control block.

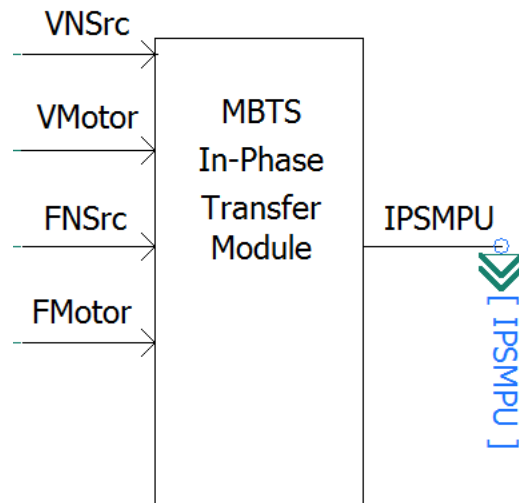


Figure 5-13 Motor bus transfer system in-phase module

The transfer should be accomplished when the new source voltage is in phase coincidence with the motor bus voltage. This requires that the new source breaker must be closed by predicting movement towards phase coincidence between the motor bus voltage and the new source voltage. To accomplish such phase angle coincidence, the close command to the new source breaker should occur at a phase angle in advance of phase coincidence between the motor bus and the new source. The phase angle in advance is the new breaker's closing time. This is controlled internally in the in-phase transfer module implemented in PSCAD/EMTDC.

The concept of sending a command to close the circuit breaker in advance is graphically explained in Figure 5-14. The motor bus phase "a" voltage is the one leading the source voltage and it is moving toward the source phase coincidence. The circuit breaker closing angle depends on the a) voltage phase angle difference between the new source and the motor bus, b) slip frequency between the new source and the motor bus, c) circuit breaker closing time, d) phase angle difference caused by the motor bus frequency rate of change and by the frequency acceleration of change. The motor bus frequency and the voltage magnitude are changing rapidly therefore only during the first phase angle coincidences there are good possibilities to perform the transfer based on the In-Phase method.

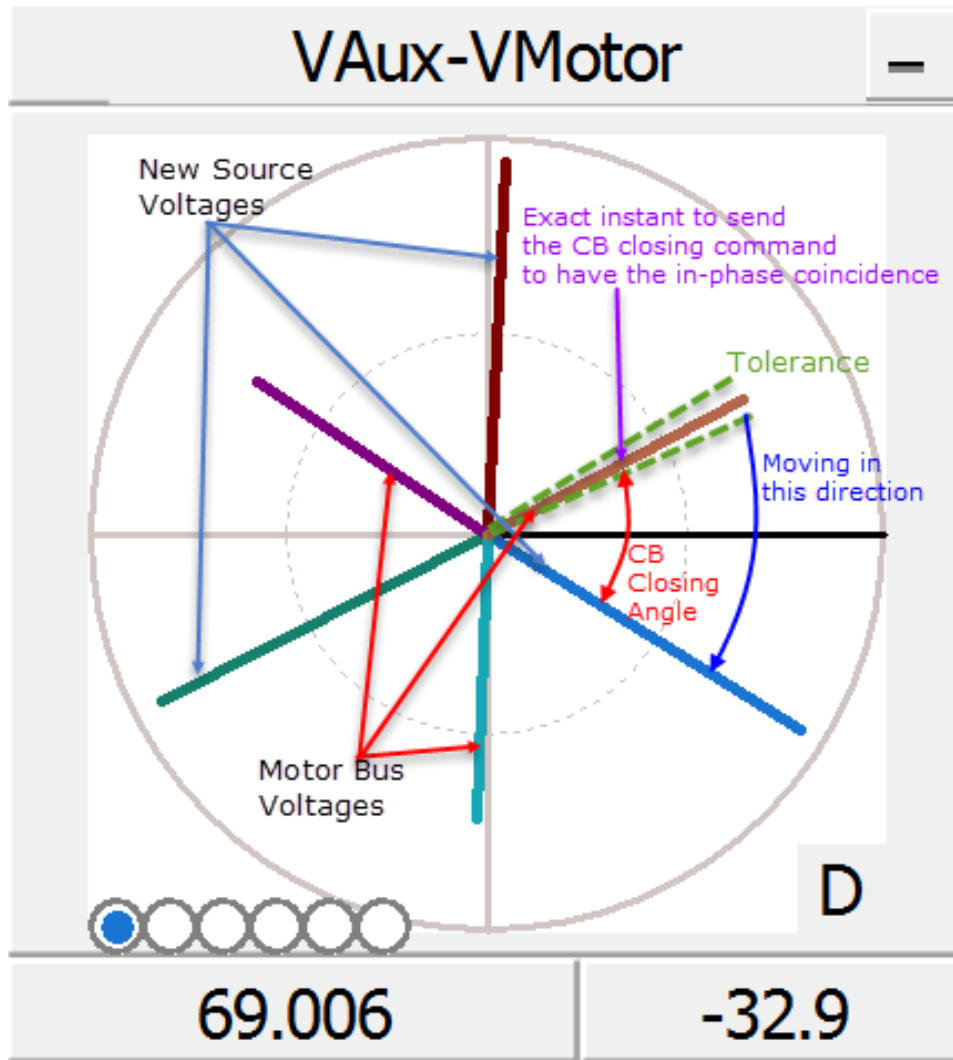


Figure 5-14 In-Phase transfer concept

The detailed MBTS in-phase transfer module is shown in Figure 5-15. The module is comprised of three components (as recommended in [12]): a) circuit breaker close in advance algorithm, b) a supervision of the slip frequency between the new source voltage frequency and the motor bus frequency, and c) a supervision of the upper and lower voltage limit of the new source.

In the present example, the voltage upper limit was set to 1.15 p.u., the lower voltage limit was set to 0.85 p.u., and the frequency difference or slip frequency was set to 10 Hertz.

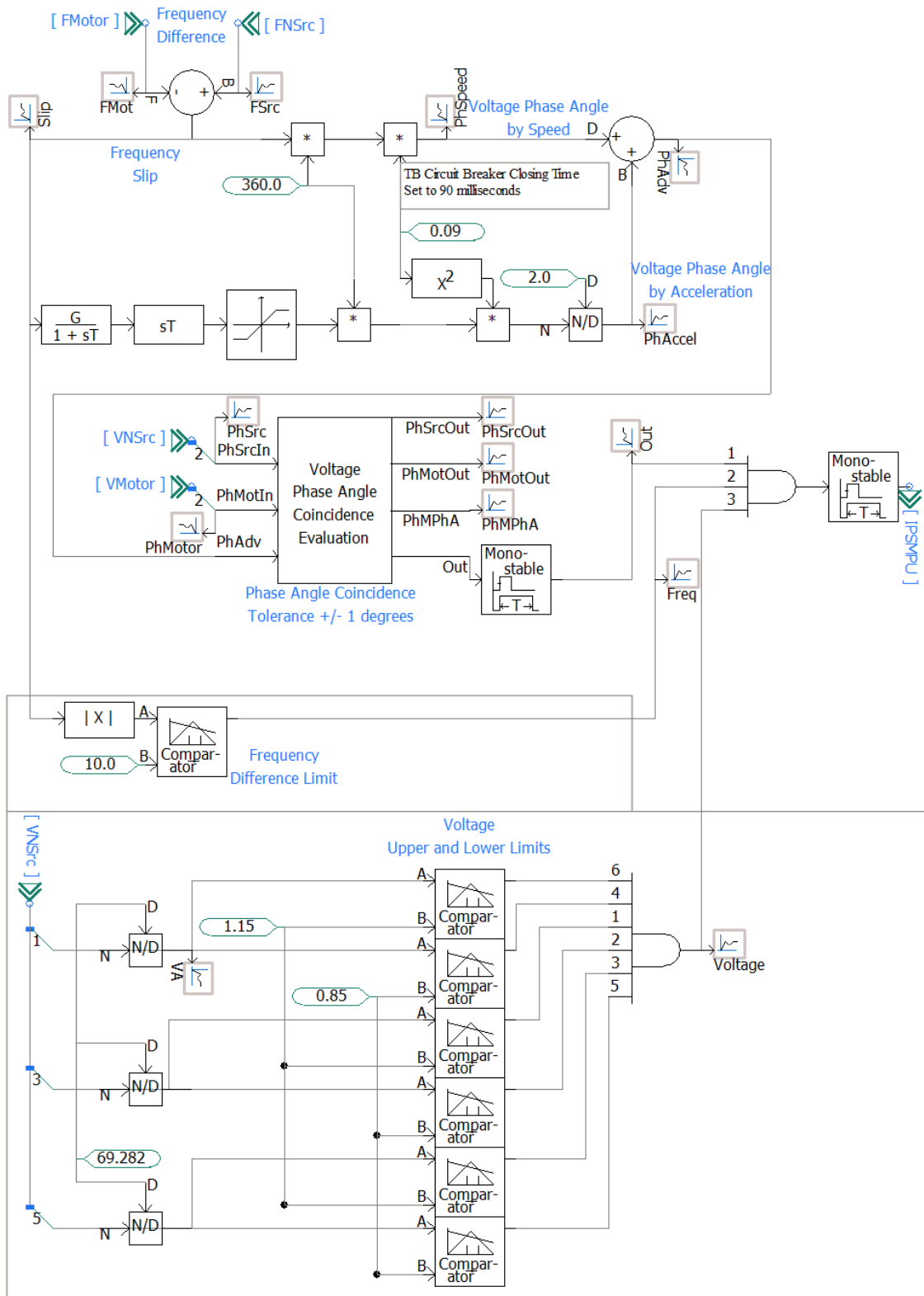


Figure 5-15 MBTS in-phase module details

#### 5.4.3.1 Frequency Difference

The absolute value of the difference between the new source and motor bus frequencies is computed and the resultant value is compared to a set value of 10Hz in this simulation. Reference [15] recommends setting this value from 6 to 10Hz.

$$\Delta F = |F_{\text{NSrc}} - F_{\text{Motor}}| \quad (5-11)$$

Where the limit for transfer is:

$$\Delta F \leq 10 \text{ Hz} \quad (5-12)$$

The frequency difference module is shown in the left-top part of Figure 5-15, where FNSrc and FMotor are the voltage frequency at the new source and motor bus respectively. The limit comparator is shown in the left center part of the same figure.

#### 5.4.3.2 New Source Upper and Lower Voltage Supervision

The voltage magnitude supervisor module is shown in the lower part of Figure 5-15, and it verifies that the new source voltage magnitude is between an upper and a lower limit. The 3-phase voltage magnitudes (input VNSrc) are converted to per unit on a 120 L-L volts' base reference (69.282 L-N volts) and then these per unit values are compared to the upper and lower limits. The limits were established as  $\pm 15\%$  of the rated voltage to coordinate such values with the motor bus under voltage unit.

#### 5.4.3.3 Motor Bus Transfer System Circuit Breaker Close Angle

In order to perform a motor bus transfer using the in-phase transfer method, the motor bus voltage phase angle and the new source voltage phase should be in phase coincidence. To accomplish this, the new source circuit breaker should receive the close command in advance to the in-phase coincidence.

According to reference [10] the phase angle in advance at the instant of breaker closing can be predicted using the estimated delta frequency, the rate of change of delta frequency and the breaker closing time as described in equation (5-13).

$$\Delta\theta_{\text{advance}_{\text{radians}}} = \Delta\theta + 2\pi \left( \Delta F_e + \frac{1}{2} d \left( \frac{\Delta F_e}{dt} \right) (T_B) \right) T_B \text{ radians} \quad (5-13)$$

Rewriting this equation in degrees:

$$\Delta\theta_{\text{advance}} = \Delta\theta + 360 \Delta F_e T_B + \frac{1}{2} d \left( \frac{\Delta F_e}{dt} \right) (T_B^2) \quad (5-14)$$

Where:

$\Delta\theta$  = Voltage phase angle difference between the new source and the motor bus in degrees

$\Delta F_e$  = Frequency difference between the new source and the motor bus

$T_B$  = Circuit breaker closing time

$360 \times \Delta F_e \times T_B$  = Phase angle in degrees caused by the speed of change

$\frac{1}{2} d \left( \frac{\Delta F_e}{dt} \right) (T_B^2)$  = Phase angle in degrees caused by the acceleration of change

Equation (5-14) was implemented in PSCAD/EMTDC as shown in the upper part of Figure 5-15.

The frequency difference is computed subtracting the motor bus frequency  $F_{\text{Motor}}$  from the new source frequency  $F_{\text{NSrc}}$ . Then, the voltage phase angles in degrees caused by the rate of change of frequency and by the acceleration of change of frequency are computed according to equation (5-14). In this example, the circuit breaker closing time  $T_B$  was set to 0.09 seconds (90 milliseconds). The sum

of these two phase-angles together with the motor bus phase A angle  $V_{Motor}$  and the new source voltage phase A angle  $V_{NSrc}$  are passed to the voltage phase angle coincidence module as inputs  $PhAdv$ ,  $PhMotIn$ ,  $PhSrcIn$  respectively. The voltage phase angle coincidence module adds the motor bus phase A angle input to the  $PhAdv$  input, and the resultant value is compared to input  $PhSrcIn$ . If there is a predicted phase angle coincidence with a tolerance of  $\pm 1$  degree, the output  $Out$  is sent.

#### 5.4.4 Motor Bus Transfer System Residual Voltage Transfer Module

The MBTS residual voltage transfer module is shown in Figure 5-16. The residual voltage module has four inputs and one output which are described as follows: a)  $V_{Motor}$  that receives the motor bus voltage phasor, b)  $V_{NSrc}$  that receives the new source voltage phasor ( $V_{Aux}$  if the transfer is from the start-up to the auxiliary system or  $V_{Start}$  if the transfer is from the auxiliary to the start-up system), c)  $F_{Motor}$  which receives the motor bus voltage frequency, and d)  $F_{NSrc}$  that receives the new source voltage frequency ( $F_{Aux}$  if the transfer is from the start-up to the auxiliary system or  $F_{Start}$  if the transfer is from the auxiliary to the start-up system). The MBTS residual voltage transfer module processes the inputs using the standard residual voltage algorithm and if the conditions are met then it outputs a command  $RVSMPU$  which is then passed to the circuit breaker control block.

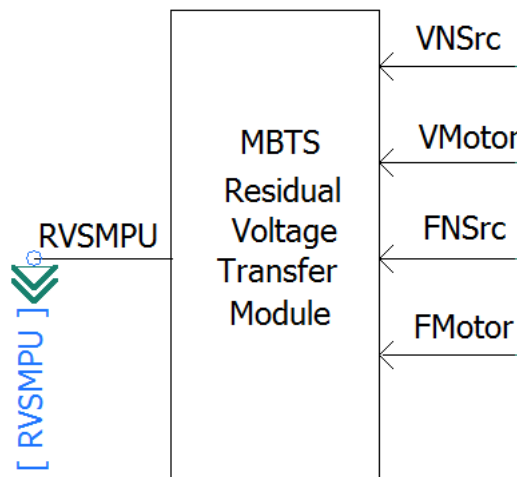


Figure 5-16 Motor bus transfer system residual voltage module

Figure 5-17 shows the phase “a” residual voltage of a motor bus (red plot). It is also shown both the new source voltage (plot in blue) and the old source voltage and its phase angle change when the motor bus is disconnected from it (plot in purple). The transfer is performed when the residual voltage is lower than the residual voltage limit and when the computed volts/Hertz is lower than the 1.33 V/Hz standard limit.

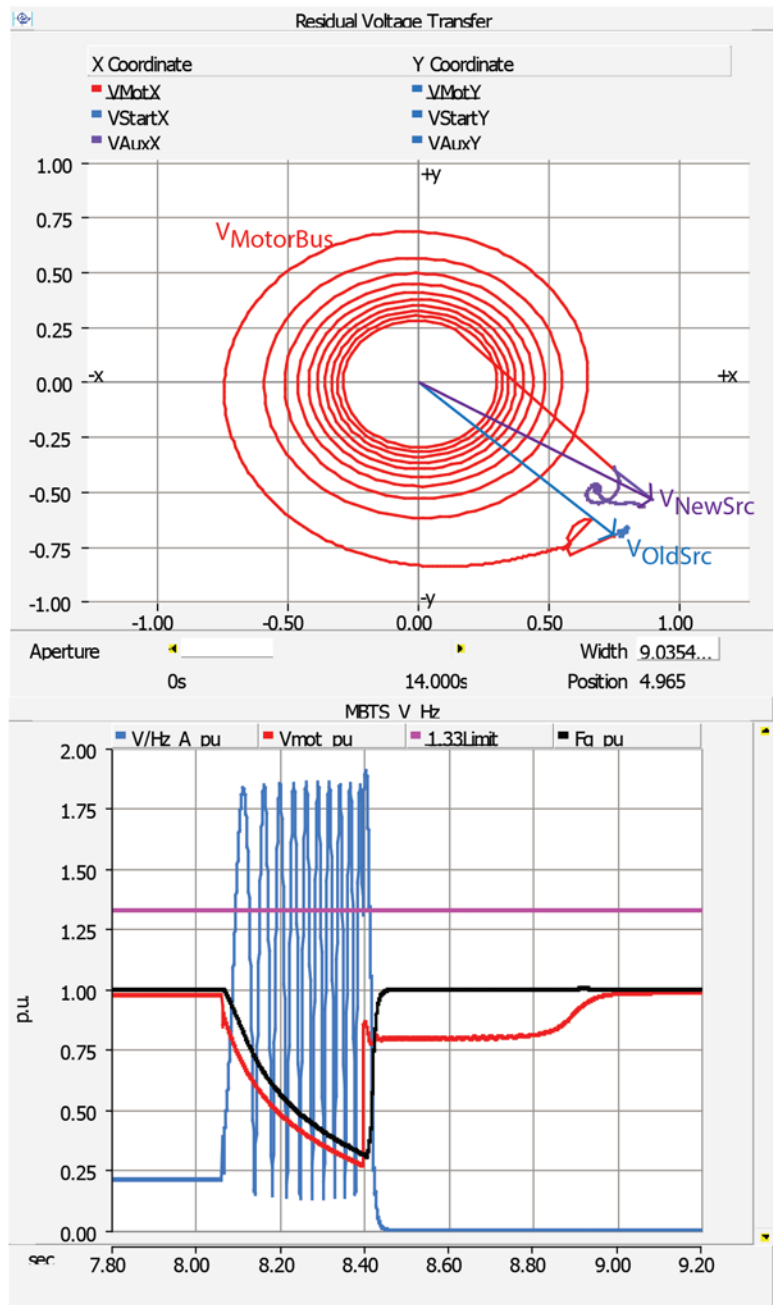


Figure 5-17 Residual voltage transfer concept

The detailed MBTS residual voltage transfer module is shown in Figure 5-18. The residual voltage module computes the phasor voltage/Hz per unit difference between the new source and the motor bus. This difference is compared to the maximum limit of 1.33 per unit Volts/Hz phasor difference recommended by NEMA MG-1-2006 [24] and ANSI C50.41-2000 [25].

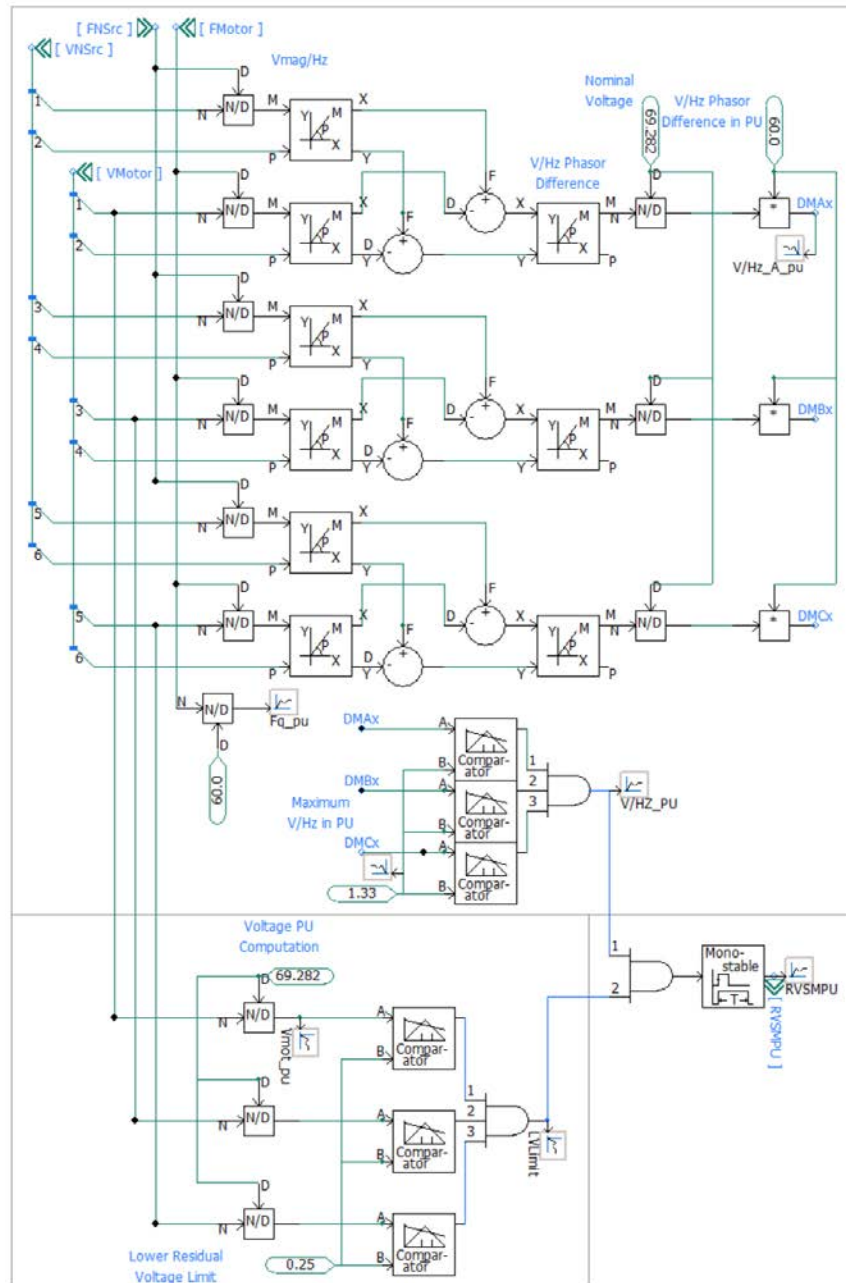


Figure 5-18 MBTS residual voltage module components



#### 5.4.4.1 Lower Residual Voltage Limit

The residual module also computes the per unit motor bus decaying voltage on a base of 120 L-L volts (69.282 V L-N) to perform the motor bus transfer when the decaying residual voltage is equal to or lower than a lower residual voltage limit, which in this example was set to 0.25 p.u. Reference [1] states that this residual voltage usually is lower than 0.25 p.u. and it ensures compliance with the 1.33 p.u. V/Hz limit.

#### 5.4.4.2 Volts/Hertz

The per unit volts/Hz shown in Figure 5-18 is computed as follows:

$$\frac{V}{\text{Hz}_{\text{pu}}} = \frac{\left| \frac{|V_{\text{NSrc}}|}{F_{\text{NSrc}}} \angle \theta_{\text{NS}} - \frac{|V_{\text{Motor}}|}{F_{\text{Motor}}} \angle \theta_{\text{MB}} \right|}{V_{\text{nominal}}} \times 60\text{Hz} \quad (5-15)$$

$$\frac{V}{\text{Hz}_{\text{pu}}} = \frac{\left| \left( \frac{|V_{\text{NSrc}}|}{F_{\text{NSrc}}} \angle \theta_{\text{NSrc}_x} - \frac{|V_{\text{Motor}}|}{F_{\text{Motor}}} \angle \theta_{\text{Motor}_x} \right) + j \left( \frac{|V_{\text{NSrc}}|}{F_{\text{NSrc}}} \angle \theta_{\text{NSrc}_y} - \frac{|V_{\text{Motor}}|}{F_{\text{Motor}}} \angle \theta_{\text{Motor}_y} \right) \right|}{V_{\text{nominal}}} \times 60\text{Hz} \quad (5-16)$$

$$\frac{V}{\text{Hz}_{\text{pu}}} = \frac{\sqrt{\left( \frac{|V_{\text{NSrc}}|}{F_{\text{NSrc}}} \angle \theta_{\text{NSrc}_x} - \frac{|V_{\text{Motor}}|}{F_{\text{Motor}}} \angle \theta_{\text{Motor}_x} \right)^2 + \left( \frac{|V_{\text{NSrc}}|}{F_{\text{NSrc}}} \angle \theta_{\text{NSrc}_y} - \frac{|V_{\text{Motor}}|}{F_{\text{Motor}}} \angle \theta_{\text{Motor}_y} \right)^2}}{V_{\text{nominal}}} \times 60\text{Hz} \quad (5-17)$$

Equation (5-17) was implemented in PSCAD/EMTDC as shown in the top part of Figure 5-18. The source voltage phasor magnitudes  $V_{\text{NSrc}}$  and motor bus voltage phasor magnitudes  $V_{\text{Motor}}$  are divided by the frequency  $F_{\text{NSrc}}$  and  $F_{\text{Motor}}$  respectively. Then, the V/Hz phasor difference is computed for each phase. Then the V/Hz phasor difference magnitudes per unit are computed dividing the magnitude of the V/Hz phasor difference of each phase by the nominal L-N voltage magnitude of 69.282 Volts and multiplying the resultant values by nominal frequency of 60Hz (outputs  $\text{DMA}_x$ ,  $\text{DMB}_x$  and  $\text{DMC}_x$ ). Finally, these outputs are compared to the 1.33 V/Hz limit and the combined output together with the lower residual voltage supervisor output trigger the output signal  $\text{RVSM}_{\text{PU}}$  which is then passed to the circuit breaker control block.

## 5.5 Circuit Breaker Control Block

The circuit breaker control block is presented in Figure 5-19. The module has nine inputs and two outputs. Input RTrip is received from the module described in the relay trip and manual command; Section 5.2. Inputs Coastdown and SysSel inputs are received from the module described in the auxiliary controls; Section 5.3. Inputs FTSMPU, IPSMPU, RVSMPU are received from the MBTS process unit described in Section 5.4. Inputs FTT, IPT and RVT are received from the control panel to control the motor bus transfer simulation modes, fast transfer, in-phase, and residual voltage respectively. These signals are only used to test the implemented motor transfer algorithms individually.

The circuit breaker control module performs all the control actions needed to open or close the auxiliary or start-up breakers and the complete detailed module is shown in Figure 5-20.

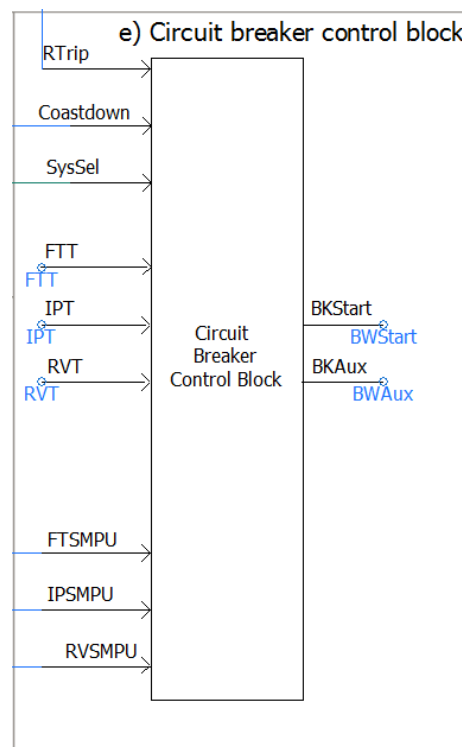


Figure 5-19 Circuit breaker control block

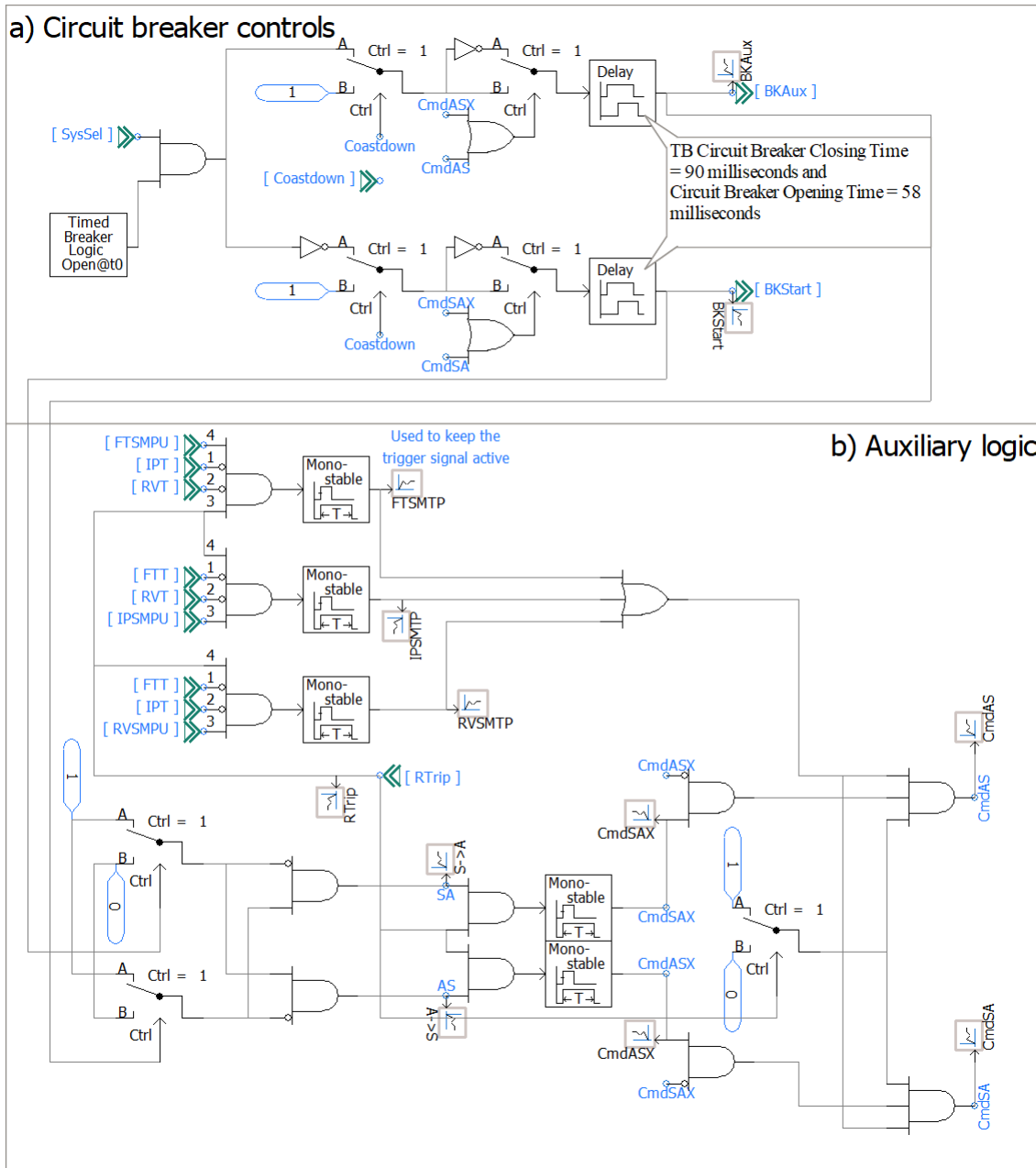


Figure 5-20 Circuit breaker controls block in details

Basically, there are two functional blocks in the circuit breaker control block, the first one is shown in the upper part of Figure 5-20. It is the block in charge of the operation of the circuit breakers, and the output signals are used directly by PSCAD/EMTDC to open or close the breakers at the auxiliary or start-up side. The command signals to operate the breakers are:

- 1) Coastdown: to open or close the auxiliary and start-up breakers during a coast-down simulation.
- 2) CmdAS and CmdASx: to open the old source when the old source is the auxiliary system.
- 3) CmdSA and CmdSAx: to open the start-up system when it is used as the old source.
- 4) BKAux and BKStart: are the outputs sent to open or close the auxiliary and start-up breakers.

The second functional block (auxiliary logic) illustrated in Figure 5-20, executes the following actions.

- 1) The upper part executes the trip logic for motor bus transfer based on the trip signal RTrip and pick-up signals from the MBTS process unit (FTSMPU) for the fast transfer method; or (IPSMPU) for the in-phase transfer method; or (RVSMPU) for the residual voltage method.
- 2) The lower part is the section that defines the operating condition of the auxiliary and start-up breakers, in other words it finds if the breakers are opened or closed.
- 3) CmdAS and CmdSA signals are sent to circuit breaker control to open or close the breakers.

## CHAPTER 6 - SIMULATIONS AND RESULTS

### 6.1 Introduction

This chapter discusses the results of the simulation testing of the motor bus transfer system using the PSCAD/EMTDC software. As described in Chapter 3, the motor bus transfer system model used to perform the motor bus transfer may select three motor transfer algorithms. As modeled in this research, the motor bus transfer may be performed manually or automatically. The initial breaker action is initiated manually or by the auxiliary transformer differential protection, or by the transmission line distance protective relay or by an under-voltage relay modeled in the motor bus process unit. Note: In nuclear power plants the second level of voltage protection may initiate the transfer as well.

The motor bus transfer system modeled uses a simultaneous transfer in which both the opening and closing commands are sent at the same time so that the time the breakers are simultaneously open is minimized.

Section 6.2 discusses all three algorithms performance during test: a) fast transfer, b) in-phase transfer and c) residual voltage transfer. Section 6.3 discusses the performance during manual transfer and Section 6.4 discusses the performance during automatic transfer initiation.

### 6.2 Testing Mode

#### 6.2.1 Fast Transfer Algorithm Component Response

The fast transfer method requires the voltage, phase angle and frequency differences between the new source and the motor bus to be within their specified limits. When the conditions are met, the transfer should happen during the first cycles after the transfer initiation.

To test the algorithm's performance, four tests were carried out. All tests were performed under the same voltage, phase angle and frequency conditions of the auxiliary and start-up systems but with different motor bus transfer initiation times of a quarter of cycle between every subsequent test.

The motor bus transfer system controls used for this test are shown in Figure 6-1. Control SysSel was set to position BWS (transfer simulation from the start-up to the auxiliary system), manual transfer switch MTransfer set to 0, transfer initialization time MTTime set to 14 seconds, TType was set to 1 (fast transfer test mode). Control Coast Down was set to off, control Coast Down Time was set to 99 seconds (coast down simulating motors spinning down in group was not performed), Ind Coast Down Time was set to 99 seconds (coast down simulating motors spinning individually was not performed).

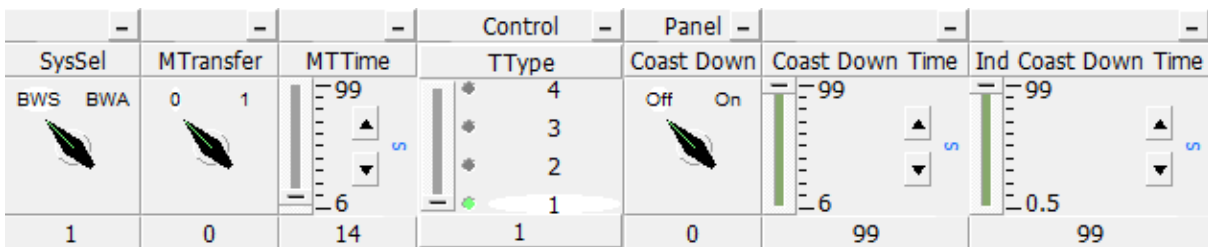


Figure 6-1 Motor bus transfer system controls for a fast transfer test, initiated at  $t=14$  sec.

The start-up breaker opened at  $t=14.058$  seconds (phase B current was interrupted at  $t= 14.0588$  s, phase A current at  $t= 14.0629$  s and phase C current at  $t = 14.0629$  s.). The transfer was accomplished at  $t=14.09$  seconds when the auxiliary breaker closed, 90 milliseconds after the transfer initiation; which basically is the breaker closing time. The close command was given at the same time of the trip command so that the time the breakers are simultaneously open is minimized.

Figure 6-2 shows the phase A instantaneous voltage of the auxiliary bus (light blue plot), start-up bus (purple plot) and motor bus (red plot) during the fast transfer test. The motor bus was transferred from the start-up side to the auxiliary side.

The start-up bus voltage magnitude before the transfer initiation was 4.1267 kV L-L and after the bus transfer the voltage magnitude was 4.3098 kV. The auxiliary voltage magnitude before the transfer initiation was 4.3430 kV and after the bus transfer it was 4.1932 kV. During the loss of power supply, the motor bus voltage magnitude decayed to 3.669 kV.

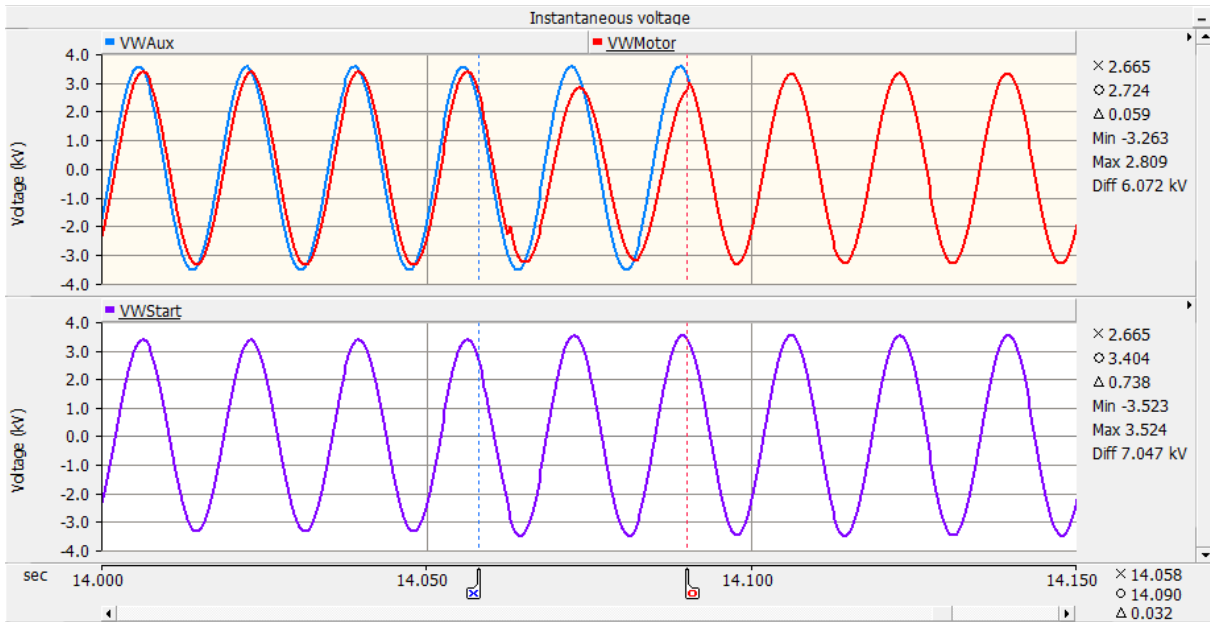


Figure 6-2 Phase A instantaneous voltage in kV during a fast transfer test, initiated at t=14 sec.

Figure 6-3 shows the per unit phase A RMS voltage of the auxiliary bus (light blue plot), start-up bus (purple plot) and motor bus (red plot) during the fast transfer test. The start-up voltage magnitude changed from 0.992 p.u. (in a reference of 4.16 kV L-L) before the bus transfer to 1.036 p.u. after the bus transfer. The auxiliary side voltage magnitude before the bus transfer was 1.044 p.u. and after the transfer was 1.008 p.u.

When the start-up breaker opened, the motor bus voltage magnitude decayed to 0.886 p.u. The motor bus voltage magnitude and the auxiliary bus voltage magnitude took approximately 210 milliseconds to recover once the motor bus was connected to the auxiliary source.

Whereas the instantaneous voltage of the motor bus and the auxiliary bus changed immediately to the same value when the motor bus is connected to the auxiliary bus voltage, the RMS computed values of the motor and auxiliary bus meters took approximately one cycle at fundamental frequency to change to the same value due to their time response.

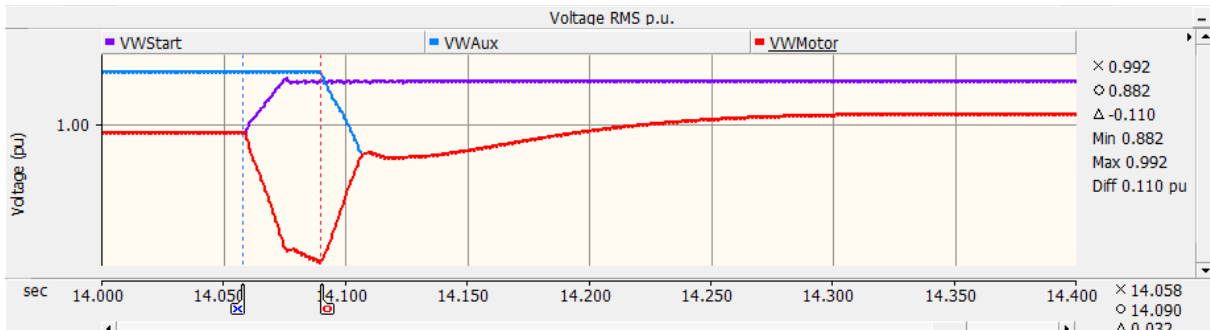


Figure 6-3 Phase A RMS voltage in per unit during a fast transfer test, initiated at  $t=14$  sec.

Figure 6-4 shows the voltage frequency of the auxiliary bus (light blue plot), start-up bus (purple plot) and motor bus (red plot) during the fast transfer test. The motor bus voltage frequency decayed down to 58.23 Hz on loss of power supply. When the auxiliary breaker closed, the electromagnetic transient caused the motor bus frequency to increase up to 63 Hz. The motor bus frequency took approximately 210 milliseconds to change from its decaying magnitude to the new source frequency once the motor bus was connected to the auxiliary source.

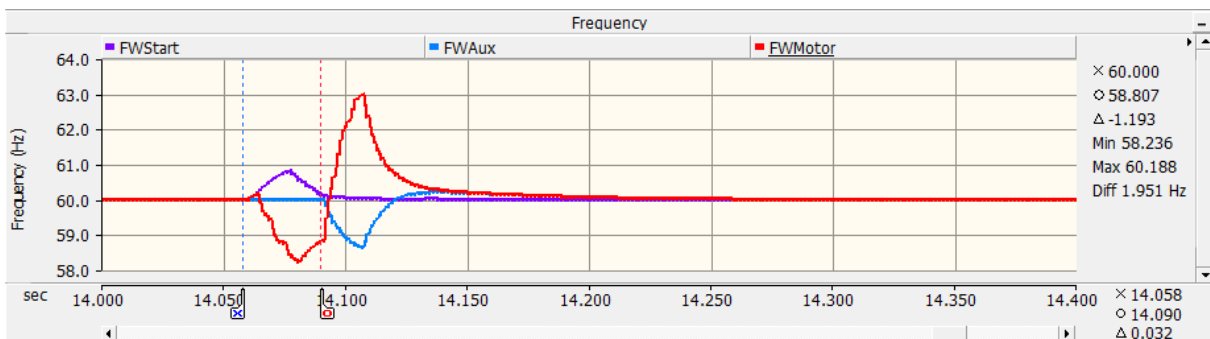


Figure 6-4 Voltage frequency in Hertz during a fast transfer test, initiated at  $t=14$  sec.

Figure 6-5 shows the phase A voltage angle of the auxiliary (light blue plot), start-up (purple plot) and motor buses (red plot) during the fast transfer test. The motor bus voltage phase A angle changed from its steady state operating angle of  $-45.079$  degrees to  $-63.484$  degrees before the auxiliary breaker closed. The motor bus phase A voltage angle took 210 milliseconds more or less to change to the new steady state value once the motor bus was connected to the auxiliary source.



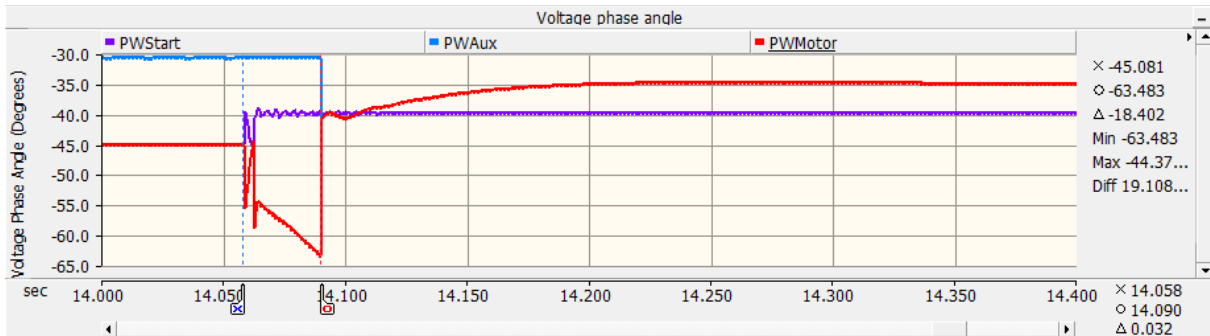


Figure 6-5 Phase A voltage phase angle in degrees during a fast transfer test, initiated at t=14 sec.

The logic timing of the motor bus transfer system elements and circuit breaker contact operations is shown in Figure 6-6, where:

RTrip	Element activated by manual transfer, relay trip, and test mode initialization time
FTSMTP	Fast transfer trip element
IPSMTP	In-phase transfer trip element
RVSMTP	Residual voltage transfer trip element
S->A	Element to enable bus transfer from start-up to auxiliary system
A->S	Element to enable bus transfer from auxiliary to start-up system
BKStart	Start-up side breaker
BKAux	Auxiliary side breaker

Before the transfer initialization, the elements RTrip, FTSMTP were active but not operated; elements IPSMTP, RVSMTP were disabled during the whole simulation, elements S->A and A->S were enabled and disabled respectively; BKStart was closed and BKAux was open.

When the simulation time was equal to the time-controlled signal MTime, set to  $t = 14$  seconds, the element RTrip and the fast transfer trip element FTSMTM tripped instantaneously. With both element tripped, the breakers BKStart and BKAux started their opening and closing operations respectively. Breaker BKStart opened 58 milliseconds after receiving the tripping signal and at that moment the element S->A changed its status from enabled to disabled. Breaker BKAux closed 90 milliseconds after receiving the closing signal and the element A->S changed its status from disabled to enabled. The transfer was accomplished at  $t = 14.090$  seconds.

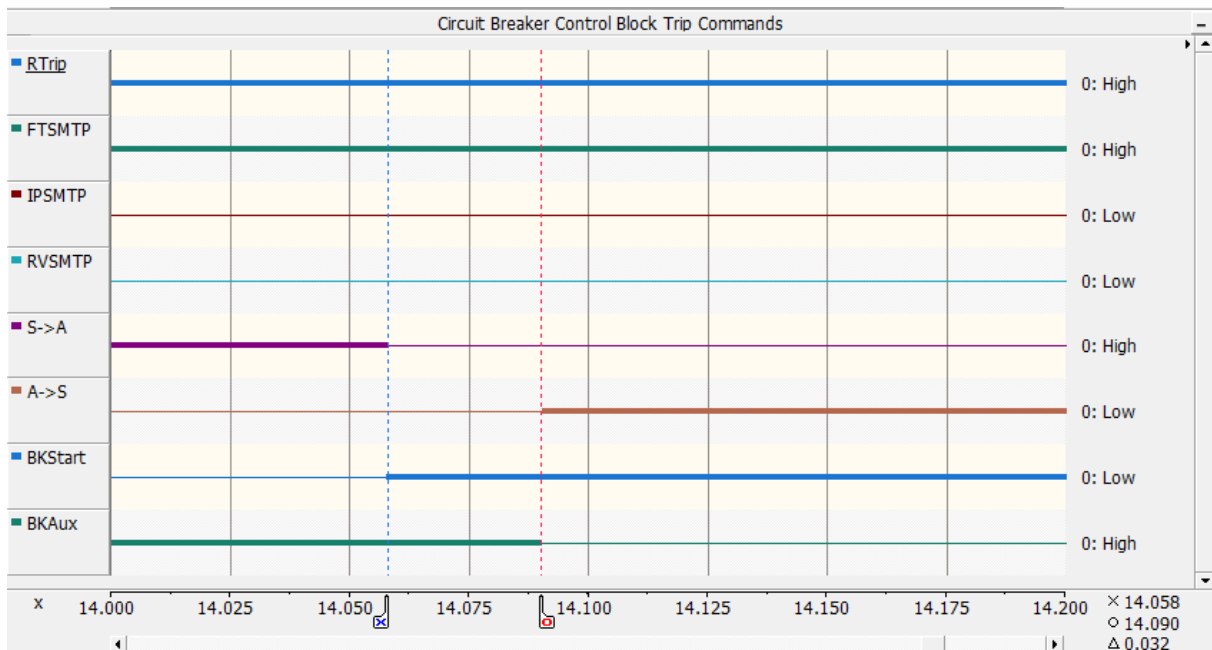


Figure 6-6 Motor bus transfer system element and circuit breaker contact operations during a fast transfer test, initiated at  $t = 14$  sec.

The logic timing of the motor bus transfer system elements and circuit breaker contacts operated correctly.

Figure 6-7 shows the 9000 HP induction motor current and transient torque behavior during the fast transfer simulation. The first graph (blue plot) shows the motor phase A instantaneous current. Before the loss of power supply, the motor phase A current was 1153.95 A RMS and after the start-up breaker opened the motor current decayed and during the time of loss of power supply, the motor supplied approximately 146.26 A RMS from the other motors connected to the motor bus. When the motor bus was reconnected to the auxiliary system the motor phase A current increased to a maximum peak value of -6.833 kA. After the transient settling time the current was 927.30 A.

The second graph (red plot) shows the motor RMS phase A current in p.u. Before the start-up breaker opened, the motor phase A current was 1.073 p.u., when the start-up breaker opened, the motor current started decaying to a minimum of 0.136 p.u. and when the auxiliary breaker closed, the reconnecting transient caused the motor phase A current to increase to 3.231 p.u. The motor phase A RMS current transient settling time was close to 210 milliseconds, and after this time the motor phase A current was 1.006 p.u. The small difference between the current before the loss of power supply and the current after reconnection is because the motor was reconnected to a different source.

The third graph shows the load torque (red plot) and the electromagnetic torque (blue plot). The load torque was practically not disturbed during the motor bus transfer and during the reconnection to the new incoming source. The electromagnetic torque changed from 0.983 p.u. during nominal operating conditions to a minimum of -0.205 p.u. during the loss of power supply. The 9000 HP induction motor behaved as an induction generator, therefore it was supplying current to the other motors. When the auxiliary breaker closed reconnecting the motor bus the electromagnetic torque changed rapidly to 3.763 p.u. (positive torque), close to 25% more than the maximum torque during motor starting process. The transient torque settling time was close to 210 milliseconds.

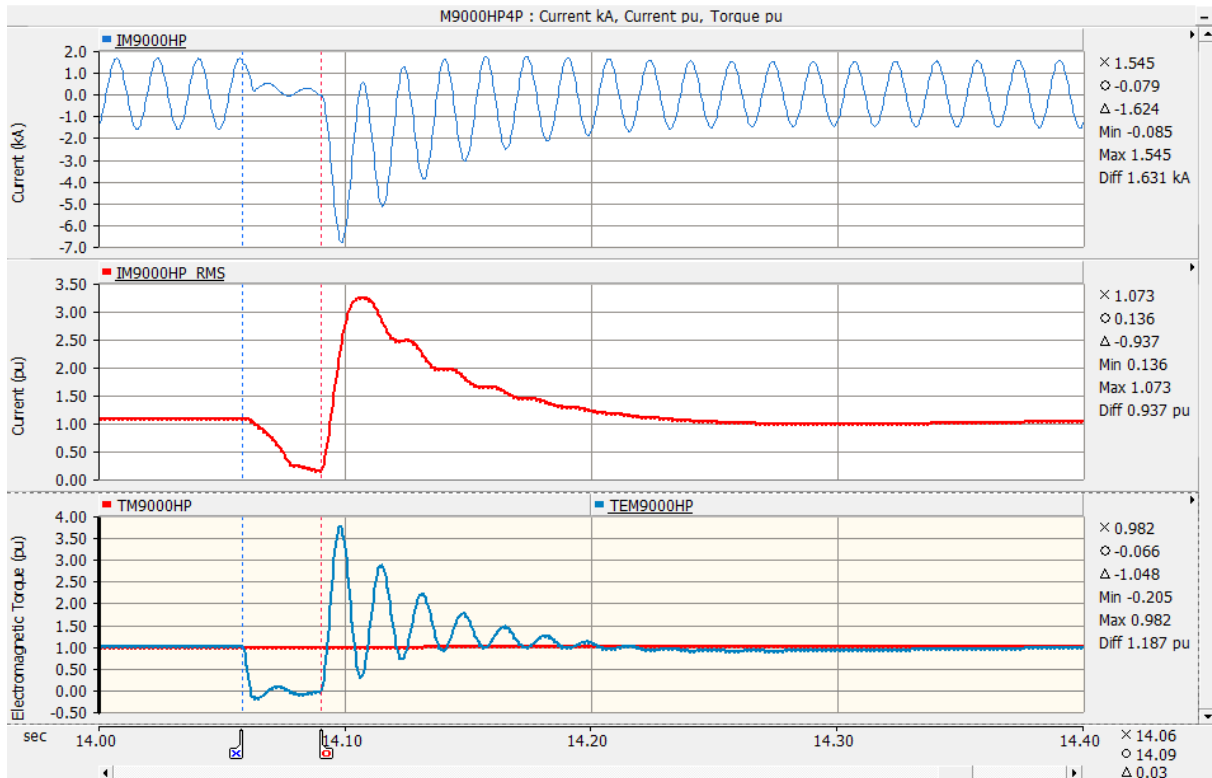


Figure 6-7 9000 HP Motor phase A instantaneous and RMS current, and torque transient response during a fast transfer test, initiated at t=14 sec.

Figure 6-8 shows the 6000 HP induction motor current and transient torque behavior during the fast transfer simulation. The first graph (blue plot) shows the motor phase A instantaneous current. Before the loss of power supply, the motor phase A current was 943.89 A RMS and after the start-up breaker opened the motor current decayed and during the time of loss of power supply, the motor drew approximately 181.62 A RMS from the other motors connected to the motor bus. When the motor bus was reconnected to the auxiliary system the motor phase A current increased to a maximum peak value of -2.639 kA. After the transient settling time the current was 927.30 A.

The second graph (red plot) shows the motor RMS phase A current in p.u. Before the start-up breaker opened, the motor phase A current was 1.081 p.u., when the start-up breaker opened, the motor current started decaying to a minimum of 0.12 p.u. and when the auxiliary breaker closed, the reconnecting transient caused the motor phase A current to increase to 2.59 p.u. The motor phase A RMS current transient settling time was close to 210 milliseconds, and after this time the motor phase A current was 1.062 p.u. The small difference between the current before the loss of power supply and the current after reconnection is because the motor was reconnected to a different source.

The third graph shows the load torque (red plot) and the electromagnetic torque (blue plot). The load torque was practically not disturbed during the motor bus transfer and during the reconnection to the new incoming source. The electromagnetic torque changed from 0.966 p.u. during nominal operating conditions to a minimum of -0.034 p.u. during the loss of power supply. When the auxiliary breaker closed reconnecting the motor bus the electromagnetic torque changed rapidly to 2.573 p.u. (positive torque), close to 11% more than the maximum torque during motor starting process. The transient torque settling time was close to 210 milliseconds.

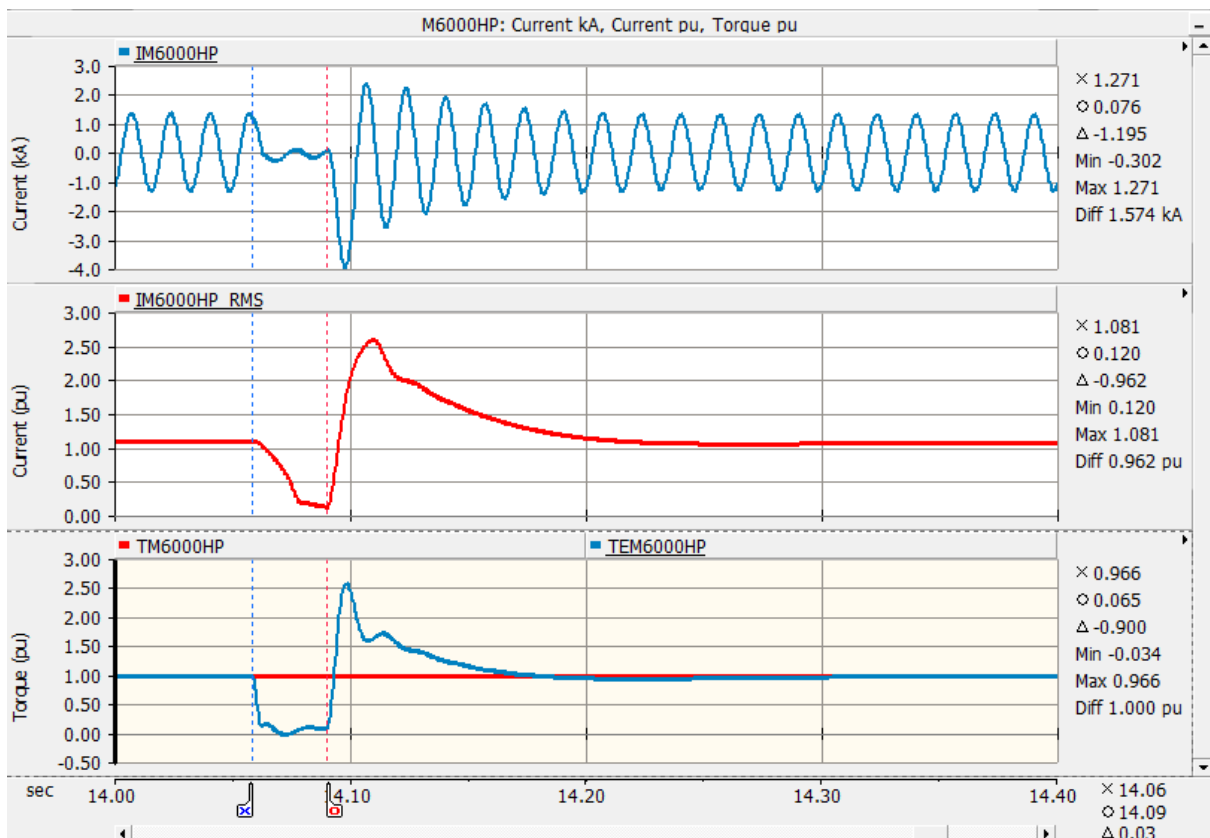


Figure 6-8 6000 HP Motor phase A instantaneous and RMS current, and torque transient response during a fast transfer test, initiated at t=14 sec.

Figure 6-9 shows the 3200 HP induction motor current and torque transient behavior during the fast transfer simulation. The first graph (blue plot) shows the motor phase A instantaneous current. Before the loss of power supply, the motor phase A current was 436.26 A RMS and after the start-up breaker opened the motor current decayed. During the time of loss of power supply, the motor drew approximately 30.08 A RMS to the other motors connected to the motor bus. When the motor bus was reconnected from the auxiliary system the motor phase A current increased up to a maximum peak value of -2.195 kA. After the transient settling time the current was 457.65 A.

The second graph (red plot) shows the motor phase A current in p.u. Before the start-up breaker opened, the motor phase A current was 1.029 p.u., when the start-up breaker opened, the motor phase A current went to 0.071 p.u. and when the auxiliary breaker closed, the reconnecting transient caused the motor phase A current to increase to 2.852 p.u. The motor phase A current transient settling time was close to 210 milliseconds, and after this time the motor phase A current was 1.08 p.u. The small difference between the current before the loss of power supply and the current after reconnection is because the motor was reconnected to a different source.

The third graph shows the load torque (red plot) and the electromagnetic torque (blue plot). The load torque was practically not disturbed during the motor bus transfer and during the reconnection to the new incoming source. The electromagnetic torque changed from 1.029 p.u. during nominal operating conditions to a minimum of -0.133 p.u. (negative torque) during the loss of power supply. The 3200 HP induction motor behaved as an induction generator, therefore it was supplying current to the other motors. When the auxiliary breaker closed reconnecting the motor bus the electromagnetic torque changed rapidly to 3.032 p.u. (positive torque), close to 11.2% more than the maximum torque during motor starting process. The torque transient settling time was close to 210 milliseconds.

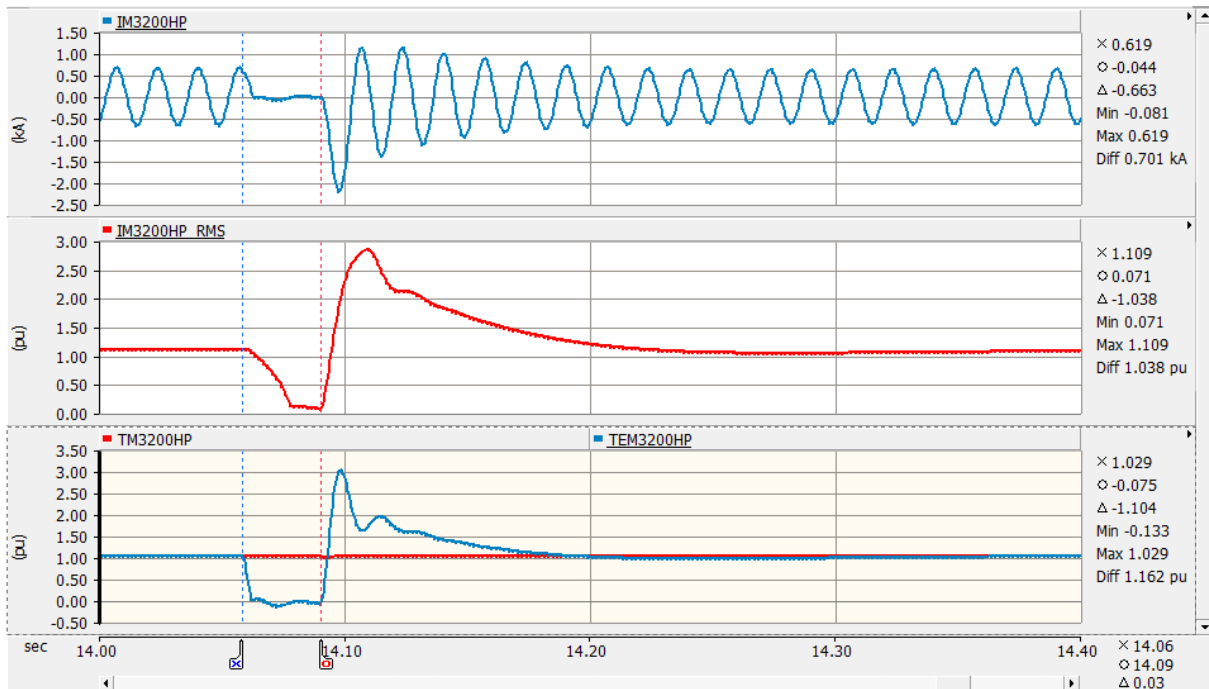


Figure 6-9 3200 HP Motor phase A instantaneous and RMS current, and torque transient response during a fast transfer test, initiated at t=14 sec.

Figure 6-10 shows the 1400 HP induction motor current and torque transient behavior during the fast transfer simulation. The first graph (blue plot) shows the phase A instantaneous current. Before the loss of power supply, the motor phase A current was 221.98 A RMS and after the start-up breaker opened the motor current decayed and during the time of loss of power supply, the motor drew current (approximately 35 A RMS) from other motors connected to the motor bus. When the motor bus was reconnected to the auxiliary system the motor phase A current increased to a maximum peak value of -0.913 kA. After the transient settling time the current was 219.53 A.

The second graph (red plot) shows the RMS phase A current in p.u. Before the start-up breaker opened the motor phase A current was 1.089 p.u., when the start-up breaker opened, the current went to 0.176 p.u. and when the auxiliary breaker closed, the reconnecting transient caused the phase A current to increase to 2.528 p.u. The phase A current transient settling time was close to 210 milliseconds, and after this time the phase A current was 1.077 p.u. The small difference between the current before the loss of power supply and the current after reconnection is because the motor was reconnected to a different source.

The third graph shows the load torque (red plot) and the electromagnetic torque (blue plot). The load torque was practically not disturbed during the motor bus transfer and during the reconnection to the new incoming source. The electromagnetic torque changed from 0.969 p.u. during nominal operating conditions to a minimum of 0.038 p.u. during the loss of power supply. When the auxiliary breaker closed reconnecting the motor bus the electromagnetic torque changed rapidly to 2.512 p.u. (positive torque), close to 11.13% more than the maximum torque during motor starting process. The torque transient settling time was close to 210 milliseconds.

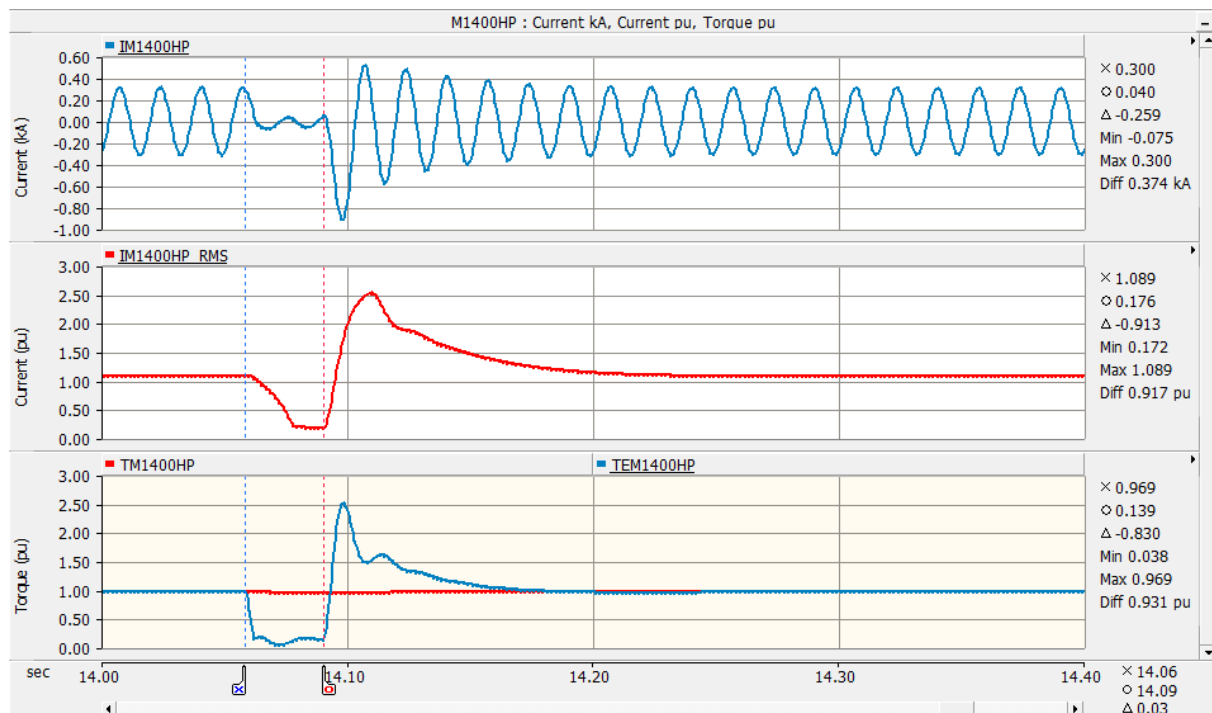


Figure 6-10 1400 HP Motor phase A instantaneous and RMS current, and torque transient response during a fast transfer test, initiated at  $t=14$  sec.

Figure 6-11 shows the 1000 HP induction motor current and torque transient behavior during the fast transfer simulation. The first graph (blue plot) shows the phase A instantaneous current. Before the loss of power supply, the motor phase A current was 158.62 A RMS and after the start-up breaker opened the motor current started decaying. During the loss of power supply, the motor drew current (approximately 17.89 A RMS) from other motors connected to the motor bus. When the motor bus was reconnected from the auxiliary system the motor phase A current increased up to a maximum peak value of -662 A. After the transient settling time the current was 154.25 A.



The second graph (red plot) shows the motor RMS phase A current in p.u. Before the start-up breaker opened, the motor phase A current was 1.09 p.u., during the loss of power supply the current went to a minimum of 0.123 p.u. and when the auxiliary breaker closed, the reconnecting transient caused the motor phase A current to increase to 2.587 p.u. The phase A current transient settling time was close to 210 milliseconds, and after this time the phase A current was 1.06 p.u. The small difference between the current before the loss of power supply and the current after reconnection is because the motor was reconnected to a different source.

The third graph shows the load torque (red plot) and the electromagnetic torque (blue plot). The load torque was practically not disturbed during the motor bus transfer and during the reconnection to the new incoming source. The electromagnetic torque was 0.973 during nominal operating conditions and during the loss of power supply it changed to a minimum of -0.028 p.u. When the auxiliary breaker closed reconnecting the motor bus the electromagnetic torque changed rapidly to 2.57 p.u. (positive torque), close to 11.05% more than the maximum torque during motor starting process. The torque transient settling time was close to 210 milliseconds.

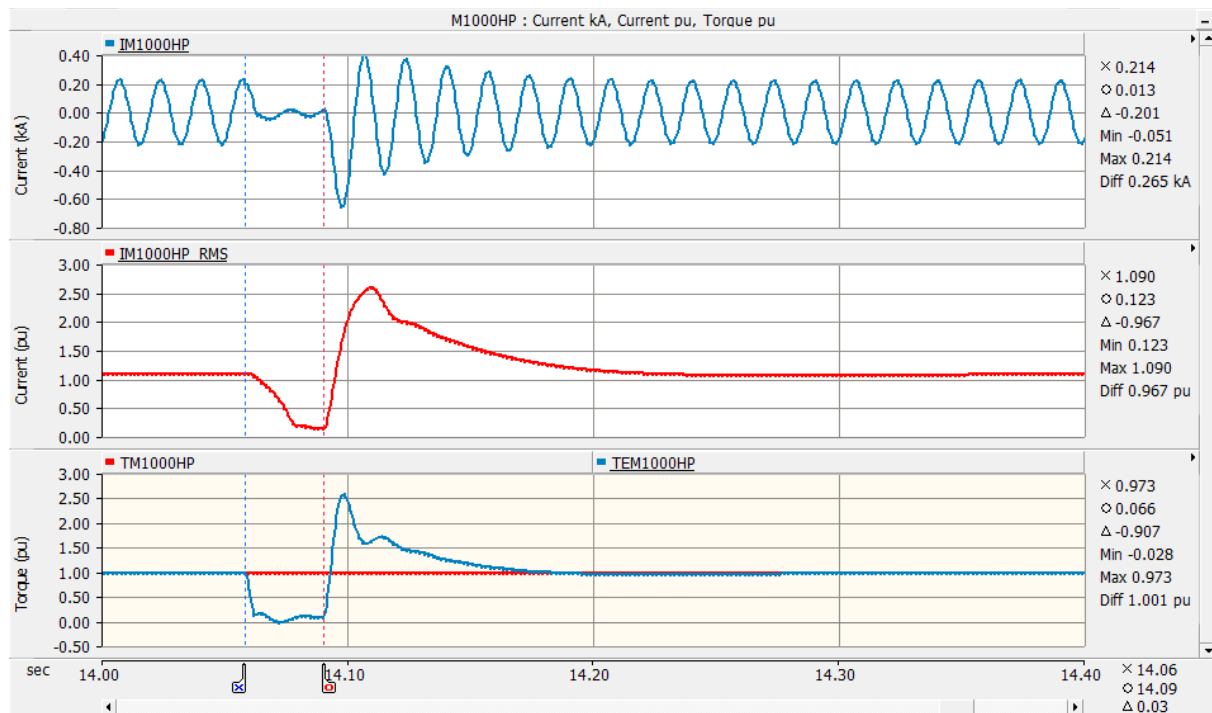


Figure 6-11 1000 HP Motor phase A instantaneous and RMS current, and torque transient response during a fast transfer test, initiated at t=14 sec.

Figure 6-12 shows the 470 HP induction motor current and torque transient behavior during the fast transfer simulation. The first graph (blue plot) shows the motor phase A instantaneous current. Before the loss of power supply, the motor phase A current was 68.89 A RMS and after the start-up breaker opened the motor current decayed. During the time of loss of power supply, the motor supplied current (approximately 4.54 A RMS) to the other motors connected to the motor bus. When the motor bus was reconnected from the auxiliary system the motor phase A current increased up to a maximum peak value of 323 A. After the transient settling time the current was 66.96 A.

The second graph (red plot) shows the motor RMS phase A current in p.u. Before the start-up breaker opened, the motor phase A current was 1.107 p.u., during the loss of power supply the motor phase A current was 0.073 p.u. and when the auxiliary breaker closed, the reconnecting transient caused the phase A current to increase to 2.859 p.u. The motor phase A current transient settling time was close to 210 milliseconds, and after this time the phase A current was 1.076 p.u. The small difference between the current before the loss of power supply and the current after reconnection is because the motor was reconnected to a different source.

The third graph shows the load torque (red plot) and the electromagnetic torque (blue plot). The load torque was practically not disturbed during the motor bus transfer and during the reconnection to the new incoming source. The electromagnetic torque changed from 1.030 p.u. during nominal operating conditions to a torque of -0.134 p.u. behaving as an induction generator during the loss of power supply, therefore it was supplying current to other. When the auxiliary breaker closed reconnecting the motor bus the electromagnetic torque changed rapidly to 3.04 p.u. (positive torque), close to 11.22% more than the maximum torque during motor starting process. The torque transient settling time was close to 210 milliseconds.

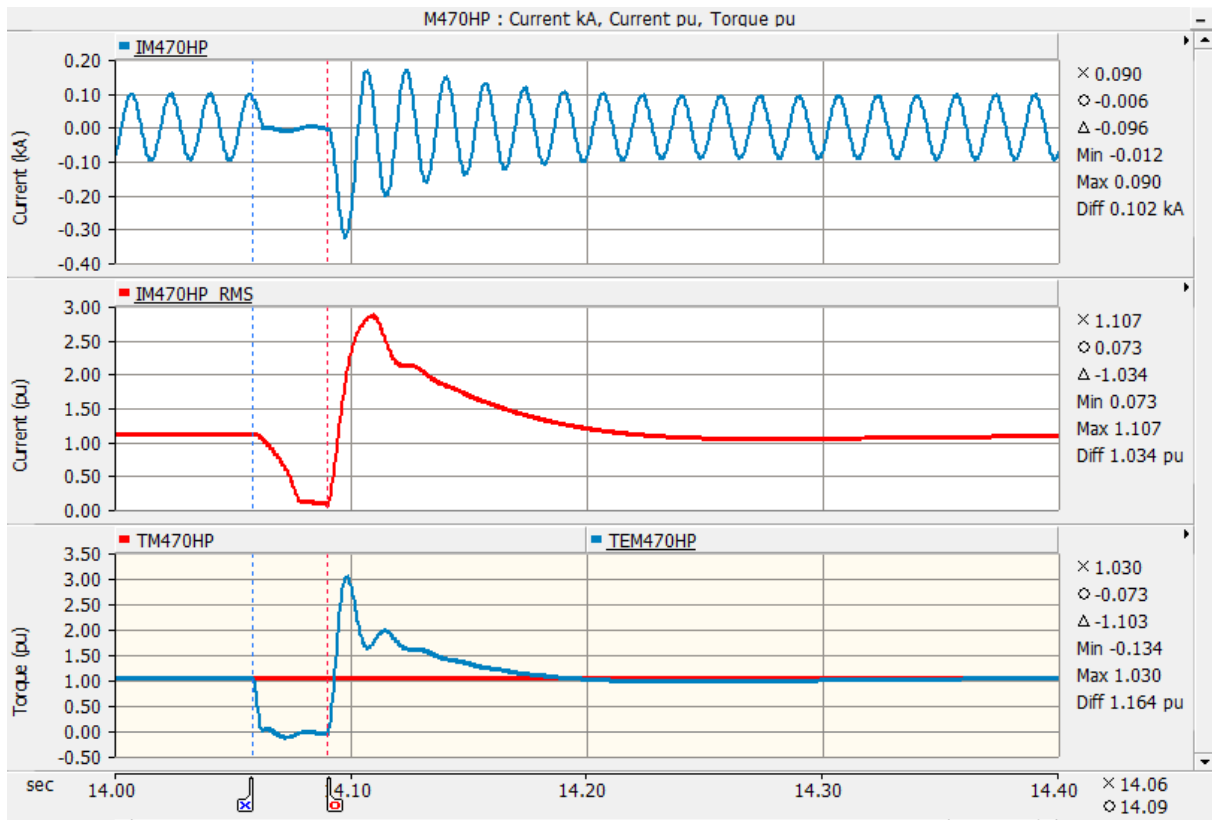


Figure 6-12 470 HP Motor phase A instantaneous and RMS current, and torque transient response during a fast transfer test, initiated at  $t=14$  sec.

Figures 6-13 to 6-15 show the instantaneous voltage, frequency and phase angle of the auxiliary, start-up and motor buses during fast transfer tests initiated at  $t=14.004167$  s,  $t=14.00333$  s and  $t=14.01250$  s respectively. The performance of the fast transfer algorithm during all the tests was the same as in the previous tests.

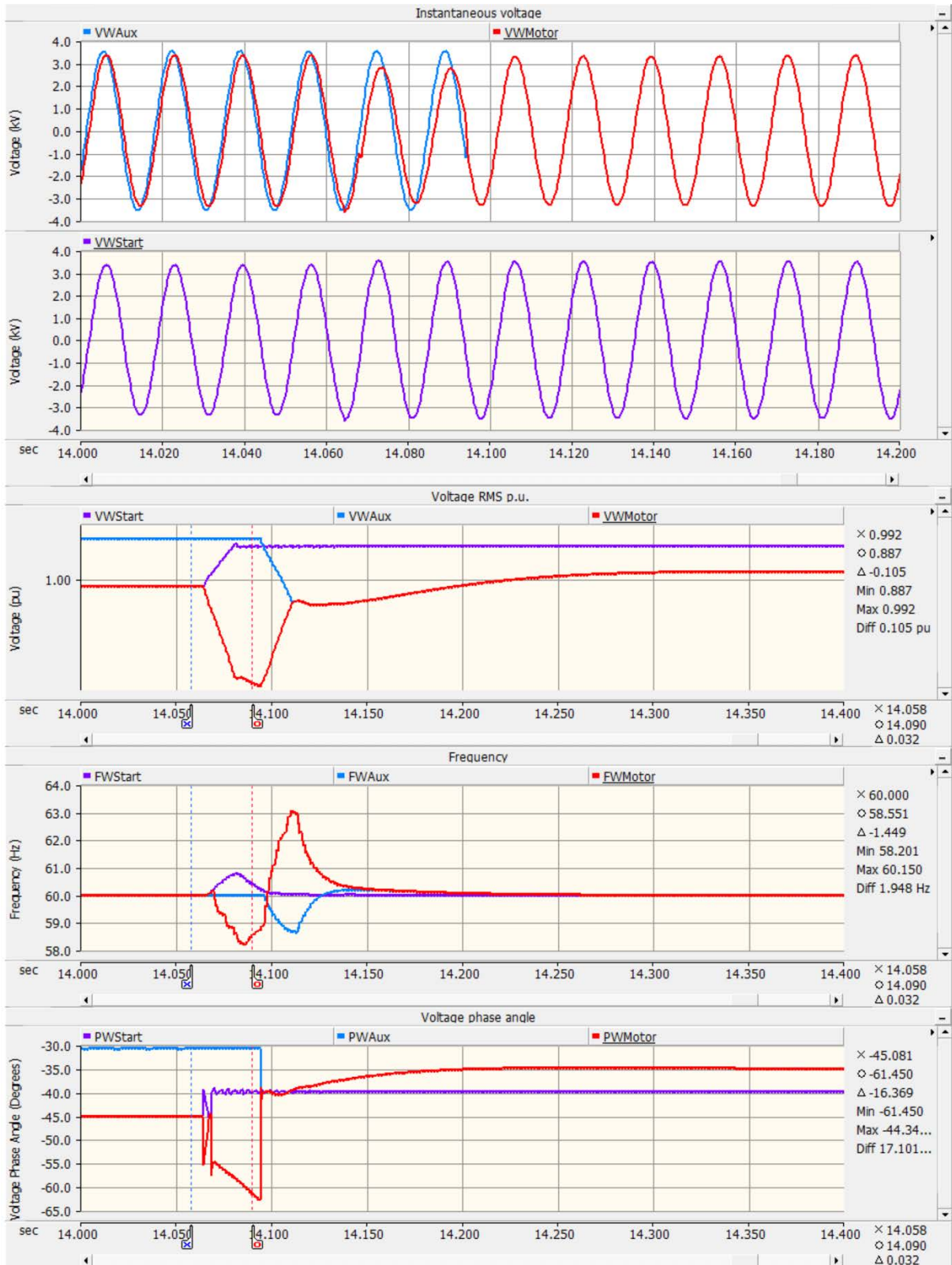


Figure 6-13 Phase A instantaneous voltage in kV, phase A RMS voltage in p.u., voltage frequency in Hz and phase A voltage phase angle during a fast transfer test, initiated at t=14.004167 sec.

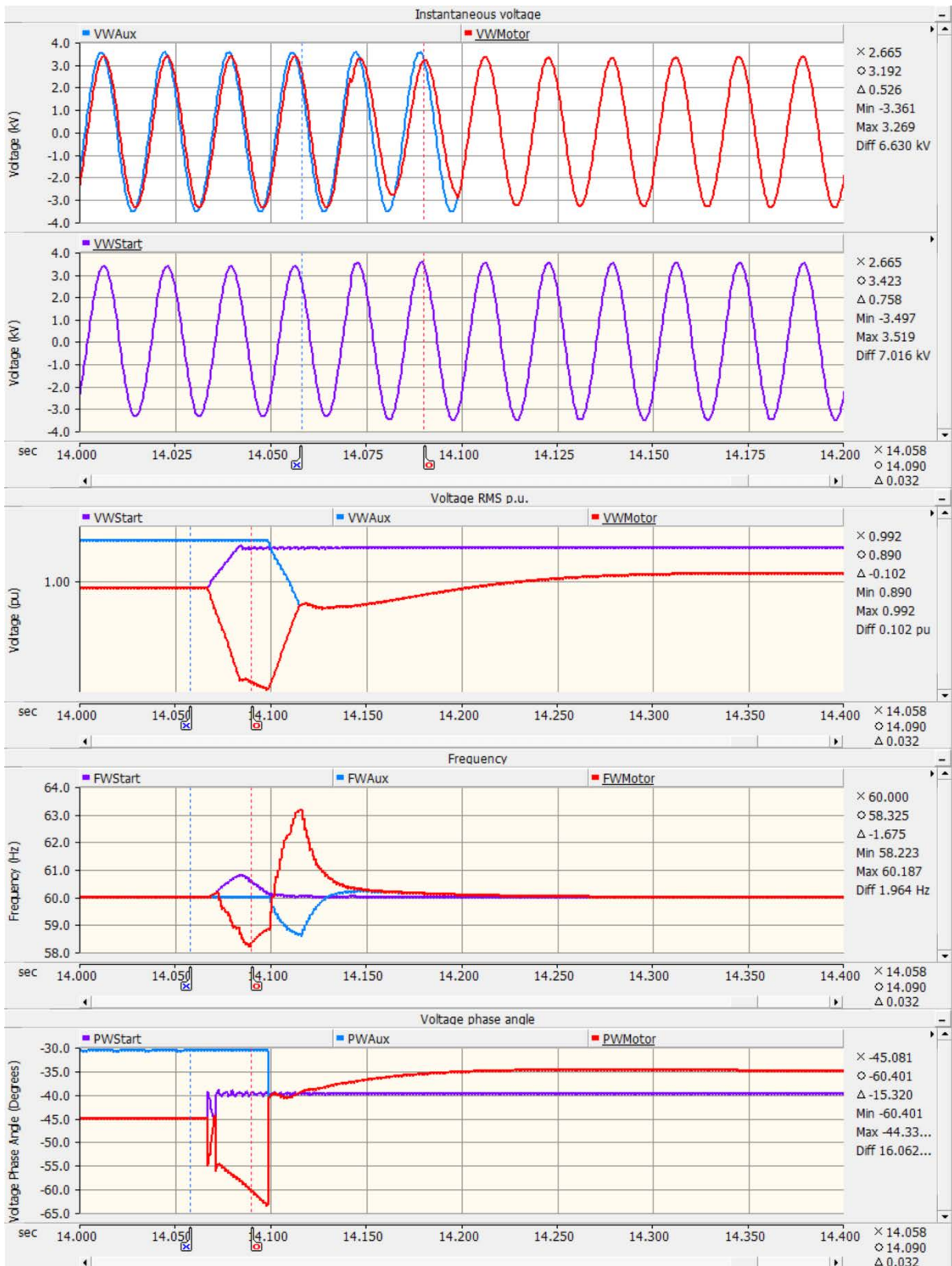


Figure 6-14 Phase A instantaneous voltage in kV, phase A RMS voltage in p.u., voltage frequency in Hz and phase A voltage phase angle during a fast transfer test, initiated at t=14.00833 sec.



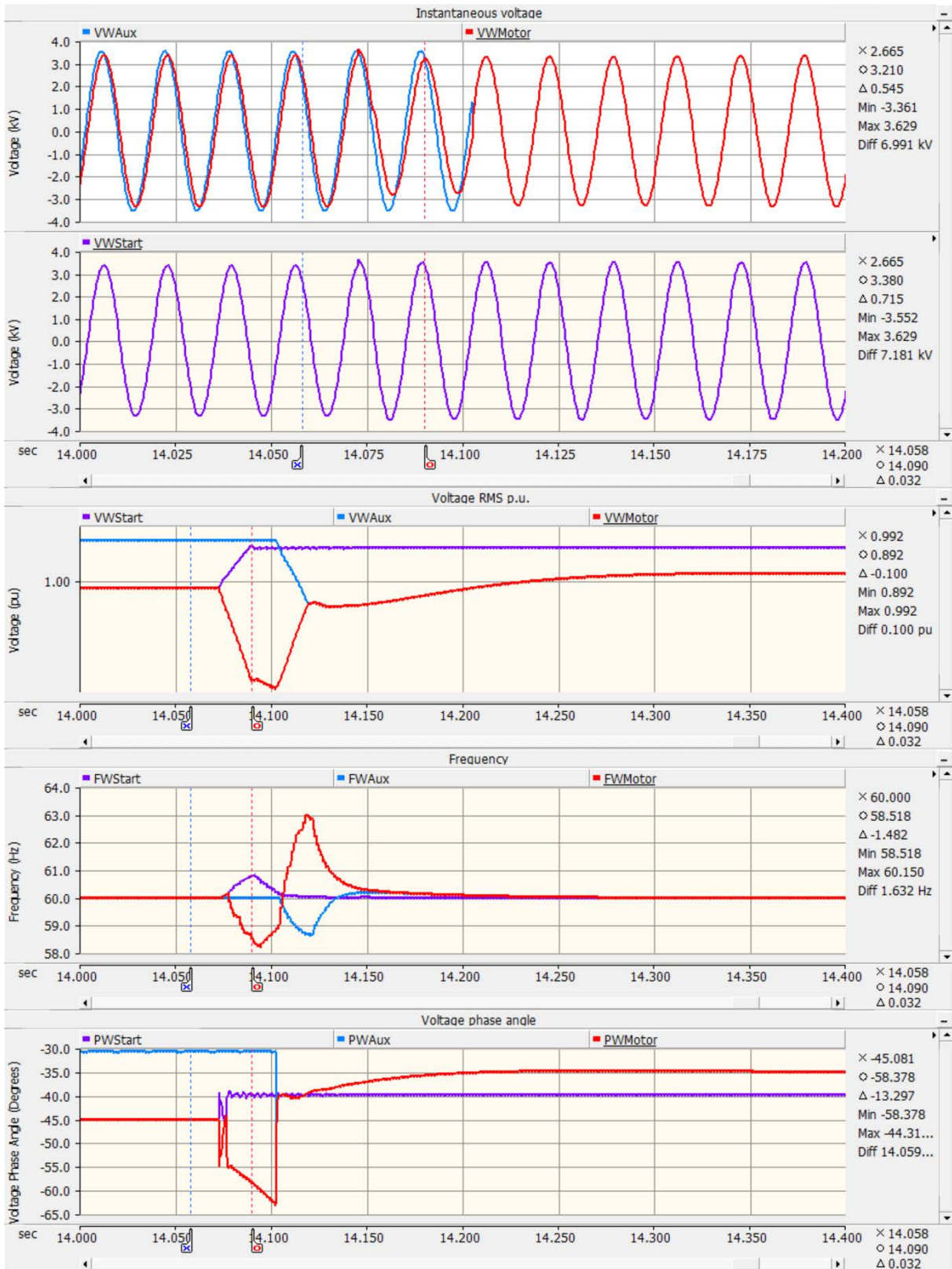


Figure 6-15 Phase A instantaneous voltage in kV, phase A RMS voltage in p.u., voltage frequency in Hz and phase A voltage phase angle during a fast transfer test, initiated at t=14.0125 sec.

Table 6-1 shows the summary of the fast transfer component response. The results cover the simulations for fast transfer test initiated at  $t=14.0$  sec,  $t=14.004167$  sec,  $t=14.00833$  sec,  $t=14.0125$  sec.

Initiation time	$t=14.0$ sec	$t=14.004167$ sec	$t=14.00833$ sec	$t=14.0125$ sec
<b>Motor bus phase A</b>				
a) Maximum peak voltage prior motor bus transfer	3.364 kV	3.364 kV	3.364 kV	3.364 kV
b) Positive peak voltage during loss of potential	2.985 kV	2.776 kV	3.207 kV	3.210 kV
c) Negative peak voltage during loss of potential	-3.205 kV	-3.220 kV	-2.954 kV	-2.779 kV
c) Maximum peak voltage after motor bus transfer	3.424 kV	3.424 kV	3.424 kV	3.424 kV
<b>Motor bus phase A voltage</b>				
a) Prior to motor bus transfer	0.992 p.u.	0.992 p.u.	0.992 p.u.	0.992 p.u.
b) Minimum value during loss of potential	0.882 p.u.	0.884 p.u.	0.882 p.u.	0.884 p.u.
c) After motor bus transfer	1.009 p.u.	1.009 p.u.	1.009 p.u.	1.009 p.u.
<b>Motor bus frequency</b>				
a) Prior to motor bus transfer	60.0 Hz	60.0 Hz	60.0 Hz	60.0 Hz
b) Minimum value during loss of power	58.23 Hz	58.2 Hz	58.22 Hz	58.23 Hz
c) Maximum value during reconnection	63.02 Hz	63.069 Hz	63.164 Hz	62.98 Hz
d) After motor bus transfer	60.0 Hz	60.0 Hz	60.0 Hz	60.0 Hz
<b>Motor bus phase A voltage angle</b>				
a) Prior to motor bus transfer	-45.08 degrees	-45.08 degrees	-45.08 degrees	-45.08 degrees
b) Minimum value during loss of power	-63.48 degrees	-62.91 degrees	-66.92 degrees	-62.94 degrees
d) After motor bus transfer	-34.97 degrees	-34.97 degrees	-34.97 degrees	-34.97 degrees

*Table 6-1 Summary of the fast transfer component response*

### 6.2.2 In-Phase Transfer Algorithm Component Response

The in-phase transfer method requires that the motor bus voltage and the new source voltage be in phase coincidence at the instant of transfer.

To test the algorithm's performance, four tests were carried out. All tests were performed under the same voltage, phase angle and frequency conditions of the auxiliary and start-up systems but with different motor bus transfer initiation times.

The motor bus transfer system controls and the motor bus transfer system test mode used for this test are shown in Figure 6-16. Control SysSel was set to position BWS (transfer simulation from the start-up to the auxiliary system), manual transfer switch MTransfer set to 0, transfer initialization time MTime set to 14 seconds, TType was set to 2 (in-phase transfer test mode). Control Coast Down was set to off, control Coast Down Time was set to 99 seconds (coast down simulating motors spinning down in group was not performed), Ind Coast Down Time was set to 99 seconds (coast down simulating motors spinning individually was not performed).

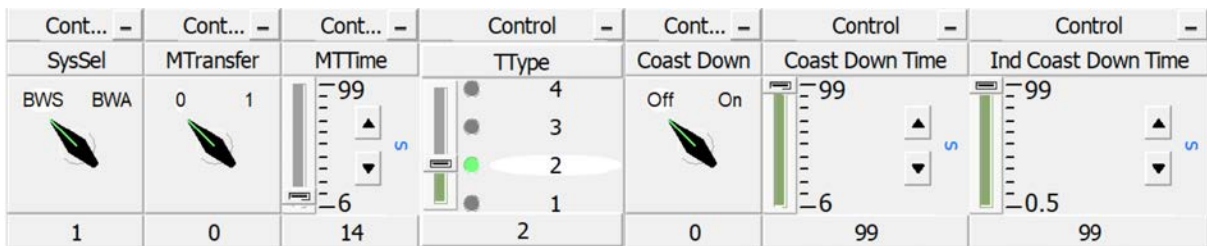


Figure 6-16 Motor bus transfer system controls for an in-phase test, initiated at t=14 sec.

The in-phase bus transfer was initiated at t=14 seconds and the start-up breaker opened at t=14.058 seconds (phase B current was interrupted at t=8.0588 s, phase A current at t= 14.0629 s and phase C current at t=14.0629 s.). The transfer was accomplished at t=14.477 seconds, at the first voltage phase angle coincidence between the motor bus and the auxiliary bus voltage.



Figure 6-17 shows the phase A instantaneous voltage of the auxiliary bus (light blue plot), start-up bus (purple plot) and motor bus (red plot) during the in-phase transfer test. The motor bus was transferred from the start-up side to the auxiliary side.

The start-up bus voltage magnitude before the transfer initiation was 4.126 kV L-L and after the bus transfer the voltage magnitude was 4.3098 kV. The auxiliary bus voltage magnitude before the transfer initiation was 4.3430 kV and after the bus transfer it was 4.193 kV. During the loss of power supply, the motor bus voltage magnitude decayed, at the instant before the reconnection to the auxiliary source the motor bus voltage magnitude was -0.628 kV. The first voltage phase angle coincidence was at 25 cycles of a 60 Hz frequency after the transfer initiation.

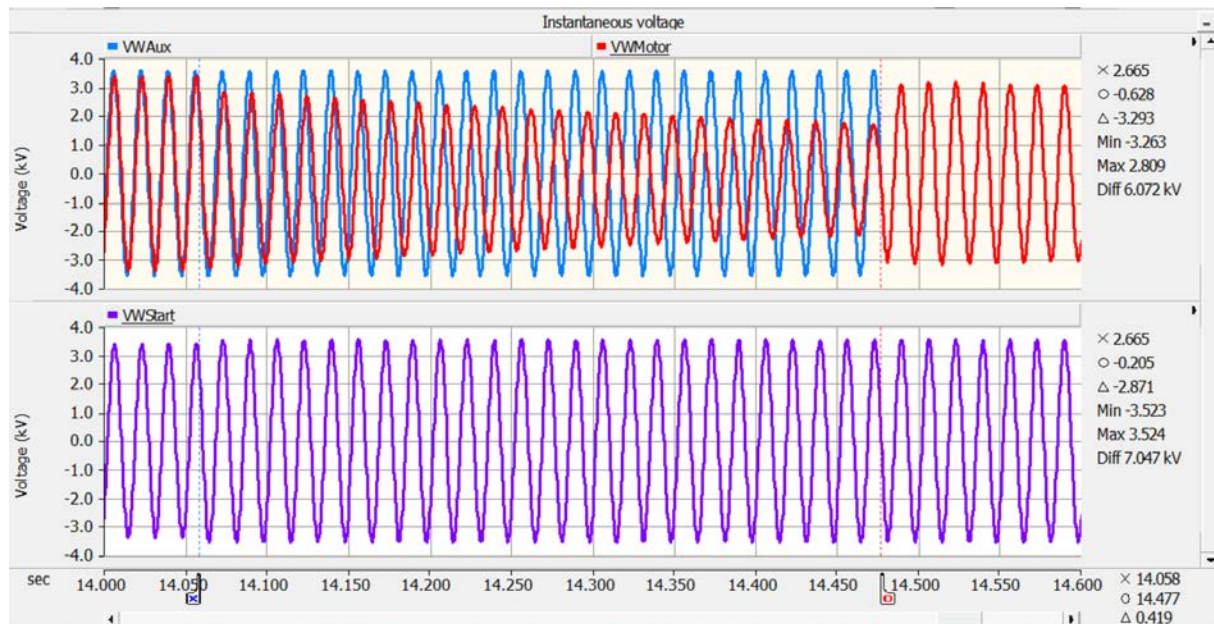


Figure 6-17 Phase A Instantaneous Voltage in kV during an in-phase transfer test, initiated at  $t=14$  sec.

Figure 6-18 shows the per unit phase A RMS voltage of the auxiliary bus (light blue plot), start-up bus (purple plot) and motor bus (red plot) during the fast transfer test. The start-up voltage magnitude changed from 0.992 p.u. (in a reference of 4.16 kV L-L) before the bus transfer to 1.036 p.u. after the bus transfer. The auxiliary side voltage magnitude before the bus transfer was 1.044 p.u. and after the bus transfer was 1.008 p.u.

When the start-up breaker opened, the motor bus voltage magnitude decayed to 0.894 p.u., and continued decaying to 0.575 p.u. at the moment before the auxiliary breaker closed. When the auxiliary breaker closed, the motor bus voltage took 820 milliseconds to recover.

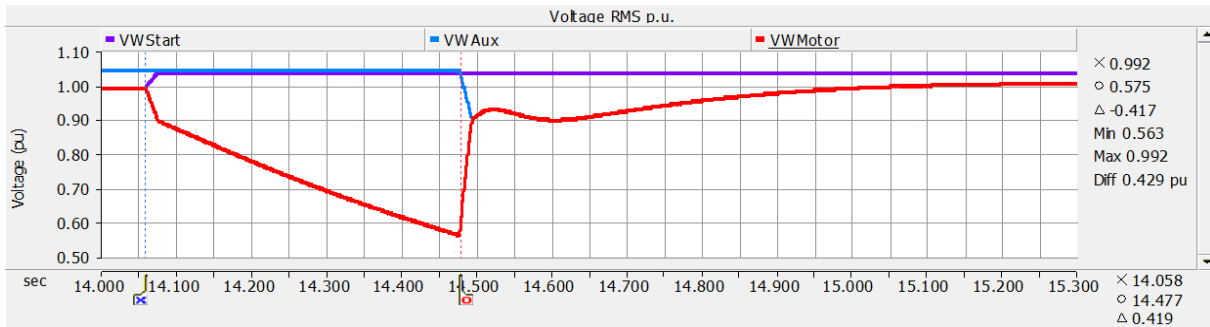


Figure 6-18 Phase A RMS voltage in per unit during an in-phase transfer test, initiated at t=14 sec.

Figure 6-19 shows the frequency of the auxiliary bus (light blue plot), start-up bus (purple plot) and motor bus (red plot) during the in-phase transfer test. The motor bus voltage frequency decayed to 58.93 Hz on loss of power supply and continued decaying up to 56.49Hz before the auxiliary medium voltage breaker closed. The motor bus frequency took 820 milliseconds to recover once the motor bus was reconnected from the auxiliary source.

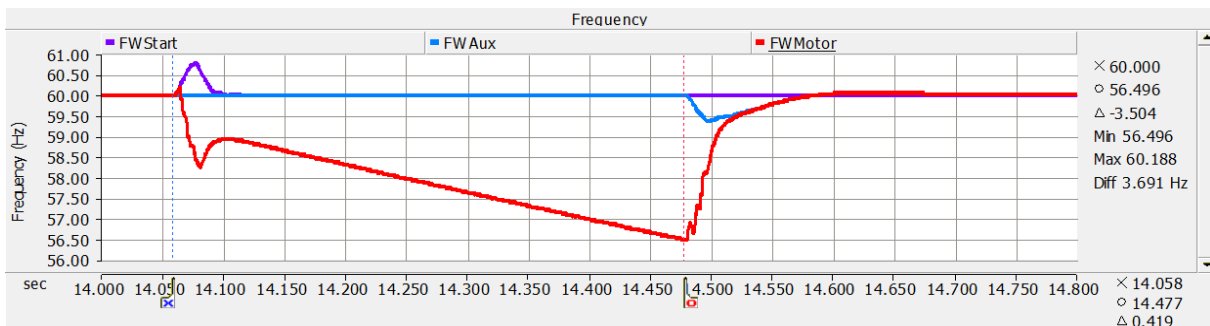


Figure 6-19 Voltage frequency in Hertz during an in-phase transfer test, initiated at t=14 sec.

Figure 6-20 shows the phase A voltage angle of the auxiliary bus (light blue plot), start-up bus (purple plot) and motor bus (red plot) during the in-phase transfer test. The start-up phase A voltage phase angle before the transfer was -45.08 degrees and after the transfer was -39.1 degrees. The auxiliary phase A voltage phase angle changed from -30.729 degrees before the bus transfer to -35.07 degrees after the transfer. The motor bus voltage phase A angle changed from its steady state operating angle of -45.08 degrees to -54.5 degrees immediately after the loss of power supply, then the phase angle continued changing and the auxiliary breaker closed in-phase coincidence at t=14.477 seconds.

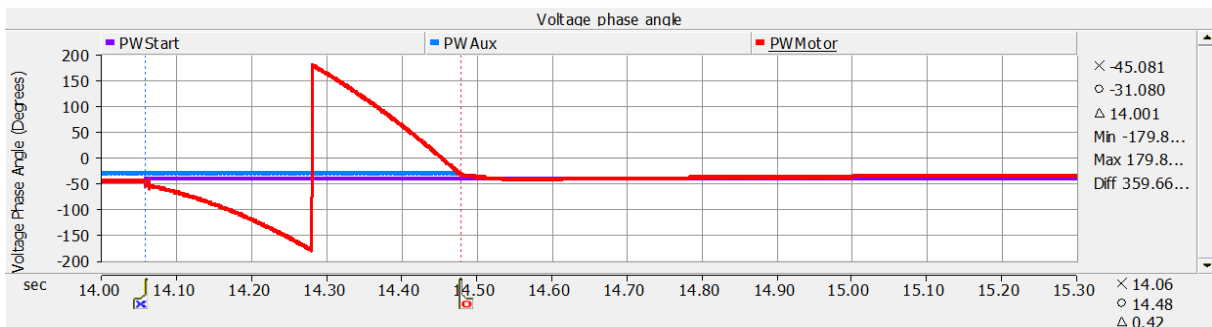


Figure 6-20 Phase A Voltage phase angle in degrees during an in-phase transfer test, initiated at t=14 sec.

The logic timing of the motor bus transfer system elements and circuit breaker contact operations is shown in Figure 6-21, where:

RTrip	Element activated by manual transfer, relay trip, and test mode initialization time
FTSMTP	Fast transfer trip element
IPSMTP	In-phase transfer trip element
RVSMTTP	Residual voltage transfer trip element
S->A	Element to enable bus transfer from start-up to auxiliary system
A->S	Element to enable bus transfer from auxiliary to start-up system

BKStart      Start-up side breaker

BKAux        Auxiliary side breaker

Before the transfer initialization the elements RTrip and IPSMTP were enabled; elements FTSMTP and RVSMTP were disabled during the whole simulation, elements S->A (motor bus transfer from start-up source to auxiliary source) was enabled and A->S (motor bus transfer from auxiliary source to start-up source) was disabled; BKStart was closed and BKAux was open.

When time of the simulation was equal to the setting of the signal MTime,  $t = 14$  seconds, the element RTrip tripped instantaneously and the tripping signal was sent to the start-up breaker BKStart which opened at  $t = 14.058$  seconds and the element S->A changed its status from enabled to disabled. The in-phase algorithm computed the first in-phase angle coincidence between the auxiliary voltage phase angle and the changing motor bus voltage phase angle. At  $t = 14.387$  the in-phase element IPSMTP tripped and the signal was sent to the auxiliary breaker BKAux which closed 90 milliseconds after receiving the closing signal, and the element A->S changed its status from disabled to enabled. The transfer was finally accomplished at  $t = 14.477$  seconds.

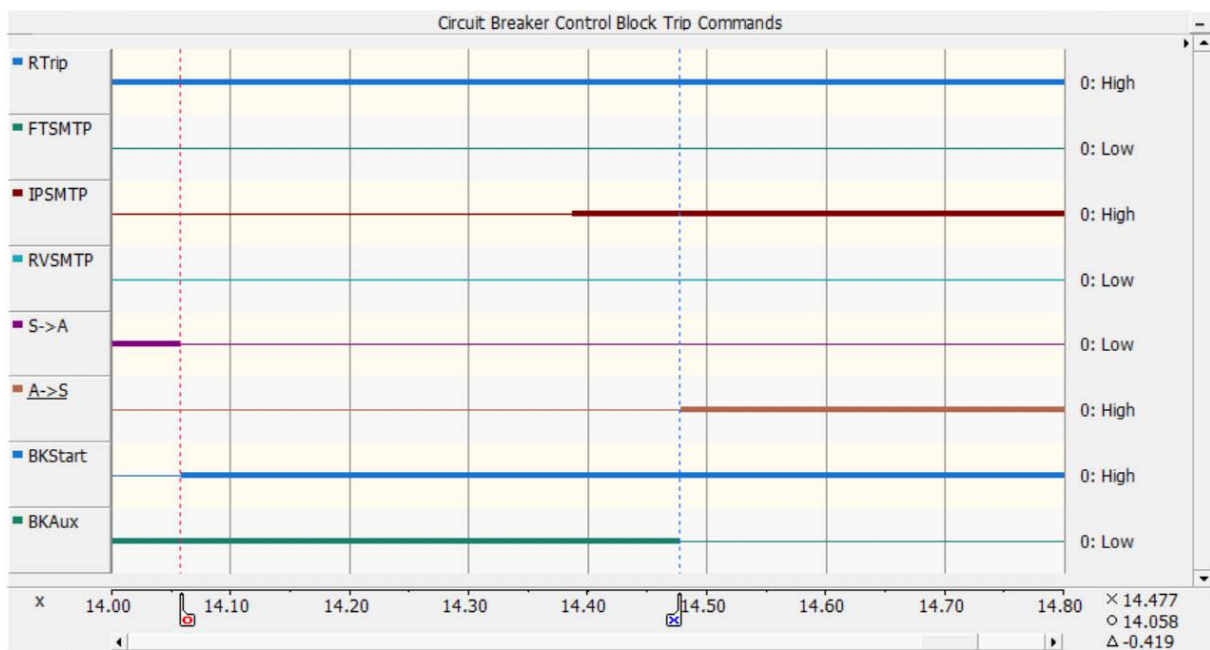


Figure 6-21 Motor bus transfer system element and circuit breaker contact operations during an in-phase transfer test, initiated at  $t = 14$  sec.

The logic timing of the motor bus transfer system elements and circuit breaker contacts operated correctly.

Figure 6-22 shows the 9000 HP induction motor current and torque transient behavior during the in-phase transfer simulation. The first graph (blue plot) shows the motor phase A instantaneous current. Before the loss of power supply the motor phase A current was 1.15395 kA RMS and during the time of loss of power supply, the motor supplied current to other motors. At the instant after the loss of power supply the motor supplied approximately 144.11 A RMS and at moment before the auxiliary breaker closed, reconnecting the motor bus, the 6000 HP was supplying 130.01 A to the other motors connected to the motor bus. When the motor bus was reconnected from the auxiliary system the motor phase A current increased up to a maximum peak value of -5.478 kA. After the transient settling time the current was 1.14642 kA.

The second graph (red plot) shows the RMS phase A current in p.u. Before the start-up breaker opened the phase A current was 1.073 p.u., the moment after the start-up breaker opened, the current went to 0.134 p.u. and the moment before the auxiliary breaker closed the phase A current in RMS was 0.121 p.u. When the auxiliary breaker closed, the reconnecting transient caused the phase A current to increase to 3.398 p.u. The phase A current transient settling time was close to 820 milliseconds, and after this time the phase A current was 1.066 p.u. The small difference between the current before the loss of power supply and the current after reconnection is because the motor was reconnected to a different source.

The third graph shows the load torque (red plot) and the electromagnetic torque (blue plot). The electromagnetic torque changed from 0.982 p.u. during nominal operating conditions to 0.235 p.u. when the start-up breaker opened. When the auxiliary breaker closed reconnecting the motor bus the electromagnetic torque changed rapidly to 2.618 p.u. (positive torque), close to 87.56% of the maximum torque during motor starting process. The torque transient settling time was close to 820 milliseconds. It may be observed the damped oscillatory behavior due to the large frequency difference between the motor bus voltage and the new source voltage.

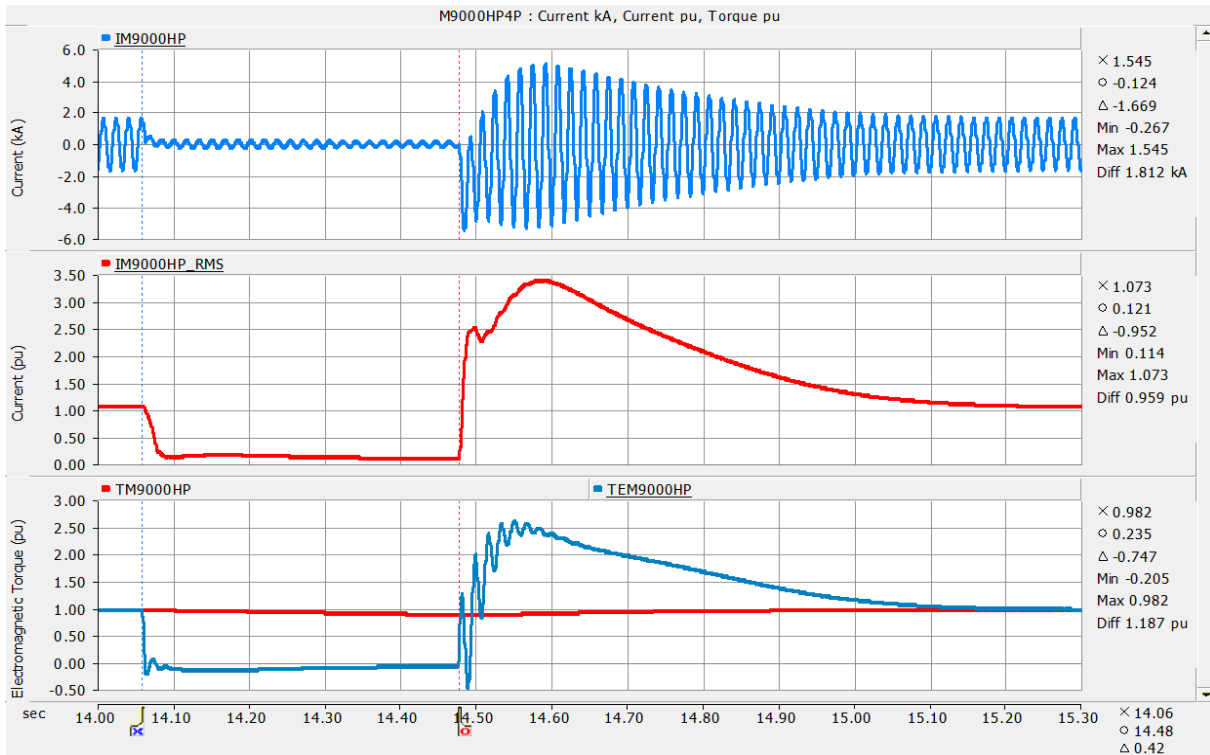


Figure 6-22 9000 HP Motor phase A instantaneous and RMS current and torque transient response during an in-phase transfer test, initiated at  $t=14$  sec.

Figure 6-23 shows the 6000 HP induction motor current and torque transient behavior during the in-phase transfer simulation. The first graph (blue plot) shows the motor phase A instantaneous current. Before the loss of power supply the motor phase A current was 943.89 A RMS and during the time of loss of power supply, the motor increasingly drew current from other motors. At the instant after the loss of power supply it drew approximately 104.78 A RMS and at moment before the auxiliary breaker closed, reconnecting the motor bus, the 6000 HP was drawing 164.15 A from the other motors connected to the motor bus. When the motor bus was reconnected from the auxiliary system the motor phase A current increased up to a maximum peak value of -3.329 kA. After the transient settling time the current was 964.85 A.

The second graph (red plot) shows the RMS phase A current in p.u. Before the start-up breaker opened the phase A current was 1.081 p.u., the moment after the start-up breaker opened, the current went to 0.120 p.u. and the moment before the auxiliary breaker closed the phase A current in RMS was 0.188 p.u. When the auxiliary breaker closed, the reconnecting transient caused the phase A current to increase to 2.691 p.u. The phase A current transient settling time was close to 820 milliseconds, and

after this time the phase A current was 1.105 p.u. The small difference between the current before the loss of power supply and the current after reconnection is because the motor was reconnected to a different source.

The third graph shows the load torque (red plot) and the electromagnetic torque (blue plot). The electromagnetic torque changed from 0.966 p.u. during nominal operating conditions to a minimum of 0.362 p.u. when the start-up breaker opened. When the auxiliary breaker closed reconnecting the motor bus the electromagnetic torque changed rapidly to 1.888 p.u. (positive torque), close to 81.37% of the maximum torque during motor starting process. The torque transient settling time was close to 820 milliseconds.

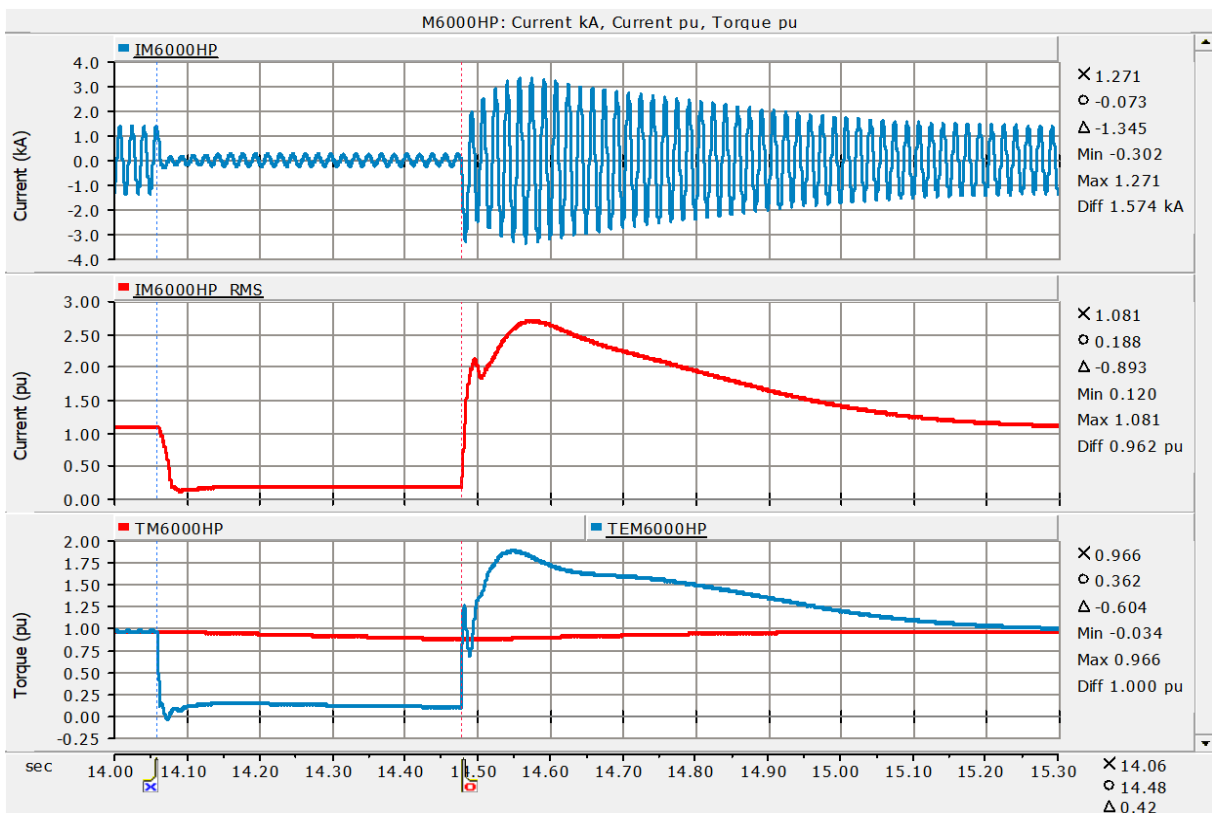


Figure 6-23 6000 HP Motor phase A instantaneous and RMS current and torque transient response during an in-phase transfer test, initiated at  $t=14$  sec.

Figure 6-24 shows the 3200 HP induction motor current and torque transient behavior during the in-phase transfer simulation. The first graph (blue plot) shows the phase A instantaneous current. Before the loss of power supply the motor phase A current was 469.93 A RMS. During the time of loss of power supply, the motor was supplying current. At the moment after the loss of power supply it supplied approximately 22.45 A RMS and at the moment before the auxiliary breaker closed, reconnecting the motor bus, the 3200 HP was supplying 48.73 A to other motors connected to the motor bus. When the motor bus was reconnected from the auxiliary system the motor phase A current increased up to a maximum negative peak value of -1.833 kA. After the transient settling time the current was 473.74 A.

The second graph (red plot) shows the RMS phase A current in p.u. Before the start-up breaker opened the phase A current was 1.109 p.u., the moment after the start-up breaker opened, the current went to 0.053 p.u. and the moment before the auxiliary breaker closed the phase A current in RMS was 0.115 p.u. When the auxiliary breaker closed, the reconnecting transient caused the phase A current to increase to 3.067 p.u. The phase A current transient settling time was close to 820 milliseconds, and after this time the phase A current was 1.118 p.u. The small difference between the current before the loss of power supply and the current after reconnection is because the motor was reconnected to a different source.

The third graph shows the load torque (red plot) and the electromagnetic torque (blue plot). The electromagnetic torque changed from 1.029 p.u. during nominal operating conditions to -0.133 p.u. (negative torque) the moment after when the start-up breaker opened, and during the loss of power supply the 3200 HP induction motor behaved as an induction generator, therefore it was supplying current to the other motors. The moment before the auxiliary breaker closed reconnecting the motor bus, the electromagnetic torque was 0.238 p.u. When the auxiliary breaker closed the 3200 HP induction motor torque changed rapidly to 2.194 p.u. (positive torque); close to 80.98% of the maximum torque during motor starting process. The torque transient settling time was close to 820 milliseconds.



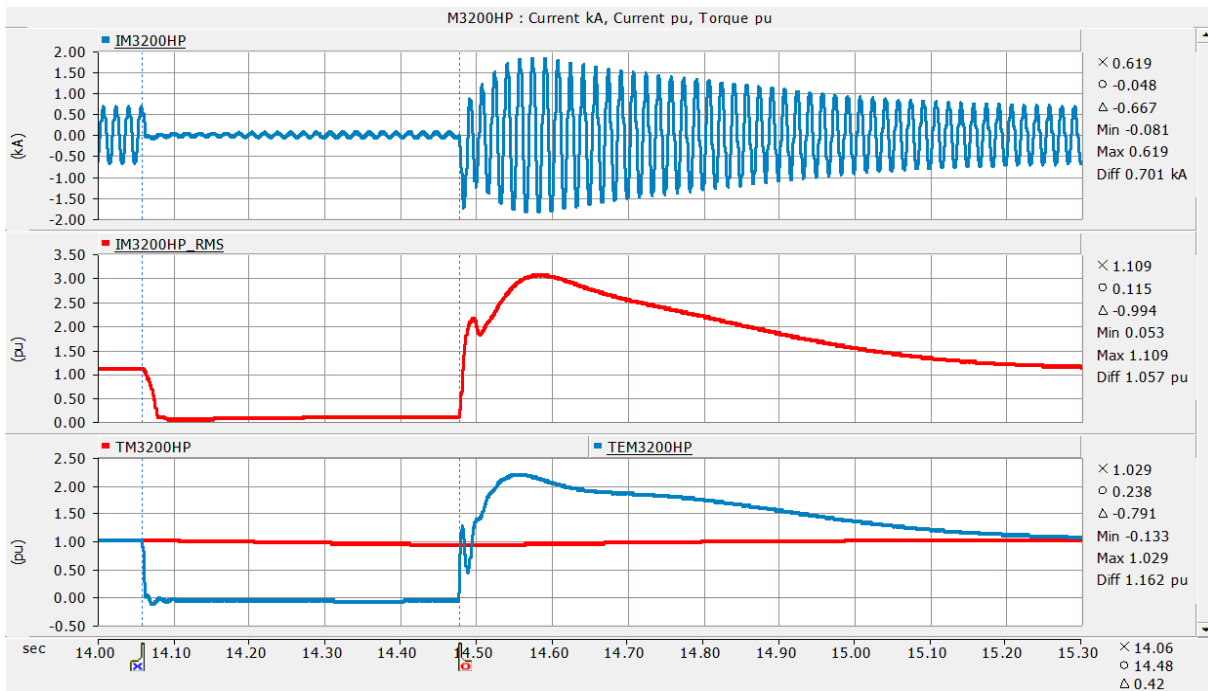


Figure 6-24 3200 HP Motor phase A instantaneous and RMS current and torque transient response during an in-phase transfer test, initiated at  $t=14$  sec.

Figure 6-25 shows the 1400 HP induction motor current and torque transient behavior during the in-phase transfer simulation. The first graph (blue plot) shows the motor phase A instantaneous current. Before the loss of power supply the motor phase A current was 221.98 A RMS. The first cycles after the moment of the loss of power supply the 1400 HP induction motor drew approximately 37.5 A RMS and during the last cycles of the loss of power supply the motor drew current to other motors. At the moment before the auxiliary breaker closed, reconnecting the motor bus, the 1400 HP motor was drawing 15.49 A from the other motors connected to the motor bus. When the motor bus was reconnected from the auxiliary system the motor phase A current increased up to a maximum peak value of -718 A. After the transient settling time the current was 225.85 A.

The second graph (red plot) shows the motor RMS phase A current in p.u. Before the start-up breaker opened the motor phase A current was 1.089 p.u. At the instant after the start-up breaker opened, the current went to 0.184 p.u. and the moment before the auxiliary breaker closed the RMS phase A current was 0.076 p.u. It may be observed that during the loss of power supply the motor was drawing current from other motors.

When the auxiliary breaker closed, the reconnecting transient caused the motor phase A current to increase to 2.429 p.u. The motor phase A current transient settling time was close to 820 milliseconds, and after this time the phase A current was 1.108 p.u. The small difference between the current before the loss of power supply and the current after reconnection is because the motor was reconnected to a different source.

The third graph shows the load torque (red plot) and the electromagnetic torque (blue plot). The electromagnetic torque changed from 0.969 p.u. during nominal operating conditions to 0.052 p.u. During the first cycles after the start-up breaker the motor torque was 0.013 p.u. The moment before the auxiliary breaker closed, the electromagnetic torque was 0.265. When the auxiliary breaker closed reconnecting the motor bus the electromagnetic torque changed rapidly to 1.737 p.u. (positive torque), close to 77.02% of the maximum torque during motor starting process. The torque transient settling time was close to 820 milliseconds.

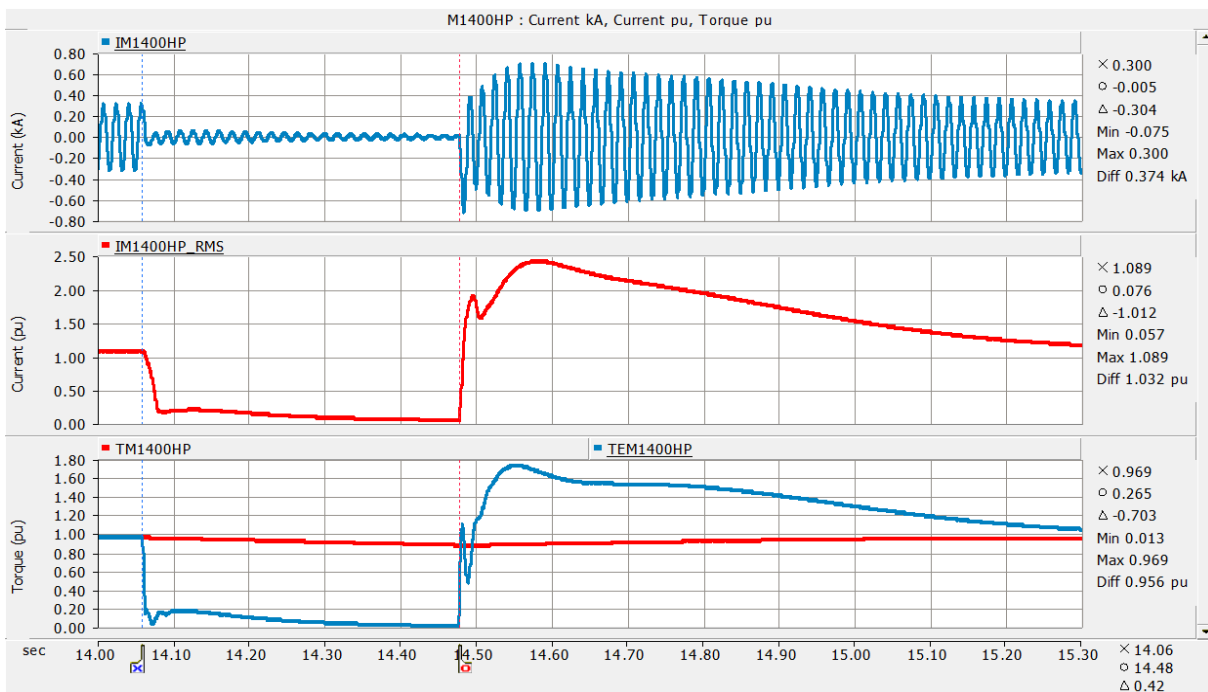


Figure 6-25 1400 HP Motor phase A instantaneous and RMS current and torque transient response during an in-phase transfer test, initiated at t=14 sec.

Figure 6-26 shows the 1000 HP induction motor current and torque transient behavior during the in-phase transfer simulation. The first graph (blue plot) shows the phase A instantaneous current. Before the loss of power supply, the motor phase A current was 158.62 A RMS and at the moment after the loss of power supply the 1400 HP induction motor drew approximately 24.15 A RMS and at the instant before the auxiliary breaker closed, reconnecting the motor bus, the 1000 HP motor was supplying 16.44 A to the other motors connected to the motor bus. When the motor bus was reconnected to the auxiliary system the motor phase A current increased up to a maximum peak value of -548 A. After the transient settling time the current was 160.66 A.

The second graph (red plot) shows the RMS phase A current in p.u. Before the start-up breaker opened, the motor phase A current was 1.09 p.u. At the moment after the start-up breaker opened, the current went to 0.166 p.u. and the moment before the auxiliary breaker closed the phase A current in RMS was 0.113 p.u. When the auxiliary breaker closed, the reconnecting transient caused the phase A current to increase to 2.662 p.u. The phase A current transient settling time was close to 820 milliseconds, and after this time the phase A current was 1.104 p.u. The small difference between the current before the loss of power supply and the current after reconnection is because the motor was reconnected to a different source.

The third graph shows the load torque (red plot) and the electromagnetic torque (blue plot). The electromagnetic torque changed from 0.973 p.u. during nominal operating conditions to -0.028 p.u. the moment after the start-up breaker opened. The moment before the auxiliary breaker closed, the electromagnetic torque was 0.314. When the auxiliary breaker closed reconnecting the motor bus the electromagnetic torque changed rapidly to 1.865 p.u. (positive torque), close to 80.21% of the maximum torque during motor starting process. The torque transient settling time was close to 820 milliseconds.

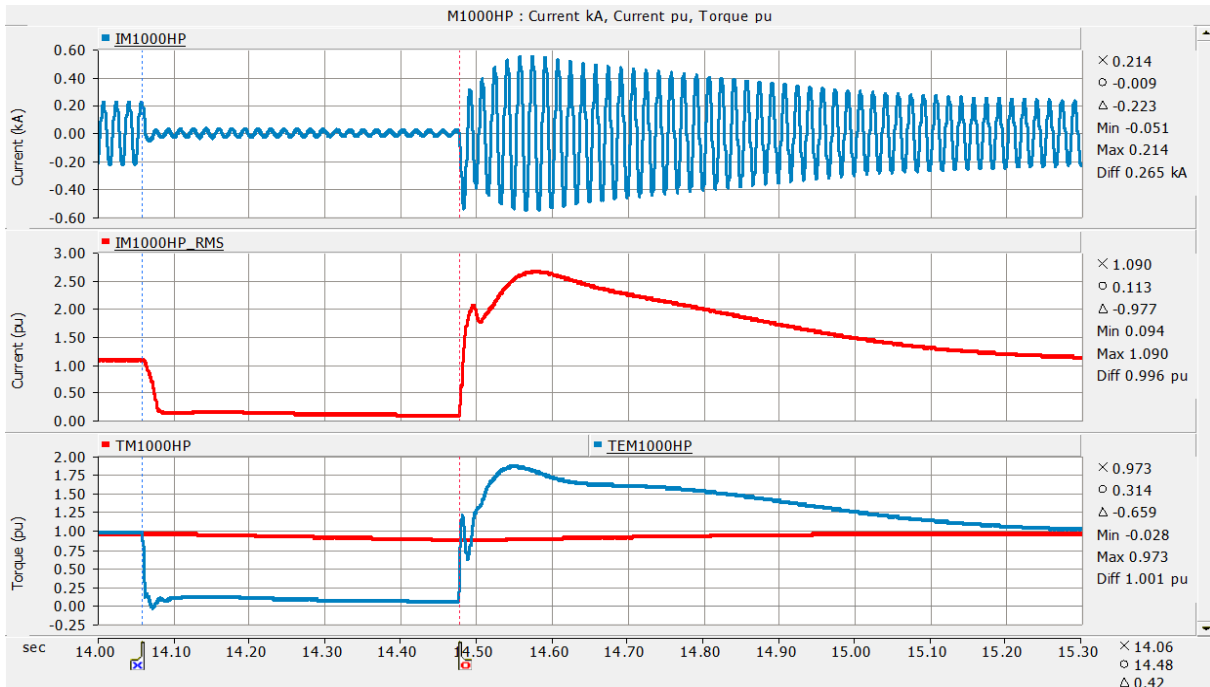


Figure 6-26 1000 HP Motor phase A instantaneous and RMS current and torque transient response during an in-phase transfer test, initiated at  $t=14$  sec.

Figure 6-27 shows the 470 HP induction motor current and torque transient behavior during the in-phase transfer simulation. The first graph (blue plot) shows the motor phase A instantaneous current. Before the loss of power supply, the motor phase A current was 68.89 A RMS, at the moment after the loss of power supply the 470 HP induction motor supplied approximately 3.36 A RMS and at the moment before the auxiliary breaker closed, reconnecting the motor bus, the 470 HP motor was supplying 5.16 A to the other motors connected to the motor bus. When the motor bus was reconnected from the auxiliary system the motor phase A current increased up to a maximum peak value of -271 A. After the transient settling time the current was 68.89 A.

The second graph (red plot) shows the motor RMS phase A current in p.u. Before the start-up breaker opened, the motor phase A current was 1.107 p.u. At the moment after the start-up breaker opened, the current went to 0.054 p.u. and the moment before the auxiliary breaker closed the motor phase A current in RMS was 0.083 p.u. When the auxiliary breaker closed, the reconnecting transient caused the phase A current to increase to 3.088 p.u. The phase A current transient settling time was close to 820 milliseconds, and after this time the phase A current was 1.107 p.u. The small difference between

the current before the loss of power supply and the current after reconnection is because the motor was reconnected to a different source.

The third graph shows the load torque (red plot) and the electromagnetic torque (blue plot). The electromagnetic torque changed from 1.03 p.u. during nominal operating conditions to -0.116 p.u. (negative torque) when the start-up breaker opened. The moment before the auxiliary breaker closed, the electromagnetic torque was 0.269. When the auxiliary breaker closed reconnecting the motor bus the electromagnetic torque changed rapidly to 2.209 p.u. (positive torque), close to 81.54% of the maximum torque during motor starting process. The torque transient settling time was close to 820 milliseconds.

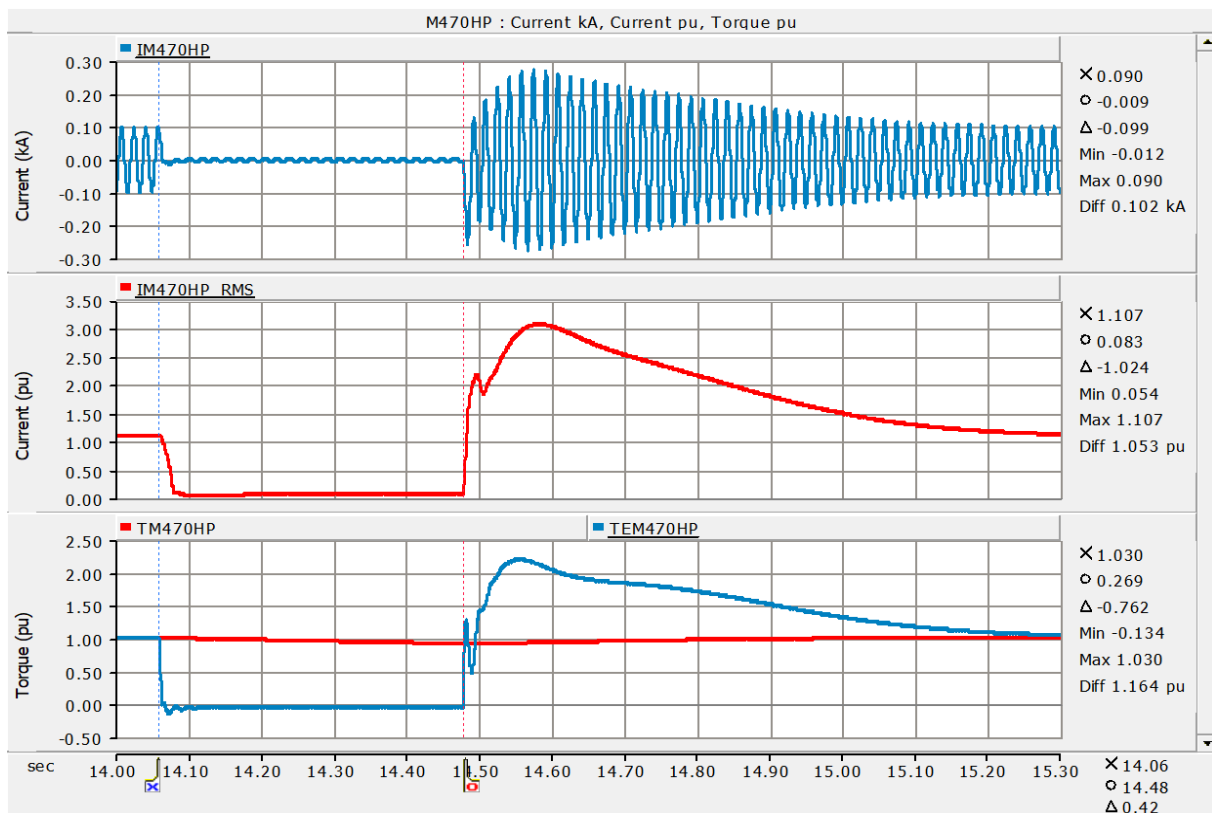


Figure 6-27 470 HP Motor phase A instantaneous and RMS current and torque transient response during an in-phase transfer test, initiated at  $t=14$  sec.

Figures 6-28 to 6-30 show the instantaneous voltage, frequency and phase angle of the auxiliary, start-up and motor bus during in-phase transfer tests initiated at  $t=14.004167$  s,  $t=14.00833$  s and

$t=14.01250$  s respectively. The performance of the in-phase transfer algorithm during all the tests was the same as in the previous tests.

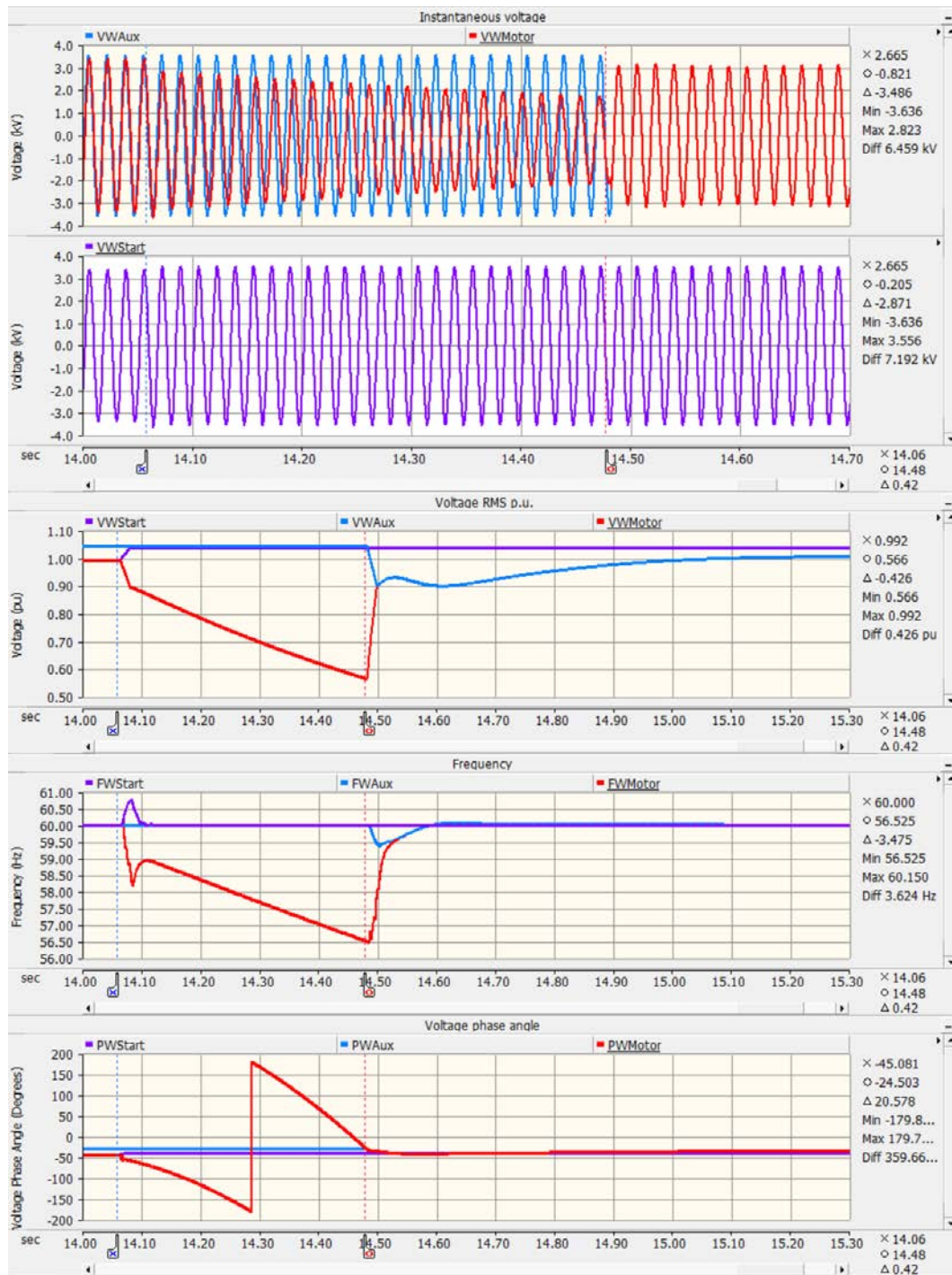


Figure 6-28 Phase A instantaneous voltage in kV, phase A RMS voltage in p.u., voltage frequency in Hz and phase A voltage phase angle during an in-phase transfer test, initiated at  $t=14.004167$  sec.



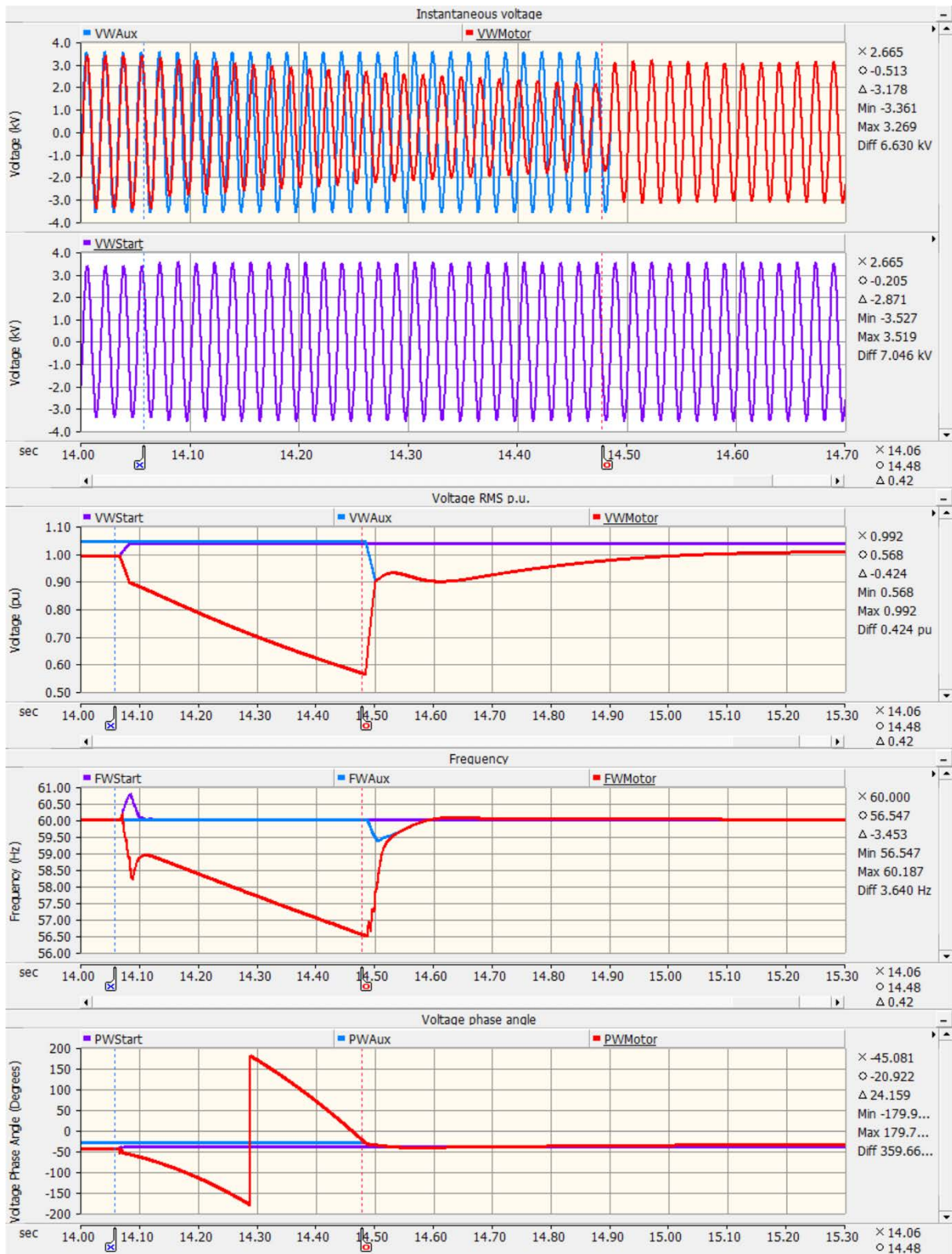


Figure 6-29 Phase A instantaneous voltage in kV, phase A RMS voltage in p.u., voltage frequency in Hz and phase A voltage phase angle during an in-phase transfer test, initiated at t=14.00833 sec.

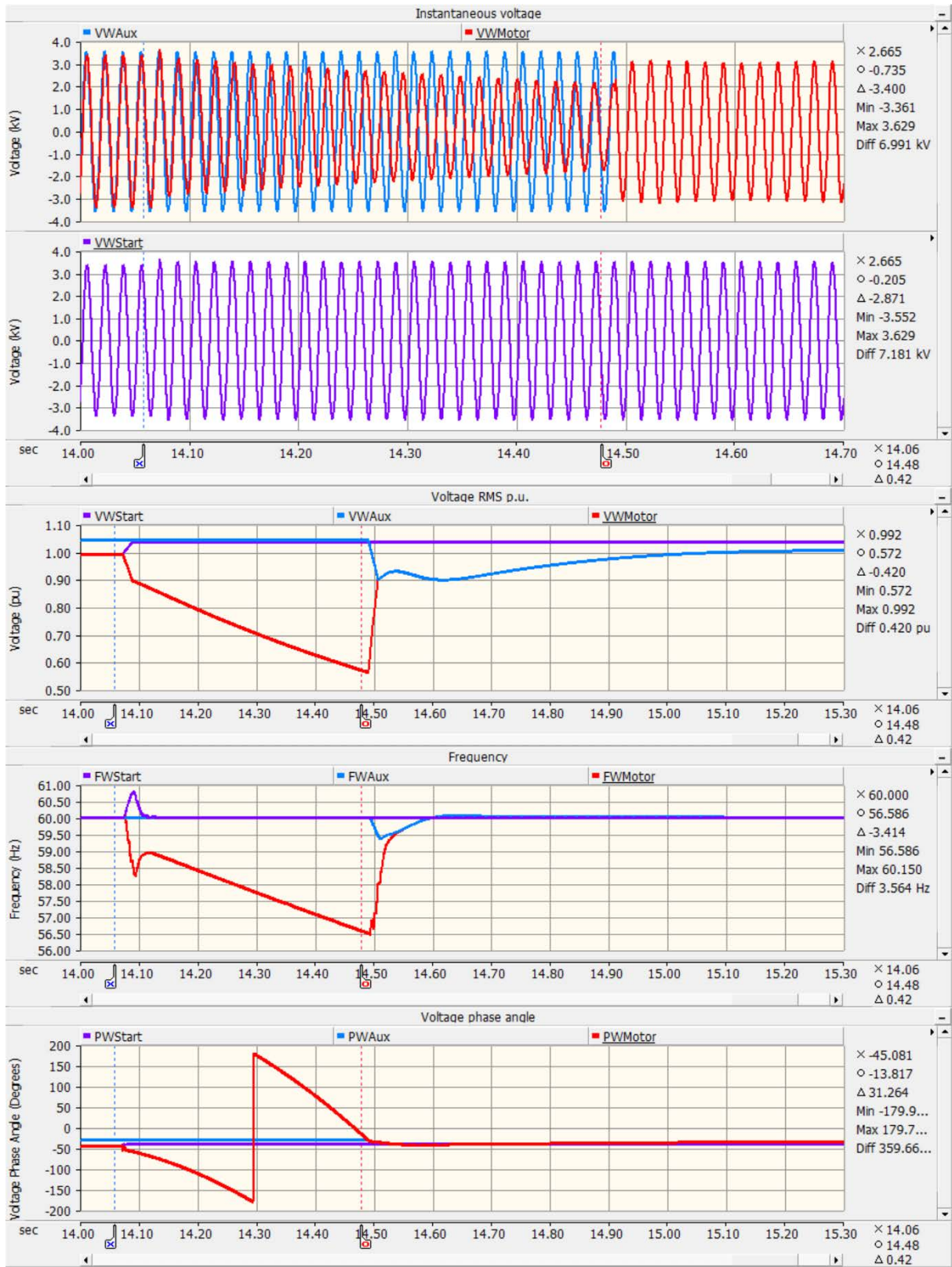


Figure 6-30 Phase A instantaneous voltage in kV, phase A RMS voltage in p.u., voltage frequency in Hz and phase A voltage phase angle during an in-phase transfer test, initiated at t=14.0125 sec.



Table 6-2 shows the summary of the in-phase transfer component response. The results cover the simulations for fast transfer test initiated at t=14.0 sec, t=14.004167 sec, t=14.00833 sec, t=14.0125 sec.

Initiation time	t=14.0 sec	t=14.004167 sec	t=14.00833 sec	t=14.0125 sec
<b>Motor bus phase A</b>				
a) Maximum peak voltage prior motor bus transfer	3.364 kV	3.364 kV	3.364 kV	3.364 kV
b) Positive peak voltage during loss of potential	1.698 kV	2.033 kV	2.130 kV	2.142 kV
c) Negative peak voltage during loss of potential	-2.128 kV	-2.323 kV	-1.693 kV	-1.710 kV
c) Maximum peak voltage after motor bus transfer	3.424 kV	3.424 kV	3.424 kV	3.424 kV
<b>Motor bus phase A voltage</b>				
a) Prior to motor bus transfer	0.992 p.u.	0.992 p.u.	0.992 p.u.	0.992 p.u.
b) Minimum value during loss of potential	0.575 p.u.	0.566 p.u.	0.563 p.u.	0.563 p.u.
c) After motor bus transfer	1.009 p.u.	1.009 p.u.	1.009 p.u.	1.009 p.u.
<b>Motor bus frequency</b>				
a) Prior to motor bus transfer	60.0 Hz	60.0 Hz	60.0 Hz	60.0 Hz
b) Minimum value during loss of power	56.48 Hz	56.48 Hz	56.48 Hz	56.48 Hz
c) Maximum value during reconnection	63.188 Hz	60.006 Hz	60.006 Hz	60.006 Hz
d) After motor bus transfer	60.0 Hz	60.0 Hz	60.0 Hz	60.0 Hz
<b>Motor bus phase A voltage angle</b>				
a) Prior to motor bus transfer	-45.08 degrees	-45.08 degrees	-45.08 degrees	-45.08 degrees
b) Minimum value during loss of power	-179.84 degrees	-179.84 degrees	-179.84 degrees	-179.84 degrees
d) After motor bus transfer	-35.07 degrees	-35.07 degrees	-35.07 degrees	-35.07 degrees

Table 6-2 Summary of the in-phase transfer component response

### 6.2.3 Residual Voltage Algorithm Component Response

The residual voltage algorithm requires the voltage of the motor bus has decayed to low voltages during the motor bus transfer process. As it has been indicated in Chapter 4, the volts/Hertz element was set to 1.33 p.u. and the motor bus undervoltage value requirement to 0.25 p.u.

To test the algorithm's performance, four tests were carried out. All tests were performed under the same voltage, phase angle and frequency conditions of the auxiliary and start-up systems but with different motor bus transfer initiation times.

The motor bus transfer system controls settings used for this test are shown in Figure 6-31. Control SysSel was set to position BWS (transfer simulation from the start-up to the auxiliary system), manual transfer switch MTransfer set to 0, transfer initialization time MTime set to 14 seconds, TType was set to 3 (residual voltage transfer test mode). Control Coast Down was set to off, control Coast Down Time was set to 99 seconds (coast down simulating motors spinning down in group was not performed), Ind Coast Down Time was set to 99 seconds (coast down simulating motors spinning individually was not performed)

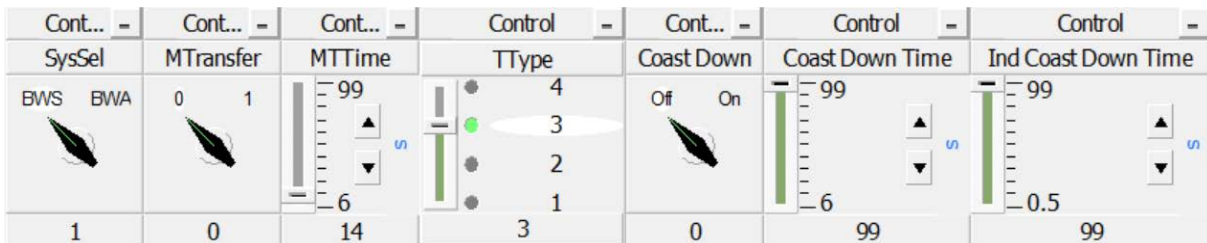


Figure 6-31 Motor bus transfer system controls for the residual voltage transfer test, initiated at t=14 sec.

The start-up breaker opened at t=14.058 seconds (phase A and phase C currents were interrupted at t= 14.0628 s, and phase B current at t = 14.058 s.). The transfer was accomplished at t=15.2352 seconds when the auxiliary breaker closed, 90 milliseconds after the residual voltage element tripped.

Figure 6-32 shows the phase A instantaneous voltage of the auxiliary bus (light blue plot), start-up bus (purple plot) and motor bus (red plot) during the residual voltage transfer test mode. The motor bus was transferred from the start-up side to the auxiliary side.

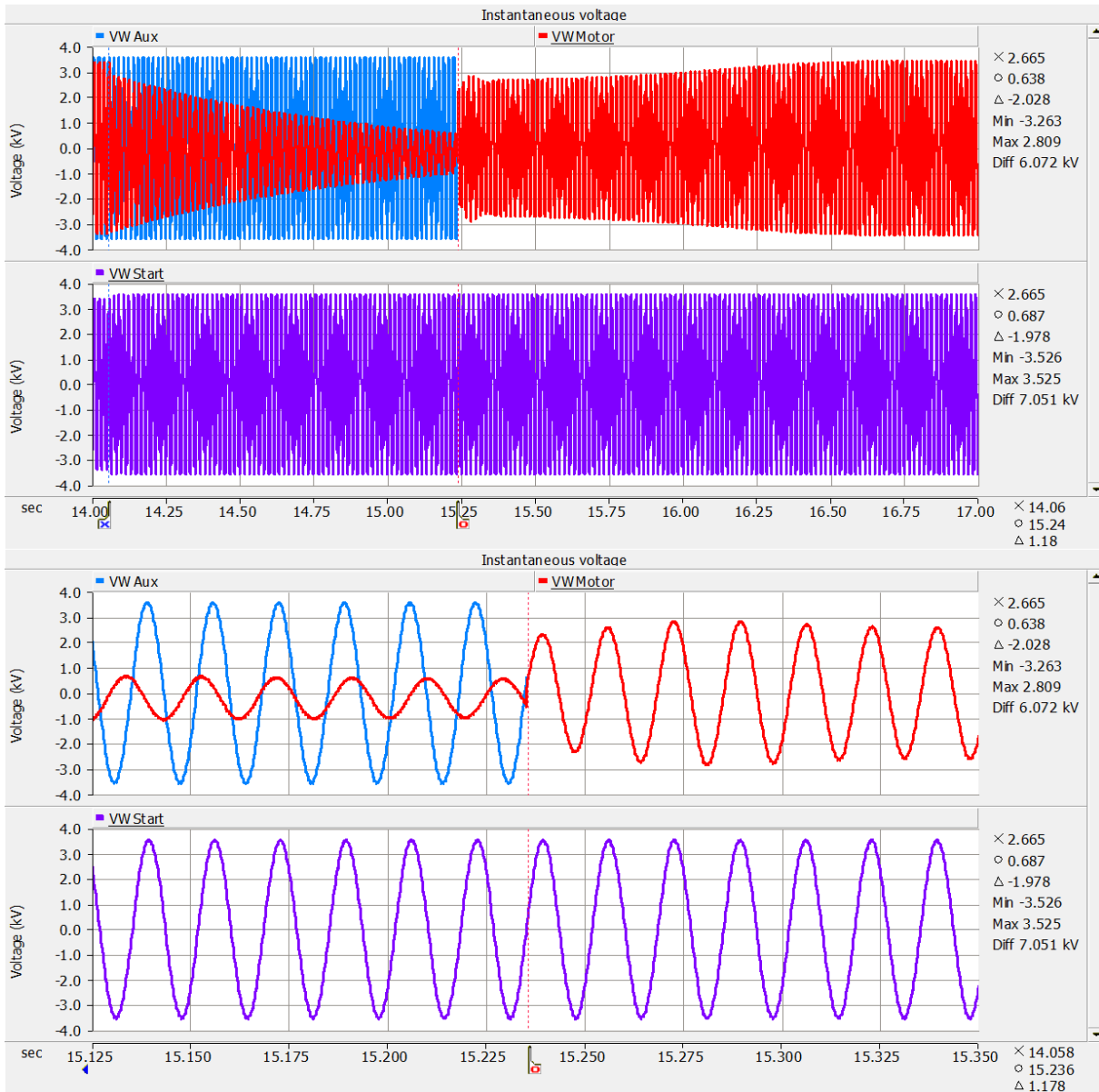


Figure 6-32 Phase A Instantaneous voltage in kV during a residual voltage transfer test, initiated at t=14 sec.

The start-up bus voltage magnitude before the bus transfer initiation was 4.1267 kV L-L and after the bus transfer the voltage magnitude was 4.3097 kV. The auxiliary bus voltage before the bus transfer initiation was 4.343 kV and after the bus transfer was 4.2057 kV. The instant after the loss of power supply, the motor bus voltage magnitude decayed to 3.6608 kV. The instant before the auxiliary breaker closed the residual voltage magnitude was 1.04 kV ( $4.16 \text{ kV} \times 0.25 = 1.04 \text{ kV}$  which was the setting of the lower voltage limit). When the auxiliary breaker closed the motor bus voltage magnitude changed to 3.2032 kV and then after 1.76 seconds the voltage magnitude was 4.2057 kV. The plots in the lower part of Figure 6-32 shows the voltage of the auxiliary and start-up side systems and the

motor bus voltage at the instant when the auxiliary breaker closed. It may be observed the motor bus voltage phase change at the reconnection due to the residual voltage transfer method does not have a voltage phase angle difference limit between the motor bus and the new incoming source voltages.

Figure 6-33 shows the per unit phase A RMS voltage in per unit of the auxiliary bus (light blue plot), start-up bus (purple plot) and motor bus (red plot) during the residual voltage transfer test. After the start-up breaker opened, the motor bus voltage magnitude decayed to 0.25 p.u. before the auxiliary breaker closed. The motor bus voltage magnitude took 1.76 seconds to recover once the motor bus was reconnected to the start-up source. When the start-up breaker opened the voltage magnitude at the start-up side recovered from 0.992 p.u. to 1.036 p.u.

It can be clearly seen the residual voltage decay from the moment when the start-up breaker opened to the moment when the auxiliary breaker closed at  $t = 15.2352$  seconds. The medium voltage start-up bus voltage magnitude dropped to 0.7 p.u. at the instant the start-up breaker took the motor bus load. The startup side voltage magnitude reached the new steady state after 1.76 seconds.

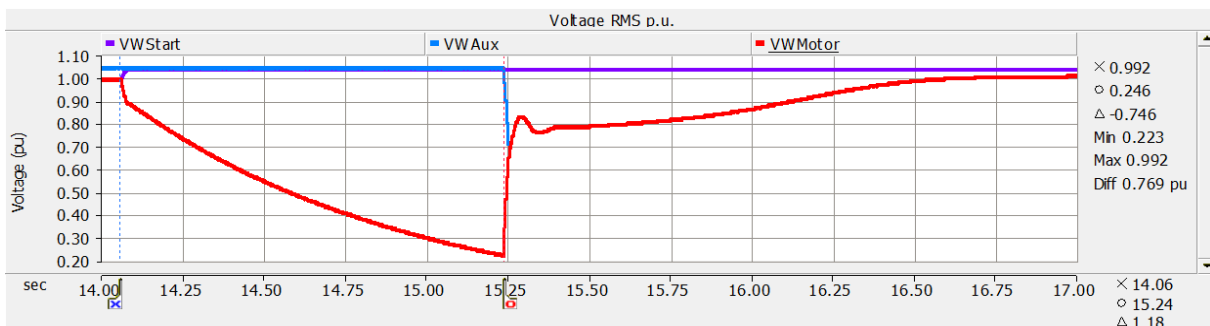


Figure 6-33 Phase A RMS voltage in per unit during a residual voltage transfer test, initiated at  $t = 14$  sec.

Figure 6-34 shows the voltage frequency of the auxiliary bus (light blue plot), start-up bus (purple plot) and motor bus (red plot) during the residual voltage transfer test mode. The motor bus voltage frequency decayed to 58.936 Hz immediately after the loss of power supply and continued decaying to 52.068 Hz at the instant before the auxiliary medium voltage breaker closed.

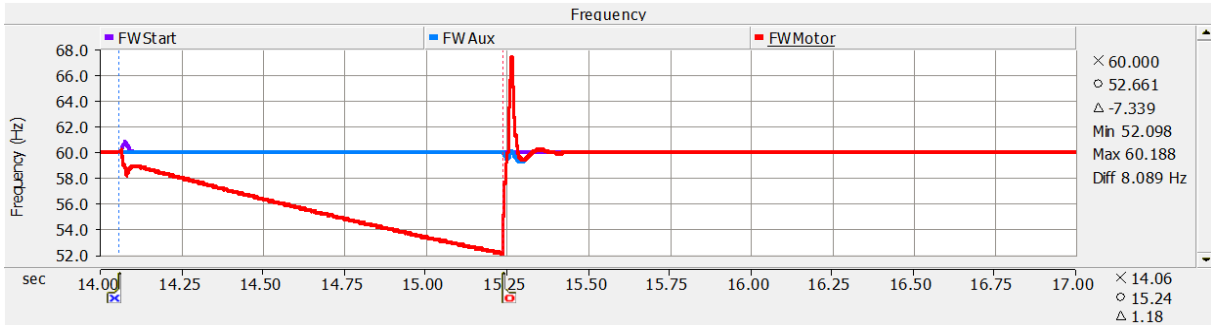


Figure 6-34 Voltage frequency in Hertz during a residual voltage transfer test, initiated at t=14 sec.

Figure 6-35 shows the phase A voltage angle of the auxiliary bus (light blue plot), start-up bus (purple plot) and motor bus (red plot) during the in-phase transfer test mode. The upper plot shows the motor bus voltage phase angle during the simulation and as the frequency changed quickly, so did the phase angle. The plot at the lower part shows a zoom of the voltage phase angle at the instant of the reconnection to the auxiliary side, the motor bus voltage phase angle changed from 161.703 degrees to -32.246 degrees.

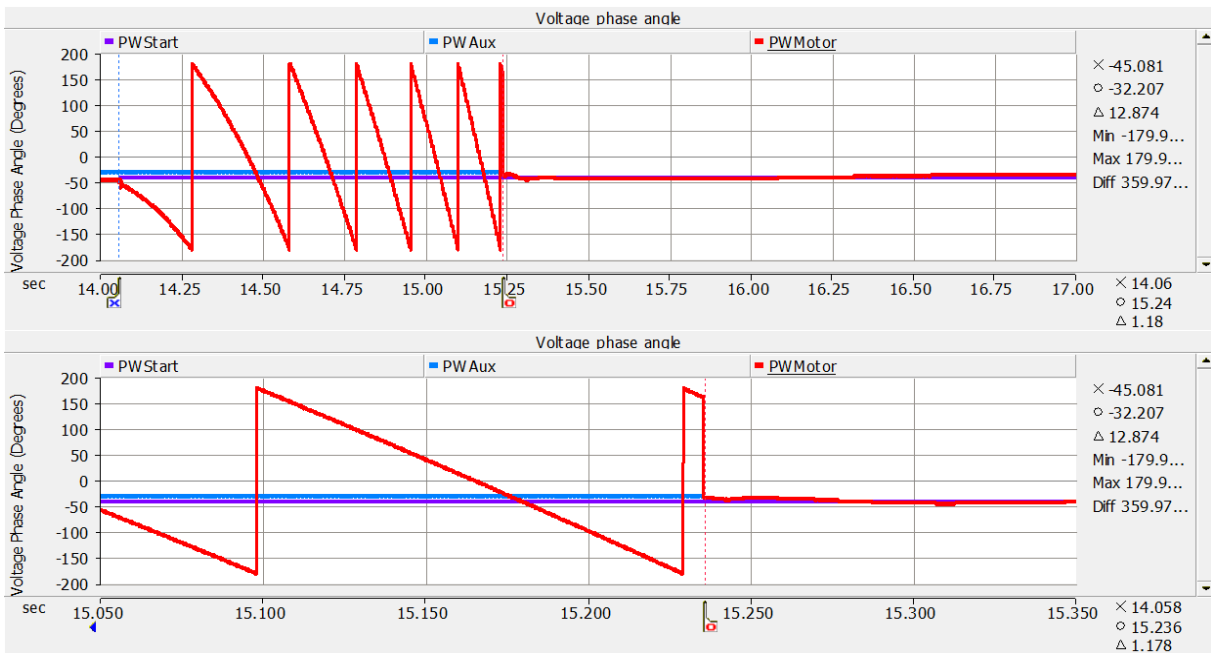


Figure 6-35 Phase A Voltage phase angle in degrees during a residual voltage transfer test, initiated at t=14 sec.

The logic timing of the motor bus transfer system elements and circuit breaker contacts operations is shown in Figure 6-36, where:

RTrip	Element activated by manual transfer, relay trip, and test mode initialization time
FTSMTP	Fast transfer trip element
IPSMTP	In-phase transfer trip element
RVSMTP	Residual voltage transfer trip element
S->A	Element to enable bus transfer from start-up to auxiliary system
A->S	Element to enable bus transfer from auxiliary to start-up system
BKStart	Start-up side breaker
BKAux	Auxiliary side breaker

Before the transfer initialization, the elements RTrip, RVSMTP, were enabled; elements FTSMTP and IPSMTP were disabled during the simulation, element S->A (motor bus transfer from start-up source to auxiliary source) was enabled and element A->S (motor bus transfer from auxiliary source to start-up source) was disabled; BKStart was closed and BKAux was open.

When time of the simulation was equal to the setting of the signal MTime,  $t = 14$  seconds, the element RTrip tripped instantaneously and the tripping signal was sent to the start-up breaker BKStart which opened at  $t = 15.058$  seconds and the element S->A changed its status from enabled to disabled. The residual voltage algorithm computed the volts/Hertz per unit and supervised the lower voltage limit. At  $t = 15.1452$  seconds, the residual voltage element RVSMTP tripped and the signal was sent to the auxiliary breaker BKAux which closed 90 milliseconds after receiving the closing signal, and the element

A->S changed its status from disabled to enabled. The transfer was accomplished at  $t= 15.2352$  seconds.

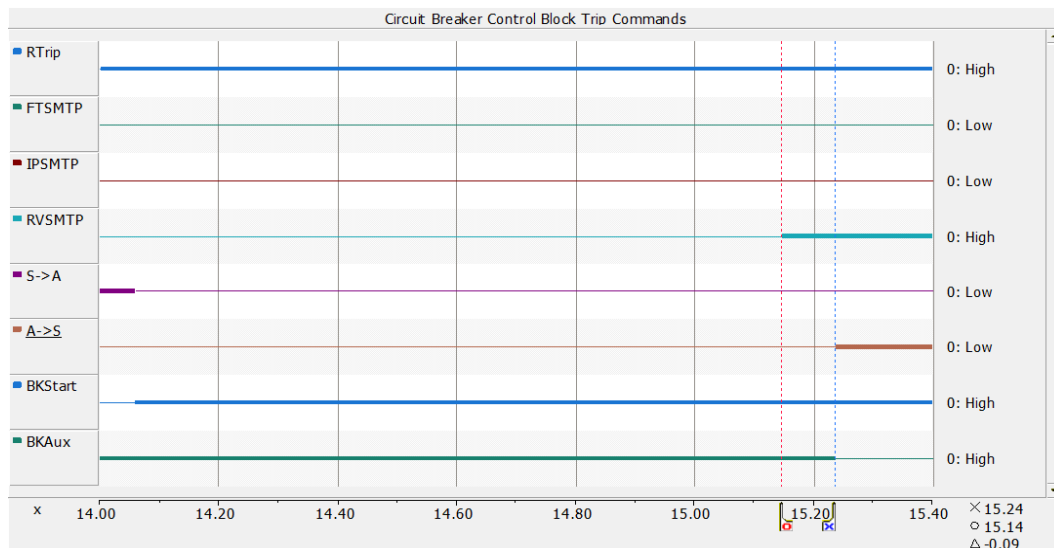


Figure 6-36 Motor bus transfer system element and circuit breaker contact operations during a residual voltage transfer test, initiated at  $t=14$  sec.

The logic timing of the motor bus transfer system elements and circuit breaker contacts operated correctly.

Figure 6-37 shows the phase A instantaneous current and electromagnetic torque transient behavior of the 9000 HP motor during the motor bus transfer reconnection with the motor starting process.

The maximum peak starting current (first five seconds of the simulation) was 10.572 kA whereas the maximum positive peak current at reconnection was 15.484 kA and the maximum negative peak current was -6.925kA. The maximum positive peak current was 46.46% higher than the maximum peak starting current.

The maximum torque during motor starting was 2.899 p.u. in contrast when the motor bus was reconnected the maximum negative torque was -1.762 p.u. and the maximum positive torque was 2.423 p.u. The maximum negative torque was 60.77% of the maximum torque during the starting process.

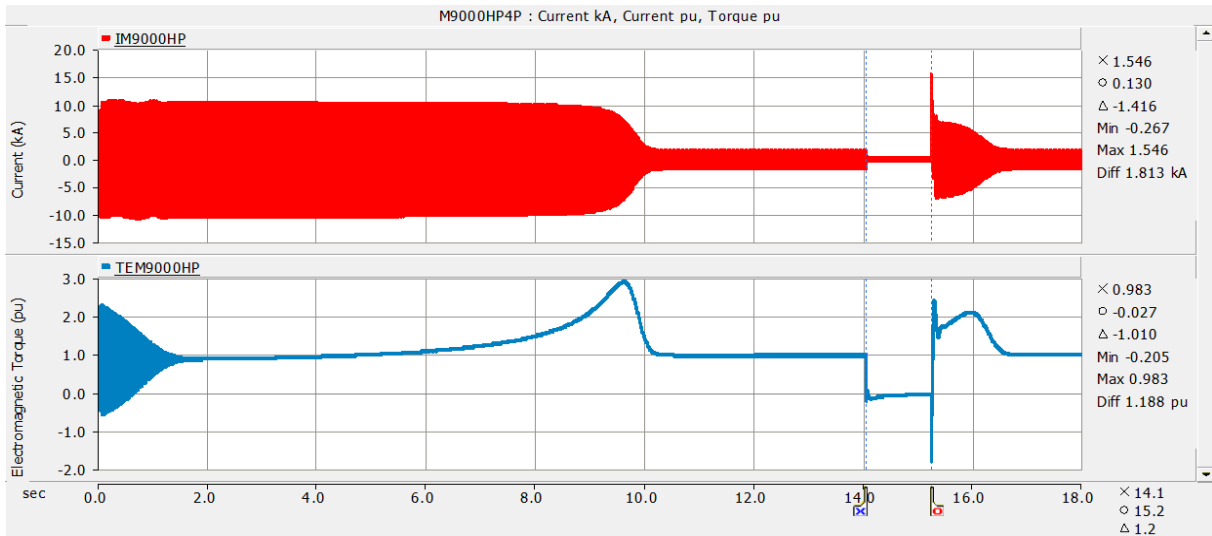


Figure 6-37 9000 HP Motor phase A instantaneous current and electromagnetic torque transient response comparison between the motor starting process and the reconnection after a residual voltage transfer test, initiated at t=14 sec.

Figure 6-38 zoom in on Figure 6-37 and shows the damped oscillatory response of the motor phase A instantaneous current and electromagnetic torque when the motor bus was reconnected to the auxiliary system. There were two cycles in which the torque was oscillating between negative and positive magnitudes. This damped oscillatory behavior of the torque causes harmful and accumulative stress on the motors. After this transient the motor required about 1.46 seconds to reaccelerate and reach steady state operation.

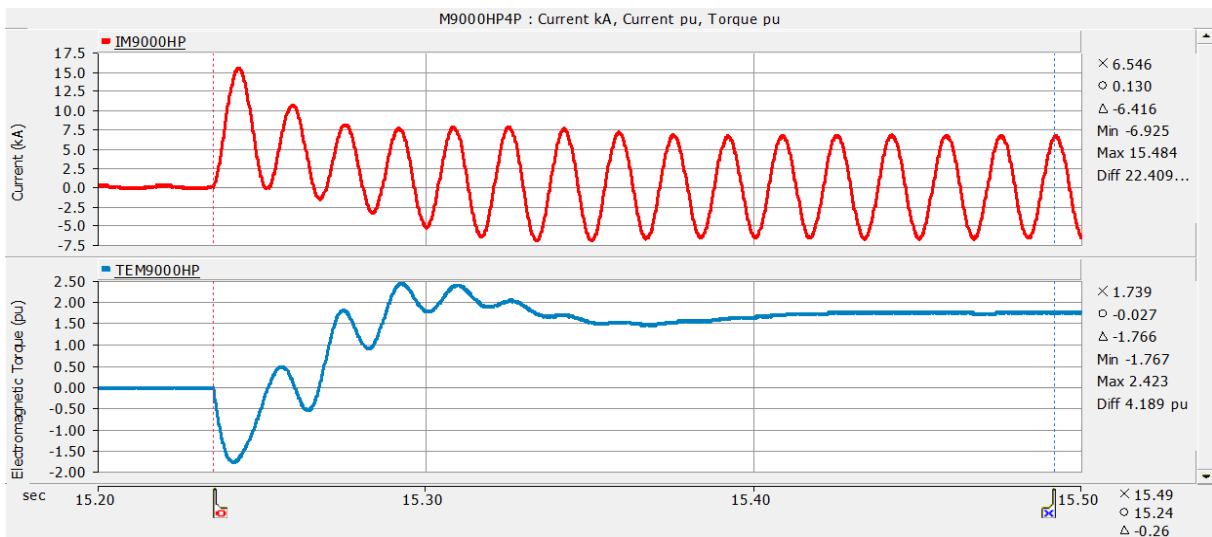


Figure 6-38 9000 HP Motor phase A instantaneous current and electromagnetic torque transient response at the moment of reconnection to the start-up system during a residual voltage transfer test, initiated at t=14 sec.



Figure 6-39 shows the 9000 HP motor phase A current in per unit versus motor speed in per unit during the simulation. The starting current curve is the plot section from letter a to letter b. The steady state operating point is marked with letter b. Current versus speed at the instant of loss of power supply is marked with letter c. Letter d shows the current versus speed at the instant before the reconnection to the auxiliary system, it may be observed that the speed of the motor decayed to 0.871 per unit at the moment before the reconnection (letter d), at that instant the current was approximately zero. The maximum current when the auxiliary breaker closed is shown with letter e. The curve from e to f is a damped oscillatory behavior of the motor during the reconnection. The curve from letter f to b shows the reaccelerating current. The maximum current (7.232 p.u.) was higher than the maximum starting current (6.809 p.u.).

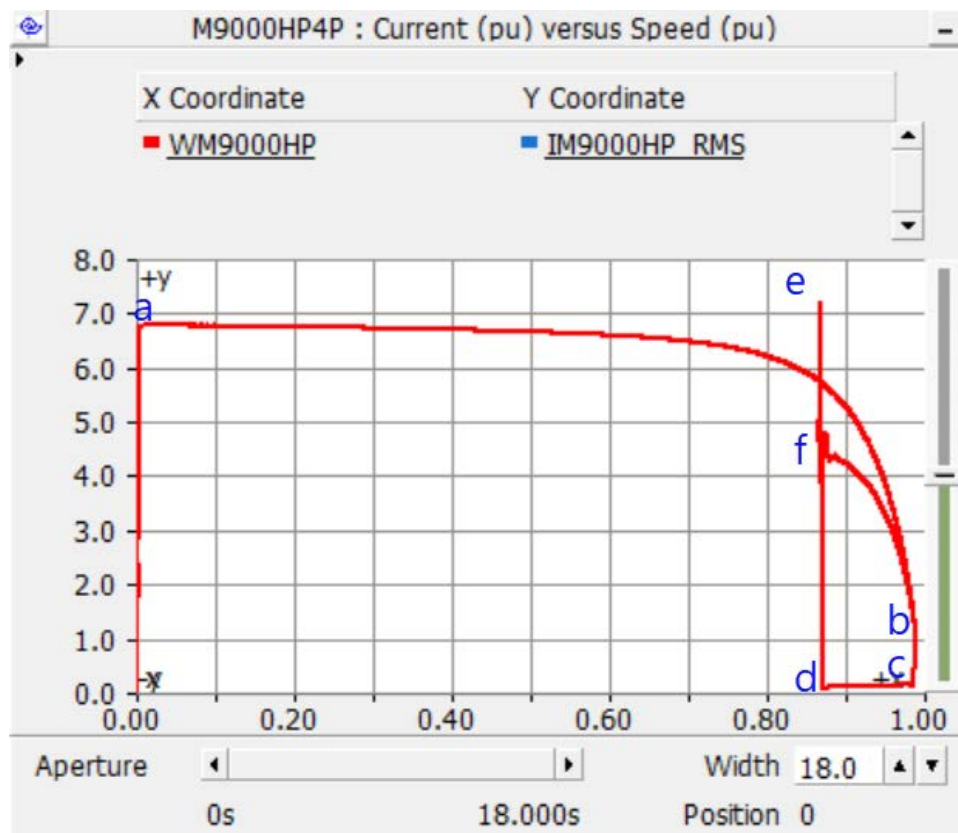


Figure 6-39 9000 HP Motor phase A current versus speed in per unit transient response comparison between the motor starting process and the reconnection after a residual voltage transfer test, initiated at  $t=14$  sec.

Figure 6-40 shows the 9000 HP motor electromagnetic torque versus the speed in per unit during the simulation. The starting torque curve is shown from letter a to b and c, the maximum starting torque is identified with letter b. The steady state operating point is marked with letter c. Letter d shows the torque at the instant of loss of power supply. Letter e shows the torque at the instant before the reconnection to the start-up system, it may be observed that the speed of the motor decayed close to 0.871 per unit at that moment. The curve from e to h is a damped oscillatory behavior of the motor torque. The maximum negative torque was close to 1.767 per unit when the start-up breaker closed and is shown with letter f. Letter g shows the maximum positive torque when the start-up breaker closed. The reaccelerating torque is identified with letter h and finally, the torque reached the steady state operating point which was very close to the point of letter c.

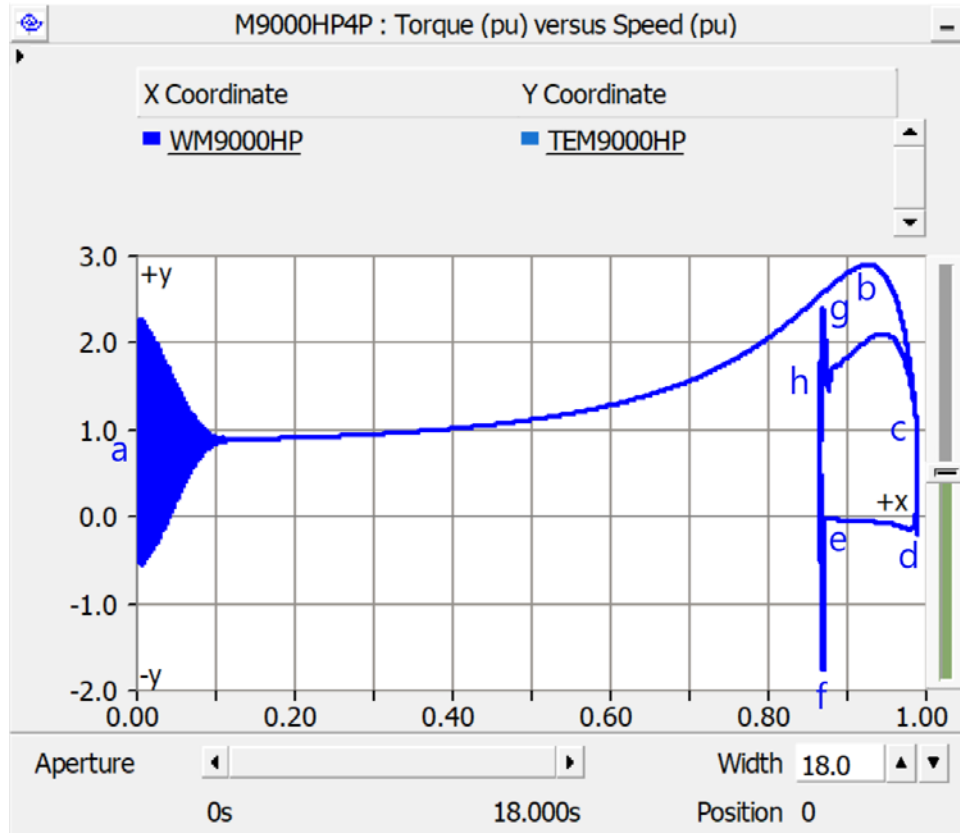


Figure 6-40 9000 HP Motor electromagnetic torque versus speed transient response comparison during starting process and at the reconnection after a residual voltage transfer test, initiated at  $t=14$  sec.

Figure 6-41 shows the phase A instantaneous current and electromagnetic torque transient behavior of the 6000 HP motor (motor with medium inertia) during the motor bus transfer reconnection with the motor starting process.

The maximum peak starting current (first five seconds of the simulation) was 7.56 kA whereas the maximum negative peak current at reconnection was -4.903 kA and the maximum positive peak current was 8.286 kA. The maximum positive peak current was 9.6% higher than the maximum peak starting current.

The maximum torque during motor starting was 2.248 p.u. in contrast when the motor bus was reconnected the maximum negative torque was -1.376 p.u. and the maximum positive torque was 1.883 p.u. The maximum negative torque was 61.2% of the maximum torque during the starting process.

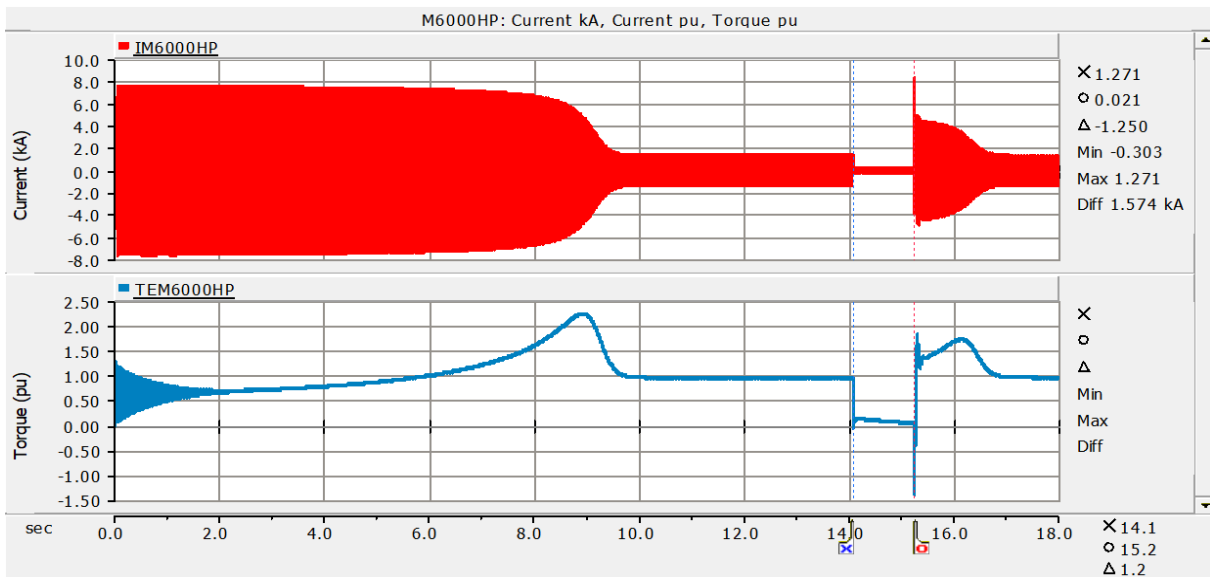


Figure 6-41 6000 HP Motor phase A instantaneous current and electromagnetic torque transient response comparison between the motor starting process and the reconnection after a residual voltage transfer test, initiated at t=14 sec.

Figure 6-42 zoom in on Figure 6-41 and shows the damped oscillatory response of the motor phase A instantaneous current and electromagnetic torque when the motor bus was reconnected to the auxiliary system. After this transient the motor required about 1.68 seconds to reaccelerate and reach steady state operation.

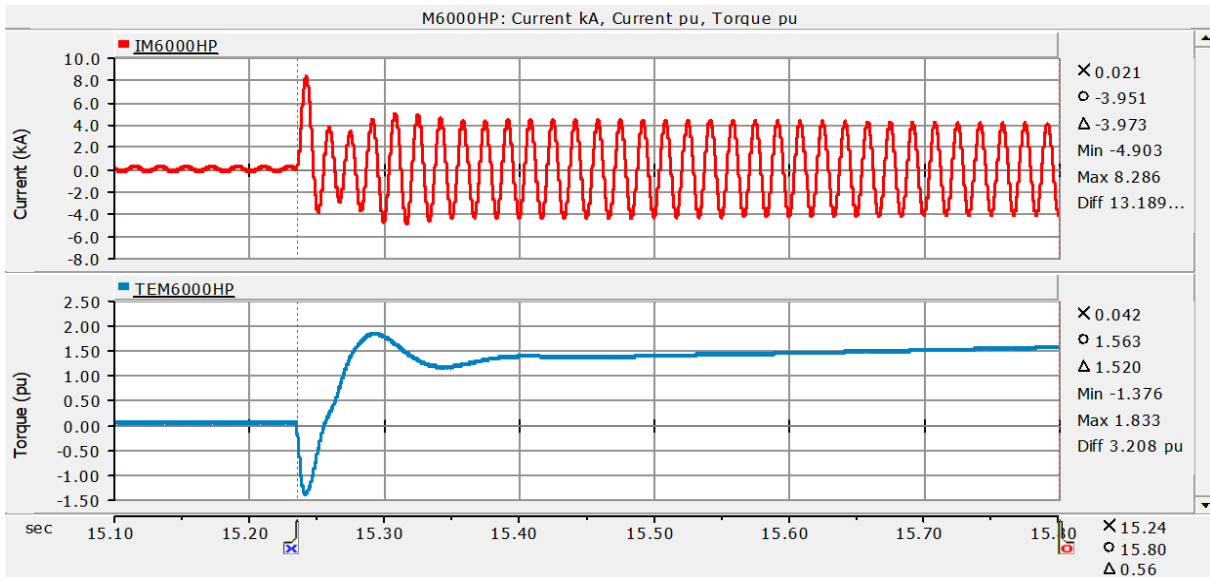


Figure 6-42 6000 HP Motor phase A instantaneous current and electromagnetic torque transient response at the moment of reconnection to the start-up system during a residual voltage transfer test, initiated at  $t=14$  sec.

Figure 6-43 shows the 6000 HP motor phase A current in per unit versus motor speed in per unit during the simulation. The starting current curve is the plot section from letter a to letter b. The steady state operating point is marked with letter b. Current versus speed at the instant of loss of power supply is marked with letter c. Letter d shows the current versus speed at the instant before the reconnection to the auxiliary system, it may be observed that the speed of the motor decayed to 0.856 per unit at the moment before the reconnection (letter d), at that instant the current was approximately 0.171 p.u. The maximum current when the auxiliary breaker closed is shown with letter e. The curve from e to f is a damped oscillatory behavior of the motor during the reconnection. The curve from letter f to b shows the reaccelerating current. The maximum current (5.89 p.u.) was lower than the maximum starting current (5.986 p.u.).

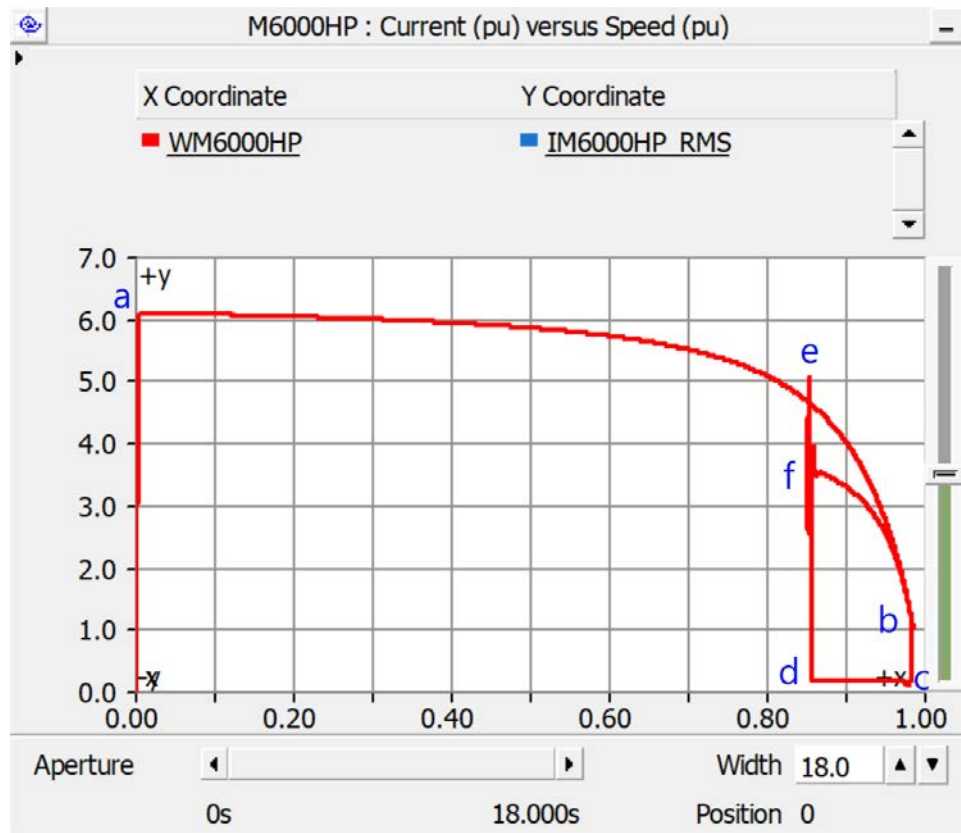


Figure 6-43 6000 HP Motor phase A current versus speed in per unit transient response comparison between the motor starting process and the reconnection after a residual voltage transfer test, initiated at  $t=14$  sec.

Figure 6-44 shows the 6000 HP motor electromagnetic torque versus the speed in per unit during the simulation. The starting torque curve is shown from letter a to b and c, the maximum starting torque is identified with letter b. The steady state operating point is marked with letter c. Letter d shows the torque at the instant of loss of power supply. Letter e shows the torque at the instant before the reconnection to the start-up system, it may be observed that the speed of the motor decayed close to 0.856 per unit at that moment. The curve from e to h is a damped oscillatory behavior of the motor torque. The maximum negative torque was close to 1.376 per unit when the start-up breaker closed and is shown with letter f. Letter g shows the maximum positive torque when the start-up breaker closed. When the motor was reconnected, the motor deaccelerated even more because of negative torques and the speed reduced to 0.852 p.u. and then it reaccelerates. The reaccelerating torque is identified with letter h and finally, the torque reached the steady state operating point which was very close to the point of letter c.

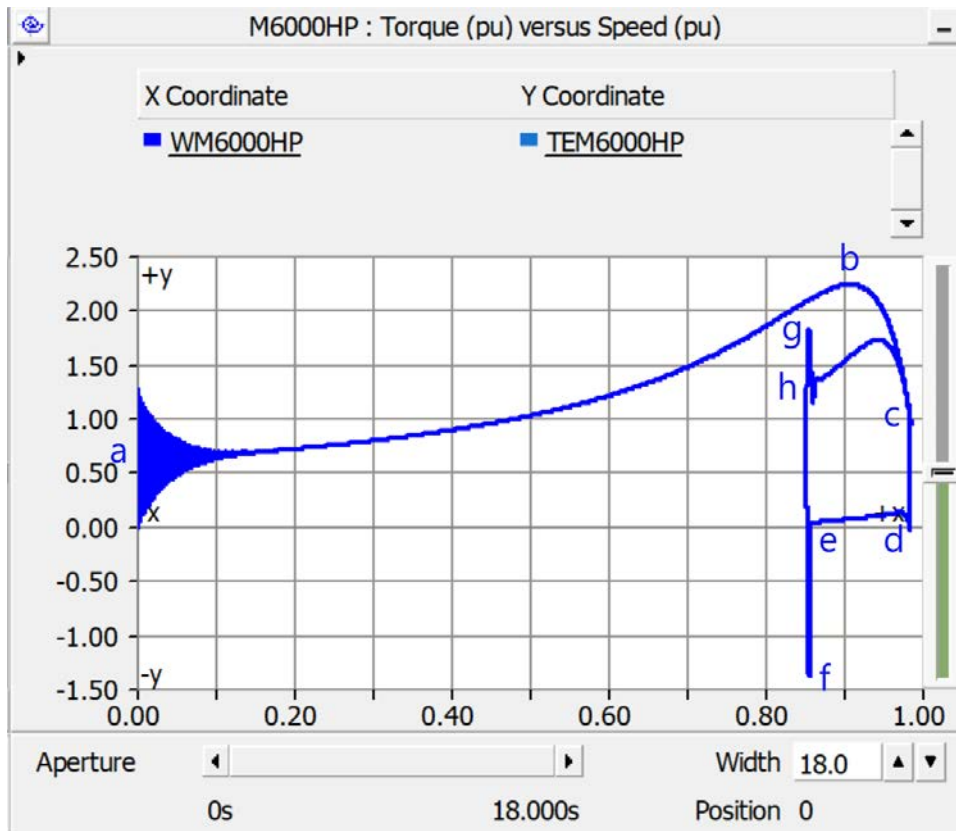


Figure 6-44 6000 HP Motor electromagnetic torque versus speed transient response comparison during starting process and at the reconnection after a residual voltage transfer test, initiated at  $t=14$  sec.

Figure 6-45 shows the phase A instantaneous current and electromagnetic torque transient behavior of the 3200 HP motor (motor with high inertia) during the motor bus transfer reconnection with the motor starting process.

The maximum peak starting current (first seven seconds of the simulation) was 4.121 kA whereas the maximum negative peak current at reconnection was 2.653 kA and the maximum positive peak was 4.847 kA. The maximum positive peak was 17.6% higher than the maximum peak starting current.

The maximum torque during motor starting was 2.642 p.u. in contrast when the motor bus was reconnected the maximum negative torque was 1.546 p.u. and the maximum positive torque was 2.053 p.u. The maximum negative torque was 58.5% of the maximum torque during the starting process.

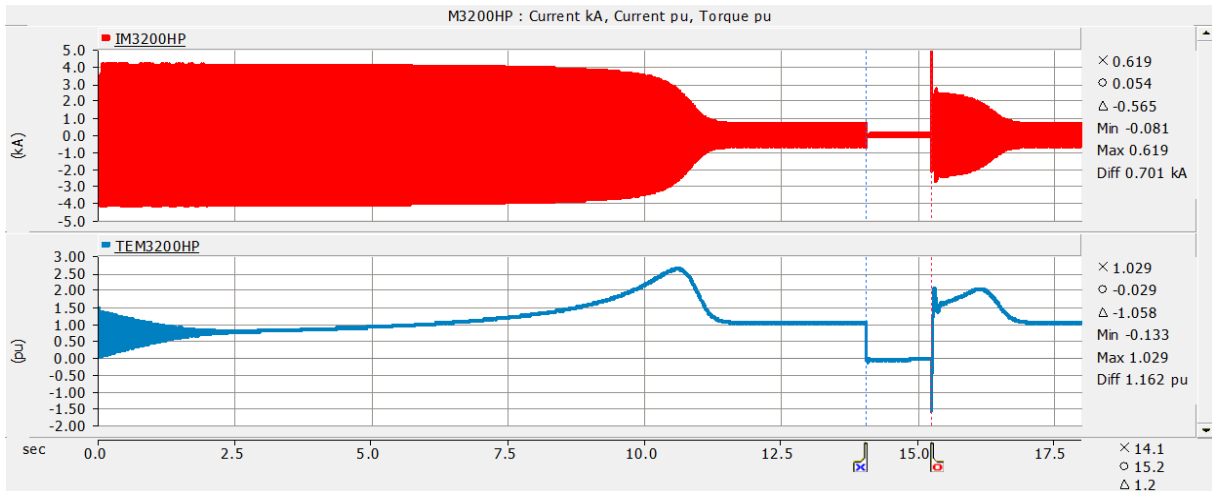


Figure 6-45 3200 HP Motor phase A instantaneous current and electromagnetic torque transient response during a residual voltage transfer test, initiated at t=14 sec.

Figure 6-46 zooms in on Figure 6-45 and shows the damped oscillatory response of the phase A instantaneous current and electromagnetic torque when the motor bus was reconnected to the start-up system. The motor required about 1.96 seconds to reaccelerate and reach steady state operation.

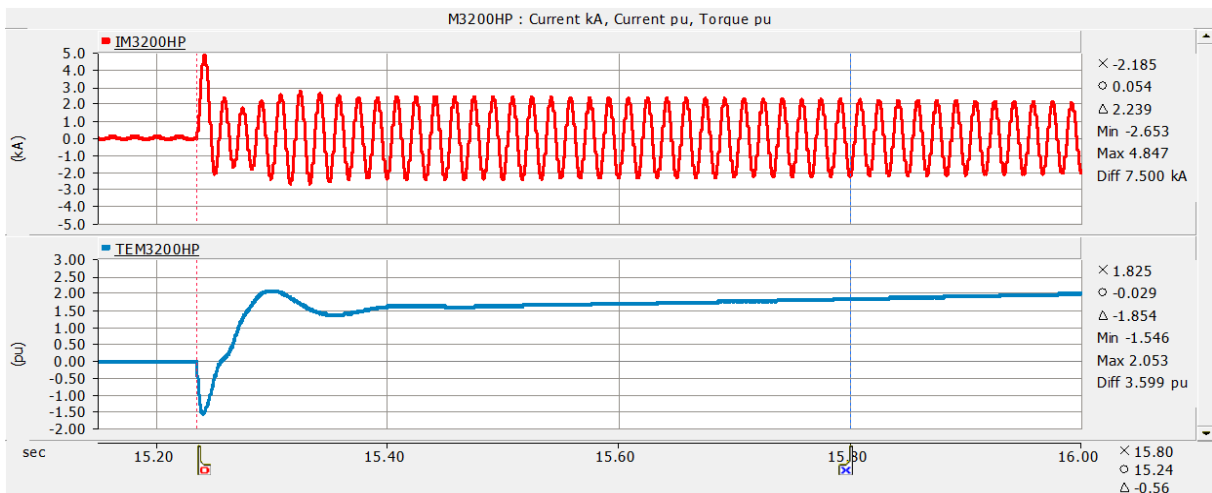


Figure 6-46 3200 HP Motor phase A instantaneous current and electromagnetic torque transient response at the moment of reconnection to the start-up system during a residual voltage transfer test, initiated at t=14 sec.

Figure 6-47 shows the phase A current in per unit versus the speed in per unit during the simulation. It may be observed that the maximum current was 6.093 p.u. at the instant after the reconnection (identified with letter e) which was lower than the starting current (identified with letter a). The speed

before the reconnection was 0.873 p.u. (identified with letter d). The curve from e to f is a damped oscillatory behavior of the motor during the reconnection to the new power supply.

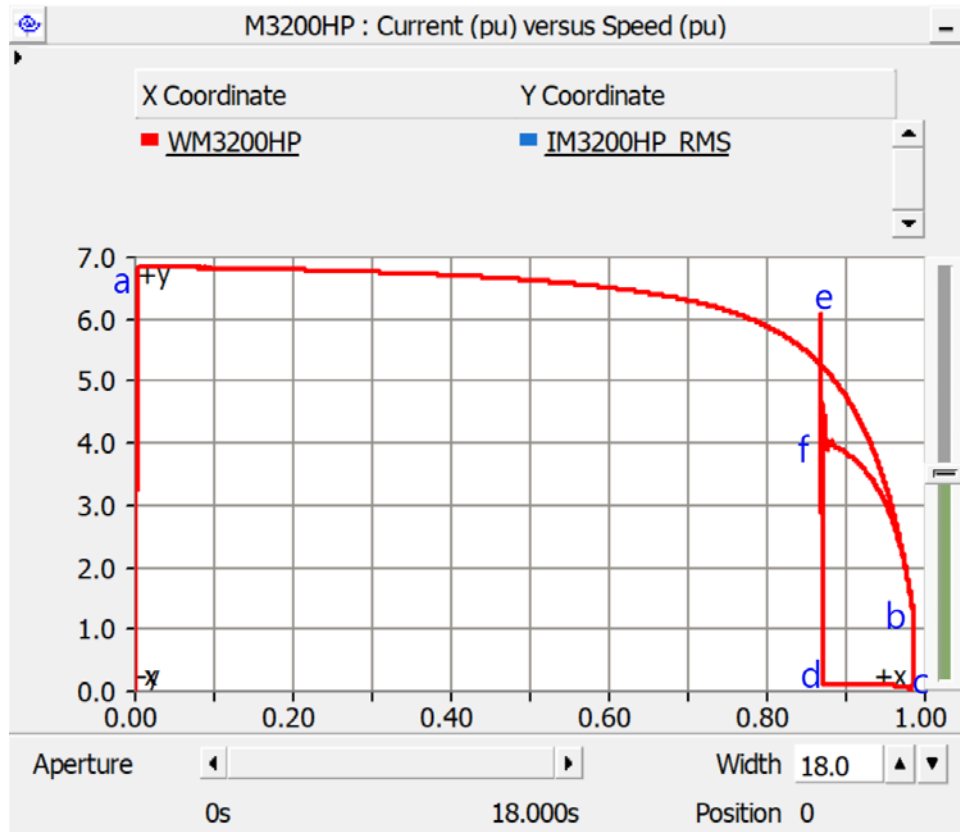


Figure 6-47 3200 HP Motor phase A current versus speed in per unit transient response comparison between the motor starting process and the reconnection after a residual voltage transfer test, initiated at  $t=14$  sec.

Figure 6-48 shows the electromagnetic torque in per unit versus the speed in per unit during the simulation. It may be observed that the maximum negative torque was 1.546 p.u. at the instant after the reconnection (letter f) which was lower than the maximum starting torque (letter b). The speed of the motor decayed to 0.873 per unit at the moment before the reconnection. It may be observed that this motor was behaving as an induction generator during the loss of power supply, curve from letter d to letter e. The curve from e to h shows the damped oscillating behavior of the motor when connected to the new source.



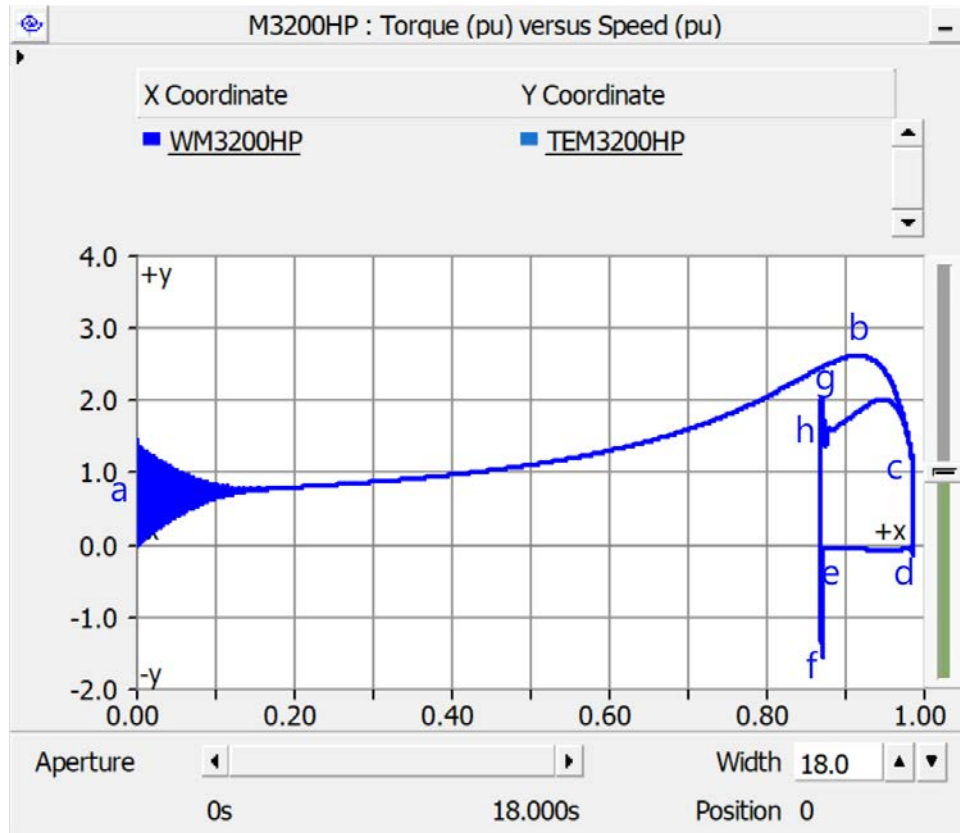


Figure 6-48 3200 HP Motor electromagnetic torque versus speed transient response comparison during starting process and at the reconnection after a residual voltage transfer test, initiated at  $t=14$  sec.

Figure 6-49 compares the phase A instantaneous current and electromagnetic torque transient behavior of the 1400 HP motor (motor with medium inertia) during the motor bus transfer reconnection with the motor starting process, to observe the high damped oscillating currents and high negative and damped oscillating torques that may be produced during the residual voltage transfer method.

During the starting process that lasted approximately 11.5 seconds, the maximum peak current was 1.682 kA and during the reconnection the maximum positive peak current was 1.887 and the maximum negative peak was 1.03 kA.

The maximum torque during motor starting was 2.183 p.u. in contrast when the motor bus was reconnected the maximum negative torque was -1.298 p.u. and the maximum positive torque was 1.738 p.u. The maximum negative torque was 59.45% of the maximum torque during the starting process.

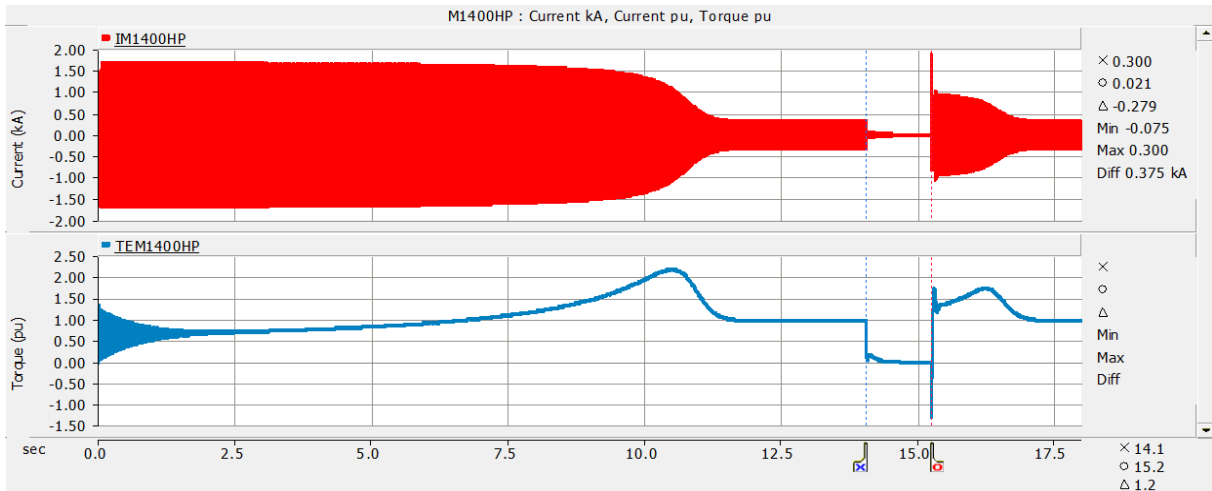


Figure 6-49 1400 HP Motor phase A instantaneous current and electromagnetic torque transient response during a residual voltage transfer test, initiated at t=14 sec.

Figure 6-50 is a zoom in time of Figure 6-49 and shows the damped oscillatory response of the phase A instantaneous current and electromagnetic torque when the motor bus was reconnected to the auxiliary system. The motor required about 2 seconds to reaccelerate and reach steady state operation.

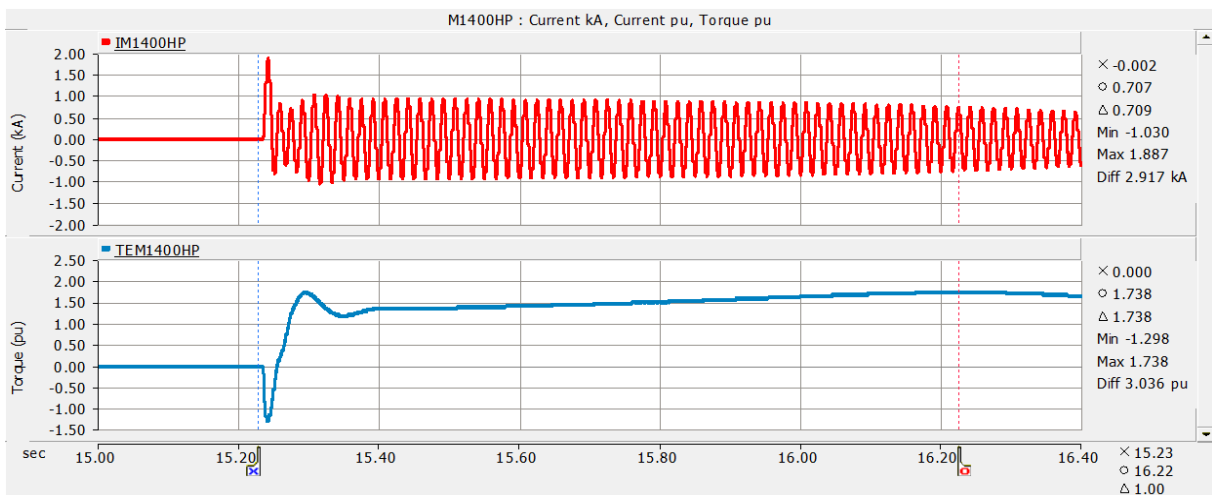


Figure 6-50 1400 HP Motor phase A instantaneous current and electromagnetic torque transient response at the moment of reconnection to the start-up system during a residual voltage transfer test, initiated at t=14 sec.

Figure 6-51 shows the phase A current in per unit versus the speed in per unit during the simulation. The maximum current was 4.935 p.u. at the instant after the reconnection (indicated with letter e) which was lower than the starting current that was 5.828 p.u.(shown with letter a). The speed before

the reconnection was 0.867 p.u. (letter d). The curve from e to f is a damped oscillatory behavior of the motor during the reconnection.

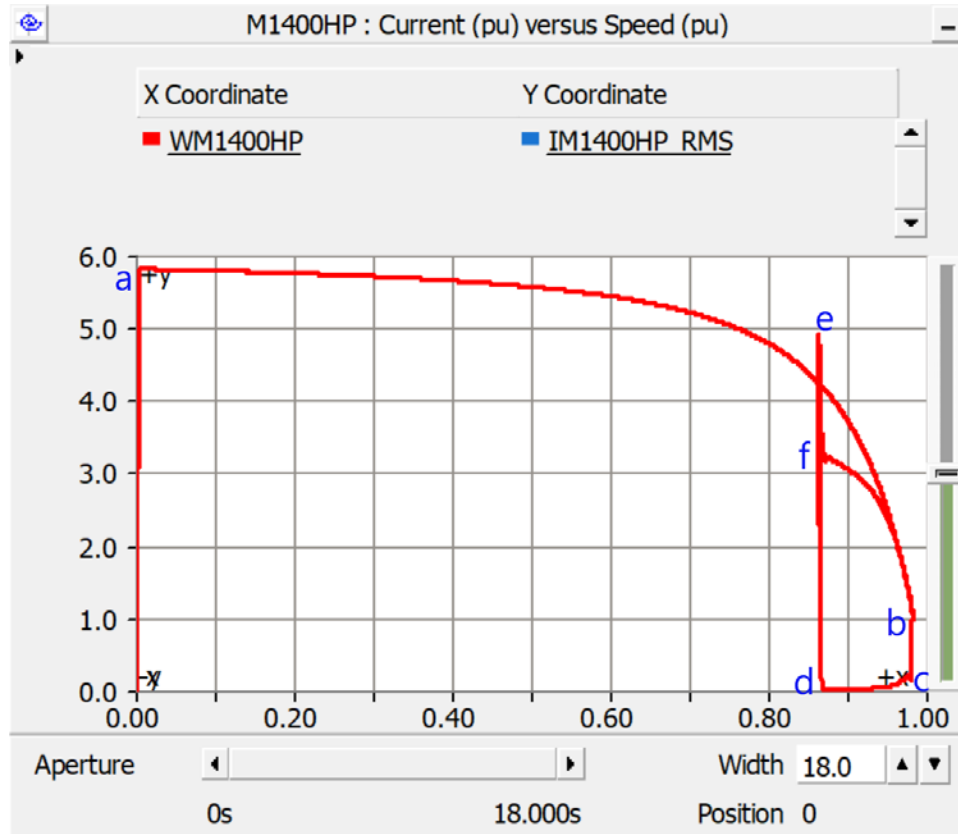


Figure 6-51 1400 HP Motor phase A current versus speed in per unit transient response comparison between the motor starting process and the reconnection after a residual voltage transfer test, initiated at  $t=14$  sec.

Figure 6-52 shows the electromagnetic torque in per unit versus the speed in per unit during the simulation. It may be observed that the maximum negative torque was -1.298 p.u. at the instant after the reconnection (letter f) which was lower than the maximum starting torque (letter b). The speed of the motor decayed to 0.867 per unit at the moment before the reconnection (letter e). The curve from e to h shows the damped oscillating behavior of the motor torque during the reconnection.

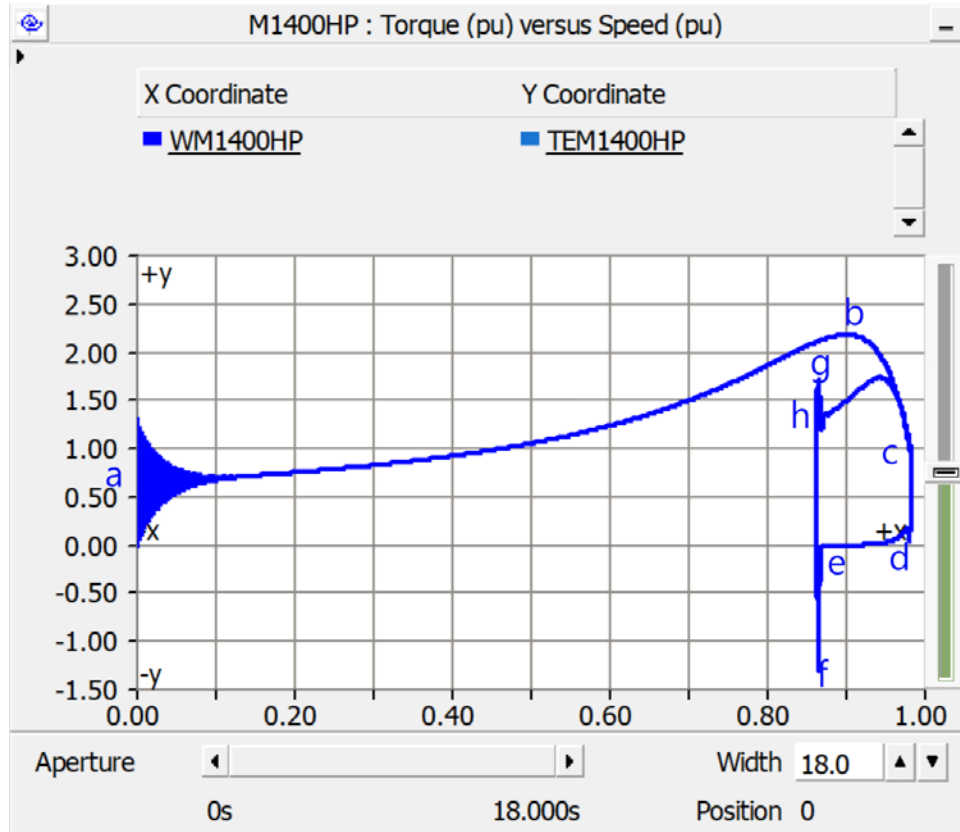


Figure 6-52 1400 HP Motor electromagnetic torque versus speed transient response comparison during starting process and at the reconnection after a residual voltage transfer test, initiated at  $t=14$  sec.

Figure 6-53 shows the phase A instantaneous current and electromagnetic torque transient behavior of the 1000 HP motor during the motor bus transfer reconnection with the motor starting process.

During the starting process that lasted approximately 11.1 seconds, the maximum peak current was 1.260 kA and during the reconnection the maximum negative peak current was -0.807 kA and the maximum positive peak was 1.393 kA. The maximum positive peak was 110% higher than the maximum peak starting current.

The maximum torque during motor starting was 2.252 p.u. in contrast when the motor bus was reconnected the maximum negative torque was -1.364 p.u. and the maximum positive torque was 1.819 p.u. The maximum positive torque was 80.77% lower than the maximum torque during the starting process.

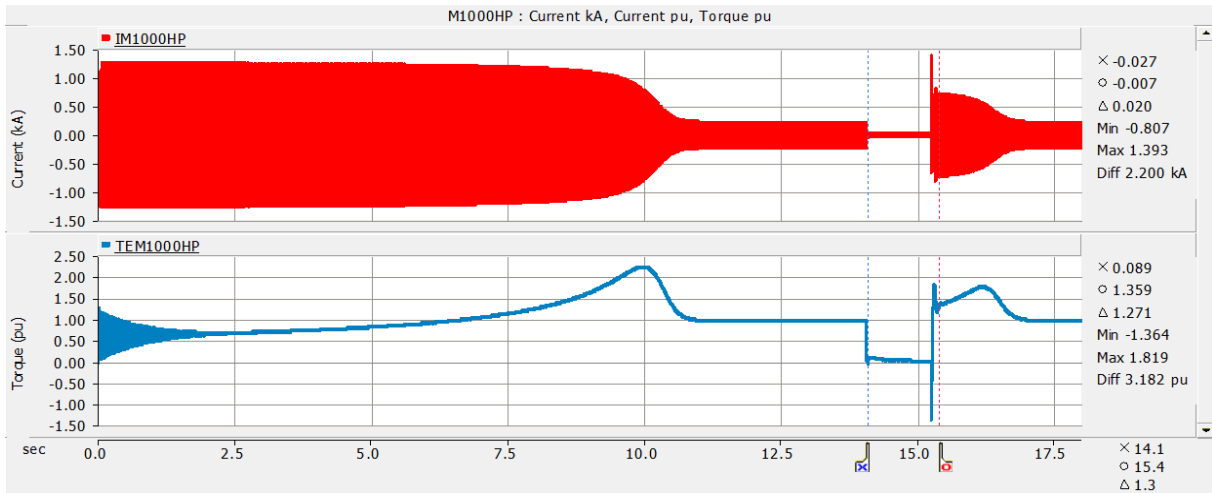


Figure 6-53 1000 HP Motor phase A instantaneous current and electromagnetic torque transient response during a residual voltage transfer test, initiated at t=14 sec.

Figure 6-54 is a zoom in time of Figure 6-53 and shows the damped oscillatory response of the phase A instantaneous current and electromagnetic torque when the motor bus was reconnected to the auxiliary system. The motor required about 1.88 seconds to reaccelerate and reach steady state operation.

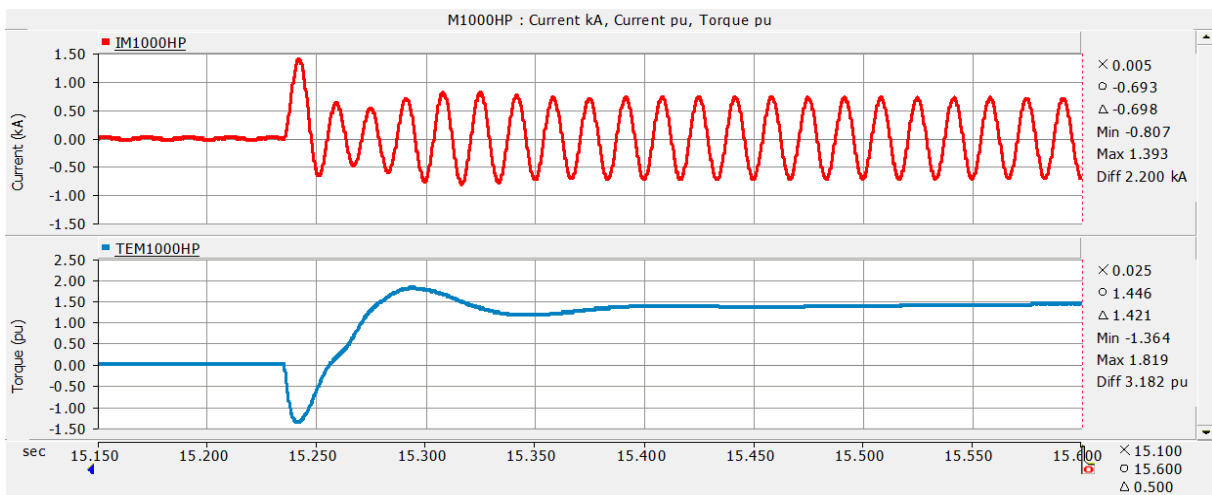


Figure 6-54 1000 HP Motor phase A instantaneous current and electromagnetic torque transient response at the moment of reconnection to the start-up system during a residual voltage transfer test, initiated at t=14 sec.

Figure 6-55 shows the phase A current in per unit versus the speed in per unit during the simulation. The maximum current was 5.148 p.u. at the instant after the reconnection (indicated with letter e) which was lower than the starting current that was 6.114 p.u. (shown with letter a). The speed before the reconnection was 0.864 p.u. (identified with letter d). The curve from e to f shows the damped oscillating behavior of the motor during the reconnection.

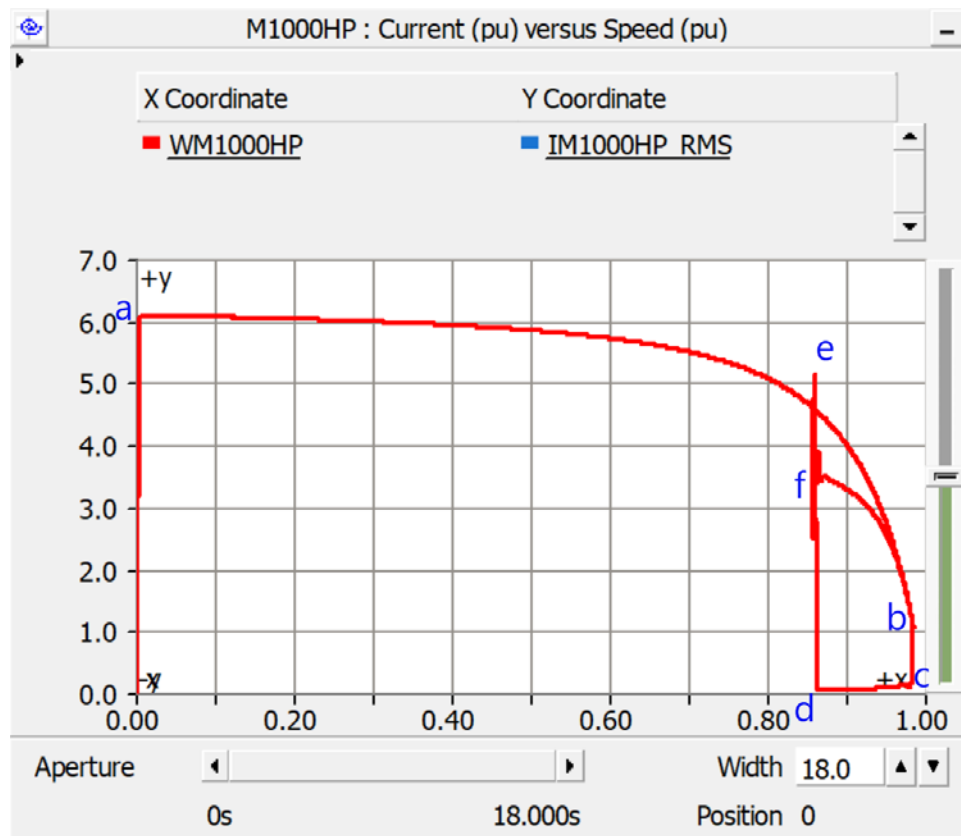


Figure 6-55 1000 HP Motor phase A current versus speed in per unit transient response comparison between the motor starting process and the reconnection after a residual voltage transfer test, initiated at  $t=14$  sec.

Figure 6-56 shows the electromagnetic torque in per unit versus the speed in per unit during the simulation. The maximum negative torque was -1.364 p.u. at the instant after the reconnection (shown with letter f) which was lower than the maximum starting torque. The speed of the motor decayed to 0.864 per unit at the moment before the reconnection. The curve from e to h shows the damped oscillating behavior of the motor when reconnected to the new source.

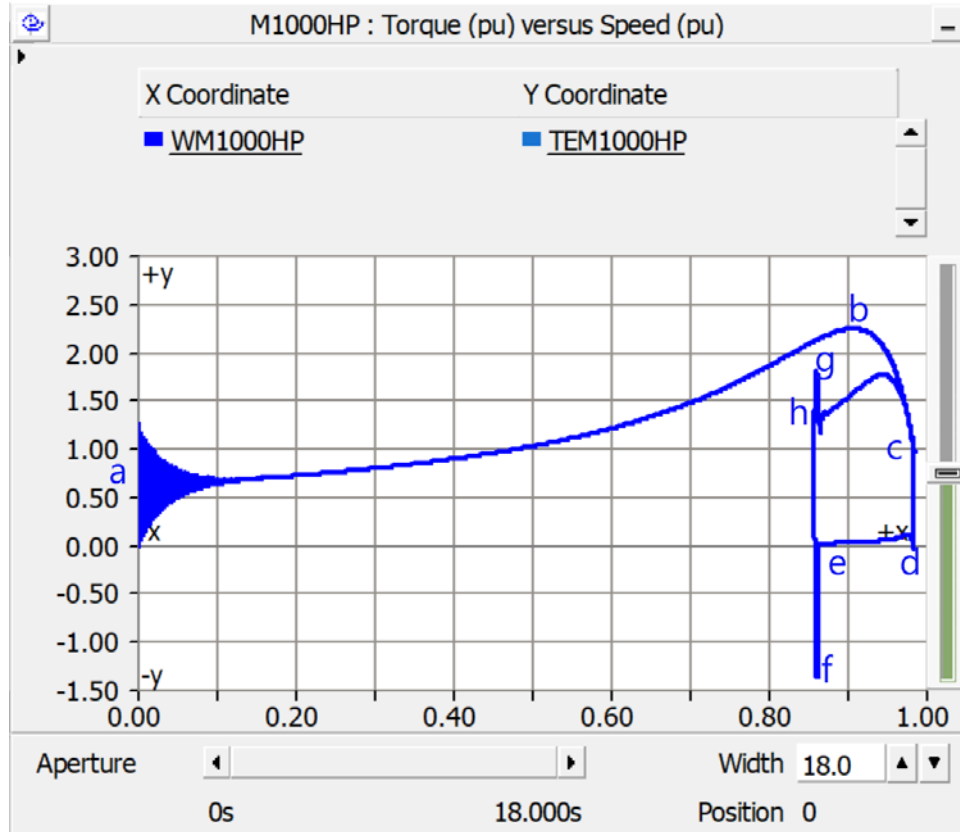


Figure 6-56 1000 HP Motor electromagnetic torque versus speed transient response comparison during starting process and at the reconnection after a residual voltage transfer test, initiated at  $t=14$  sec.

Figure 6-57 shows the phase A instantaneous current and electromagnetic torque transient behavior of the 470 HP motor during the motor bus transfer reconnection with the motor starting process.

The maximum peak starting current (first 7.7 seconds of the simulation) was 0.605 kA whereas the maximum negative peak current at reconnection was 0.555 kA and the maximum positive peak was 0.710 kA. The maximum positive peak was 11.7% higher than the maximum peak starting current.

The maximum torque during motor starting was 2.625 p.u. in contrast when the motor bus was reconnected the maximum negative torque was -1.57 p.u. and the maximum positive torque was 2.064 p.u. The maximum negative torque was 59.8% of the maximum torque during the starting process.

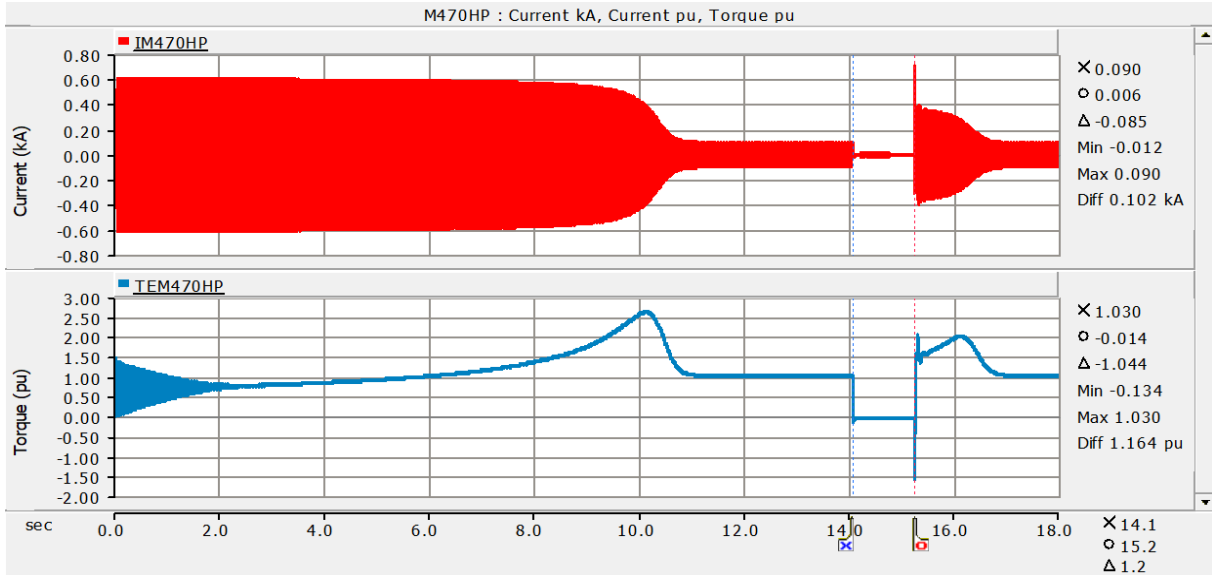


Figure 6-57 470 HP Motor phase A instantaneous current and electromagnetic torque transient response during a residual voltage transfer test, initiated at t=14 sec.

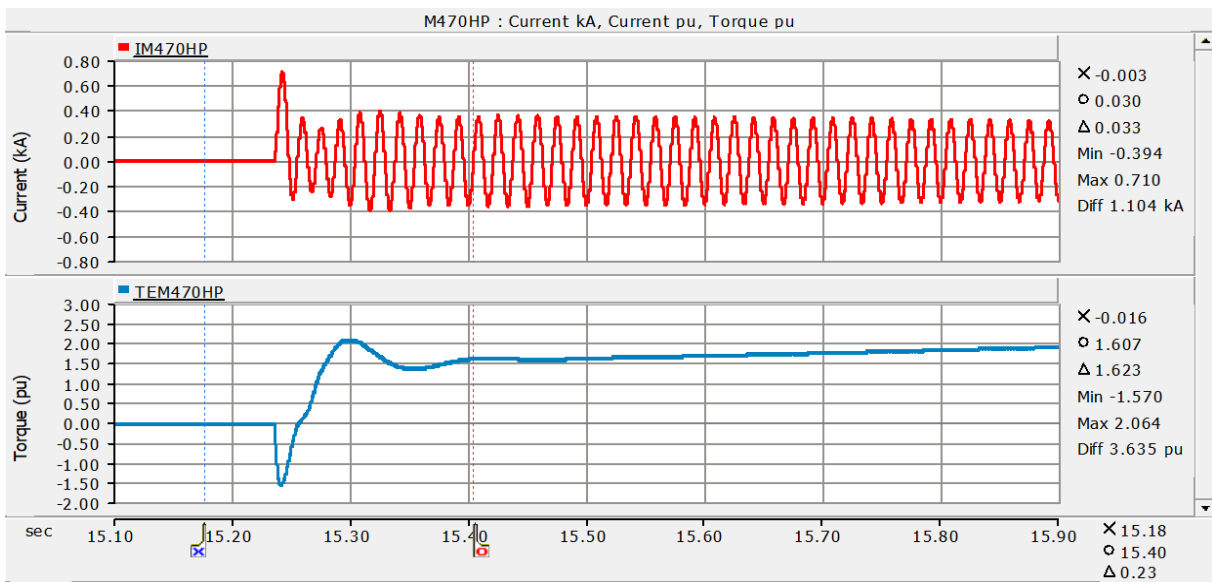


Figure 6-58 470 HP Motor phase A instantaneous current and electromagnetic torque transient response at the moment of reconnection to the start-up system during a residual voltage transfer test, initiated at t=14 sec.

Figure 6-58 zooms in on Figure 6-57 and shows the damped oscillatory response of the phase A instantaneous current and electromagnetic torque when the motor bus was reconnected to the auxiliary system. The motor required about 1.96 seconds to reaccelerate and reach steady state operation.



Figure 6-59 shows the phase A current in per unit versus the speed in per unit during the simulation. The maximum current was 6.069 p.u. at the instant after the reconnection (indicated with letter e) which was lower than the starting current (shown with letter a). The speed before the reconnection was 0.87 p.u. (identified with letter d). The curve from e to f shows the damped oscillating behavior of the motor during the reconnection.

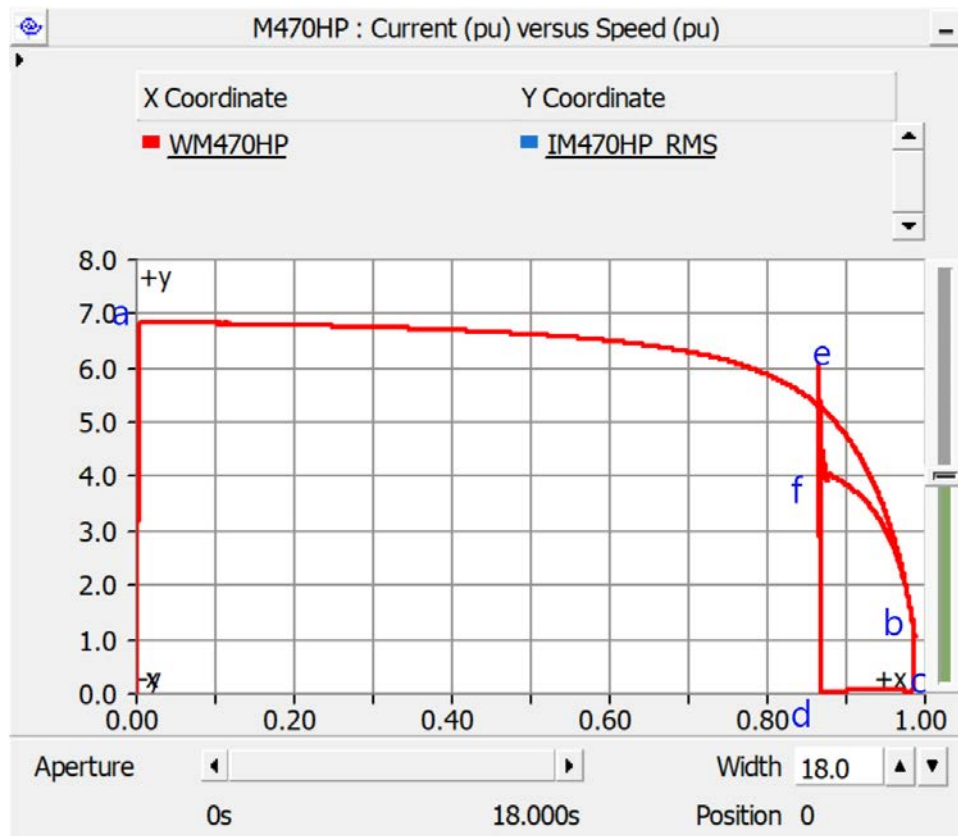


Figure 6-59 470 HP Motor phase A current versus speed in per unit transient response comparison between the motor starting process and the reconnection after a residual voltage transfer test, initiated at  $t=14$  sec.

Figure 6-60 shows the electromagnetic torque in per unit versus the speed in per unit during the simulation. The maximum negative torque was -1.57 p.u. at the instant after the reconnection (identified with letter f) which was lower than the maximum starting torque. The speed of the motor decayed to 0.87 per unit at the moment before the reconnection. The curve from e to h shows the damping oscillating behavior of the motor during the reconnection to the new power supply.

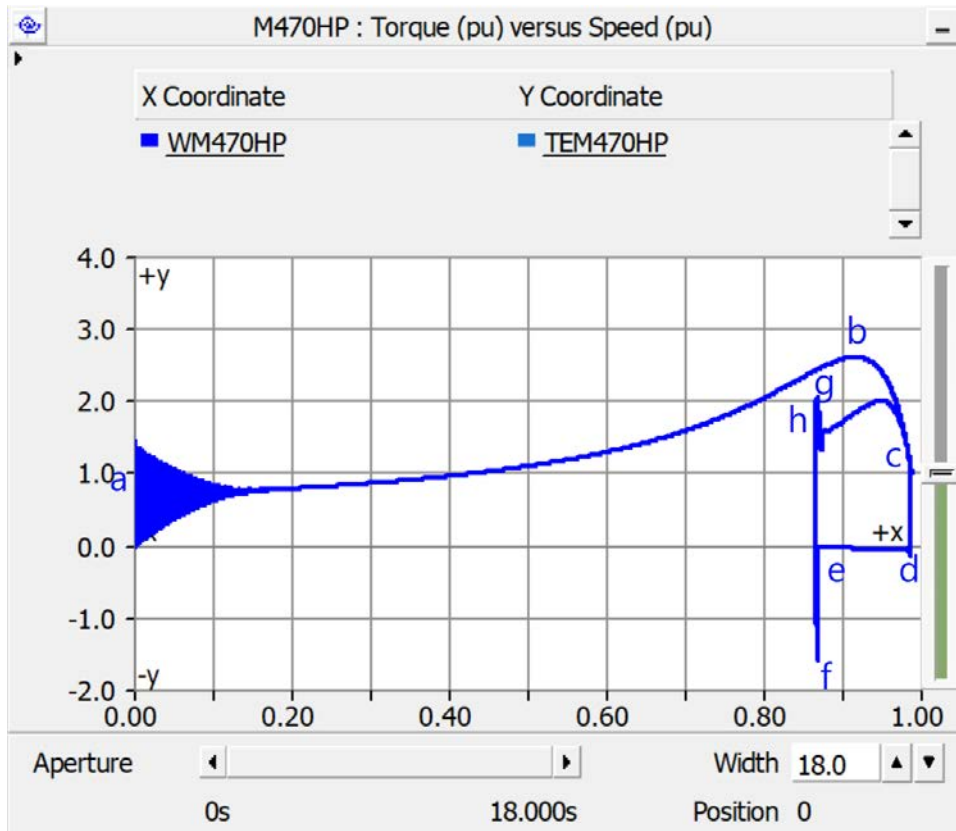


Figure 6-60 470 HP Motor electromagnetic torque versus speed transient response comparison during starting process and at the reconnection after a residual voltage transfer test, initiated at  $t=14$  sec.

Figures 6-61 to 6-67 show the phase A instantaneous voltages of the auxiliary and motor buses, and the current and electromagnetic torque versus speed in per unit for each motor during a residual voltage transfer tests initiated at t=8.004167 s.

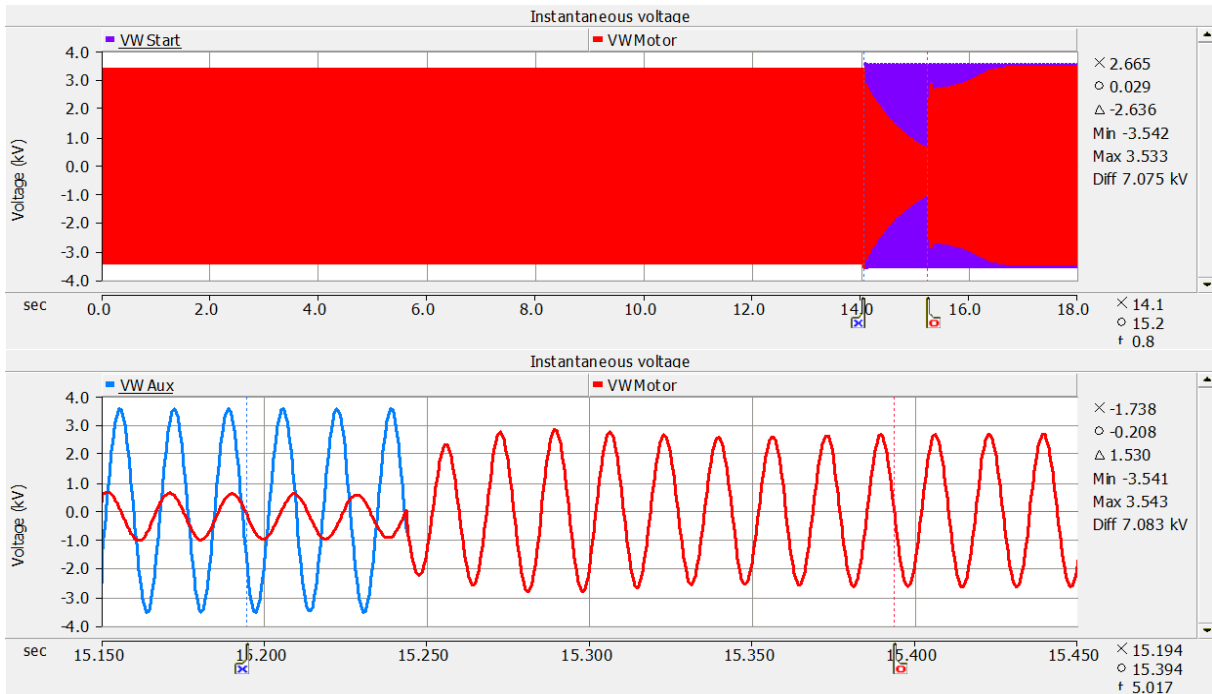


Figure 6-61 Phase A instantaneous voltage in kV, during a residual voltage transfer test, initiated at t=14.004167 sec.

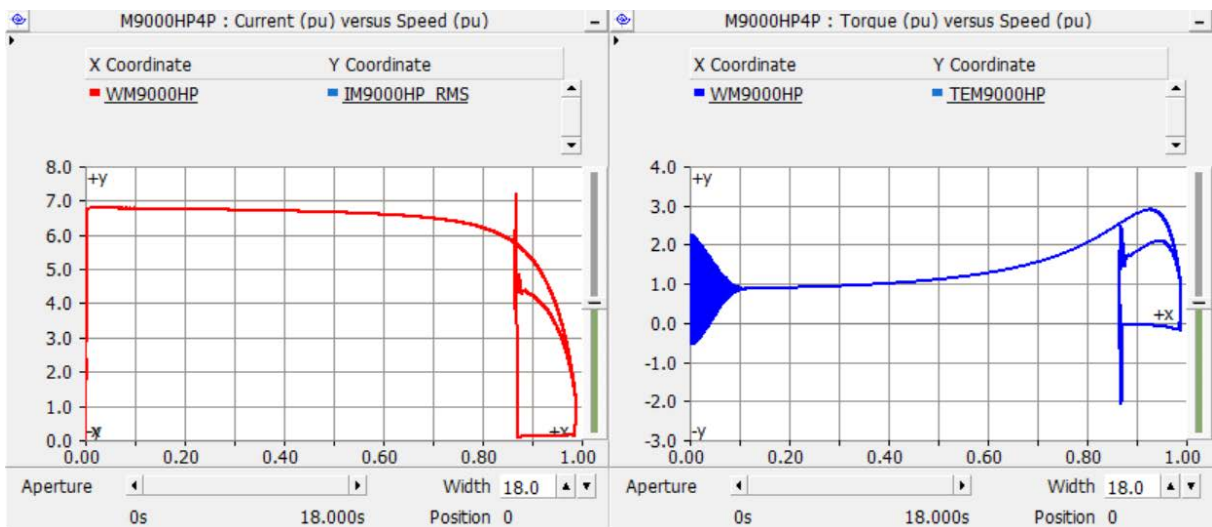


Figure 6-62 9000 HP motor phase A current and electromagnetic torque versus speed in per unit transient response comparison during starting process and at the reconnection after a residual voltage transfer test, initiated at t=14.004167 sec.

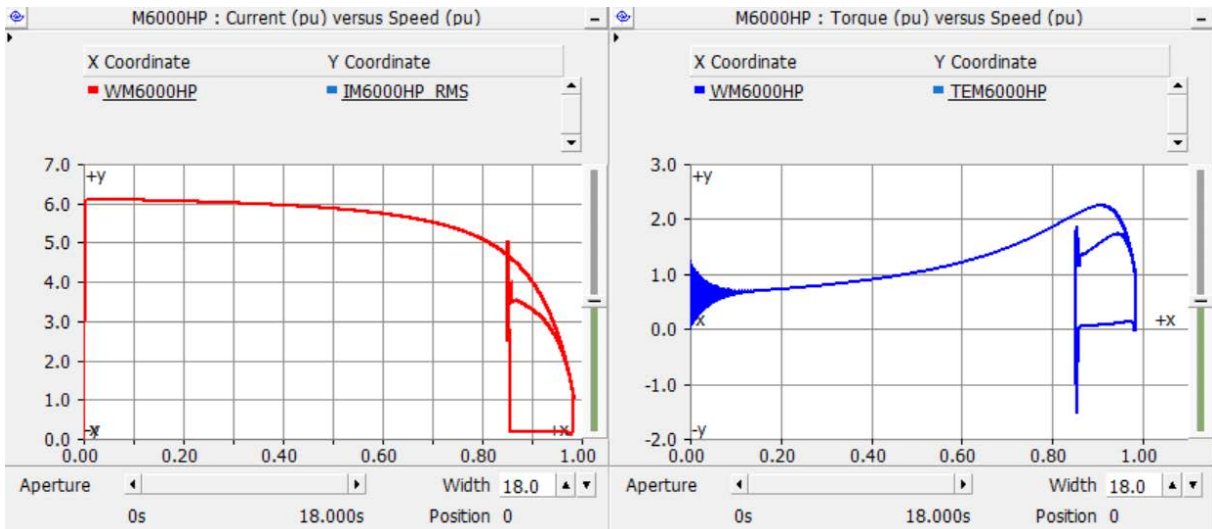


Figure 6-63 6000 HP motor phase A current and electromagnetic torque versus speed in per unit transient response comparison during starting process and at the reconnection after a residual voltage transfer test, initiated at t=14.004167 sec.

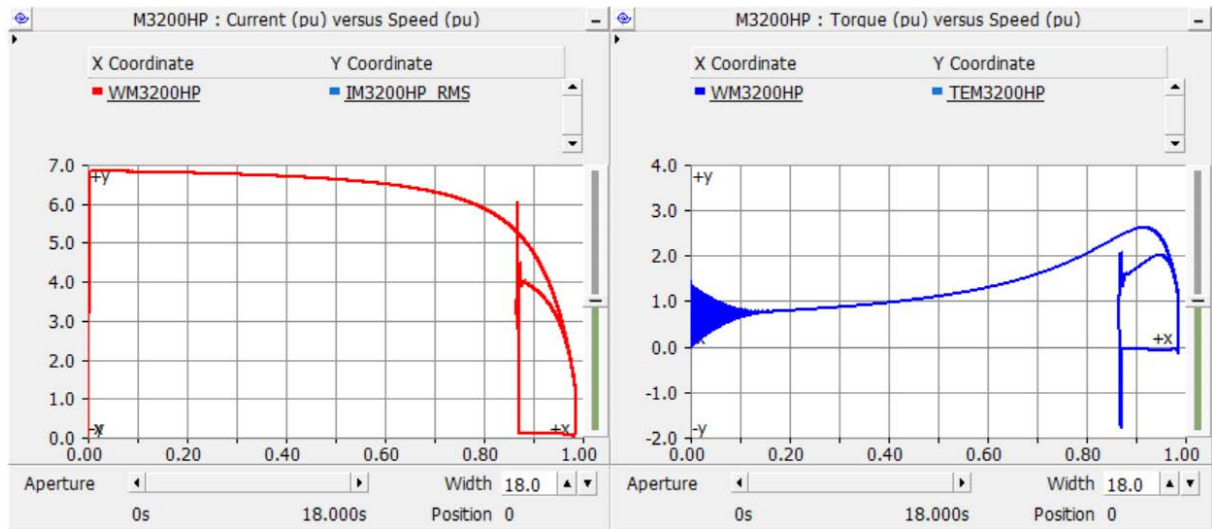


Figure 6-64 3200 HP motor phase A current and electromagnetic torque versus speed in per unit transient response comparison during starting process and at the reconnection after a residual voltage transfer test, initiated at t=14.004167 sec.

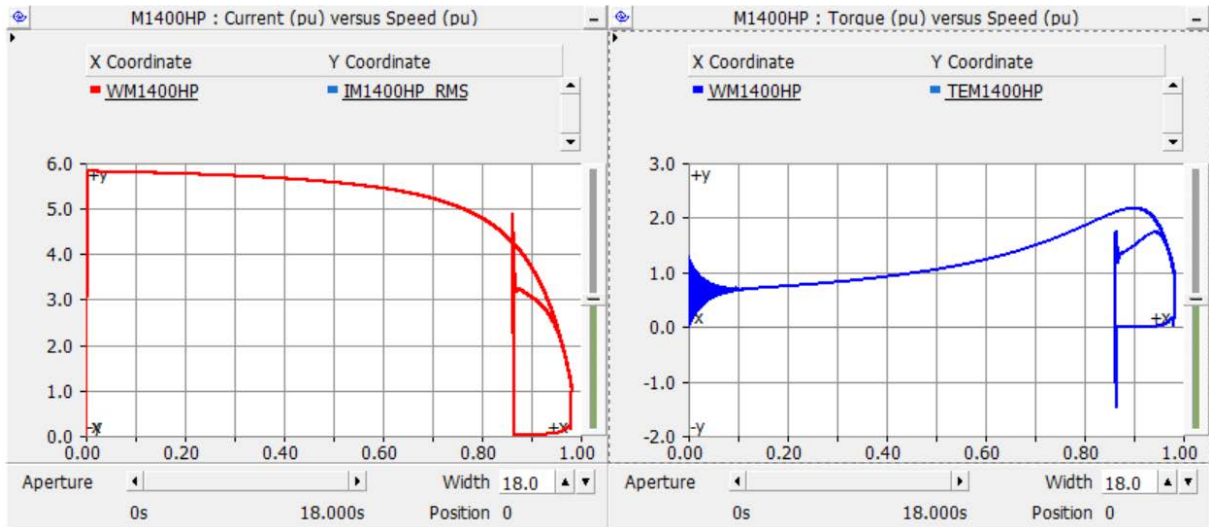


Figure 6-65 1400 HP motor phase A current and electromagnetic torque versus speed in per unit transient response comparison during starting process and at the reconnection after a residual voltage transfer test, initiated at t=14.004167 sec.

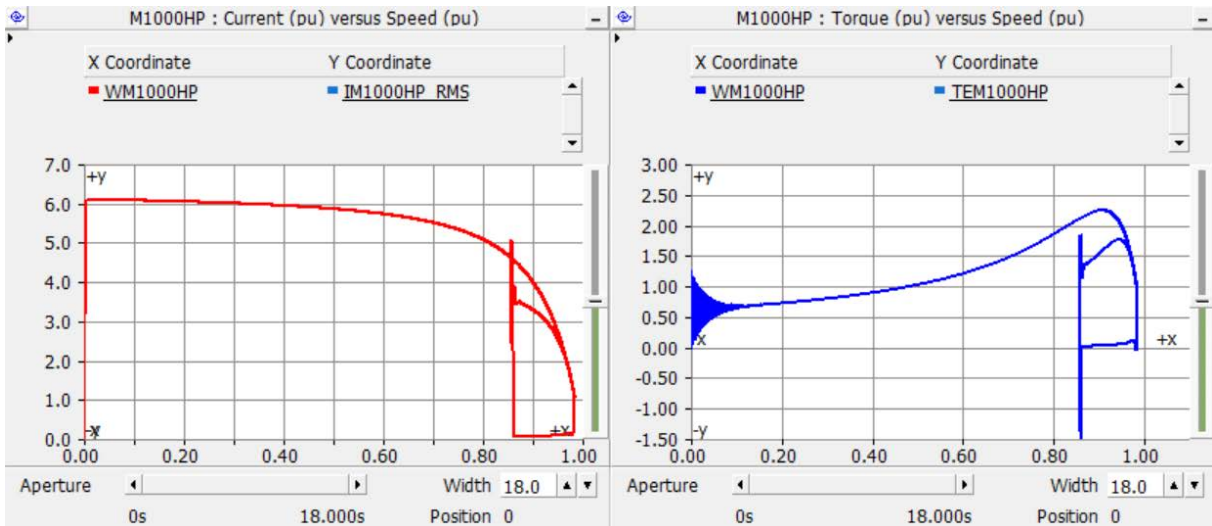


Figure 6-66 1000 HP motor phase A current and electromagnetic torque versus speed in per unit transient response comparison during starting process and at the reconnection after a residual voltage transfer test, initiated at t=14.004167 sec.

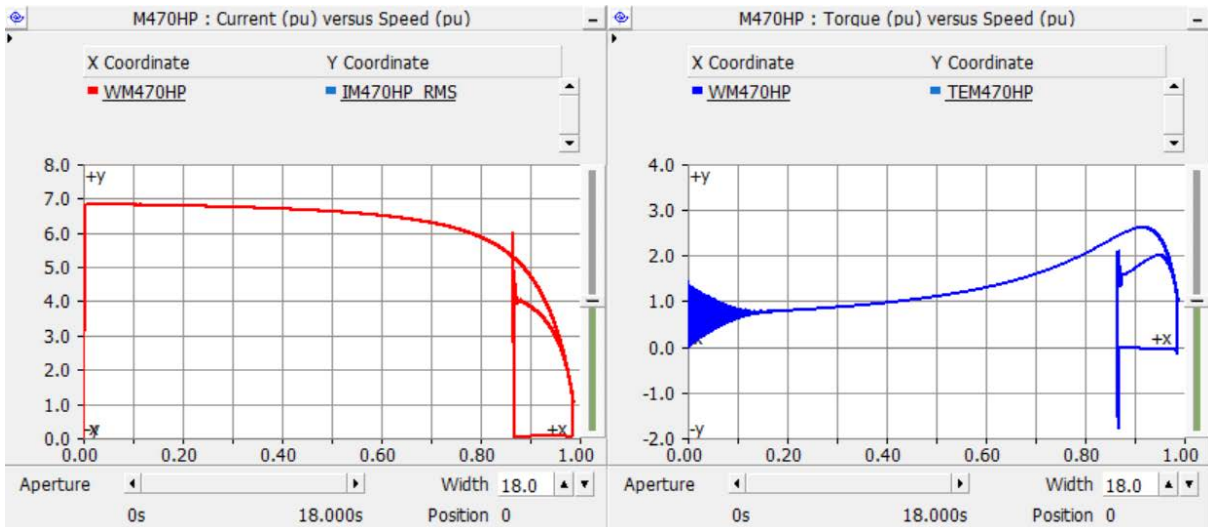


Figure 6-67 470 HP motor phase A current and electromagnetic torque versus speed in per unit transient response comparison during starting process and at the reconnection after a residual voltage transfer test, initiated at  $t=14.004167$  sec.

The performance of the residual voltage transfer algorithm during the test was the same as in the previous test and the maximum current and electromagnetic torque changed according to the point on wave at the instant of loss of power supply and reconnection.

Figures 6-68 to 6-74 show the phase A instantaneous voltages of the auxiliary and motor buses, and the current and electromagnetic torque versus speed in per unit for each motor during a residual voltage transfer tests initiated at  $t=14.00833$  s.

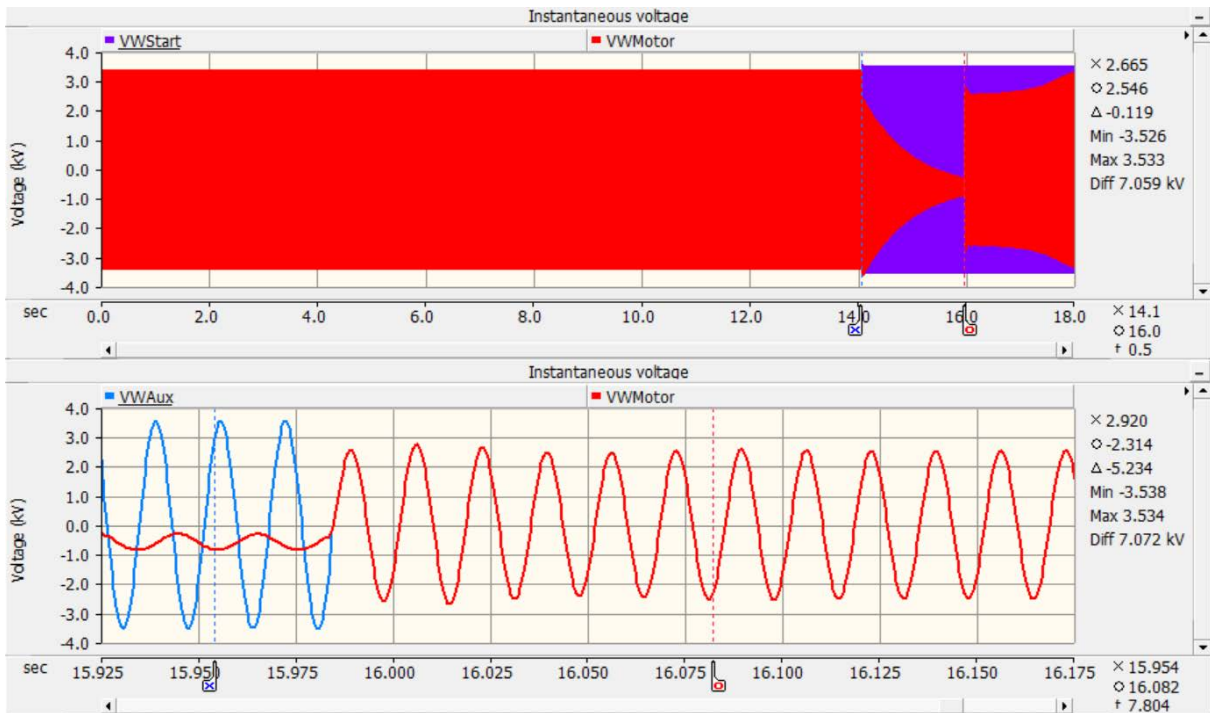


Figure 6-68 Phase A instantaneous voltage in kV, during a residual voltage transfer test, initiated at t=14.00833 sec.

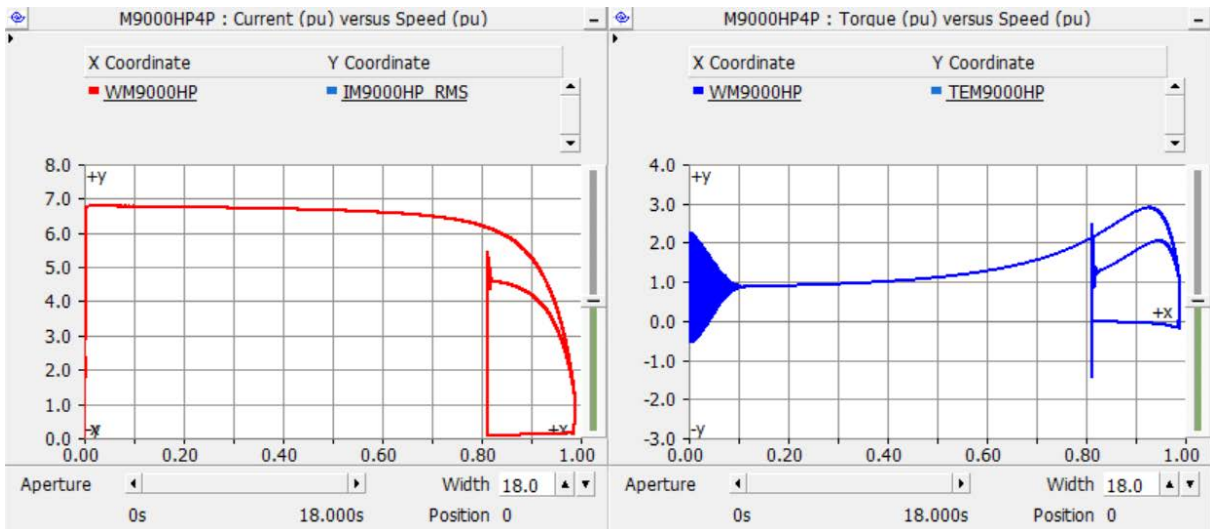


Figure 6-69 9000 HP motor phase A current and electromagnetic torque versus speed in per unit transient response comparison during starting process and at the reconnection after a residual voltage transfer test, initiated at t=14.00833 sec.



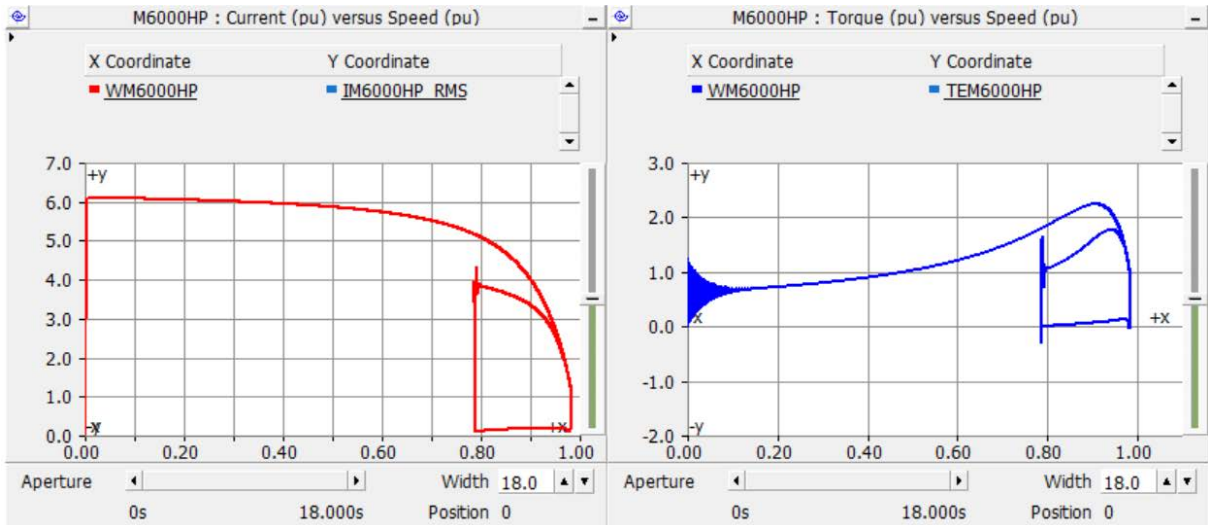


Figure 6-70 6000 HP motor phase A current and electromagnetic torque versus speed in per unit transient response comparison during starting process and at the reconnection after a residual voltage transfer test, initiated at  $t=14.00833$  sec.

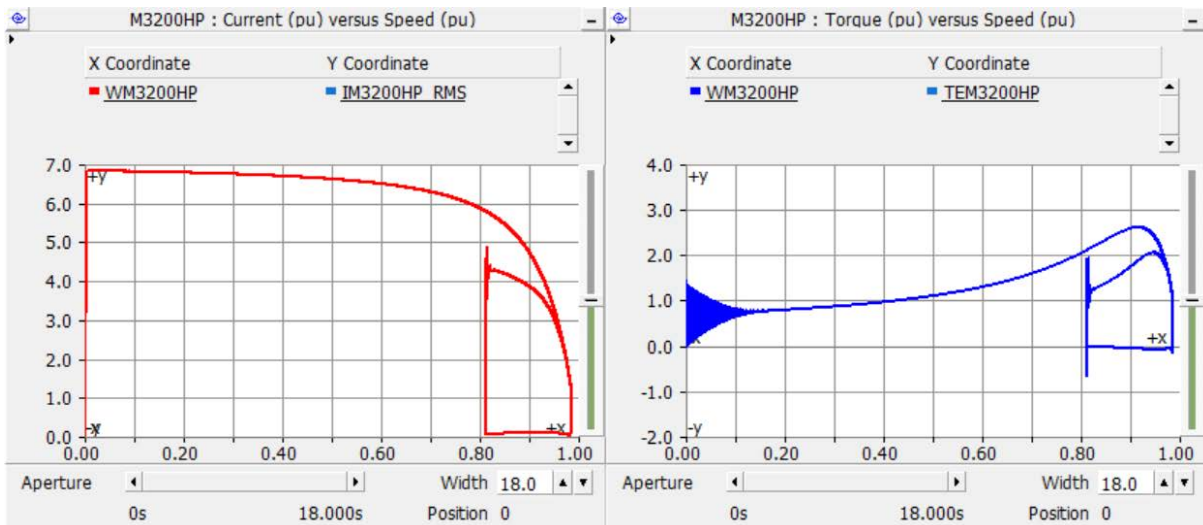


Figure 6-71 3200 HP motor phase A current and electromagnetic torque versus speed in per unit transient response comparison during starting process and at the reconnection after a residual voltage transfer test, initiated at  $t=14.00833$  sec.



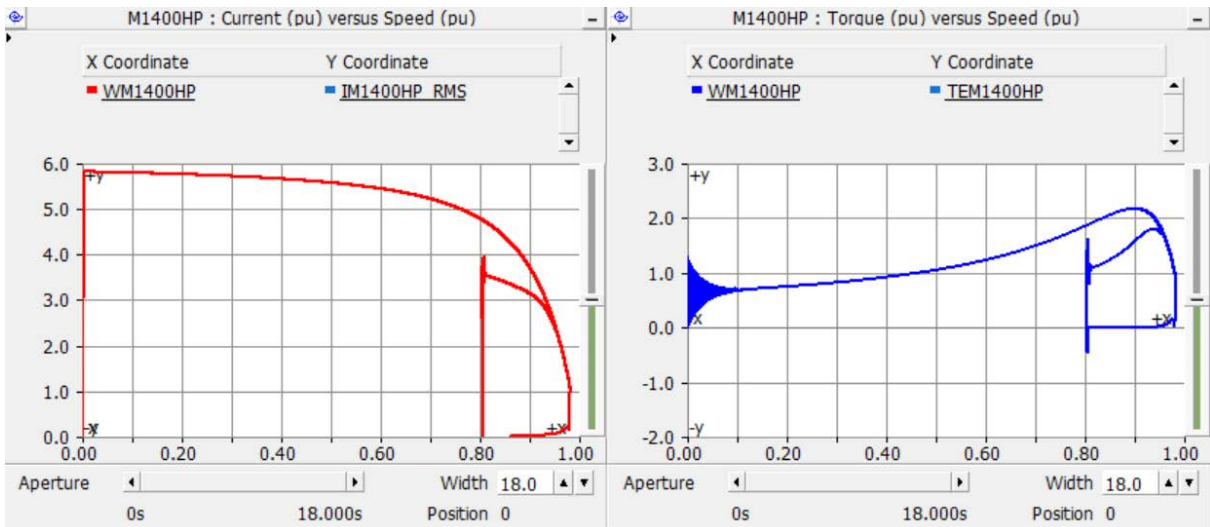


Figure 6-72 1400 HP motor phase A current and electromagnetic torque versus speed in per unit transient response comparison during starting process and at the reconnection after a residual voltage transfer test, initiated at  $t=14.00833$  sec.

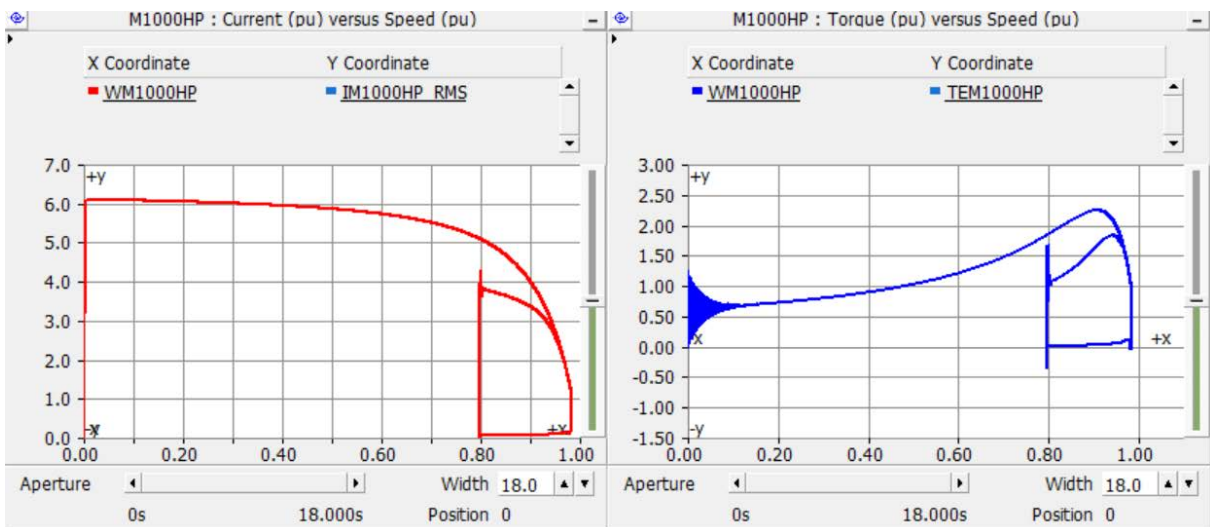


Figure 6-73 1000 HP motor phase A current and electromagnetic torque versus speed in per unit transient response comparison during starting process and at the reconnection after a residual voltage transfer test, initiated at  $t=14.00833$  sec.

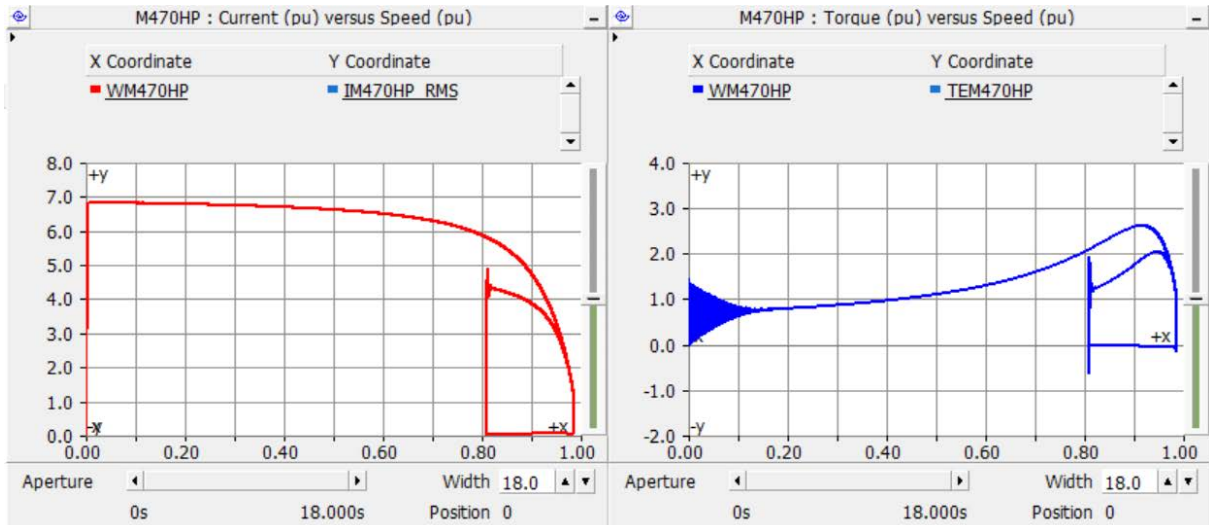


Figure 6-74 470 HP motor phase A current and electromagnetic torque versus speed in per unit transient response comparison during starting process and at the reconnection after a residual voltage transfer test, initiated at  $t=14.004167$  sec.

The performance of the residual voltage transfer algorithm during the test was the same as in the previous test and the maximum current and electromagnetic torque changed according to the point on wave at the instant of loss of power supply and reconnection.

Figures 6-75 to 6-81 show the phase A instantaneous voltages of the auxiliary and motor buses, and the current and electromagnetic torque versus speed in per unit for each motor during a residual voltage transfer tests initiated at t=14.00125 s.

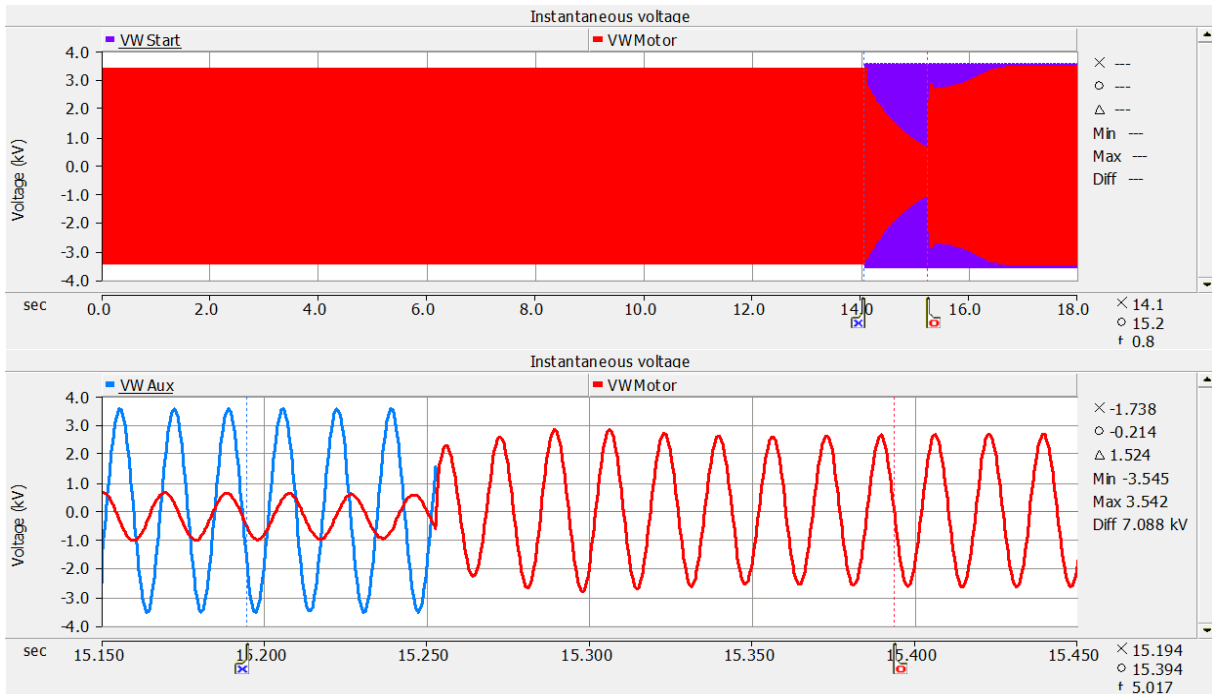


Figure 6-75 Phase A instantaneous voltage in kV, during a residual voltage transfer test, initiated at t=14.0125 sec.

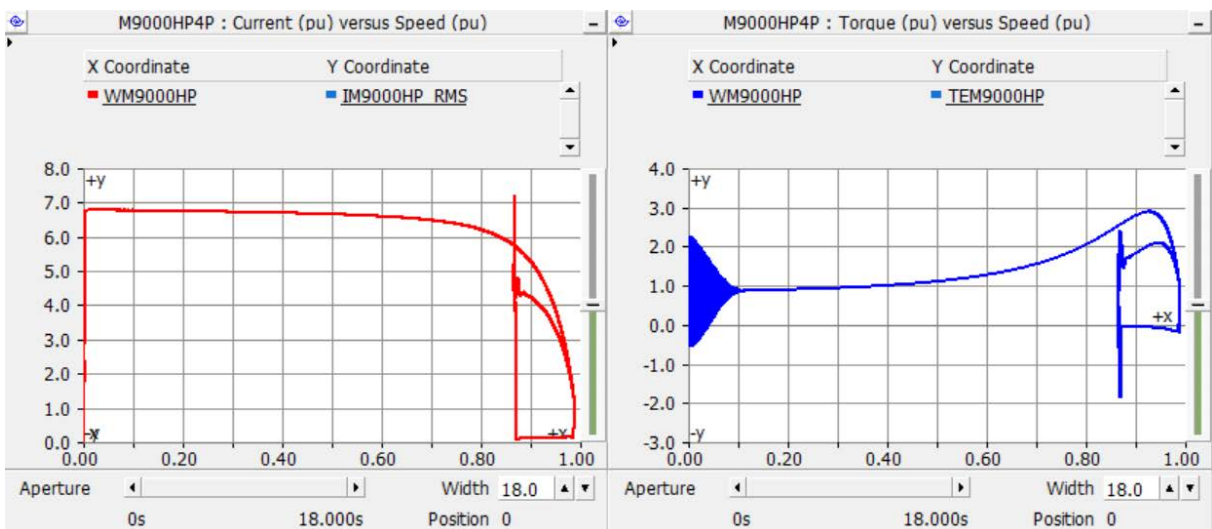


Figure 6-76 9000 HP motor phase A current and electromagnetic torque versus speed in per unit transient response comparison during starting process and at the reconnection after a residual voltage transfer test, initiated at t=14.0125 sec.

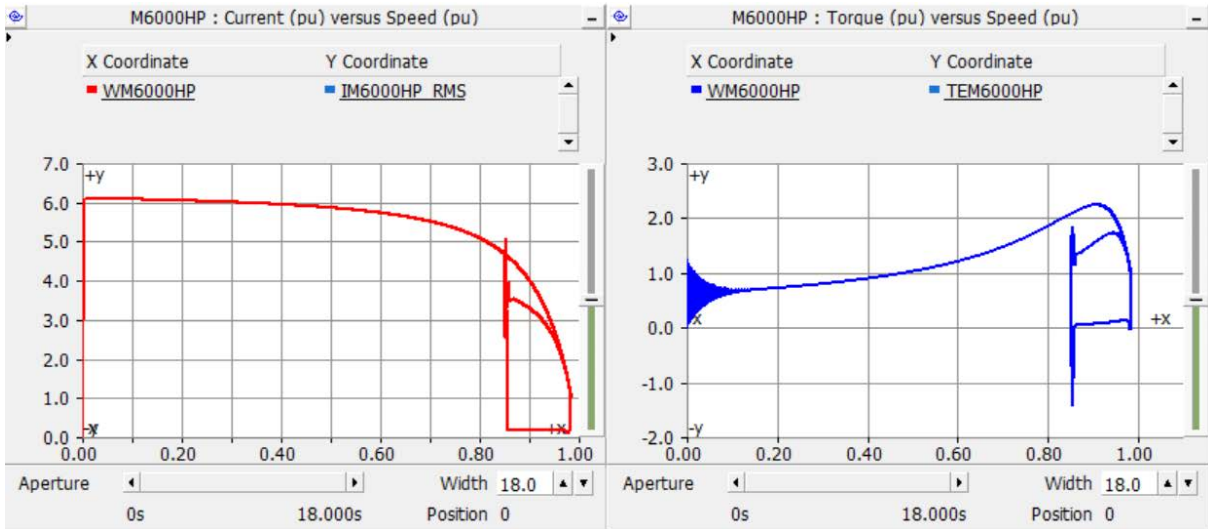


Figure 6-77 6000 HP motor phase A current and electromagnetic torque versus speed in per unit transient response comparison during starting process and at the reconnection after a residual voltage transfer test, initiated at  $t=14.0125$  sec.

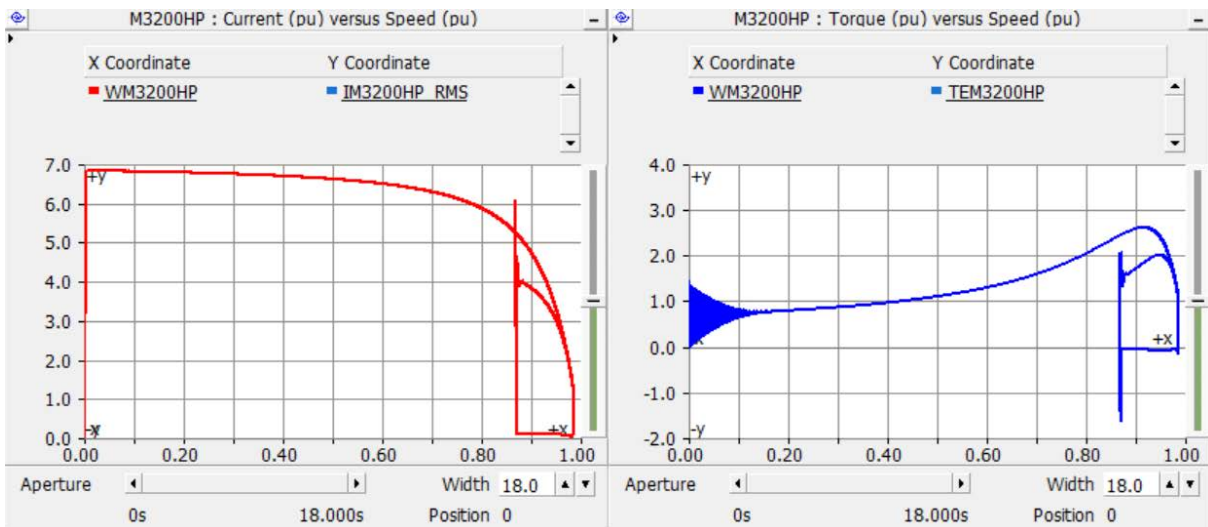


Figure 6-78 3200 HP motor phase A current and electromagnetic torque versus speed in per unit transient response comparison during starting process and at the reconnection after a residual voltage transfer test, initiated at  $t=14.0125$  sec.

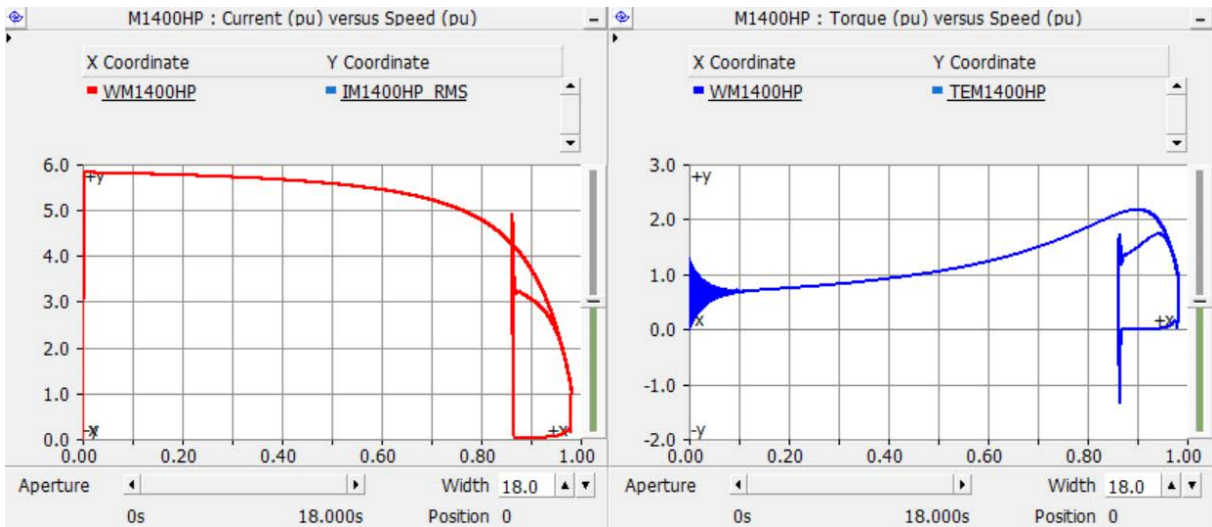


Figure 6-79 1400 HP motor phase A current and electromagnetic torque versus speed in per unit transient response comparison during starting process and at the reconnection after a residual voltage transfer test, initiated at  $t=14.0125$  sec.

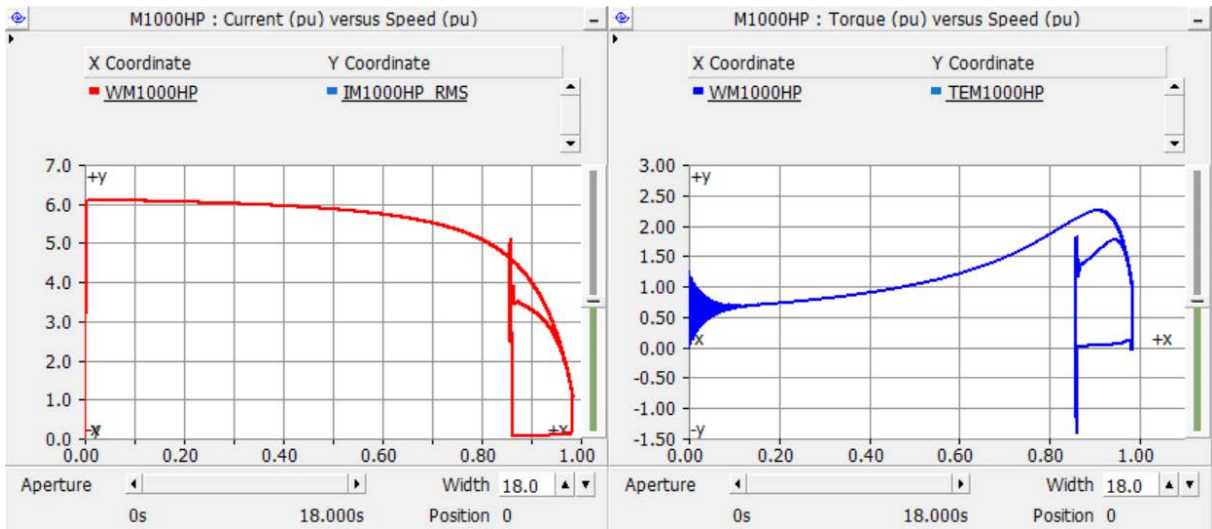


Figure 6-80 1000 HP motor phase A current and electromagnetic torque versus speed in per unit transient response comparison during starting process and at the reconnection after a residual voltage transfer test, initiated at  $t=14.0125$  sec.

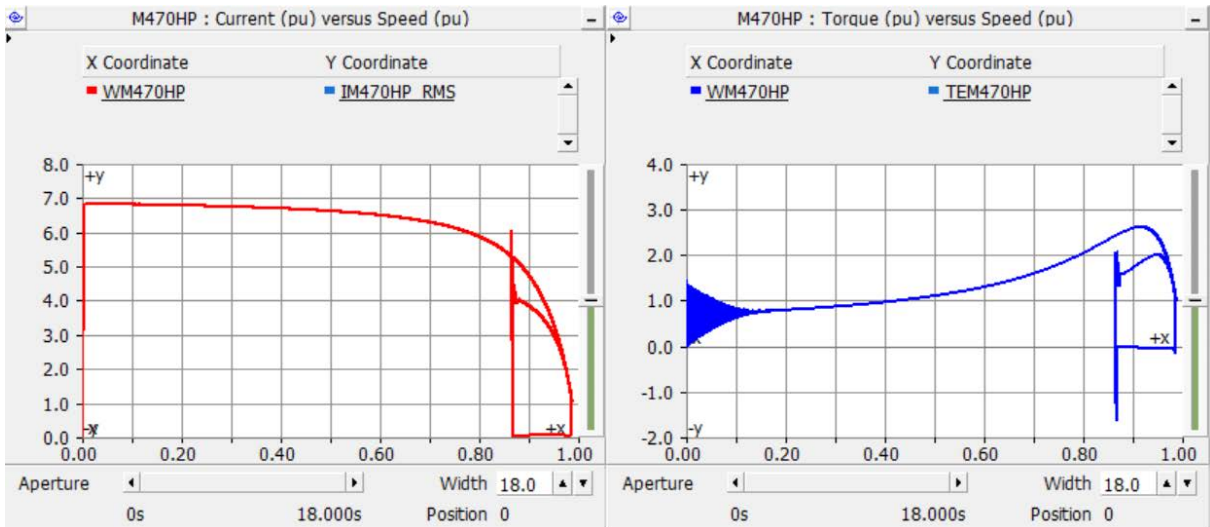


Figure 6-81 470 HP motor phase A current and electromagnetic torque versus speed in per unit transient response comparison during starting process and at the reconnection after a residual voltage transfer test, initiated at  $t=14.0125$  sec.

Figures 6-82 to 6-89 show the phase A instantaneous voltages of the auxiliary and motor buses, and the current and electromagnetic torque versus speed in per unit for each motor during a residual voltage transfer tests initiated at  $t=14.02$  s and the residual voltage limit set to 0.33 p.u.

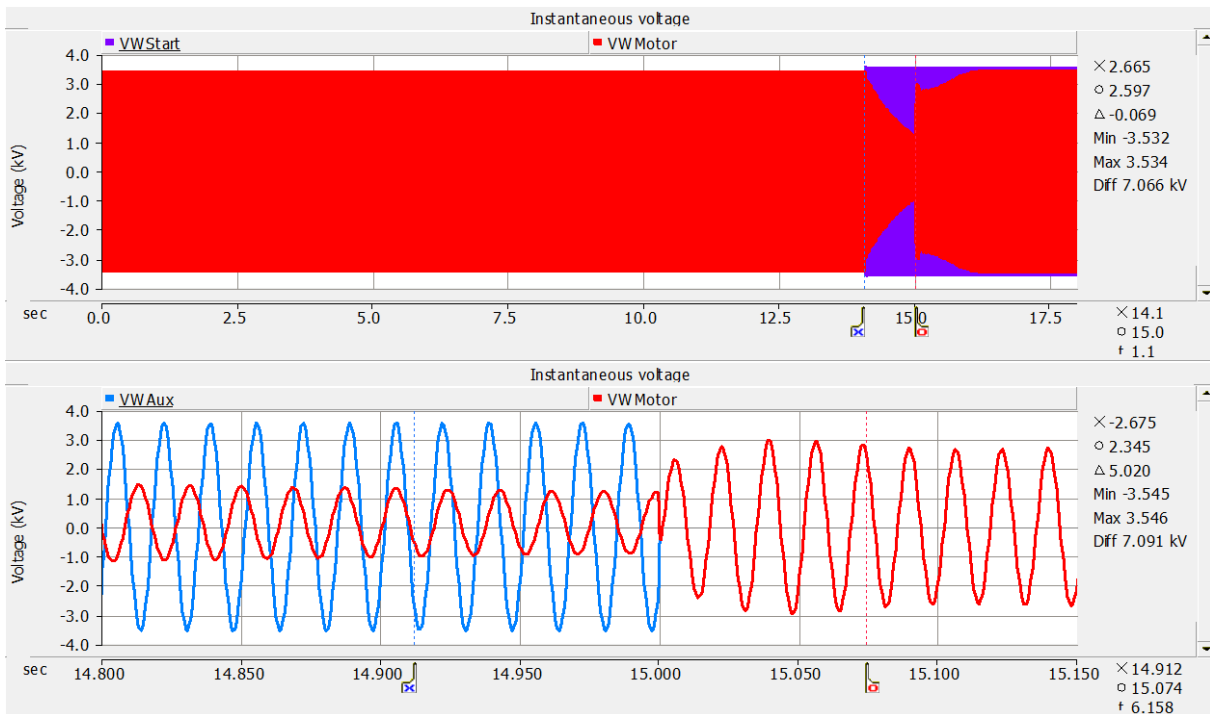


Figure 6-82 Phase A instantaneous voltage in kV, during a residual voltage transfer test, initiated at  $t=14.02$  sec.

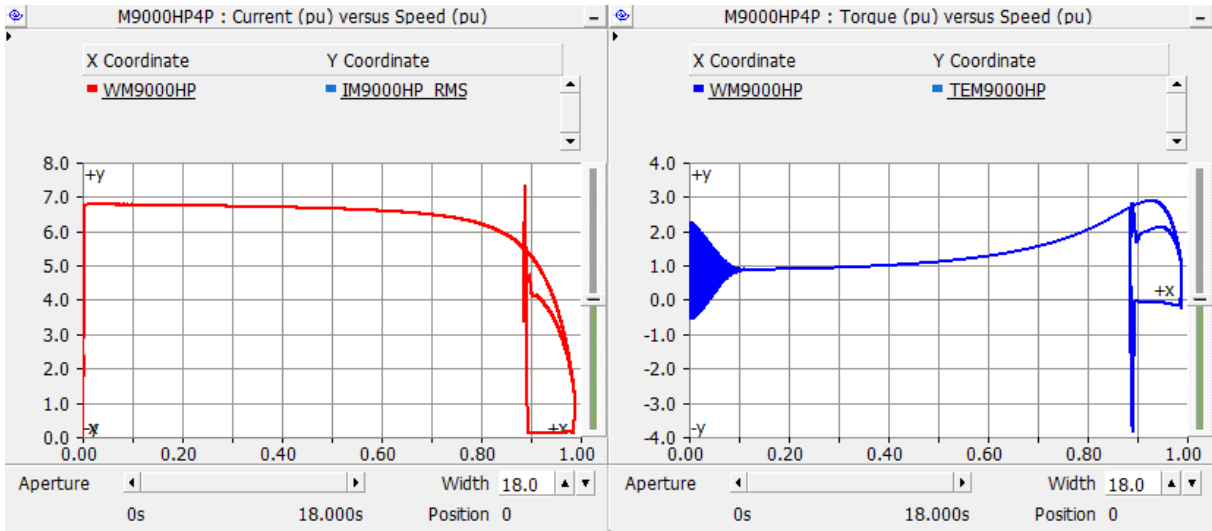


Figure 6-83 9000 HP motor phase A current and electromagnetic torque versus speed in per unit transient response comparison during starting process and at the reconnection after a residual voltage transfer test, initiated at t=14.02 sec.

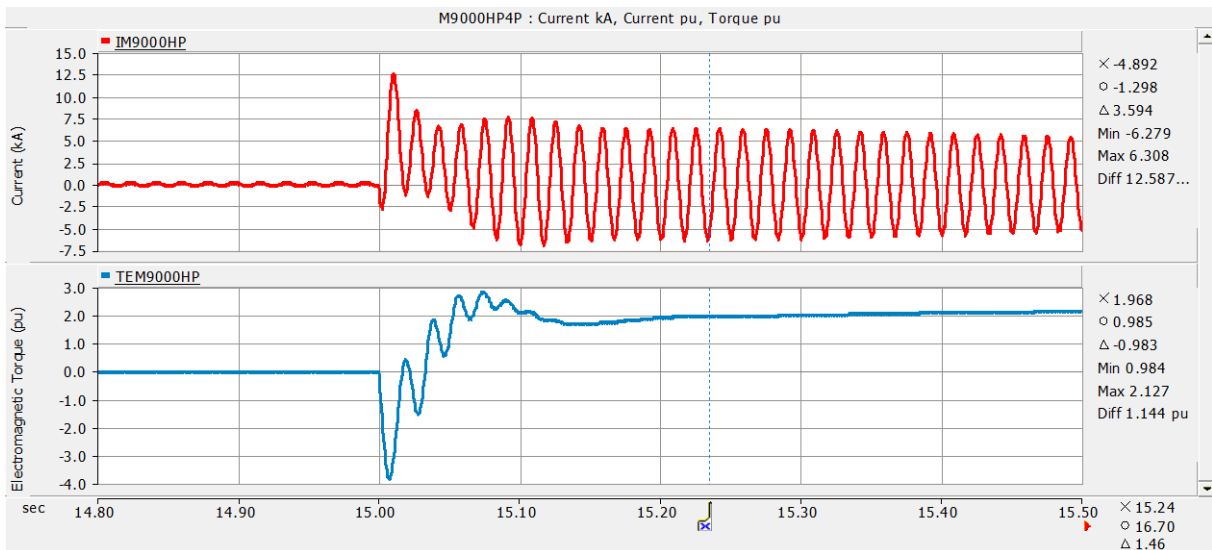


Figure 6-84 9000 HP motor phase A current and electromagnetic torque transient response at the reconnection after a residual voltage transfer test, initiated at t=14.02 sec.



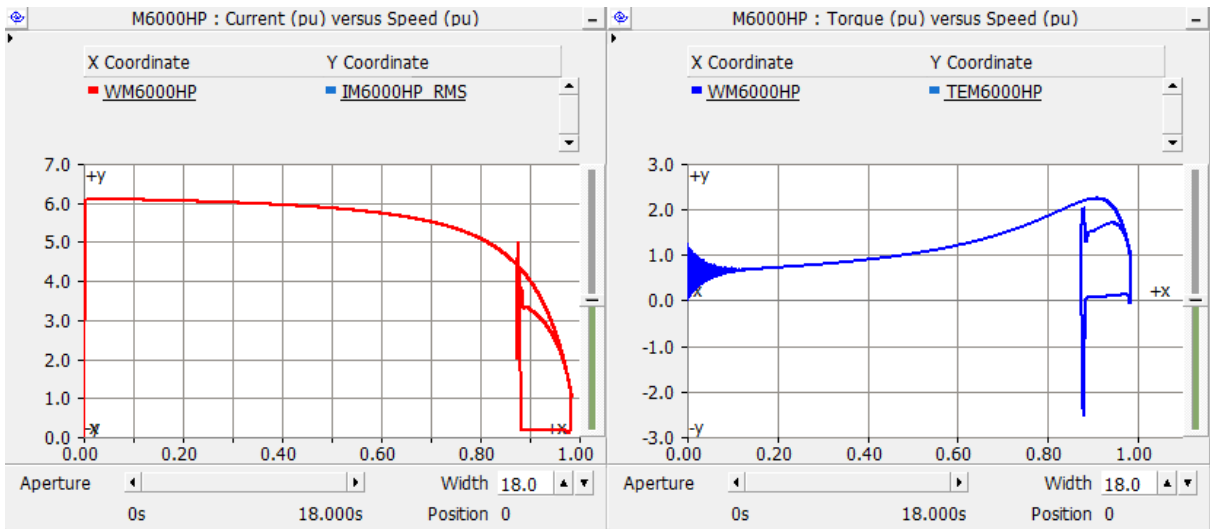


Figure 6-85 6000 HP motor phase A current and electromagnetic torque versus speed in per unit transient response comparison during starting process and at the reconnection after a residual voltage transfer test, initiated at t=14.02 sec.

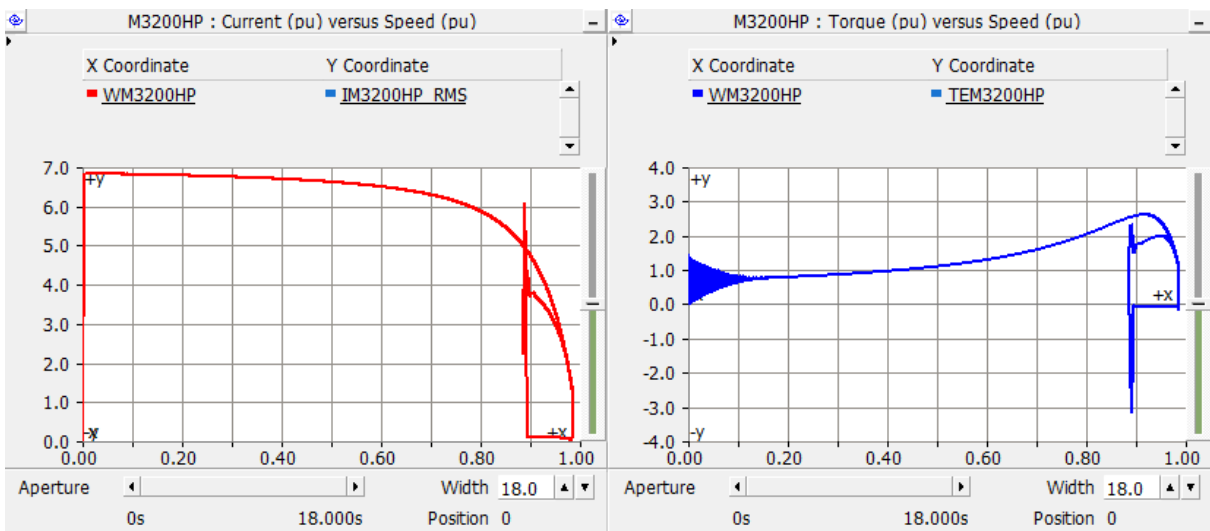


Figure 6-86 3200 HP motor phase A current and electromagnetic torque versus speed in per unit transient response comparison during starting process and at the reconnection after a residual voltage transfer test, initiated at t=14.02 sec.



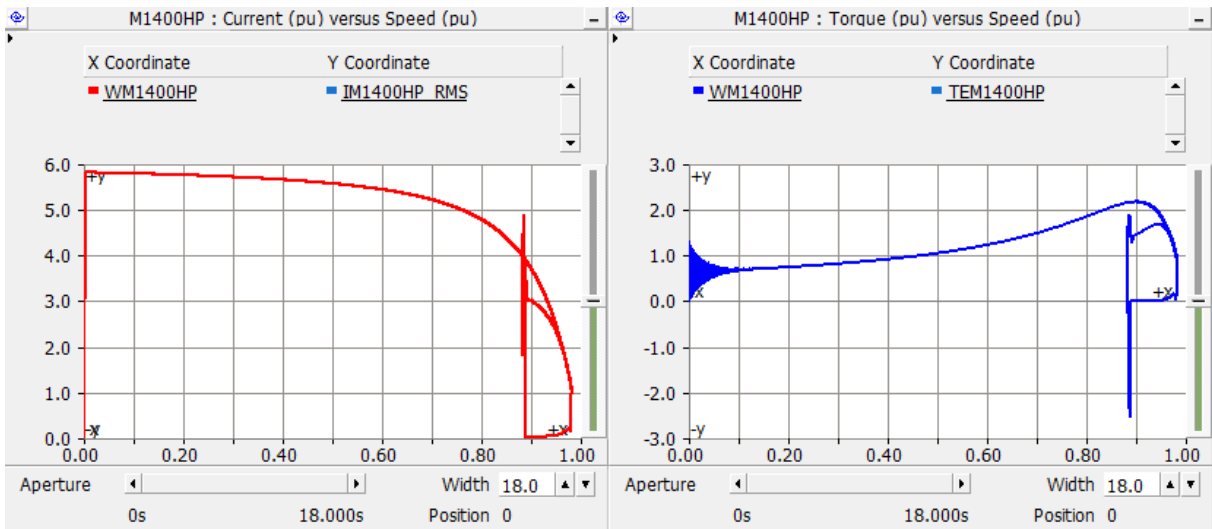


Figure 6-87 1400 HP motor phase A current and electromagnetic torque versus speed in per unit transient response comparison during starting process and at the reconnection after a residual voltage transfer test, initiated at  $t=14.02$  sec.

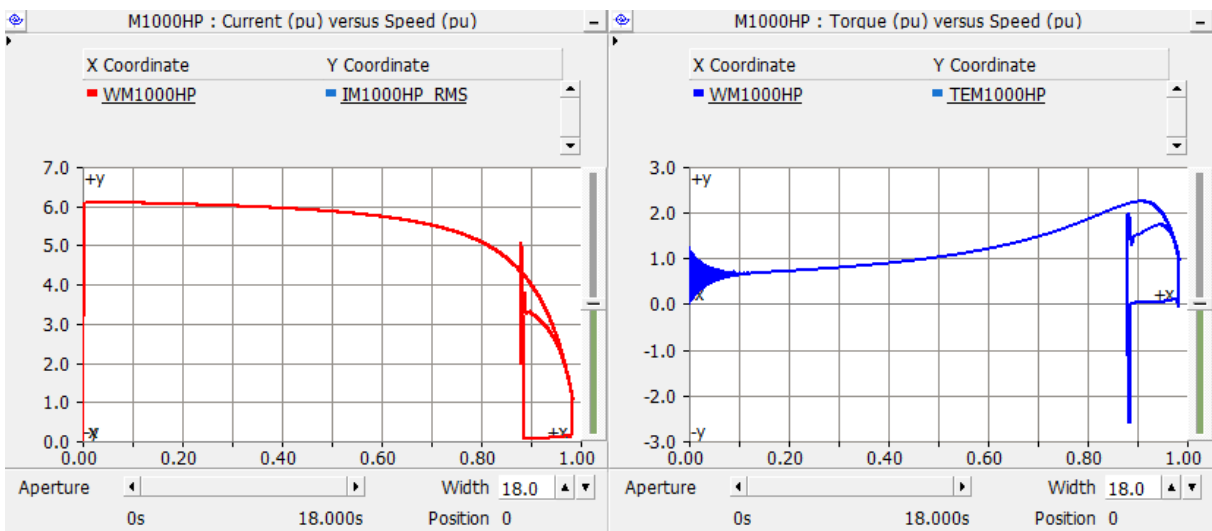


Figure 6-88 1000 HP motor phase A current and electromagnetic torque versus speed in per unit transient response comparison during starting process and at the reconnection after a residual voltage transfer test, initiated at  $t=14.0125$  sec.

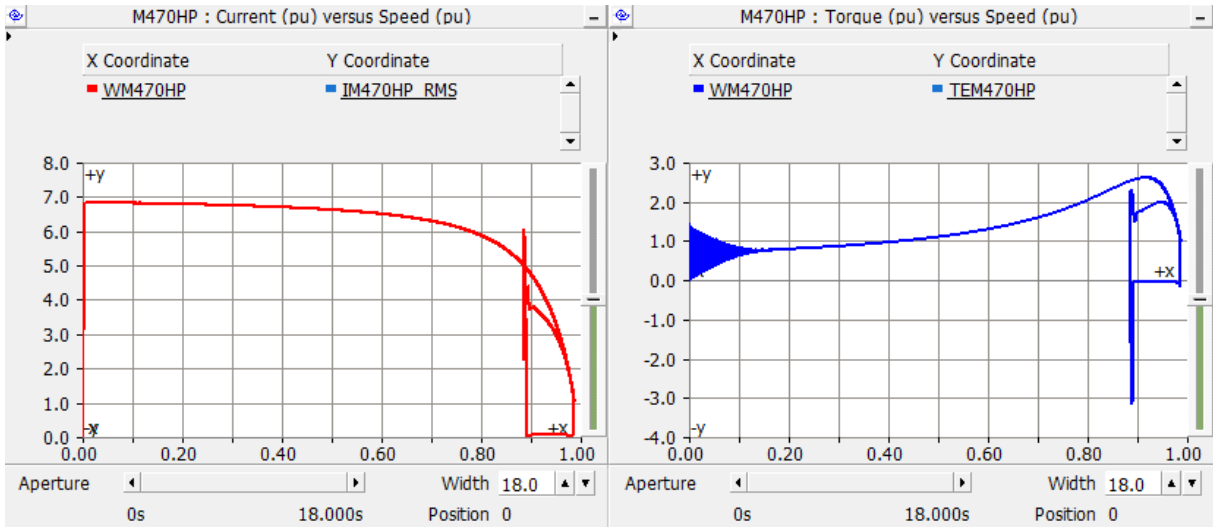


Figure 6-89 470 HP motor phase A current and electromagnetic torque versus speed in per unit transient response comparison during starting process and at the reconnection after a residual voltage transfer test, initiated at  $t=14.02$  sec.

The performance of the residual voltage transfer algorithm during the test was the same as in the previous test and the maximum current and electromagnetic torque changed according to the point on wave at the instant of loss of power supply and reconnection.

Table 6-3 shows a summary of maximum current and electromagnetic torque of the 6000 HP induction motor during several motor bus transfer conditions. The first two columns identified as a) and b) are improper transfer conditions which may cause damage to the motors.

6000 HP Induction Motor Reconnecting the motor bus under:	a) Maximum motor bus – new source voltage difference	b) Large motor bus - new source voltage frequency difference	Fast Transfer	In-phase Transfer	c) Residual Voltage Transfer
<b>Current</b>					
a) Maximum starting current in p.u.	6.0	6.0	6.0	6.0	6.0
b) Maximum current during reconnection in p.u.	9.53	7.55	2.59	2.69	5.0
c) $I_{\text{reconnecting}} / I_{\text{starting}}$ in p.u.	1.59	1.25	0.43	0.45	0.83
<b>Electromagnetic Torque</b>					
a) Maximum starting torque in p.u.	2.3	2.3	2.3	2.3	2.3
b) Maximum torque during reconnection in p.u.	-6.39	-3.62	2.57	1.89	-2.5
c) $T_{\text{reconnecting}} / T_{\text{starting}}$ in p.u.	2.78	1.57	1.11	0.82	1.08

*Table 6-3 Summary of maximum current and electromagnetic torque of the 6000 HP motor during several motor bus transfer conditions*

Table 6-4 shows a summary of maximum current and electromagnetic torque of the 3200 HP induction motor during several motor bus transfer conditions. Columns identified as a) and b) and c) are improper transfer conditions which may cause damage to the motors.

3200 HP Induction Motor Reconnecting the motor bus under:	a) Maximum motor bus – new source voltage difference	b) A high motor bus - new source voltage frequency difference	Fast Transfer	In-phase Transfer	c) Residual Voltage Transfer
Current					
a) Maximum starting current in p.u.	6.8	6.8	6.8	6.8	6.8
b) Maximum current during reconnection in p.u.	11.2	8.71	2.85	3.06	6.1
c) $I_{reconnecting}$ to $I_{starting}$ in p.u.	1.65	1.28	0.42	0.45	0.90
Electromagnetic Torque					
a) Maximum starting torque in p.u.	2.6	2.6	2.6	2.6	2.6
b) Maximum torque during reconnection in p.u.	-7.44	-4.56	3.03	2.19	-3.1
c) $T_{reconnecting}$ to $T_{starting}$ in p.u.	2.86	1.75	1.17	0.84	1.19

*Table 6-4 Summary of maximum current and electromagnetic torque of the 3200 HP motor during several motor bus transfer conditions*

## 6.3 Manual Transfer

### 6.3.1 Transfer from Start-up System to Auxiliary System

This section shows the results of the manual transfer test when transferring the motor bus from the start-up to the auxiliary system.

The motor bus transfer system controls used for this test are shown in Figure 6-90. Control SysSel was set to position BWS (transfer simulation from the start-up to auxiliary system), transfer initialization time MTime set to 99 seconds (this control is used only when fast, in-phase or residual voltage algorithms are tested individually), TType was set to 4 (fast transfer, in-phase and residual voltage algorithms were enabled). Control Coast Down was set to off, control Coast Down Time was set to 99 seconds (coast down simulating motors spinning down in group was not performed), Ind Coast Down Time was set to 99 seconds (coast down simulating motors spinning individually was not performed). The manual transfer was initiated when the switch button MTransfer was changed from 0 to 1 at  $t=14.1312$  seconds, which was therefore the transfer initiation time.

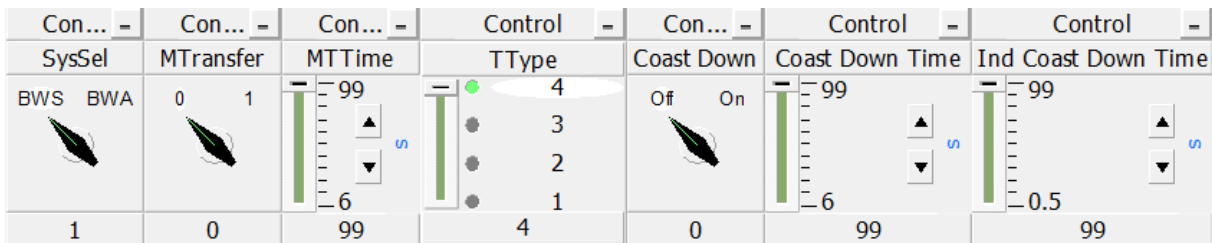


Figure 6-90 Motor bus transfer system controls for a manual transfer test, initiated at  $t=14.1312$  sec.

The start-up breaker opened at  $t=14.1892$  seconds (phase B current was interrupted at  $t= 8. 14.19244$  s, phase A current at  $t= 14.19602$  s and phase C current at  $t = 14.19602$  s.). The transfer was accomplished at  $t=14.2218$  seconds when the auxiliary breaker closed, approximately 90 milliseconds after the transfer initiation; which is basically the breaker closing time.

Figure 6-91 shows the phase A instantaneous voltage of the start-up (purple plot), auxiliary (light blue plot) and motor bus (red plot) during a manual transfer test. The start-up voltage magnitude before the transfer initiation was 4.1267 kV L-L and after the bus transfer the voltage magnitude was 4.309 kV. The auxiliary voltage magnitude before the transfer initiation was 4.343 kV and after the bus

transfer it was 4.1932 kV. During the loss of power supply, the motor bus voltage magnitude decayed to 3.6892 kV.

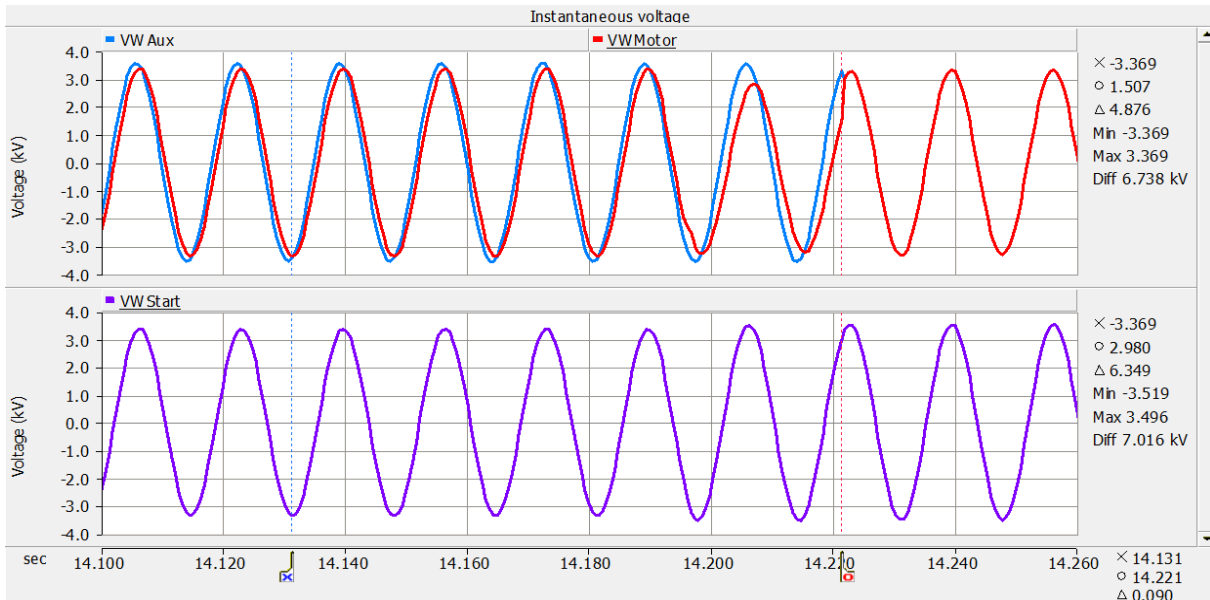


Figure 6-91 Phase A Instantaneous voltage in kV during a manual transfer test, initiated at  $t=14.1312$  sec.

Figure 6-92 shows the per unit phase A RMS voltage of the start-up (purple plot), auxiliary (light blue plot) and motor bus (red plot) during the fast transfer test mode. The start-up voltage magnitude changed from 0.992 p.u. (in a reference of 4.16 kV L-L) before the bus transfer to 1.036 p.u. after the bus transfer. The auxiliary medium voltage side voltage magnitude before the bus transfer was 1.044 p.u. and after the transfer was 1.008 p.u.

When the start-up breaker opened, the motor bus voltage magnitude decayed to 0.89 p.u. The motor bus voltage took 250 milliseconds to recover once the motor bus was reconnected from the auxiliary source.

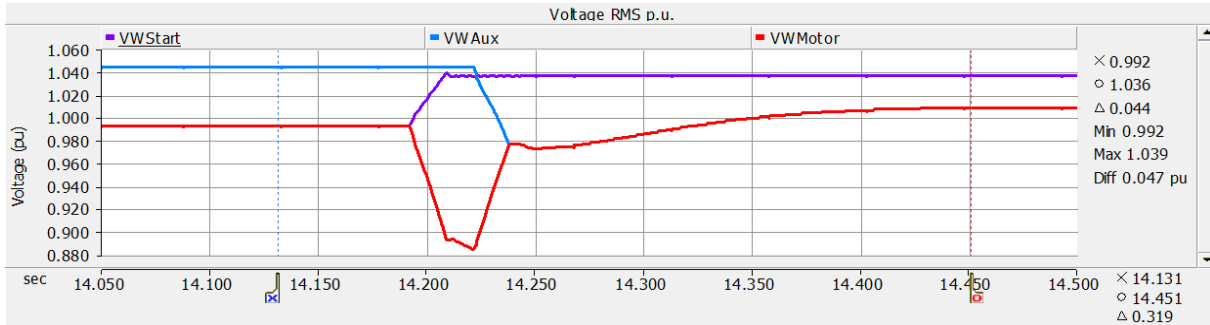


Figure 6-92 Phase A RMS voltage in per unit during a manual transfer test, initiated at  $t=14.1312$  sec.

Figure 6-93 shows the voltage frequency of the start-up (purple plot), auxiliary (light blue plot) and motor bus (red plot) during the fast transfer test mode. The motor bus voltage frequency decayed to 58.223 Hz on loss of power supply. When the auxiliary breaker closed, the motor bus frequency increased to 63.30 Hz and then decayed during 250 milliseconds to settle in 60 Hz.

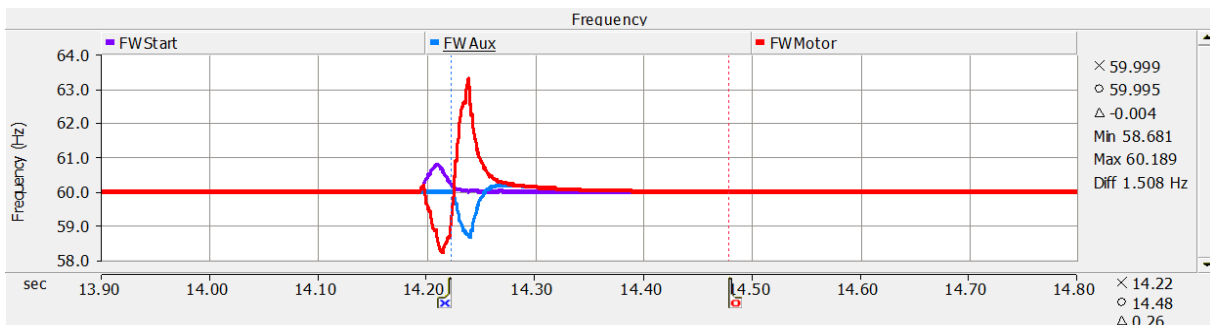


Figure 6-93 Voltage frequency in Hertz during a manual transfer test, initiated at  $t=14.1312$  sec.

Figure 6-94 shows the voltage phase A angle of the start-up (purple plot), auxiliary (light blue plot) and motor bus (red plot) during the fast transfer test mode. The start-up phase A voltage phase angle before the transfer was  $-45.083$  degrees and after the transfer was  $-39.84$  degrees. The auxiliary phase A voltage phase angle changed from  $-30.757$  degrees before the bus transfer to  $-34.995$  degrees after the transfer. During the bus transfer, the motor bus phase A voltage phase angle decayed to  $-62.713$  degrees.

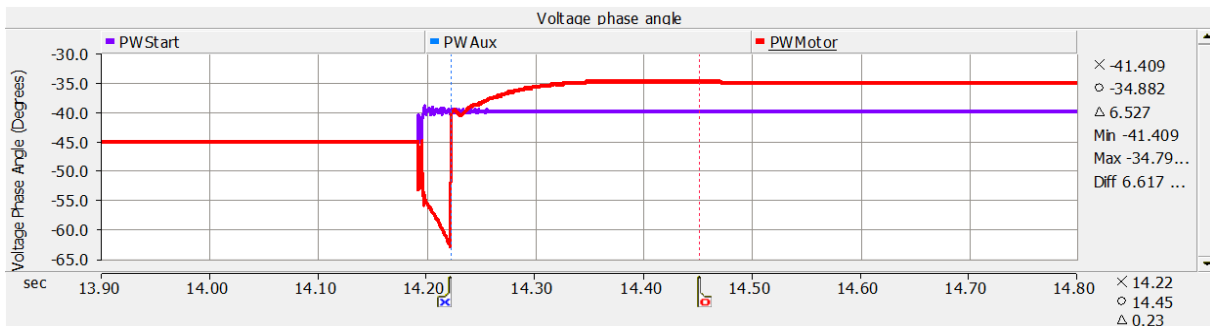


Figure 6-94 Phase A voltage phase angle in degrees during a manual transfer test, initiated at  $t=14.1312$  sec.

The timing logic for the motor bus transfer system elements and circuit breaker contact operations is shown in Figure 6-95, where:

RTrip	Element activated by manual transfer, relay trip, and test mode initialization time
FTSMTP	Fast transfer trip element
IPSMTP	In-phase transfer trip element
RVSMTP	Residual voltage transfer trip element
S->A	Element to enable bus transfer from start-up to auxiliary system
A->S	Element to enable bus transfer from auxiliary to start-up system
BKStart	Start-up side breaker
BKAux	Auxiliary side breaker

Before the transfer initialization, the elements RTrip, FTSMTP, IPSMTP, RVSMTP were enabled; elements S->A (motor bus transfer from start-up source to auxiliary source) was enabled and A->S



(motor bus transfer from auxiliary source to start-up source) was disabled; BKStart was closed and BKAux was open.

When the manual transfer control switch was manually changed from 0 to 1 the simulation time was  $t = 14.1312$  seconds, and instantaneously the RTrip element tripped and the fast transfer trip element FTSMTMP also tripped, with both element RTrip and FTSMTMP tripped, the breakers BKStart and BKAux started their opening and closing operations respectively. Breaker BKStart opened 58 milliseconds after receiving the tripping signal and at that moment, the element S->A changed its status from enabled to disabled. Breaker BKAux closed 90 milliseconds after receiving the closing signal and the element A->S changed its status from disabled to enabled. The transfer was finally accomplished at  $t = 14.2218$  seconds.

The in-phase trip element IPSMTMP and the residual voltage trip element RVSMTP did not operate as it was expected.

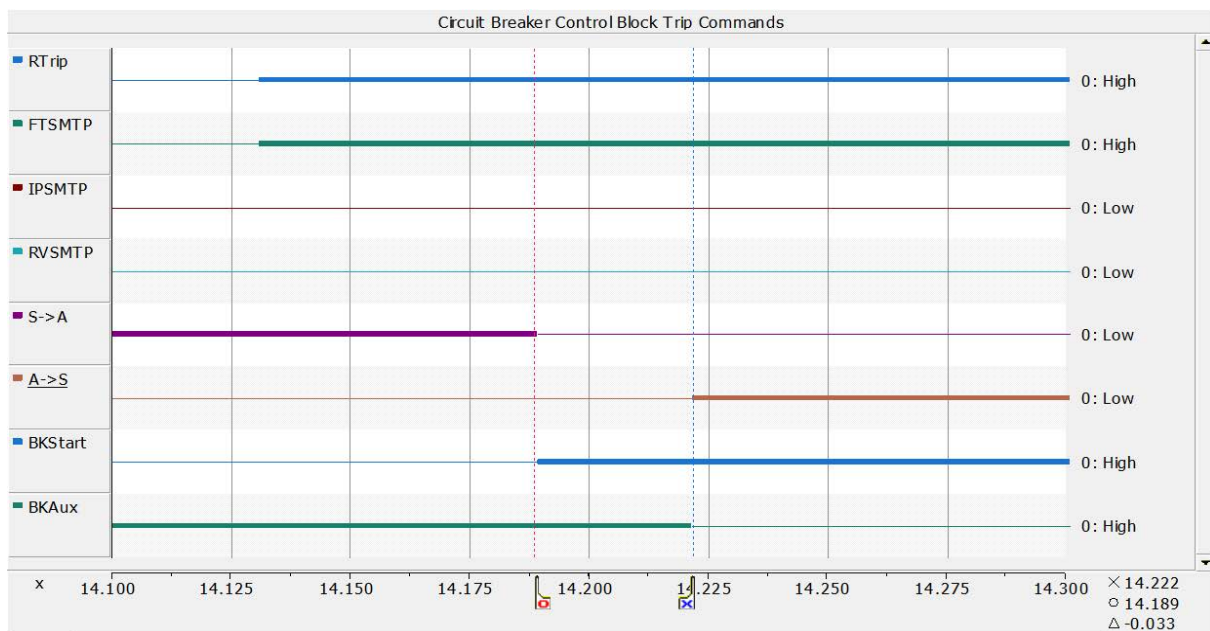


Figure 6-95 Motor bus transfer system element and circuit breaker contact operations during a manual transfer test, initiated at  $t = 14.1312$  sec.

The logic timing of the motor bus transfer system elements and circuit breaker contacts operated correctly.

### 6.3.2 Manual Transfer from Auxiliary System to Start-up System

This section shows the results of the manual transfer test when transferring the motor bus from the auxiliary to the start-up system.

The motor bus transfer system controls used for this test are shown in Figure 6-96. Control SysSel was set to position AWS (transfer simulation from the auxiliary to start-up system), transfer initialization time MTime set to 99 seconds (this control is used only when fast, in-phase or residual voltage algorithms are tested individually), TType was set to 4 (fast transfer, in-phase and residual voltage algorithms were enabled). Control Coast Down was set to off, control Coast Down Time was set to 99 seconds (coast down simulating motors spinning down in group was not performed), Ind Coast Down Time was set to 99 seconds (coast down simulating motors spinning individually was not performed). The manual transfer was initiated when the switch button MTransfer was changed from 0 to 1 at  $t=14.1042$  seconds, which was therefore the transfer initiation time.

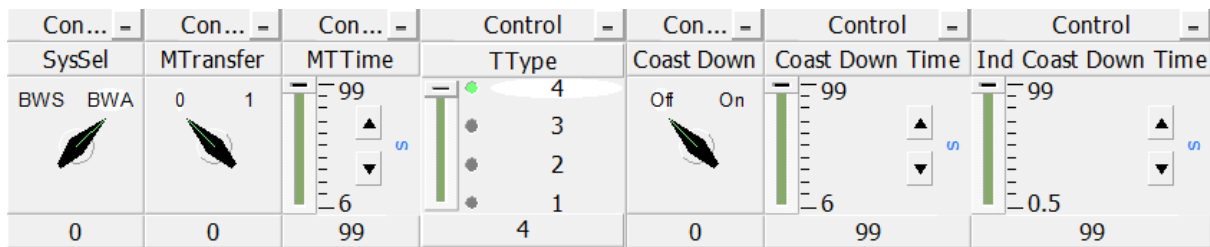


Figure 6-96 Motor bus transfer system controls for a manual transfer test, initiated at  $t=14.1042$  sec.

The auxiliary breaker opened at  $t=14.16782$  seconds (phase A current was interrupted at  $t=14.16782$ s, phase C current at  $t=14.16427$  s and phase B current at  $t=14.16782$  s.). The transfer was accomplished at  $t=14.1948$  seconds when the start-up breaker closed, approximately 90 milliseconds after the transfer initiation.

Figure 6-97 shows the phase A instantaneous voltage of the start-up (purple plot), auxiliary (light blue plot) and motor bus (red plot) during a manual transfer test. The start-up voltage magnitude before the transfer initiation was 4.309 kV L-L and after the bus transfer the voltage magnitude was 4.122 kV. The auxiliary voltage before the transfer initiation was 4.1932 kV and after the bus transfer it was 4.343 kV. During the loss of power supply, the motor bus voltage magnitude decayed to 3.744 kV.

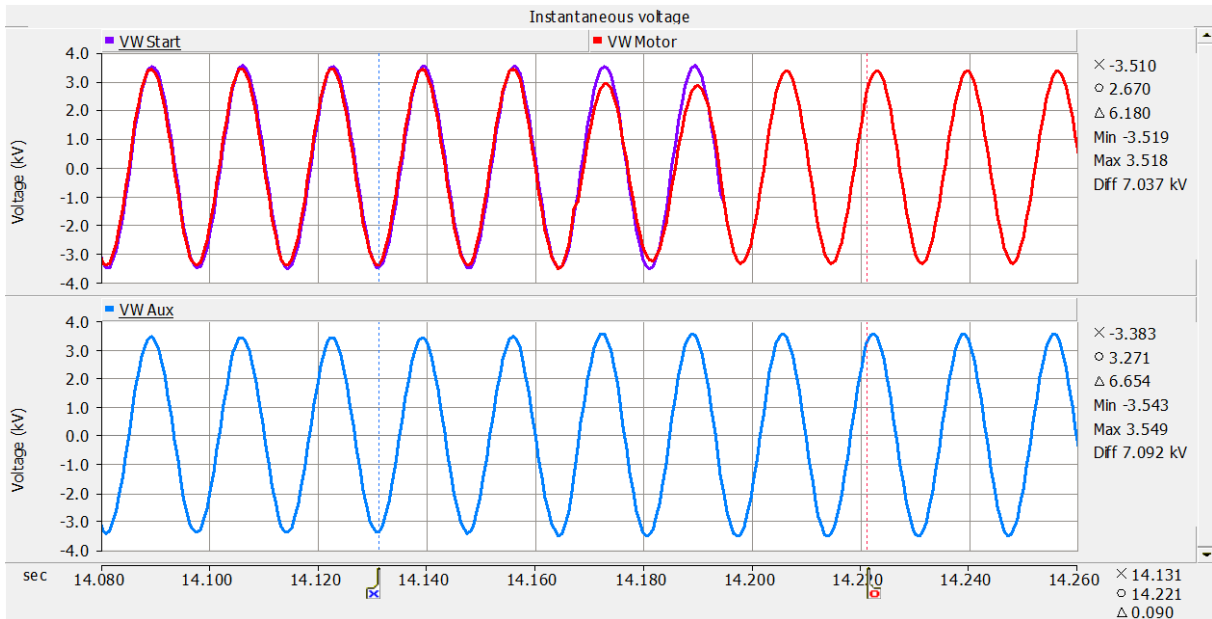


Figure 6-97 Phase A Instantaneous voltage in kV during a manual transfer test, initiated at t=14.1042 sec.

Figure 6-98 shows the per unit phase A RMS voltage of the start-up (purple plot), auxiliary (light blue plot) and motor bus (red plot) during the fast transfer test mode. The start-up voltage magnitude changed from 1.036 p.u. (in a reference of 4.16 kV L-L) before the bus transfer to 0.991 p.u. after the bus transfer. The auxiliary medium voltage side voltage magnitude before the bus transfer was 1.008 p.u. and after the transfer was 1.044 p.u.

When the auxiliary breaker opened, the motor bus voltage magnitude decayed to 0.9 p.u. The motor bus voltage took 410 milliseconds to recover once the motor bus was reconnected from the auxiliary source.

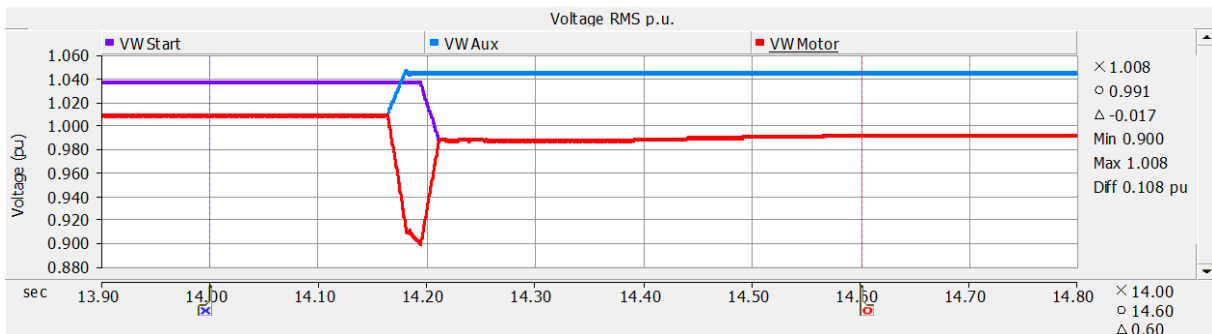


Figure 6-98 Phase A RMS voltage in per unit during a manual transfer test, initiated at t=14.1042 sec.

Figure 6-99 shows the voltage frequency of the start-up (purple plot), auxiliary (light blue plot) and motor bus (red plot) during the fast transfer test mode. The motor bus voltage frequency decayed to 58.319 Hz on loss of power supply. When the auxiliary breaker closed, the motor bus frequency increased to 60.764 Hz and then decayed during 410 milliseconds to settle in 60 Hz.

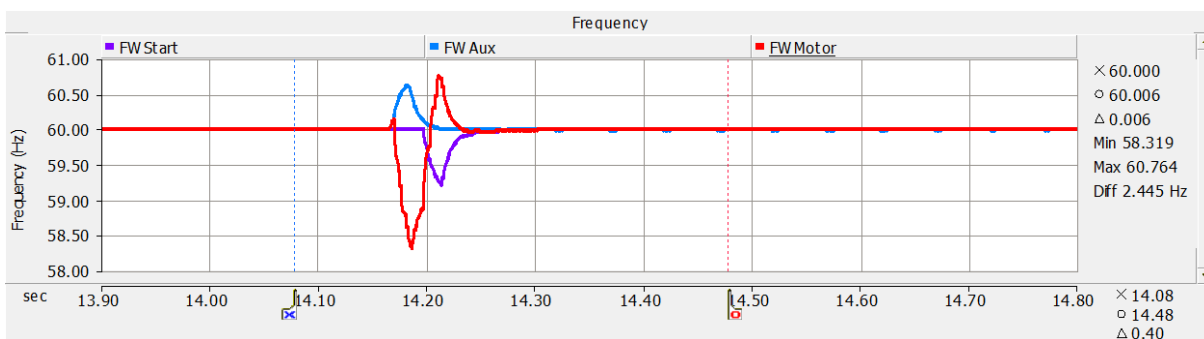


Figure 6-99 Voltage frequency in Hertz during a manual transfer test, initiated at  $t=14.1042$  sec.

Figure 6-100 shows the voltage phase A angle of the start-up (purple plot), auxiliary (light blue plot) and motor bus (red plot) during the fast transfer test mode. The start-up phase A voltage phase angle before the transfer was -39.84 degrees and after the transfer was -45.23 degrees. The auxiliary phase A voltage phase angle changed from -35.05 degrees before the bus transfer to -30.7 degrees after the transfer. During the bus transfer, the motor bus phase A voltage phase angle decayed to -52.54 degrees.

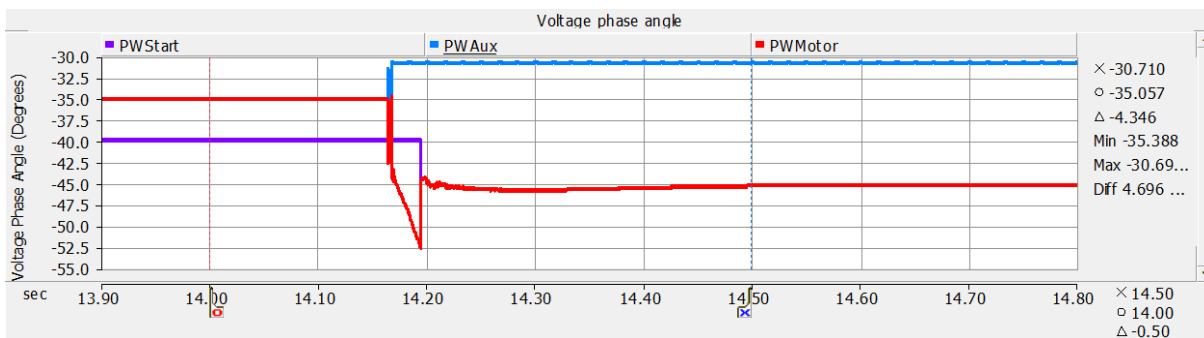


Figure 6-100 Phase A voltage phase angle in degrees during a manual transfer test, initiated at  $t=14.1042$  sec.

The timing logic for the motor bus transfer system elements and circuit breaker contact operations is shown in Figure 6-101, where:

RTrip	Element activated by manual transfer, relay trip, and test mode initialization time
FTSMTP	Fast transfer trip element
IPSMTP	In-phase transfer trip element
RVSMTP	Residual voltage transfer trip element
S->A	Element to enable bus transfer from start-up to auxiliary system
A->S	Element to enable bus transfer from auxiliary to start-up system
BKStart	Start-up side breaker
BKAux	Auxiliary side breaker

Before the transfer initialization, the elements RTrip, FTSMTP, IPSMTP, RVSMTP were enabled; elements S->A (motor bus transfer from start-up source to auxiliary source) was disabled and A->S (motor bus transfer from auxiliary source to start-up source) was enabled; BKStart was open and BKAux was closed.

When the manual transfer control switch was manually changed from 0 to 1 the simulation time was  $t = 14.1042$  seconds, and instantaneously the RTrip element and the fast transfer trip element FTSMTP tripped. With both elements tripped, the breakers BKStart and BKAux started their closing and opening operations respectively. Breaker BKAux opened 58 milliseconds after receiving the tripping signal and at that moment, the element A->S changed its status from enabled to disabled. Breaker BKStart closed

90 milliseconds after receiving the closing signal and the element S->A changed its status from disabled to enabled. The transfer was finally accomplished at t= 14.1948 seconds.

The in-phase trip element IPSMTP and the residual voltage trip element RVSMTP did not operate as it was expected.

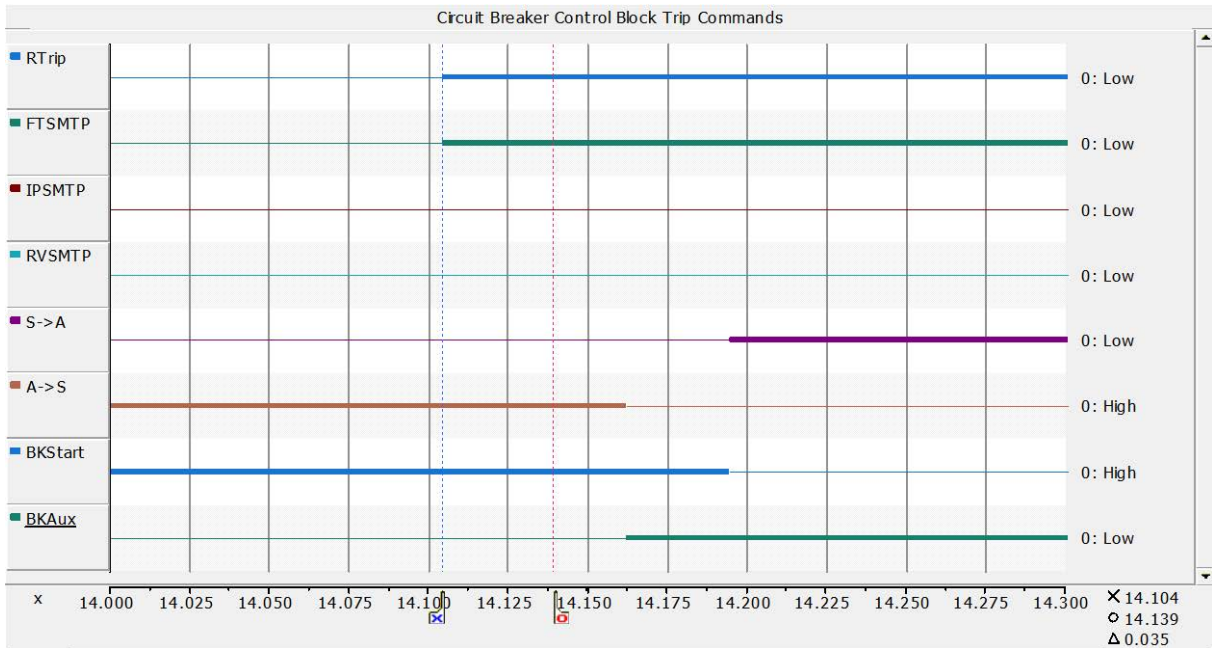


Figure 6-101 Motor bus transfer system element and circuit breaker contact operations during a manual transfer test, initiated at t=14.1042 sec.

The logic timing of the motor bus transfer system elements and circuit breaker contacts operated correctly.

## 6.4 Automatic Transfer

### 6.4.1 Automatic Transfer Initiated by the Auxiliary Transformer Differential Protective Relay

In order to test the transfer model in automatic mode, three tests were performed, the one described in this section is the automatic transfer initiated by the operation of the auxiliary transformer differential protection relay under a phase-to-ground A-G fault initiated at  $t=14.0$  seconds.

The motor bus transfer system controls used for this test are shown in Figure 6-102. Control SysSel was set to position AWS (transfer simulation from the auxiliary to start-up system), transfer initialization time MTime set to 99 seconds (this control is used only when fast, in-phase or residual voltage algorithms are tested individually), TType was set to 4 (fast transfer, in-phase and residual voltage algorithms were enabled). Control Coast Down was set to off, control Coast Down Time was set to 99 seconds (coast down simulating motors spinning down in group was not performed), Ind Coast Down Time was set to 99 seconds (coast down simulating motors spinning individually was not performed).

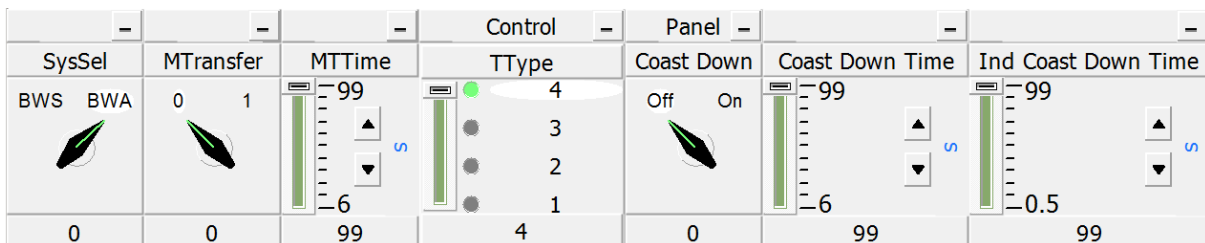


Figure 6-102 Motor bus transfer system controls for the automatic transfer

The auxiliary breaker opened at  $t=14.0616$  seconds (phase A current was interrupted at  $t=14.06123$  s, phase B and C currents at  $t=14.06529$  s). The transfer was accomplished at  $t=14.0935$  seconds when the auxiliary breaker closed, 90 milliseconds after the motor bus transfer process unit fast transfer element tripped.

Figure 6-103 shows the phase A instantaneous voltage of the auxiliary bus (light blue plot), start-up bus (purple plot) and motor bus (red plot) during the automatic transfer initiated by the auxiliary transformer differential protective relay. The auxiliary voltage magnitude before the fault initiation was 4.1932 kV and after the fault duration and bus transfer it was 4.343 kV. The start-up voltage

magnitude before the fault initiation was 4.309 kV L-L and after the fault duration and bus transfer the voltage magnitude was 4.1225 kV. During the loss of power supply, the motor bus voltage magnitude decayed to 3.6067 kV.

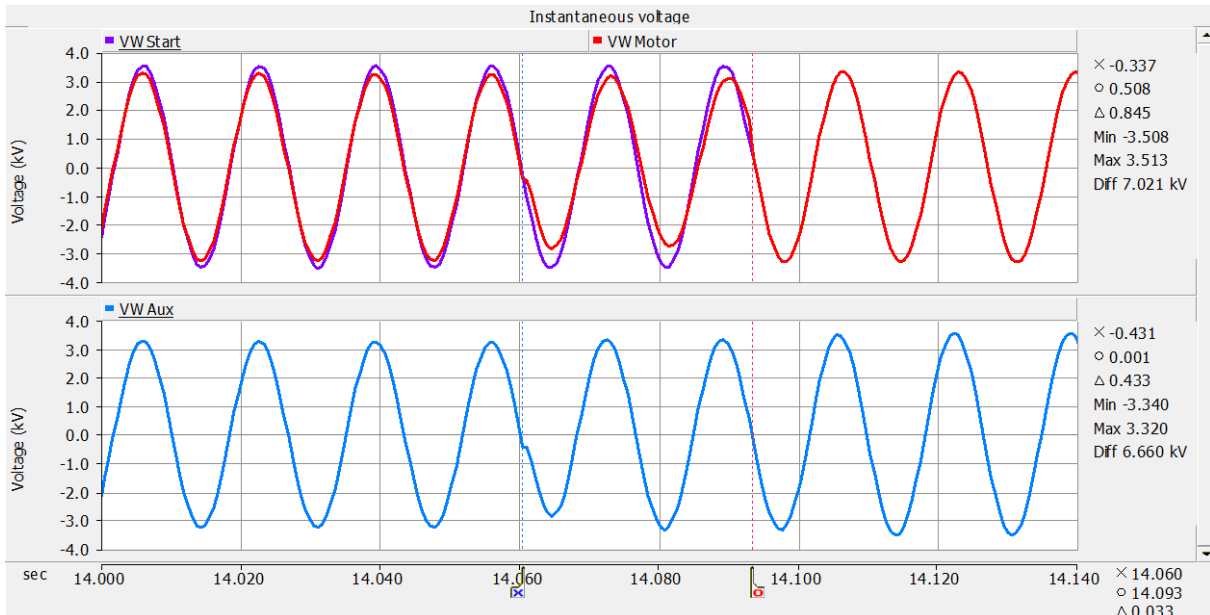


Figure 6-103 Phase A Instantaneous voltage in kV during an automatic transfer initiated by the auxiliary transformer differential protective relay operation under a phase-to-ground C-G fault initiated at  $t=14.000$  seconds

Figure 6-104 shows the per unit phase A RMS voltage of the auxiliary bus (light blue plot), start-up bus (purple plot) and motor bus (red plot) during the automatic transfer initiated by the auxiliary transformer differential protective relay. The auxiliary voltage magnitude changed from 1.008 p.u. (in a reference of 4.16 kV L-L) before the fault to 0.978 p.u. during the fault and then to 0.949 p.u. when the auxiliary breaker opened, finally after the bus transfer the voltage magnitude changed to 1.044 p.u. The start-up medium voltage side voltage magnitude before the fault was 1.036 p.u. and after the fault duration and bus transfer was 0.991 p.u. The motor bus voltage decayed to 0.867 during the loss of power supply.

The motor bus voltage magnitude took 510 milliseconds to recover once the motor bus was reconnected to the auxiliary source.



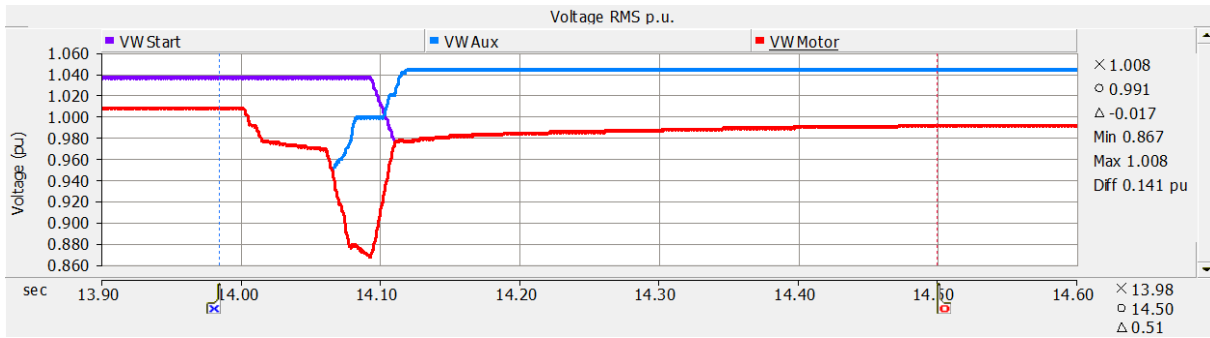


Figure 6-104 Phase A RMS voltage in per unit during an automatic transfer initiated by the auxiliary transformer differential protective relay operation under a phase-to-ground C-G fault initiated at  $t=14.000$  seconds

Figure 6-105 shows the frequencies of the auxiliary bus (light blue plot), start-up bus (purple plot) and motor bus (red plot) during the automatic transfer initiated by the auxiliary transformer differential protective relay. The motor bus voltage frequency decayed to 58.259 Hz right after the loss of power supply. When the start-up breaker closed, the motor bus frequency increased to 60.706 Hz and then decayed during 510 milliseconds to settle in 60 Hz.

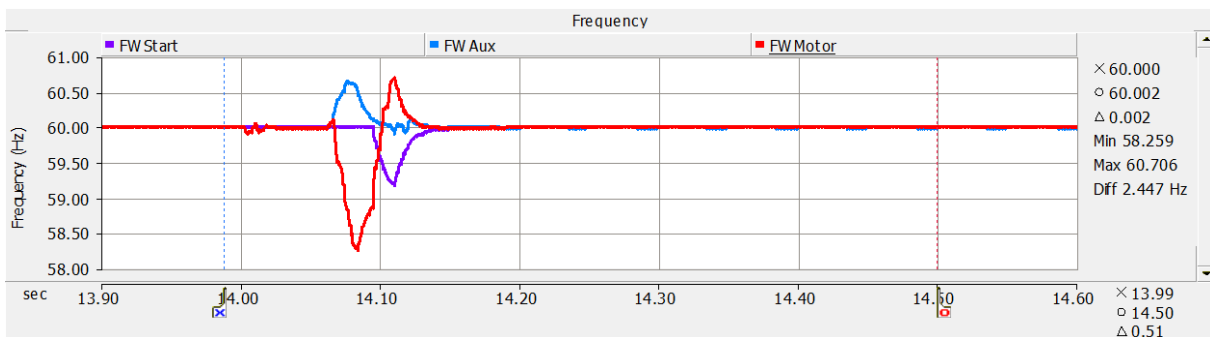


Figure 6-105 Frequency in Hertz during an automatic transfer initiated by the auxiliary transformer differential protective relay operation under a phase-to-ground C-G fault initiated at  $t=14.000$  seconds

Figure 6-106 shows the voltage phase A angle of the auxiliary bus (light blue plot), start-up bus (purple plot) and motor bus (red plot) during the automatic transfer initiated by the auxiliary transformer differential protective relay operation. The start-up phase A voltage phase angle before the fault initiation was 39.84 degrees and after the fault duration and motor bus transfer it was -45.15 degrees. The auxiliary phase A voltage phase angle changed from -35.05 degrees before the fault initiation to -30.8 degrees after the fault duration and bus transfer. During the bus transfer, the motor bus phase A voltage phase angle decayed to -54.18 degrees.

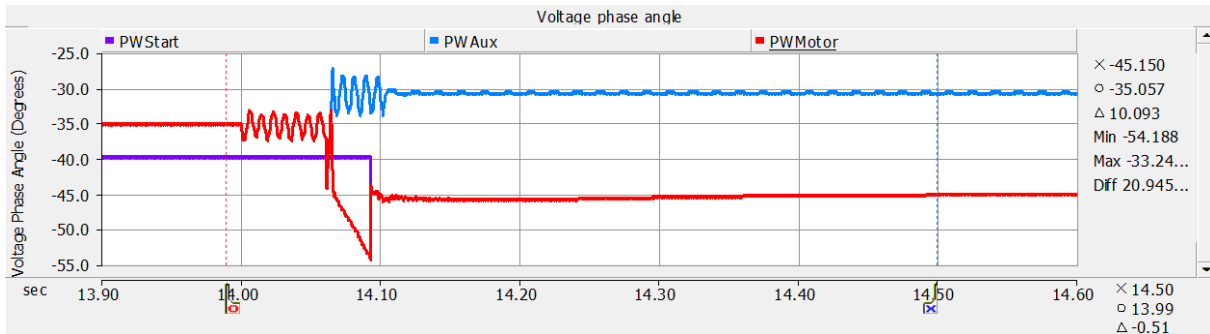


Figure 6-106 Phase A Voltage phase angle in degrees during an automatic transfer initiated by the auxiliary transformer differential protective relay operation under a phase-to-ground C-G fault initiated at  $t=14.000$  seconds

The timing logic for the motor bus transfer system elements and circuit breakers contact operations is shown in Figure 6-107, where:

21East	Eastern transmission line distance relay trip element
87Aux	Auxiliary transformer differential relay trip element
27MB	Motor bus undervoltage relay trip element
RTrip	Element activated by manual transfer, relay trip, and test mode initialization time
FTSMTP	Fast transfer trip element
IPSMTP	In-phase transfer trip element
RVSMTP	Residual voltage transfer trip element
S->A	Element to enable bus transfer from start-up to auxiliary system
A->S	Element to enable bus transfer from auxiliary to start-up system

BKStart      Start-up side breaker

BKAux        Auxiliary side breaker

Before the transfer initialization, the elements RTrip, FTSMTP, IPSMTP and RVSMTP were enabled, elements S->A (motor bus transfer from start-up source to auxiliary source) was disabled and A->S (motor bus transfer from auxiliary to start-up source) was enabled; BKStart was open and BKAux was closed.

When the auxiliary transformer differential relay 87Aux tripped at  $t= 14.0035$  seconds, it sent the trip command to the element RTrip and immediately the tripping signal was sent to the auxiliary breaker BKAux which opened at  $t= 14.0616$  seconds and the element A->S changed its status from enabled to disabled. The MBTS fast transfer element FTSMTP also tripped at  $t=14.0035$  seconds and the closing signal was sent to the start-up breaker BKStart which closed 90 milliseconds after receiving the closing signal, and the element S->A changed its status from disabled to enabled. The transfer was finally accomplished at  $t= 14.0035$  seconds. Elements 21East and 27MB did not operate as was expected.

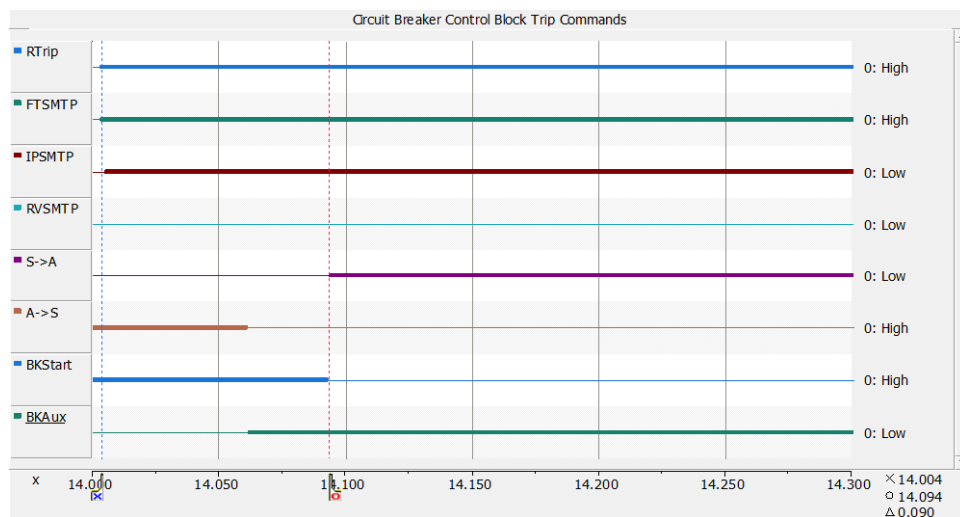


Figure 6-107 Motor bus transfer system element and circuit breaker contact operations during an automatic transfer initiated by the auxiliary transformer differential protective relay operation under a phase-to-ground C-G fault initiated at  $t=14.000$  seconds

The logic timing of the motor bus transfer system elements and circuit breaker contacts operated correctly.

#### 6.4.2 Automatic Transfer Initiated by a Transmission Line Impedance Protective Relay

This section describes the behavior and performance of the motor bus transfer system when initiated by the operation of the Eastern transmission line impedance protective relay under a phase-to-phase-to-ground, BC-G, fault initiated at  $t = 14.0$  seconds.

The motor bus transfer system controls used for this test are shown in Figure 6-108. Control SysSel was set to position AWS (transfer simulation from the auxiliary to start-up system), transfer initialization time MTime set to 99 seconds (this control is used only when fast, in-phase or residual voltage algorithms are tested individually), TType was set to 4 (fast transfer, in-phase and residual voltage algorithms were enabled). Control Coast Down was set to off, control Coast Down Time was set to 99 seconds (coast down simulating motors spinning down in group was not performed), Ind Coast Down Time was set to 99 seconds (coast down simulating motors spinning individually was not performed).

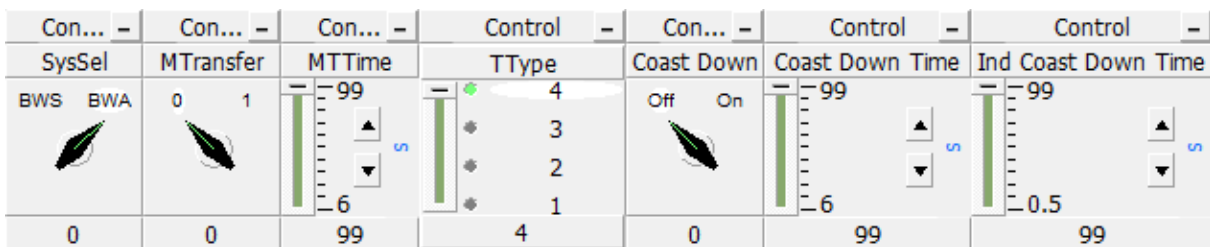


Figure 6-108 Motor bus transfer system controls for the automatic transfer

The auxiliary breaker opened at  $t = 14.0696$  seconds (phase A and B currents were interrupted at  $t = 14.07611$  s, phase C current at  $t = 14.07205$  s). The transfer was accomplished at  $t = 14.1016$  seconds when the auxiliary breaker closed, 90 milliseconds after the motor bus transfer process unit fast transfer element tripped.

Figure 6-109 shows the phase A instantaneous voltage of the auxiliary (light blue plot), start-up (purple plot) and motor buses (red plot) during the automatic transfer initiated by the Eastern transmission line impedance relay. The auxiliary voltage magnitude before the fault initiation was 4.1932 kV and after the fault duration and bus transfer, it was 4.3555 kV. The start-up voltage magnitude before the fault initiation was 4.309 kV L-L and after the fault duration and bus transfer the voltage magnitude

was 4.1225 kV. During the loss of power supply, the motor bus voltage magnitude decayed to 3.6691 kV.

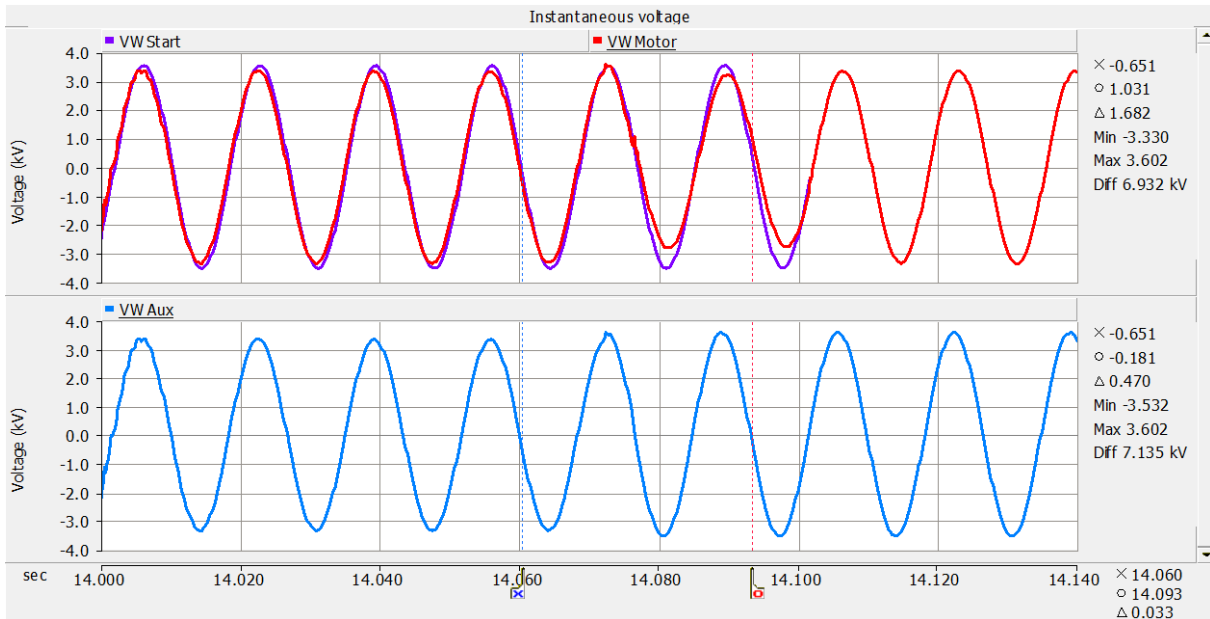


Figure 6-109 Phase A instantaneous voltage in kV during an automatic transfer initiated by the Eastern transmission line impedance protective relay operation under a phase-to-phase BC fault initiated at  $t=14.000$  seconds

Figure 6-110 shows the per unit phase A RMS voltage in per unit of the auxiliary bus (light blue plot), start-up bus (purple plot) and motor bus (red plot) during the automatic transfer initiated by the Eastern transmission line impedance relay. The auxiliary voltage magnitude changed from 1.008 p.u. (in a reference of 4.16 kV L-L) before the fault to 0.99 p.u. during the fault and then to 0.9846 p.u. when the auxiliary breaker opened. Finally, after the bus transfer the voltage magnitude changed to 1.047 p.u. The start-up medium voltage side voltage magnitude before the fault was 1.036 p.u. and after the fault duration and bus transfer was 0.991 p.u.

The motor bus voltage magnitude took 400 milliseconds to recover once the motor bus was reconnected from the auxiliary source.

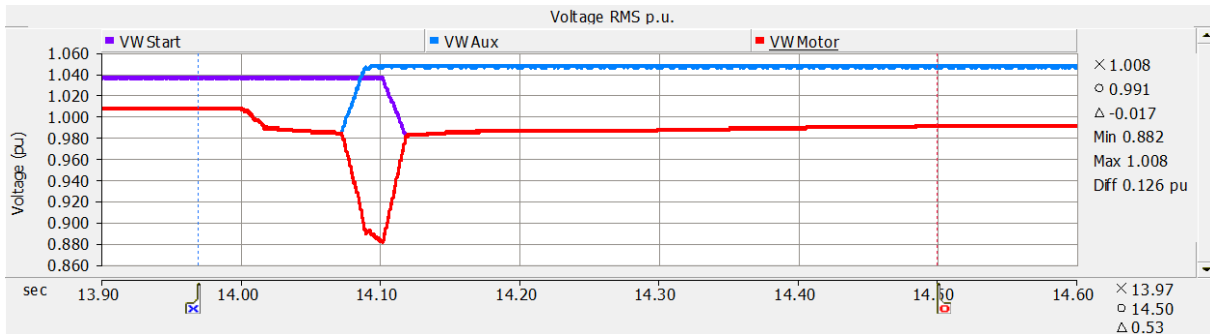


Figure 6-110 Phase A RMS voltage in per unit during an automatic transfer initiated by the Eastern transmission line impedance protective relay operation under a phase-to-phase BC fault initiated at  $t=14.000$  seconds

Figure 6-111 shows the voltage frequency of the auxiliary bus (light blue plot), start-up bus (purple plot) and motor bus (red plot) during the automatic transfer initiated by the Eastern transmission line impedance relay. The motor bus voltage frequency decayed to 58.295 Hz immediately after the loss of power supply. When the auxiliary breaker closed, the motor bus frequency increased to 60.807 Hz and then, it decayed during 400 milliseconds to settle in 60 Hz.

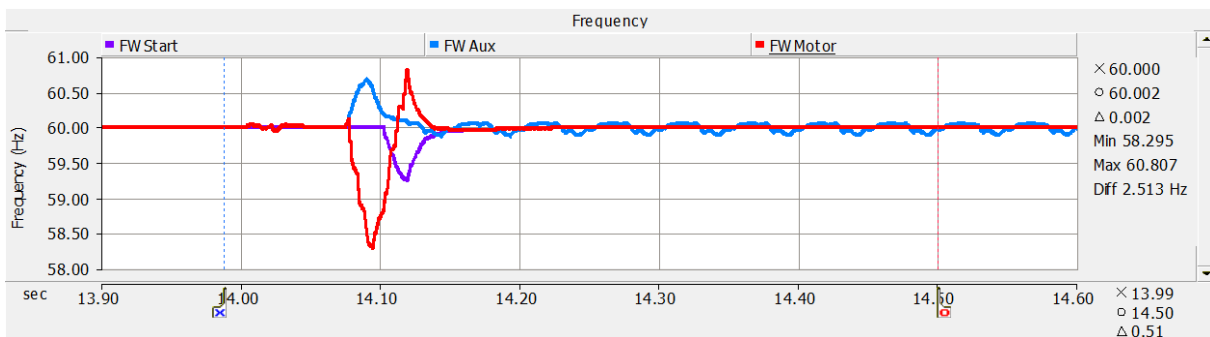


Figure 6-111 Voltage frequency in Hertz during an automatic transfer initiated by the Eastern transmission line impedance protective relay operation under a phase-to-phase BC fault initiated at  $t=14.000$  seconds

Figure 6-112 shows the voltage phase A angle of the auxiliary bus (light blue plot), start-up bus (purple plot) and motor bus (red plot) during the automatic transfer initiated by the Eastern transmission line impedance relay operation under a phase-to-phase BC fault initiated at  $t=14$  seconds. The start-up phase A voltage phase angle before the fault initiation was  $-39.84$  degrees and after the fault duration and motor bus transfer was  $-45.148$  degrees. The auxiliary phase A voltage phase angle changed from  $-35.05$  degrees before the fault initiation to  $-30.16$  degrees after the fault duration and bus transfer. During the bus transfer, the motor bus phase A voltage phase angle decayed to  $-52.21$  degrees.

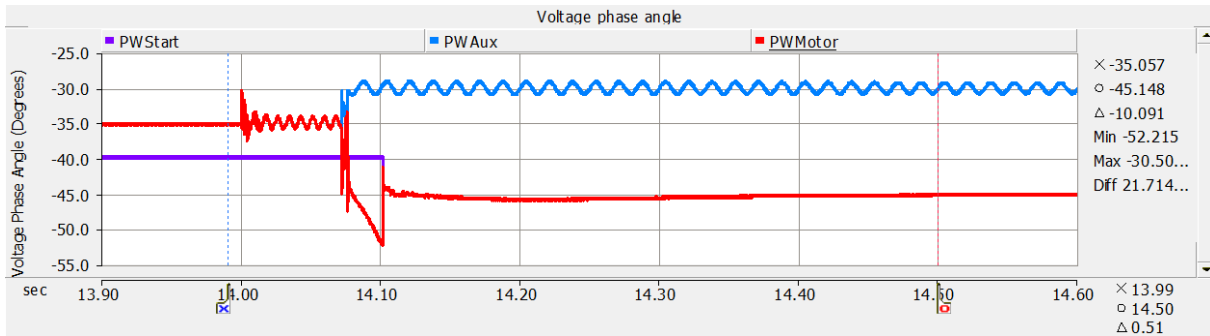


Figure 6-112 Phase A Voltage phase angle in degrees during an automatic transfer initiated by the Eastern transmission line impedance protective relay operation under a phase-to-phase BC fault initiated at  $t=14.000$  seconds

The timing logic for the motor bus transfer system elements and circuit breakers contact operations are shown in Figure 6-113, where:

21East	Eastern transmission line distance relay trip element
87Aux	Auxiliary transformer differential relay trip element
27MB	Motor bus undervoltage relay trip element
RTrip	Element activated by manual transfer, relay trip, and test mode initialization time
FTSMTP	Fast transfer trip element
IPSMTP	In-phase transfer trip element
RVSMTMP	Residual voltage transfer trip element
S->A	Element to enable bus transfer from start-up to auxiliary system
A->S	Element to enable bus transfer from auxiliary to start-up system

BKStart      Start-up side breaker

BKAux        Auxiliary side breaker

Before the transfer initialization, the elements 21East, 87Aux, 27MB, RTrip, FTSMT, IPSMT and RVSMT, were enabled, elements S->A (motor bus transfer from start-up source to auxiliary source) was disabled and A->S (motor bus transfer from auxiliary source to start-up source) was enabled; BKStart was open and BKAux was closed.

When the impedance relay 21East tripped at  $t= 14.0116$  seconds it sent the trip command to the element RTrip and immediately the tripping signal was sent to the auxiliary breaker BKAux which opened at  $t= 14.0696$  seconds and the element A->S changed its status from enabled to disabled. The MBTS fast transfer element FTSMT also tripped at  $t=14.0116$  seconds and the closing signal was sent to the start-up breaker BKStart which closed 90 milliseconds after receiving the closing signal, and the element S->A changed its status from disabled to enabled. The transfer was finally accomplished at  $t= 14.1016$  seconds. Elements 87Aux and 27MB did not operate as it was expected.

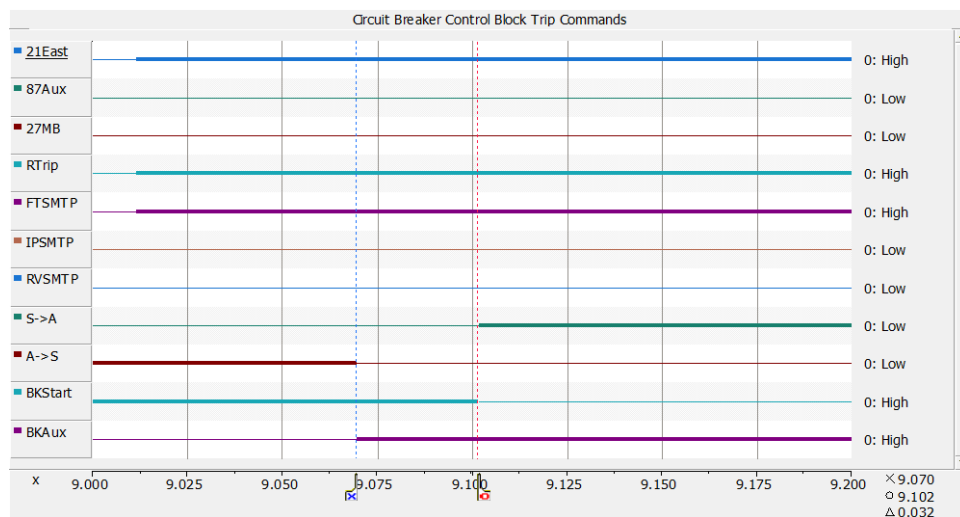


Figure 6-113 Motor bus transfer system element and circuit breaker contact operations during an automatic transfer initiated by the Eastern transmission line impedance protective relay operation under a phase-to-phase BC fault initiated at  $t=14.000$  seconds

The logic timing of the motor bus transfer system elements and circuit breaker contacts operated correctly.



### 6.4.3 Automatic Transfer Initiated by Motor Bus Undervoltage Conditions

This section describes the behavior and performance of the motor bus transfer system initiated by the operation of the motor bus under voltage relay under a low voltage condition initiated at  $t = 14.0$  seconds.

The motor bus transfer system controls used for this test are shown in Figure 6-114. Control SysSel was set to position AWS (transfer simulation from the auxiliary to start-up system), transfer initialization time MTime set to 99 seconds (this control is used only when fast, in-phase or residual voltage algorithms are tested individually), TType was set to 4 (fast transfer, in-phase and residual voltage algorithms were enabled). Control Coast Down was set to off, control Coast Down Time was set to 99 seconds (coast down simulating motors spinning down in group was not performed), Ind Coast Down Time was set to 99 seconds (coast down simulating motors spinning individually was not performed).

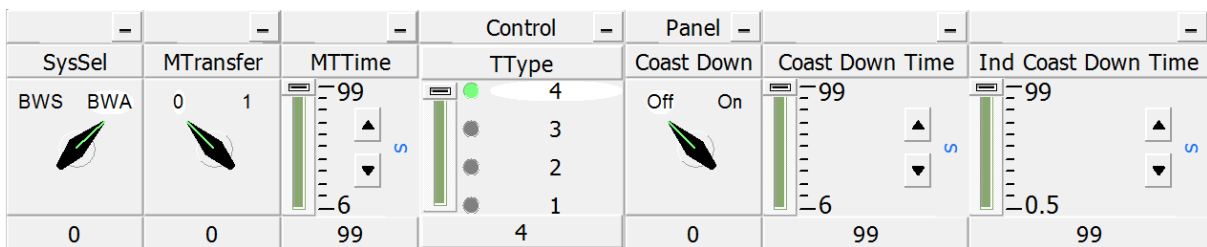


Figure 6-114 Motor bus transfer system controls for the automatic transfer

The auxiliary breaker opened at  $t = 14.0696$  seconds (phase A and phase B currents were interrupted at  $t = 14.07543$  s, phase C current at  $t = 14.07104$  s.). The transfer was accomplished at  $t = 14.1016$  seconds when the start-up breaker closed, 90 milliseconds after the motor bus transfer process unit fast transfer element tripped.

Figure 6-115 shows the phase A instantaneous voltage of the auxiliary bus (light blue plot), start-up bus (purple plot) and motor bus (red plot) during the automatic transfer initiated by the motor bus under voltage relay. The start-up voltage magnitude before the fault initiation was 4.309 kV L-L and after the fault duration and bus transfer the voltage magnitude was 4.1184 kV. The auxiliary voltage magnitude before the bus transfer initiation was 4.1932 kV, and it was 3.477 kV at the moment the

start-up breaker closed. During the loss of power supply, the motor bus voltage magnitude decayed to 3.2489 kV.

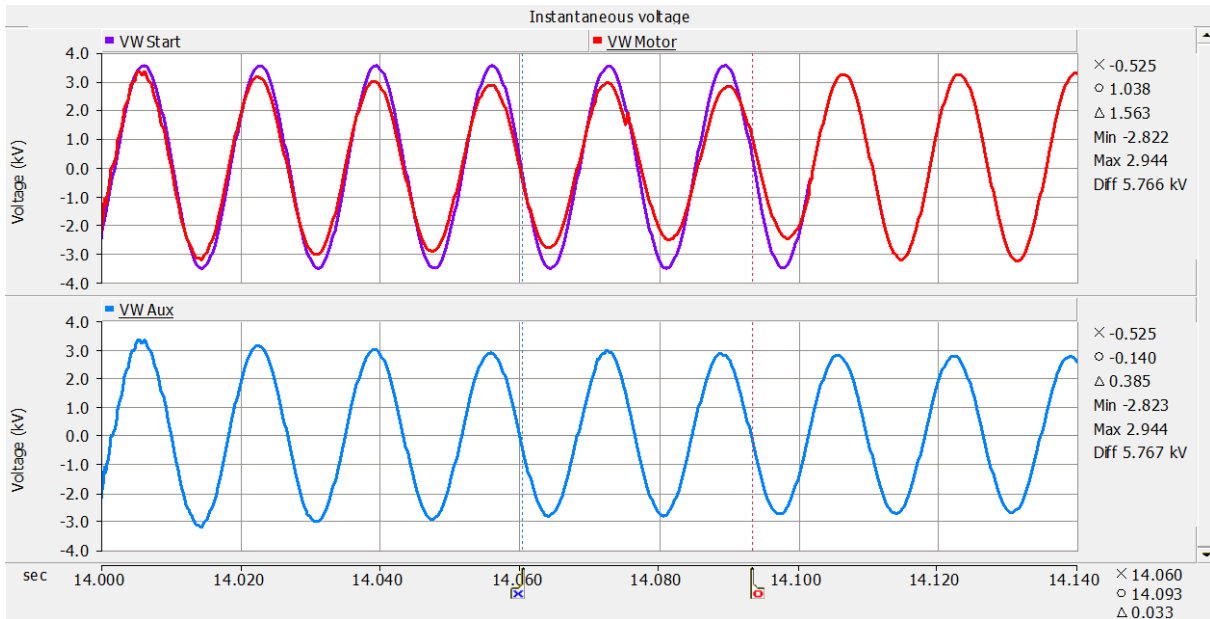


Figure 6-115 Phase A instantaneous voltage in kV during an automatic transfer initiated by the Eastern transmission line impedance protective relay operation under a phase-to-phase BC fault initiated at t=14.000 seconds

Figure 6-116 shows the per unit phase A RMS voltage in per unit of the auxiliary bus (light blue plot), start-up bus (purple plot) and motor bus (red plot) during the automatic transfer initiated by the motor bus under voltage relay. The auxiliary voltage magnitude was decaying from 1.008 p.u. (in a reference of 4.16 kV L-L) before the low voltage condition to 0.836 p.u when the auxiliary breaker opened. The start-up medium voltage side voltage magnitude before the undervoltage condition was 1.036 p.u. and after the fault duration and bus transfer was 0.99 p.u.

The motor bus voltage took 400 milliseconds to recover once the motor bus was reconnected from the auxiliary source.

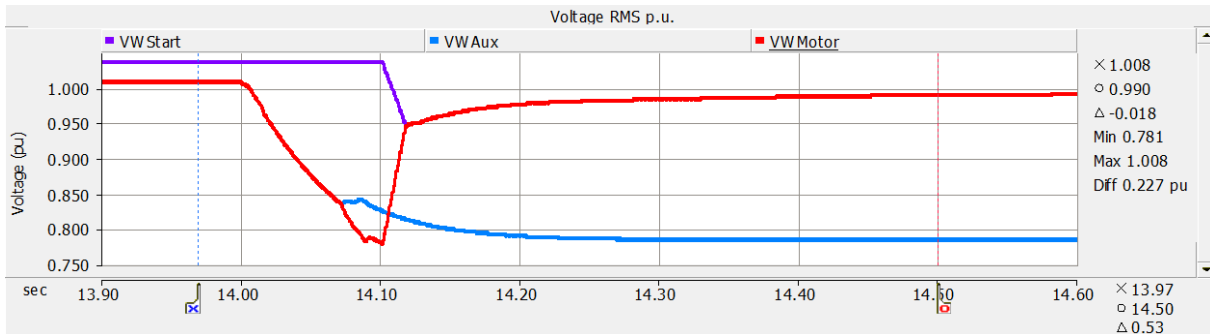


Figure 6-116 Phase A RMS voltage in per unit during an automatic transfer initiated by the Eastern transmission line impedance protective relay operation under a phase-to-phase BC fault initiated at  $t=14.000$  seconds

Figure 6-117 shows the voltage frequency of the auxiliary bus (light blue plot), start-up bus (purple plot) and motor bus (red plot) during the automatic transfer initiated by the motor bus under voltage relay. The motor bus voltage frequency decayed to 58.347 Hz right after the loss of power supply. When the auxiliary breaker closed, the motor bus frequency increased to 61.214 Hz and then decayed during 400 milliseconds to settle in 60 Hz.

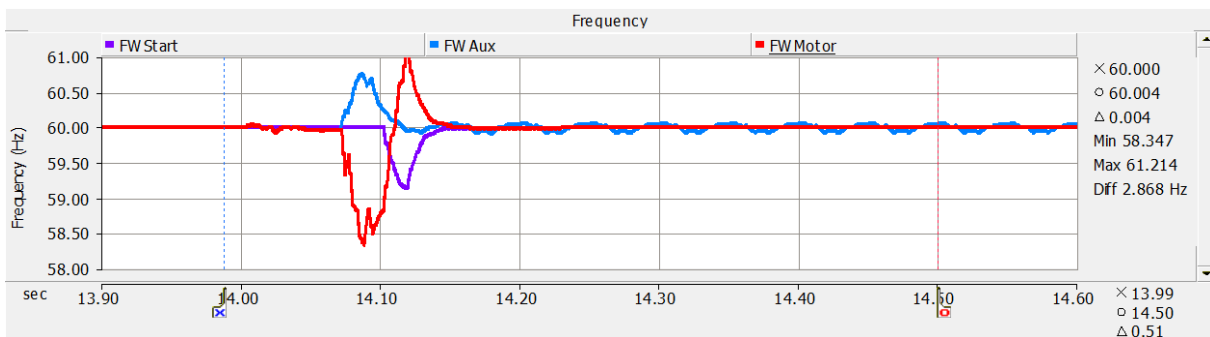


Figure 6-117 Voltage frequency in Hertz during an automatic transfer initiated by the Eastern transmission line impedance protective relay operation under a phase-to-phase BC fault initiated at  $t=14.000$  seconds

Figure 6-118 shows the voltage phase A angle of the auxiliary bus (light blue plot), start-up bus (purple plot) and motor bus (red plot) during the automatic transfer initiated by the motor bus under voltage relay. The start-up phase A voltage phase angle before the fault initiation was -39.84 degrees and after the motor bus transfer was -45.211 degrees. The auxiliary phase A voltage phase angle changed from -35.05 degrees before the fault initiation to -30.05 degrees after the bus transfer. During the bus transfer, the motor bus phase A voltage phase angle decayed to -55.857 degrees.

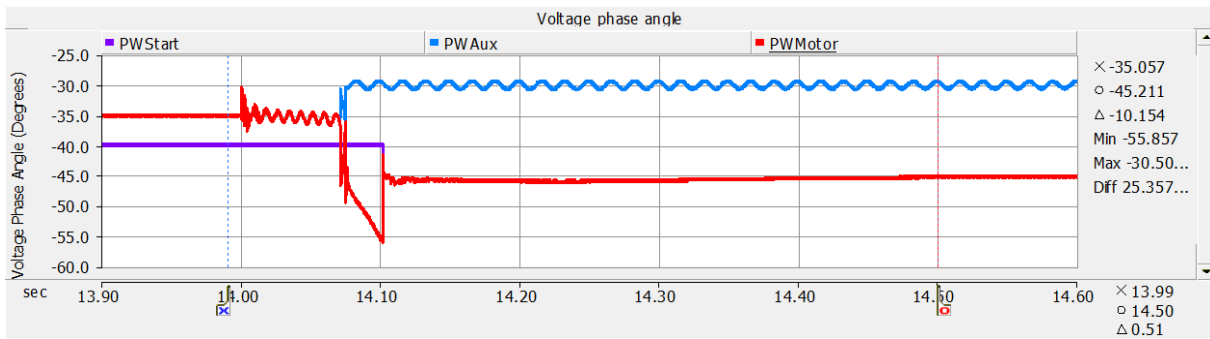


Figure 6-118 Phase A Voltage phase angle in degrees during an automatic transfer initiated by the Eastern transmission line impedance protective relay operation under a phase-to-phase BC fault initiated at  $t=14.000$  seconds

The timing logic response for the motor bus transfer system elements and circuit breakers contact operations are shown in Figure 6-113, where:

21East	Eastern transmission line distance relay trip element
87Aux	Auxiliary transformer differential relay trip element
27MB	Motor bus undervoltage relay trip element
RTrip	Element activated by manual transfer, relay trip, and test mode initialization time
FTSMTP	Fast transfer trip element
IPSMTP	In-phase transfer trip element
RVSMTMP	Residual voltage transfer trip element
S->A	Element to enable bus transfer from start-up to auxiliary system
A->S	Element to enable bus transfer from auxiliary to start-up system

BKStart      Start-up side breaker

BKAux        Auxiliary side breaker

Before the transfer initialization the elements 21East, 87Aux, 27MB, RTrip, FTSMT, IPSMT, RVSMT, were enabled, elements S->A (motor bus transfer from start-up source to auxiliary source) was disabled and A->S (motor bus transfer from auxiliary source to start-up source) was enabled; BKStart was open and BKAux was closed.

When the under voltage relay element 27MB tripped at  $t = 14.0116$  seconds sent the trip command to the element RTrip and immediately the tripping signal was sent to the auxiliary breaker BKAux which opened at  $t = 14.0696$  seconds and the element A->S changed its status from enabled to disabled. The MBTS fast transfer element FTSMT also tripped at  $t = 14.0116$  seconds and the closing signal was sent to the start-up breaker BKStart which closed 90 milliseconds after receiving the closing signal, and the element S->A changed its status from disabled to enabled. The transfer was finally accomplished at  $t = 14.1016$  seconds. Elements 21East and 87Aux did not operate as it was expected.

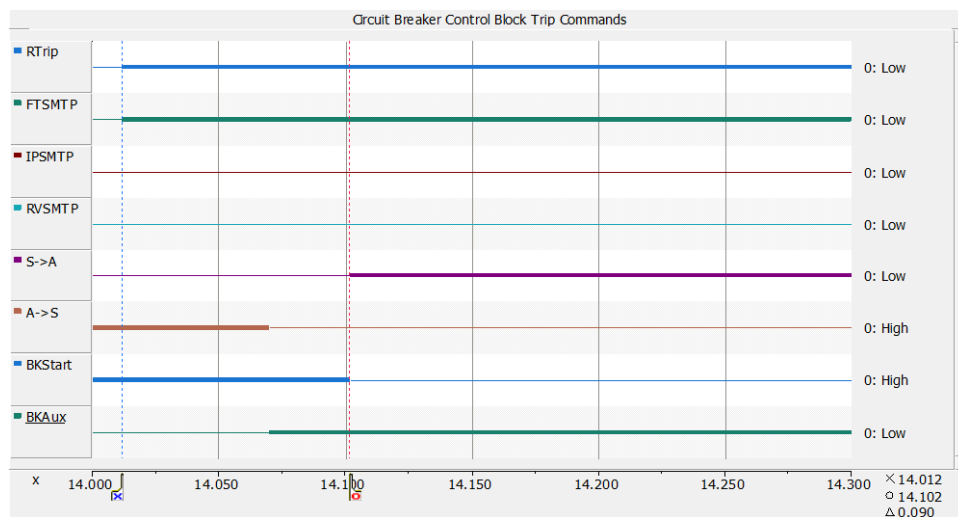


Figure 6-119 Motor bus transfer system element and circuit breaker contact operations during an automatic transfer initiated by the motor bus under voltage relay operation under low voltage conditions initiated at  $t = 14.000$  seconds

The logic timing of the motor bus transfer system elements and circuit breaker contacts operated correctly.

## 6.5 Motor Bus Transfer System Model Performance Summary

Table 6-5 shows a summary of the responses of the motor bus transfer system under different conditions. In the table “Pass” means that the motor bus transfer system model performed as predicted during the test.

Test	Transfer Initiation Time (seconds)	Test Result
Testing Mode		
Fast transfer	14.00	Pass
In-phase	14.00	Pass
Residual voltage	14.00	Pass
Testing Mode		
Fast transfer	14.00416	Pass
In-phase	14.00416	Pass
Residual voltage	14.00416	Pass
Testing Mode		
Fast transfer	14.00833	Pass
In-phase	14.00833	Pass
Residual voltage	14.00833	Pass
Testing Mode		
Fast transfer	14.0125	Pass
In-phase	14.0125	Pass
Residual voltage	14.0125	Pass
Residual voltage	14.02	Pass
Manual Transfer		
From start-up to auxiliary	14.18154	Pass
From auxiliary to start-up	14.1042	Pass
Automatic Transfer	Fault Initiation Time	
Initiated by the Auxiliary Differential Protective Relay	14.00	Pass
Initiated by the Transmission Line Distance Protective Relay	14.00	Pass
Initiated by the Motor Bus Undervoltage Protective Relay	14.00	Pass

Table 6-5 Summary of response of the motor bus transfer system

## CHAPTER 7 - CONCLUSIONS AND FUTURE WORK

In the course of the motor bus transfer process in power plants, the auxiliary induction and synchronous motors, their loads and couplings are exposed to electromechanical and electromagnetic forces that could damage them if an improper transfer schemes are implemented. The set of equations describing the behavior of the three-phase induction motors and the load was presented and the transient behavior of a single induction motor and of a group of induction motors during open and reconnection conditions were modeled. Several simulations were performed and their results (mathematically and graphically) showed the behavior of the induction motors, including worst conditions that may affect the motors during improper motor bus transfer. It has been shown that the highest voltage difference, when re-connecting, does not necessarily occur in phase opposition.

Under improper motor bus transfer, induction motors may be exposed to negative electromagnetic torques higher than 6 p.u. and inrush currents higher than twice the starting current. The large frequency difference between the new incoming source voltage frequency and the decaying frequency of the motor bus, when reconnecting, causes high and damped oscillatory phase currents and torques. The magnitude of such negative or oscillating torques may cause damage to the motor's shaft and some related power plant equipment. The ANSI 1.33 p.u. V/Hz limit is not a good criterion to reduce the induction motor electromagnetic torque when reconnecting under residual voltage transfer.

The large negative torques and high currents during reconnection to the new incoming power supply can be avoided reconnecting the new incoming source under supervision of the fast and in-phase transfer method.

A detailed search of available references concluded that the published literature does not clearly explain modeling implementation of a motor bus transfer scheme, using an electromagnetic transients program. Thus, I believe this detailed research is new work which may add to the MBTS literature and permit others to study the motor bus transfer scheme and vary the parameter settings to set them accordingly to the specific requirements and operating practices in a power plant.

This research work implemented a detailed motor bus transfer system and validated its performance during several normal and emergency conditions of the simulated power plant system, including interaction with manual and automatic controls.

The system modeled included enough detail to allow the protection and control power plant engineers to set and test every transfer method, independently or in an integrated form, permitting them to select the transfer method, depending on the power system conditions.

It was concluded that the modeled motor transfer system had sufficient controls to perform simulations of the coast-down tests of any single motor or all motors in group. It also included the modeling of the transfer scheme's full logic in order to test it before its implementation or upgrades in the field.

The results of this work concluded that all the motor bus transfer systems modeled and simulated behaved correctly. The fast, in-phase and residual voltage algorithms modeled in PSCAD/EMTDC operated as projected. All transfers from start-up power source to auxiliary power source and from the auxiliary source to the start-up source, either initiated manually or initiated automatically by the operation of protective relays, behaved as expected

Finally, in conclusion, I believe the models and simulations developed in this research work may be used, together with the PSCAD/EMTDC software, in power system classes to introduce protection and control engineers in the study and analysis of induction motor transient behavior under motor bus transfer conditions.



## 7.2 Future Work

This research work has been laid down the basis of motor bus transfer system using the standard methods described by the IEEE [1]. Based on the design concepts implemented here, further study on the model and performance of different motor bus transfer schemes can be addressed by the following;

- The standard motor bus transfer methods and power systems can also be modeled in a Real Time Digital Simulator (RTDS) in order to test the digital motor bus transfer devices already available in the market to ensure their appropriate configuration and settings previously to their installation in the field, avoiding the expensive testing currently performed in the field when commissioning those devices. Reference [14] is an extensive research on “In Phase Motor Bus Transfer and its modeling in a Real Time Digital Simulator (RTDS).
- This thesis does not include the analysis and behavior of synchronous motors on motor bus transfer. According to reference [22] synchronous motors have much larger open circuit time constant than induction motors and are more vulnerable to damage from high speed reclosing. Further work needs to be done so as to determine the impact of motor bus transfer transients on synchronous motors, and the impact of different reclosing times to the maximum current and maximum positive and negative torques that may be developed on synchronous motors.
- In the reference [14], high torques values obtained in simulations with the RTDS system under residual voltage conditions are reported. In reference [26] cases of field experience in motor bus transfer with residual voltage are reported where electromagnetic torques have been registered with magnitudes higher than 11 per unit. In the development of this research work in transfer simulations using the residual voltage method, electromagnetic torques exceeding 6 per unit were developed. It is necessary to continue with the investigation and analysis presented in section 3.5 to determine the cause of such large torques in residual voltage conditions, and to propose a transfer method in conditions of residual voltage in which the electromagnetic torques are limited to amounts that do not compromise the induction motor machines. Field and laboratory tests may be performed to further analyze and investigate those large electromagnetic torques.

**CHAPTER 8 - BIBLIOGRAPHY**

- [1] J. Gardel and D. Fredrickson, "Motor Bus Transfer Applications Issues and Considerations, J9 Working Group Report to the Rotating Machinery Protection Subcommittee of the IEEE Power System Relay Committee," IEEE-Power Systems Relay Committee, May 2012.
  
- [2] Manitoba-HVDC Research Centre, PSCAD User's Guide, Winnipeg, Manitoba: Manitoba-HVDC Research Centre, 2005.
  
- [3] Manitoba-HVDC Research Centre., EMTDC The Electromagnetic Transients and Controls Simulation Engine, Winnipeg, Manitoba: Manitoba-HVDC Research Centre, 2004.
  
- [4] P. C. Krause and C. H. Thomas, "Simulation of Symmetrical Induction Machinery," in *IEEE Transactions on Power Apparatus and Systems*, Vol. PAS-84, No. 11, November 1965.
  
- [5] W. S. Meyer and H. K. Lauw, "Universal Machine Modeling for the Representation of Rotating Electric Machinery in an Electromagnetic Transients Program," in *IEEE Transactions on Power Apparatus and Systems*, Vol. PAS-101, No. 6, June 1981.
  
- [6] R. H. Daugherty, "Analysis of Transient Electrical Torques and Shaft Torques in Induction Motors as a Result of Power Supply Disturbances," in *IEEE Transactions on Power Apparatus and Systems*, Vol. PAS-101, No. 8, August 1982.
  
- [7] T. S. Sidhu, V. Balamourougan, M. Thakur and B. Kasztenny, "A Modern Automatic Bus Transfer Scheme," in *International Journal of Control, Automation, and Systems*, Vol. 3, No. 2, June 2005.

- [8] V. Balamourougan, T. S. Sidhu, B. Kasztenny and M. M. Thakur, "Robust Technique for Fast and Safe Transfer of Power Plant Auxiliaries," in *IEEE Transactions of Energy Conversion*, Vol. 21, No. 2, June 2006.
- [9] T. R. Beckwith and W. G. Hartmann, "Motor Bus Transfer: Considerations and Methods," in *IEEE Transactions on Industry Applications*, Vol. 42, No. 2, April 2006.
- [10] D. M. V. V. S. Yalla, "Design of a High-Speed Motor Bus Transfer System," in *Industrial & Commercial Power Systems Technical Conference - Conference Record 2009 IEEE*, Calgary, AB, Canada, May 2009.
- [11] R. D. Pettigrew and P. Powell, "Motor Bus Transfer, A Report Prepared by the Motor Bus Transfer Working Group of the Power System Relaying Committee," in *IEEE Transactions on Power Delivery*, Vol. 8, No. 4, October 1993.
- [12] G. Hunswadkar and N. R. Viju, "Considerations and Methods for an Effective Fast Bus Transfer System," in *Power System Protection and Automation*, New Delhi, India, December 2010.
- [13] A. Raje, A. Raje, J. McCall and A. Chaudhary, "Bus Transfer Systems: Requirements, Implementation, and Experiences," in *IEEE Transactions on Industry Applications*, Vol. 39, No. 1, Toronto, ON, Canada, February 2003.
- [14] N. Fischer, "In Phase Motor Bus Transfer," in *Doctorate of Philosophy Thesis at the University of Idaho*, September 2014.
- [15] Beckwith Electric Co, Inc., M-4272 Motor Bus Transfer System, Instruction Book, Largo, Florida: Beckwith Electric, Co. Inc., August 2015.

- [16] The Institute of Electrical and Electronics Engineers, Inc., "IEEE Std. 308-2012 Standard Criteria for Class 1E Power Systems for Nuclear Power Generating Stations," New York, NY, USA, 2013.
- [17] P. Pillay and V. Levin, "Mathematical Models for Induction Machines," in *Department of Electrical Engineering, University of New Orleans*, New Orleans, Louisiana, 1995.
- [18] A. E. Fitzgerald, K. Charles, Jr. and S. D. Umas, *Electric Machinery*, Sixth ed., New York, NY: Mc Graw Hill, 2003.
- [19] P. Krause, O. Wasynczuk, S. Sudhoff and S. Pekarek, *Analysis of Electric Machinery and Drive Systems*, Third Edition ed., Wiley, Ed., Piscataway, NJ: IEEE Press, Wiley, 2013.
- [20] J. C. Das, *Transients in Electrical Systems, Analysis, Recognition, and Mitigation*, First ed., New York, NY: Mc Graw Hill, 2010.
- [21] M. A. Zamani, M. D. Zadeh and T. S. Sidhu, "A Compensated DFT-Based Phase-Angle Estimation for Fast Motor-Bus Transfer Applications," in *IEEE Transactions on Energy Conversion, Volume: 30, Issue: 2*, Toronto, ON, Canada, 2015.
- [22] R. W. Patterson and G. T. Pitts, "Reclosing and Tapped Motor Load," in *Protective Relaying Conference, 61st Annual Georgia Institute of Technology*, Atlanta, GA, 2007.
- [23] EDSA Micro Corporation, *Induction Motor Parameter Estimation Based on the Sequential Augmented Lograngian Optimization Algorithm*, EDSA Micro Corporation, 2008.
- [24] NEMA Standards Publication, "NEMA Standards Publication Mg 1-2006, Motors and Generators," 2006.

- [25] American National Standard Institute, "ANSI C50.41-2000 American National Standard for Polyphase Induction Motors for Power Generation Stations," 2000.
- [26] D. M. V. Yalla and T. R. Beckwith, "Expanded Field Data Analysis in Support of a Torque-Based Motor Bus Transfer Criterion," in *Petroleum and Chemical Industry Technical Conference (PCIC)*, Calgary, AB, Canada, 2017.

## APPENDIX A

This appendix shows the electrical parameters of the elements used in the power system modeled in PSCAD/EMTDC.

### A.1 Western System PSCAD/EMTDC Input Parameters

Table A-1 to Table A-11 show the PCAD/EMTDC input parameters of the Western system elements

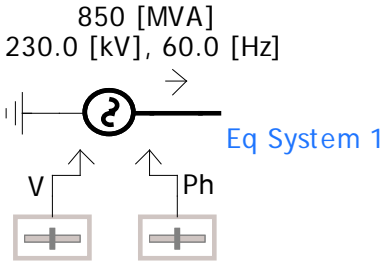
Equivalent source 1	Value
	
Source name	EqSys01
Base MVA (3-phase)	850 MVA
Base voltage (L-L, RMS)	230.0 kV
Base frequency	60.0 Hz
Voltage input time constant	0.01 sec
Infinite bus?	Yes
Positive sequence impedance	1.0 ohm
Positive sequence impedance phase angle	80.0 degrees
Positive sequence resistance	0.06 ohm
Positive sequence reactance	15.0758 ohm
Zero sequence impedance	1.0 ohm
Zero sequence impedance phase angle	80.0 degrees
Zero sequence resistance	0.12 ohm
Zero sequence reactance	8.93845 ohm

Table A-1 PSCAD/EMTDC input parameters of the Western system equivalent source 1

Equivalent source 2	Value
Source name	EqSys01
Base MVA (3-phase)	850 MVA
Base voltage (L-L, RMS)	230.0 kV
Base frequency	60.0 Hz
Voltage input time constant	0.01 sec
Infinite bus?	Yes
Positive sequence impedance	1.0 ohm
Positive sequence impedance phase angle	80.0 degrees
Positive sequence resistance	0.06 ohm
Positive sequence reactance	15.0758 ohm
Zero sequence impedance	1.0 ohm
Zero sequence impedance phase angle	80.0 degrees
Zero sequence resistance	0.12 ohm
Zero sequence reactance	8.93845 ohm

Table A-2 PSCAD/EMTDC input parameters of the Western system equivalent source 2

Transmission line from bus BusA to bus BusB – Part 1	
<p>Mid-Span Sag: 7 [m] for Conductors 6 [m] for Ground Wires</p> <p>9 [m]</p> <p>14 [m]</p> <p>10 [m]</p> <p>20 [m]</p> <p>10 [m]</p> <p>Resistivity: 100.0 [ohm*m]</p> <p>Aerial: Analytical Approximation (Deri-Semlyen) Underground: Direct Numerical Integration Mutual: Analytical Approximation (LUCCA)</p>	
General configuration	Value
Graphic conductor sag	Yes
Ideal transposition	Enabled
Shunt conductance	1.0E-11 mhos/m
Relative x-position of power centre	10 m
Height of all conductors	20 m
Horizontal spacing between conductors	20 m
Height of ground wires over lowest conductor	9 m
Spacing between ground wires	14 m
Conductor data	Value
Outer radius	0.01529 m
DC resistance (entire conductor)	0.0701 ohms/km
Relative permeability	1.0
Sag (all conductors)	7 m
Total bundle sub-conductors	3
Bundle configuration is	Symmetrical
Sub-conductor spacing	0.2 m
Bundle graphic is	Visible

Table A-3 PSCAD/EMTDC input parameters of the Western system transmission line from bus BusA to bus BusB – Part 1



Transmission line from bus BusA to bus BusB – Part 2	
Ground wire data	Value
Total number of ground wires is	2
Ground wires are	Identical
Ground wire elimination is	Enabled
Data entry method	Direct
Outer radius	0.00475 m
DC resistance	3.750 ohms/km
Relative permeability	1.0
Sag (all ground wires)	6 m
Connection Numbers	Value
Conductor 1	1
Conductor 2	2
Conductor 3	3
General information	Value
Segment name	TL9001
Steady-state frequency	60 Hz
Segment length	144.81 km
Line termination style	Local connection
Coupling of this segment to others is	Disabled

*Table A-4 PSCAD/EMTDC input parameters of the Western system transmission line from bus BusA to bus BusB – Part 2*

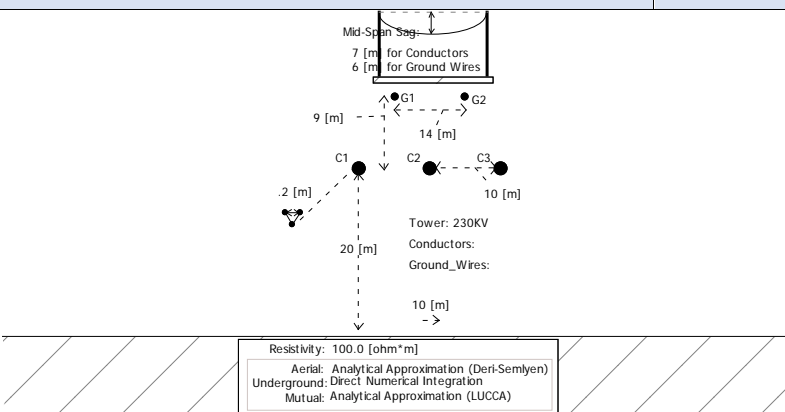
Transmission line from bus BusB to bus BusFlt_1 – Part 1	
	
General configuration	Value
Graphic conductor sag	Yes
Ideal transposition	Enabled
Shunt conductance	1.0E-11 mhos/m
Relative x-position of power centre	10 m
Height of all conductors	20 m
Horizontal spacing between conductors	20 m
Height of ground wires over lowest conductor	9 m
Spacing between ground wires	14 m
Conductor data	Value
Outer radius	0.01529 m
DC resistance (entire conductor)	0.0701 ohms/km
Relative permeability	1.0
Sag (all conductors)	7 m
Total bundle sub-conductors	3
Bundle configuration is	Symmetrical
Sub-conductor spacing	0.2 m
Bundle graphic is	Visible

Table A-5 PSCAD/EMTDC input parameters of the Western system transmission line from bus BusB to bus BusFlt\_1 – Part 1

Transmission line from bus BusB to bus BusFlt_1 – Part 2	
Ground wire data	Value
Total number of ground wires is	2
Ground wires are	Identical
Ground wire elimination is	Enabled
Data entry method	Direct
Outer radius	0.00475 m
DC resistance	3.750 ohms/km
Relative permeability	1.0
Sag (all ground wires)	6 m
Connection Numbers	Value
Conductor 1	1
Conductor 2	2
Conductor 3	3
General information	Value
Segment name	TL9002
Steady-state frequency	60 Hz
Segment length	43.443 km
Line termination style	Local connection
Coupling of this segment to others is	Disabled

*Table A-6 PSCAD/EMTDC input parameters of the Western system transmission line from bus BusB to bus BusFlt\_1 – Part 2*

Transmission line from bus BusFlt_1 to bus BusC – Part 1	
General configuration	Value
Graphic conductor sag	Yes
Ideal transposition	Enabled
Shunt conductance	1.0E-11 mhos/m
Relative x-position of power centre	10 m
Height of all conductors	20 m
Horizontal spacing between conductors	20 m
Height of ground wires over lowest conductor	9 m
Spacing between ground wires	14 m
Conductor data	Value
Outer radius	0.01529 m
DC resistance (entire conductor)	0.0701 ohms/km
Relative permeability	1.0
Sag (all conductors)	7 m
Total bundle sub-conductors	3
Bundle configuration is	Symmetrical
Sub-conductor spacing	0.2 m
Bundle graphic is	Visible

Table A-7 PSCAD/EMTDC input parameters of the Western system transmission line from bus BusFlt\_1 to bus BusC – Part 1

Transmission line from bus BusFlt_1 to bus BusC – Part 2	
Ground wire data	Value
Total number of ground wires is	2
Ground wires are	Identical
Ground wire elimination is	Enabled
Data entry method	Direct
Outer radius	0.00475 m
DC resistance	3.750 ohms/km
Relative permeability	1.0
Sag (all ground wires)	6 m
Connection Numbers	Value
Conductor 1	1
Conductor 2	2
Conductor 3	3
General information	Value
Segment name	TL9003
Steady-state frequency	60 Hz
Segment length	101.367 km
Line termination style	Local connection
Coupling of this segment to others is	Disabled

*Table A-8 PSCAD/EMTDC input parameters of the Western system transmission line from bus BusFlt\_1 to bus BusC – Part 2*

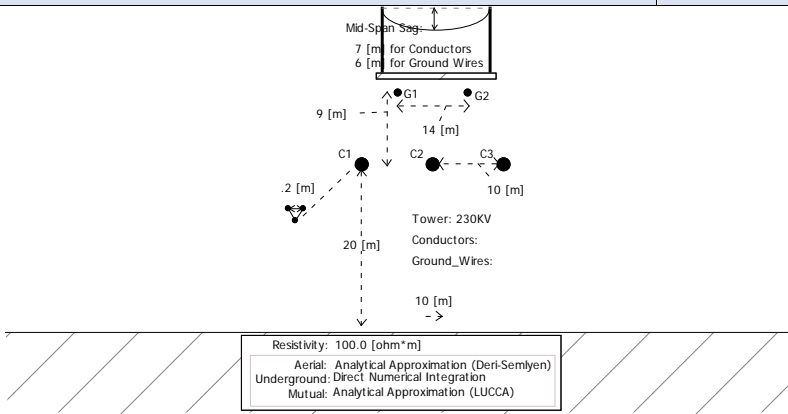
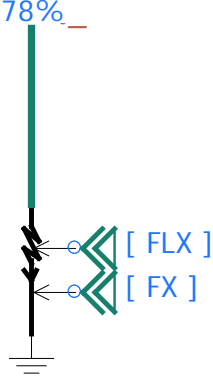
Transmission line from bus BusBF to bus BusC – Part 1	
	
General configuration	Value
Graphic conductor sag	Yes
Ideal transposition	Enabled
Shunt conductance	1.0E-11 mhos/m
Relative x-position of power centre	10 m
Height of all conductors	20 m
Horizontal spacing between conductors	20 m
Height of ground wires over lowest conductor	9 m
Spacing between ground wires	14 m
Conductor data	Value
Outer radius	0.01529 m
DC resistance (entire conductor)	0.0701 ohms/km
Relative permeability	1.0
Sag (all conductors)	7 m
Total bundle sub-conductors	3
Bundle configuration is	Symmetrical
Sub-conductor spacing	0.2 m
Bundle graphic is	Visible

Table A-9 PSCAD/EMTDC input parameters of the Western system transmission line from bus BusBF to bus BusC – Part 1

Transmission line from bus BusBF to bus BusC – Part 2	
<b>Ground wire data</b>	<b>Value</b>
Total number of ground wires is	2
Ground wires are	Identical
Ground wire elimination is	Enabled
Data entry method	Direct
Outer radius	0.00475 m
DC resistance	3.750 ohms/km
Relative permeability	1.0
Sag (all ground wires)	6 m
<b>Connection Numbers</b>	<b>Value</b>
Conductor 1	1
Conductor 2	2
Conductor 3	3
<b>General information</b>	<b>Value</b>
Segment name	TL9004
Steady-state frequency	60 Hz
Segment length	144.81 km
Line termination style	Local connection
Coupling of this segment to others is	Disabled

*Table A-10 PSCAD/EMTDC input parameters of the Western system transmission line from bus BusBF to bus BusC – Part 2*

Three Phase Fault Control	Value
	
Fault type control	External
Clear possible at any current	No
Is the neutral grounded	Yes
Graphic display	Single line view
Current chopping limit	0.0 kA
Fault ON resistance	0.001 ohm
Fault OFF resistance	1.0E9 ohm

*Table A-11 PSCAD/EMTDC input parameters of the Western system three phase fault control*



## A.2 Auxiliary Transformer PSCAD/EMTDC Input Parameters

Table A-12 show the PCAD/EMTDC input parameters of the auxiliary transformer

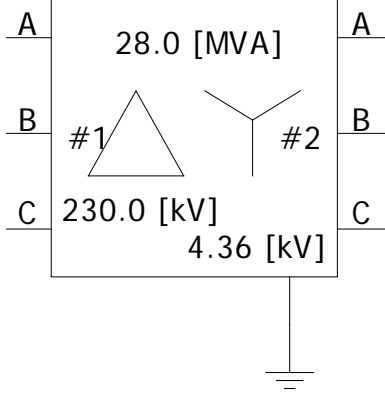
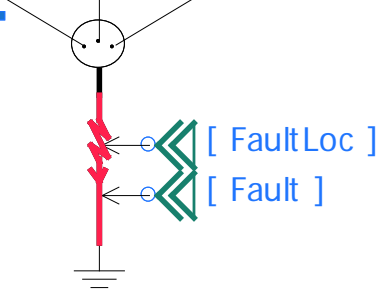
Auxiliary transformer	Value
	
Transformer name	TAux
3 phase transformer MVA	28.0 MVA
Base operation frequency	60.0 Hz
Winding #1 Type	Delta
Winding #2 Type	Y
Delta lags or leads Y	Leads
Positive sequence leakage reactance	0.1 p.u.
Ideal transformer model	No
Eddy current losses	0.0 p.u.
Copper losses	0.005 p.u.
Tap changer on winding	None
Graphic display	3 phase view
Winding 1 line to line voltage RMS	230 kV
Winding 2 line to line voltage RMS	4.36 kV

Table A-12 PSCAD/EMTDC input parameters of the auxiliary transformer

Table A-13 show the PSCAD/EMTDC input parameters of the auxiliary transformer three phase fault control.

Three Phase Fault Control	Value
	
Fault type control	External
Clear possible at any current	No
Is the neutral grounded	Yes
Graphic display	Single line view
Current chopping limit	0.0 kA
Fault ON resistance	0.001 ohm
Fault OFF resistance	1.0E9 ohm

*Table A-13 PSCAD/EMTDC input parameters of the auxiliary transformer three phase fault control*

### A.3 Eastern System PSCAD/EMTDC Input Parameters

Table A-14 to Table A-19 show the PCAD/EMTDC input parameters of the Eastern system elements

Equivalent source	Value
Source name	EqSystem
Base MVA (3-phase)	850 MVA
Base voltage (L-L, RMS)	230.0 kV
Base frequency	60.0 Hz
Voltage input time constant	0.01 sec
Infinite bus?	Yes
Positive sequence impedance	1.0 ohm
Positive sequence impedance phase angle	80.0 degrees
Positive sequence resistance	0.06 ohm
Positive sequence reactance	15.0758 ohm
Zero sequence impedance	1.0 ohm
Zero sequence impedance phase angle	80.0 degrees
Zero sequence resistance	0.12 ohm
Zero sequence reactance	8.93845 ohm

Table A-14 PSCAD/EMTDC input parameters of the Eastern system equivalent source

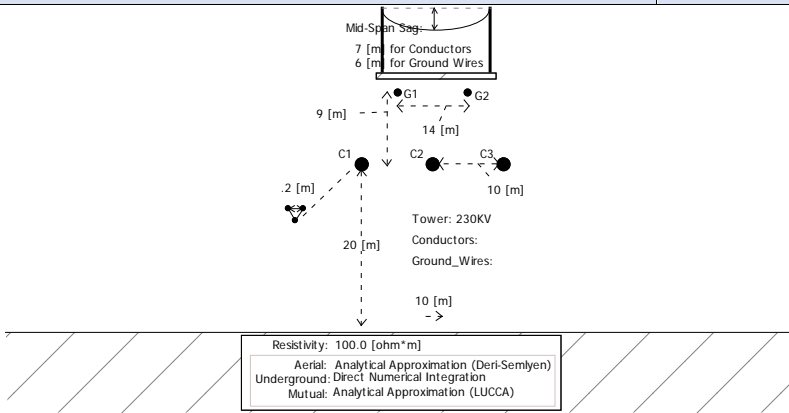
Transmission line from bus BusB to bus BusFit_1 – Part 1	
	
General configuration	Value
Graphic conductor sag	Yes
Ideal transposition	Enabled
Shunt conductance	1.0E-11 mhos/m
Relative x-position of power centre	10 m
Height of all conductors	20 m
Horizontal spacing between conductors	20 m
Height of ground wires over lowest conductor	9 m
Spacing between ground wires	14 m
Conductor data	Value
Outer radius	0.01529 m
DC resistance (entire conductor)	0.0701 ohms/km
Relative permeability	1.0
Sag (all conductors)	7 m
Total bundle sub-conductors	3
Bundle configuration is	Symmetrical
Sub-conductor spacing	0.2 m
Bundle graphic is	Visible

Table A-15 PSCAD/EMTDC input parameters of the Eastern system transmission line from bus BusB to bus BusFit\_1 – Part 1

Transmission line from bus BusB to bus BusFlt_1 – Part 2	
<b>Ground wire data</b>	<b>Value</b>
Total number of ground wires is	2
Ground wires are	Identical
Ground wire elimination is	Enabled
Data entry method	Direct
Outer radius	0.00475 m
DC resistance	3.750 ohms/km
Relative permeability	1.0
Sag (all ground wires)	6 m
<b>Connection Numbers</b>	<b>Value</b>
Conductor 1	1
Conductor 2	2
Conductor 3	3
<b>General information</b>	<b>Value</b>
Segment name	TL9021
Steady-state frequency	60 Hz
Segment length	31.8582 km
Line termination style	Local connection
Coupling of this segment to others is	Disabled

*Table A-16 PSCAD/EMTDC input parameters of the Eastern system transmission line from bus BusB to bus BusFlt\_1 – Part 2*

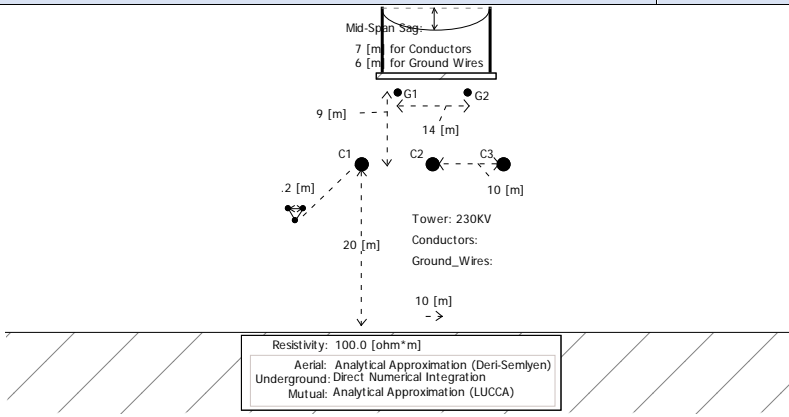
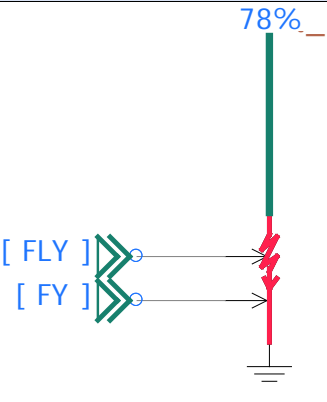
Transmission line from bus BusFlt_1 to bus BusC – Part 1	
	
General configuration	Value
Graphic conductor sag	Yes
Ideal transposition	Enabled
Shunt conductance	1.0E-11 mhos/m
Relative x-position of power centre	10 m
Height of all conductors	20 m
Horizontal spacing between conductors	20 m
Height of ground wires over lowest conductor	9 m
Spacing between ground wires	14 m
Conductor data	Value
Outer radius	0.01529 m
DC resistance (entire conductor)	0.0701 ohms/km
Relative permeability	1.0
Sag (all conductors)	7 m
Total bundle sub-conductors	3
Bundle configuration is	Symmetrical
Sub-conductor spacing	0.2 m
Bundle graphic is	Visible

Table A-17 PSCAD/EMTDC input parameters of the Eastern system transmission line from bus BusFlt\_1 to bus BusC – Part 1

Transmission line from bus BusFlt_1 to bus BusC – Part 2	
Ground wire data	Value
Total number of ground wires is	2
Ground wires are	Identical
Ground wire elimination is	Enabled
Data entry method	Direct
Outer radius	0.00475 m
DC resistance	3.750 ohms/km
Relative permeability	1.0
Sag (all ground wires)	6 m
Connection Numbers	Value
Conductor 1	1
Conductor 2	2
Conductor 3	3
General information	Value
Segment name	TL9022
Steady-state frequency	60 Hz
Segment length	110.9518 km
Line termination style	Local connection
Coupling of this segment to others is	Disabled

*Table A-18 PSCAD/EMTDC input parameters of the Eastern system transmission line from bus BusFlt\_1 to bus BusC – Part 2*

Three Phase Fault Control	Value
	
Fault type control	External
Clear possible at any current	No
Is the neutral grounded	Yes
Graphic display	Single line view
Current chopping limit	0.0 kA
Fault ON resistance	0.001 ohm
Fault OFF resistance	1.0E9 ohm

*Table A-19 PSCAD/EMTDC input parameters of the Eastern system three phase fault control*



## A.4 Main Generator PSCAD/EMTDC Input Parameters

Table A-20 shows the PCAD/EMTDC input parameters of the main generator modeled as an equivalent source.

Equivalent source	Value
Source name	MainGen
Base MVA (3-phase)	300 MVA
Base voltage (L-L, RMS)	20.0 kV
Base frequency	60.0 Hz
Voltage input time constant	0.05 sec
Infinite bus?	No
Zero seq. differs from positive seq.?	Yes
Impedance data format	Magnitude-Angle
Graphic display	Single line view
Positive sequence impedance	0.02 ohm
Positive sequence impedance phase angle	89.0 degrees
Zero sequence impedance	0.4 ohm
Zero sequence impedance phase angle	80.0 degrees

Table A-20 PSCAD/EMTDC input parameters of the main generator modeled by an equivalent source

## A.5 Main Station Transformer PSCAD/EMTDC Input Parameters

Table A-21 show the PCAD/EMTDC input parameters of the main station transformer

Main station transformer	Value
Transformer name	TMain
3 phase transformer MVA	350.0 MVA
Base operation frequency	60.0 Hz
Winding #1 Type	Delta
Winding #2 Type	Y
Delta lags or leads Y	Lags
Positive sequence leakage reactance	0.07 p.u.
Ideal transformer model	No
Eddy current losses	0.0 p.u.
Copper losses	0.003 p.u.
Tap changer on winding	None
Graphic display	3 phase view
Winding 1 line to line voltage RMS	20 kV
Winding 2 line to line voltage RMS	230 kV

Table A-21 PSCAD/EMTDC input parameters of the main station transformer

## A.6 9000 HP Induction Motor PSCAD/EMTDC Input Parameters

Table A-22 show the PSCAD/EMTDC input parameters of the 9000 HP induction motor

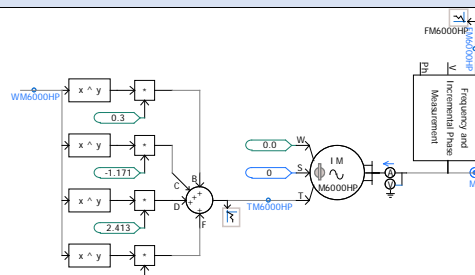
9000 HP induction motor	Value
	
Motor name	M9000HP
Data generation/entry	EMTP Type 40
Multimass interface	Disable
Number of coherent machines	1.0
Number of sub-iteration steps	1
Rated RMS phase voltage	2.40177 kV
Rated RMS phase current	1.07545 kA
Base angular frequency	376.991 rad/s
Graphic display	Single line view
Design ratio	1.0 p.u.
Power factor at rated load	0.89 p.u.
Efficiency at rated load	0.973 p.u.
Slip at full load	0.0072 p.u.
Starting current at full volts	6.9 p.u.
Starting torque at full volt / Full load torque	1 p.u.
Maximum torque / Full load torque	2.1 p.u.
Number of poles	4
Polar moment of inertia J	9.24
Units of inertia	S
Mechanical damping	0.008 p.u.

Table A-22 PSCAD/EMTDC input parameters of the 9000 HP induction motor

## A.7 6000 HP Induction Motor PSCAD/EMTDC Input Parameters

Table A-23 show the PSCAD/EMTDC input parameters of the 6000 HP induction motor

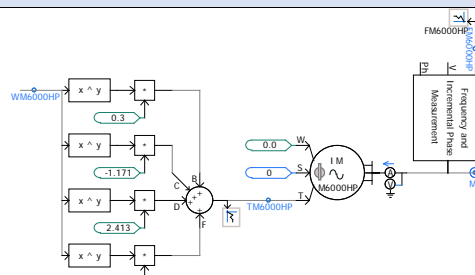
6000 HP induction motor	Value
	
Motor name	M6000HP
Data generation/entry	EMTP Type 40
Multimass interface	Disable
Number of coherent machines	1.0
Number of sub-iteration steps	1
Rated RMS phase voltage	2.309401 kV
Rated RMS phase current	0.873169 kA
Base angular frequency	376.991 rad/s
Graphic display	Single line view
Design ratio	1.0 p.u.
Power factor at rated load	0.85 p.u.
Efficiency at rated load	0.87 p.u.
Slip at full load	0.0084 p.u.
Starting current at full volts	6.2 p.u.
Starting torque at full volt / Full load torque	1 p.u.
Maximum torque / Full load torque	1.8 p.u.
Number of poles	4
Polar moment of inertia J	6.95
Units of inertia	S
Mechanical damping	0.001 p.u.

Table A-23 PSCAD/EMTDC input parameters of the 6000 HP induction motor

## A.8 3200 HP Induction Motor PSCAD/EMTDC Input Parameters

Table A-24 show the PSCAD/EMTDC input parameters of the 3200 HP induction motor

3200 HP induction motor	Value
Motor name	M3200HP
Data generation/entry	EMTP Type 40
Multimass interface	Disable
Number of coherent machines	1.0
Number of sub-iteration steps	1
Rated RMS phase voltage	2.309401 kV
Rated RMS phase current	0.423745 kA
Base angular frequency	376.991 rad/s
Graphic display	Single line view
Design ratio	1.0 p.u.
Power factor at rated load	0.903 p.u.
Efficiency at rated load	0.90 p.u.
Slip at full load	0.0084 p.u.
Starting current at full volts	7.0 p.u.
Starting torque at full volt / Full load torque	1 p.u.
Maximum torque / Full load torque	2.1 p.u.
Number of poles	6
Polar moment of inertia J	9.8
Units of inertia	S
Mechanical damping	0.008 p.u.

Table A-24 PSCAD/EMTDC input parameters of the 3200 HP induction motor

## A.9 1400 HP Induction Motor PSCAD/EMTDC Input Parameters

Table A-25 show the PSCAD/EMTDC input parameters of the 1400 HP induction motor

1400 HP induction motor	Value
Motor name	M1400HP
Data generation/entry	EMTP Type 40
Multimass interface	Disable
Number of coherent machines	1.0
Number of sub-iteration steps	1
Rated RMS phase voltage	2.309401 kV
Rated RMS phase current	0.20384 kA
Base angular frequency	376.991 rad/s
Graphic display	Single line view
Design ratio	1.0 p.u.
Power factor at rated load	0.85 p.u.
Efficiency at rated load	0.87 p.u.
Slip at full load	0.01124 p.u.
Starting current at full volts	5.9 p.u.
Starting torque at full volt / Full load torque	1 p.u.
Maximum torque / Full load torque	1.8 p.u.
Number of poles	4
Polar moment of inertia J	8.458
Units of inertia	S
Mechanical damping	0.008 p.u.

Table A-25 PSCAD/EMTDC input parameters of the 1400 HP induction motor

A.10 1000 HP Induction Motor PSCAD/EMTDC Input Parameters

Table A-26 show the PSCAD/EMTDC input parameters of the 1000 HP induction motor

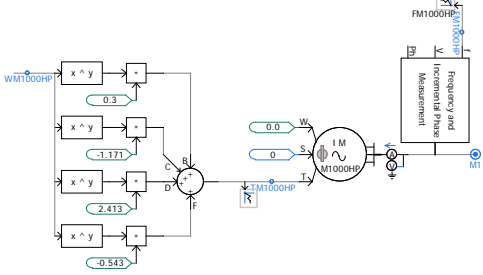
1000 HP induction motor	Value
	
Motor name	M1000HP
Data generation/entry	EMTP Type 40
Multimass interface	Disable
Number of coherent machines	1.0
Number of sub-iteration steps	1
Rated RMS phase voltage	2.309401 kV
Rated RMS phase current	0.145528 kA
Base angular frequency	376.991 rad/s
Graphic display	Single line view
Design ratio	1.0 p.u.
Power factor at rated load	0.85 p.u.
Efficiency at rated load	0.87 p.u.
Slip at full load	0.01124 p.u.
Starting current at full volts	6.2 p.u.
Starting torque at full volt / Full load torque	1 p.u.
Maximum torque / Full load torque	1.8 p.u.
Number of poles	4
Polar moment of inertia J	7.74
Units of inertia	S
Mechanical damping	0.008 p.u.

Table A-26 PSCAD/EMTDC input parameters of the 1000 HP induction motor

A.11 470 HP Induction Motor PSCAD/EMTDC Input Parameters

Table A-27 show the PSCAD/EMTDC input parameters of the 470 HP induction motor

1000 HP induction motor	Value
Motor name	M470HP
Data generation/entry	EMTP Type 40
Multimass interface	Disable
Number of coherent machines	1.0
Number of sub-iteration steps	1
Rated RMS phase voltage	2.309401 kV
Rated RMS phase current	0.062237 kA
Base angular frequency	376.991 rad/s
Graphic display	Single line view
Design ratio	1.0 p.u.
Power factor at rated load	0.903 p.u.
Efficiency at rated load	0.90 p.u.
Slip at full load	0.0084 p.u.
Starting current at full volts	7.0 p.u.
Starting torque at full volt / Full load torque	1 p.u.
Maximum torque / Full load torque	2 p.u.
Number of poles	6
Polar moment of inertia J	9.356
Units of inertia	S
Mechanical damping	0.008 p.u.

Table A-27 PSCAD/EMTDC input parameters of the 470 HP induction motor



## A.12 9000 HP Induction Motor PSCAD/EMTDC Input Parameters

Table A-28 show the PSCAD/EMTDC input parameters of the 9000 HP induction motor

9000 HP induction motor	Value
Motor name	M9000HP
Data generation/entry	EMTP Type 40
Multimass interface	Disable
Number of coherent machines	1.0
Number of sub-iteration steps	1
Rated RMS phase voltage	2.40177 kV
Rated RMS phase current	1.07546 kA
Base angular frequency	376.991 rad/s
Graphic display	Single line view
Design ratio	1.0 p.u.
Power factor at rated load	0.89 p.u.
Efficiency at rated load	0.973 p.u.
Slip at full load	0.0072 p.u.
Starting current at full volts	6.9 p.u.
Starting torque at full volt / Full load torque	1 p.u.
Maximum torque / Full load torque	2.1 p.u.
Number of poles	4
Polar moment of inertia J	7.14
Units of inertia	S
Mechanical damping	0.008 p.u.

Table A-28 PSCAD/EMTDC input parameters of the 9000 HP induction motor

A.13 6000 HP Induction Motor PSCAD/EMTDC Input Parameters

Table A-29 show the PSCAD/EMTDC input parameters of the 6000 HP induction motor

6000 HP induction motor	Value
Motor name	M6000HP
Data generation/entry	EMTP Type 40
Multimass interface	Disable
Number of coherent machines	1.0
Number of sub-iteration steps	1
Rated RMS phase voltage	2.40177 kV
Rated RMS phase current	0.71919 kA
Base angular frequency	376.991 rad/s
Graphic display	Single line view
Design ratio	1.0 p.u.
Power factor at rated load	0.89 p.u.
Efficiency at rated load	0.97 p.u.
Slip at full load	0.0072 p.u.
Starting current at full volts	6.9 p.u.
Starting torque at full volt / Full load torque	0.7 p.u.
Maximum torque / Full load torque	2.4 p.u.
Number of poles	2
Polar moment of inertia J	6.48
Units of inertia	S
Mechanical damping	0.008 p.u.

Table A-29 PSCAD/EMTDC input parameters of the 6000 HP induction motor

A.14 4000 HP Induction Motor PSCAD/EMTDC Input Parameters

Table A-30 show the PSCAD/EMTDC input parameters of the 4000 HP induction motor

4000 HP induction motor	Value
Motor name	M4000HP
Data generation/entry	EMTP Type 40
Multimass interface	Disable
Number of coherent machines	1.0
Number of sub-iteration steps	1
Rated RMS phase voltage	2.40177 kV
Rated RMS phase current	0.479458 kA
Base angular frequency	376.991 rad/s
Graphic display	Single line view
Design ratio	1.0 p.u.
Power factor at rated load	0.89 p.u.
Efficiency at rated load	0.97 p.u.
Slip at full load	0.00444 p.u.
Starting current at full volts	5.8 p.u.
Starting torque at full volt / Full load torque	0.8 p.u.
Maximum torque / Full load torque	2.0 p.u.
Number of poles	4
Polar moment of inertia J	7.27
Units of inertia	S
Mechanical damping	0.008 p.u.

Table A-30 PSCAD/EMTDC input parameters of the 4000 HP induction motor

## A.15 3500 HP Induction Motor PSCAD/EMTDC Input Parameters

Table A-31 show the PSCAD/EMTDC input parameters of the 3500 HP induction motor

3500 HP induction motor	Value
Motor name	M3500HP
Data generation/entry	EMTP Type 40
Multimass interface	Disable
Number of coherent machines	1.0
Number of sub-iteration steps	1
Rated RMS phase voltage	2.40177 kV
Rated RMS phase current	0.419958 kA
Base angular frequency	376.991 rad/s
Graphic display	Single line view
Design ratio	1.0 p.u.
Power factor at rated load	0.89 p.u.
Efficiency at rated load	0.969 p.u.
Slip at full load	0.00444 p.u.
Starting current at full volts	5.9 p.u.
Starting torque at full volt / Full load torque	1 p.u.
Maximum torque / Full load torque	2.1 p.u.
Number of poles	4
Polar moment of inertia J	7.92
Units of inertia	S
Mechanical damping	0.008 p.u.

Table A-31 PSCAD/EMTDC input parameters of the 3500 HP induction motor

## A.16 2500 HP Induction Motor PSCAD/EMTDC Input Parameters

Table A-32 show the PSCAD/EMTDC input parameters of the 2500 HP induction motor

2500 HP induction motor	Value
Motor name	M2500HP
Data generation/entry	EMTP Type 40
Multimass interface	Disable
Number of coherent machines	1.0
Number of sub-iteration steps	1
Rated RMS phase voltage	2.40177 kV
Rated RMS phase current	0.301526 kA
Base angular frequency	376.991 rad/s
Graphic display	Single line view
Design ratio	1.0 p.u.
Power factor at rated load	0.89 p.u.
Efficiency at rated load	0.964 p.u.
Slip at full load	0.00556 p.u.
Starting current at full volts	5.2 p.u.
Starting torque at full volt / Full load torque	1 p.u.
Maximum torque / Full load torque	1.8 p.u.
Number of poles	4
Polar moment of inertia J	9.5
Units of inertia	S
Mechanical damping	0.008 p.u.

Table A-32 PSCAD/EMTDC input parameters of the 2500 HP induction motor

## A.17 2000 HP Induction Motor PSCAD/EMTDC Input Parameters

Table A-33 show the PSCAD/EMTDC input parameters of the 2000 HP induction motor

2000 HP induction motor	Value
Motor name	M2000HP
Data generation/entry	EMTP Type 40
Multimass interface	Disable
Number of coherent machines	1.0
Number of sub-iteration steps	1
Rated RMS phase voltage	2.40177 kV
Rated RMS phase current	0.245746 kA
Base angular frequency	376.991 rad/s
Graphic display	Single line view
Design ratio	1.0 p.u.
Power factor at rated load	0.87 p.u.
Efficiency at rated load	0.968 p.u.
Slip at full load	0.00667 p.u.
Starting current at full volts	6.0 p.u.
Starting torque at full volt / Full load torque	1.1 p.u.
Maximum torque / Full load torque	2.1 p.u.
Number of poles	4
Polar moment of inertia J	8.79
Units of inertia	S
Mechanical damping	0.008 p.u.

Table A-33 PSCAD/EMTDC input parameters of the 2000 HP induction motor